The Geological Society of America Bulletin

Volume 72 | February 1961 | Number 2

CONTENTS

Subscriptions $15.00 per year. Printing Office: Burlington, Vt. Second-class postage paid at Burlington, Vermont. Published monthly.

Communications regarding publications should be addressed to The Geological Society of America, Dr. Frederick Betz, Jr., Secretary, 419 West 117 Street, New York 27, N. Y.

Please give notice of change of address 4 weeks in advance. Claims for nonreceipt of the Bulletin of a given month must be sent to the Secretary of the Society before the end of the second succeeding month.

PAPERS IN PRESS FOR FORTHCOMING ISSUES

Welded Tuffs and Flows in the Rhyolite Plateau of Yellowstone Park, Wyoming. Francis R. Boyd

Precambrian Rocks and Laramide Structure Along the East Flank of the Bighorn Mountains Near Buffalo, Wyoming. Richard A. Hoppin

Limnology, Sedimentation, and Microorganisms of the Salton Sea, California. Robert E. Arnal

Age and Stratigraphic Relations of the Formosa Reef Limestone of Southwestern Ontario, Canada. J. A. Fagerstrom

Hydrothermal Magnetite. William T. Holser and Cecil J. Schneer

Paleotemperature Analysis of the Plio-Pleistocene Section at Le Castella, Calabria, Southern Italy. C. Emiliani, T. Mayeda, and R. Selli

NEW FOREIGN BIBLIOGRAPHY

Bibliography and Index of Geology Exclusive of North America. Volume 23. Marie Siegrist, Mary C. Grier, and others.

Price, $13.00

Special price to Fellows and Members of GSA, $8.50

NEW MEMOIR

82. Oligocene Plants from the Upper Ruby River Basin, Southwestern Montana. Herman F. Becker

Description of a well-preserved flora (37 families, 61 genera, and 82 identifiable species, 25 of which are new) from Tertiary fossiliferous shales of the Ruby River basin. The author uses the flora to interpret the paleoecology and paleoclimatology and suggests that the Ruby and Florissant assemblages represent a single botanical province.

128 pages, 4 figures, 32 photographic plates

Price, $4.25

Special price to Fellows and Members of GSA, $3.00

MEMOIR IN PRESS

83. Biostratigraphic Studies in the Comanche (Cretaceous) Series of Northern Mexico and Texas. Bob F. Perkins

The author relates the biostratigraphy of the Aurora limestone of southwestern Coahuila to the type Aurora and to the type Lower Cretaceous of northern Texas and reports stratigraphic revisions of the Fredericksburg and Washita groups of north Texas. He describes a fauna of larger invertebrates from the upper member of the Aurora and on paleontological evidence correlates the member with the Fort Worth limestone and Grayson marl. He concludes that the Aurora limestone is of epineritic origin, deposited far from any source of terrigenous clastic material.

About 140 pages, 29 figures, 3 maps in color, 29 photographic plates

Expected date of issue February 25

Pre-publication price $5.25; post-publication price $6.00. Special price to Fellows and Members of GSA $4.50

KARL K. TUREKIAN *Dept. Geology, Yale University, New Haven, Conn.*
KARL HANS WEDEPOHL *Mineralogische-Institut der Universitat, Göttingen, Germany*

Distribution of the Elements in Some Major Units of the Earth's Crust

Abstract: This paper presents a table of abundances of the elements in the various major units of the Earth's lithic crust with a documentation of the sources and a discussion of the choice of units and data.

CONTENTS

INTRODUCTION

Several tables of the crustal abundances of the elements have been published to date (Rankama and Sahama, 1950; Goldschmidt, 1954; Fleischer, 1953; Vinogradov, 1956; Mason, 1958) either as parts of treatises on the geochemistry of the elements or as attempts to compile a list for general use. In addition, Green (1959) and Vinogradov (1956) have published charts of the distribution of many elements in various units of the Earth's crust.

We have found these tables deficient in some aspects. This awareness arose when the two of us independently were preparing articles on the geochemical distribution of the elements for the *Encyclopedia of Science and Technology* published by McGraw-Hill (Turekian, 1960) and for the new edition of *Lehrbuch der Geologie, Teil I.* by E. Kayser and R. Brinkmann, to be published by F. Enke, Stuttgart (Wedepohl).

The individual tables in these two works have been modified and collated here (Table 2) with a fuller description of the plan used in compiling the data since a brief summary article of the sort required for the encyclopedias offered no possibility of presenting the sources of information used.

Any compilation is necessarily subject to great uncertainties in the reliability of the analytical work, the sampling, and the interpretations, both of the original investigator and the compiler. Hence the accompanying table should be accepted not so much as a doctrine but as a motion on the floor to be debated, and amended or rejected.

CHOICE OF UNITS

General Statement

With the wide diversity of rock types available for sampling in the Earth's crust the choice of units for a compilation must to some degree be arbitrary. We have chosen three major groups for the presentation of the data, "igneous" rocks, sedimentary rocks, and deep-sea sediments.

"Igneous" Rocks

Under this heading we include some ultrabasic rocks and all basaltic rocks as being of undoubted igneous origin. Granitic and syenitic rocks, even though they do not all show unequivocal evidence for igneous origin, are included under "igneous" rocks for the sake of simplicity.

Peridotitic rocks were chosen whenever pos-

Geological Society of America Bulletin, v. 72, p. 175–192, February 1961

sible to represent the ultrabasic group. Ultrabasic rocks with unusual metamorphic histories were generally avoided in compiling the trace-element data. Serpentines were also avoided because several elements (boron, arsenic, and germanium, *etc.*) are notably enriched in these altered rocks relative to dunites and peridotites.

The basaltic rocks include all manifestations of rocks of basaltic composition, *i.e.*, gabbros, dolerites, and basalts. Concentrations of some elements show differences between the intrusive and the extrusive or hypabyssal representatives. In only a few cases were the differences significant in terms of the information available. In those cases the extrusive and hypabyssal rocks were weighted more heavily than the intrusive rocks to arrive at the figure in Table 2.

The granitic rocks afford some difficulty in classification. All rocks associated with a granitic terrane are considered granitic rocks although local or wider variations yield a variety of rock types such as granodiorite, quartz monzonite, *etc.* With such a wide variety of possibilities in rock types and the vagaries of meaning of some of the nomenclature presented in the literature, we decided that two categories of granitic rocks were all that were practical for the present compilation. Under the bias of a previous such consideration necessary in evaluating the geochemistry of strontium (Turekian and Kulp, 1956), we have chosen the groups in terms of their expected calcium concentrations, *viz.*, high-calcium granitic rocks with a mean gross chemical composition of a granodiorite, and low-calcium granitic rocks with a composition approaching that of an ideal granite. This choice is arbitrary. The presented data are just not any better than this gross classification.

According to the experience of field geologists, granites, granodiorites, and basaltic rocks are by far the most common rock types. We include the syenites as a type in spite of their subordinate abundance. We have generally tried to weight the values toward the syenite rather than the nepheline syenite end because the latter type is the rarer.

In the case of the granitic and syenitic rocks we have avoided using their extrusive equivalents in computing the averages. For several trace elements the extrusive acidic rocks are very different in their abundance from the intrusive chemical equivalent. Rhyolites have variable and perhaps unusual affinities.

Sedimentary Rocks

The standard breakdown of sedimentary rocks is into shales, sandstones, and carbonate rocks as end members, and other rocks as mixtures of these. This classification is based on sequences associated with Kay's (1951) miogeosynclinal areas where reasonably thorough chemical degradation of the original source rock is supposed to have occurred. There are, of course, vast amounts of sedimentary rocks which are composed to a large degree of poorly sorted more or less degraded minerals, *viz.*, conglomerates, arkoses, and graywackes. These rocks represent a great problem in the presentation of data on sedimentary rocks. It is not possible to dismiss them as the mechanical degradation products of weathering and sedimentation since in these processes a chemical differentiation from the original rocks must have taken place. However, because of the great complexity of these rock types and an uncertainty as to their manner of origin they are not included in the accompanying table. It must be noted that this is an omission because of lack of information rather than because of unimportance. Macpherson (1958) reports that Canadian Precambrian argillites and low-grade schists have the same composition for many trace elements as associated graywackes. In addition, Weber's (1960) data seem to indicate that a wide range of graywackes have similar composition with regard to most of the trace elements (zirconium seems to be an exception).

Deep-Sea Sediments

Deep-sea sediments cannot rightly be classified under the term "rock" since much of the sampling is done on material which exists permeated continuously by sea water and has not yet been subjected to lithification or extreme diagenesis.

Two end members only are considered: the pelagic clay, essentially free of calcium carbonate; and the carbonate-rich sediment in its purest sampled form containing about 10 per cent clay fraction. Further, following Goldberg and Arrhenius (1958), we assume that the dissolved solids in the water permeating the sediment are part of the sediment rather than of the hydrosphere. This means that analyses on unwashed samples are preferred. Estimating the abundance of several of the elements in the deep-sea material is complicated by the fact that their concentration is greater in the Pacific sediments than in the Atlantic. Although the Pacific is roughly three times larger than the Atlantic in area, the rate of sedimentation may be about three times greater in the Atlantic basin (Wedepohl, 1960) than in the Pacific. This being the case, where the above disparity is observed, a simple average of the Atlantic and Pacific values was used for the abundance table.

Metamorphic Rocks

We have assumed that metamorphic rocks generally retain a chemical composition similar to their unmetamorphosed equivalent. However, often a schist is sampled free of quartzofeldspathic segregations. In such a case the schist will be higher than the original rock in the concentrations of the elements associated with the mafic minerals. The whole rock, however, will probably show the composition of the original unmetamorphosed rock. Where metamorphism grades into granitization, the granitized rock is placed in the chemical category of granitic rocks, hence not treated separately.

CHOICE OF DATA

Generally the newest information was used to construct the table whenever available. Much new work has been done on the trace elements since the end of World War II and particularly since 1950.

The following is an element-by-element discussion of the sources of the information of Table 2. We have deliberately used the first person in writing because the table represents solely our judgement in compilation. There is always the risk that when such a table is published the sources and uncertainties in it may be forgotten and "the table" quoted uncritically. This must be avoided.

Lithium: The data are primarily from Horstman (1957). However, his ultrabasic value of 26 ppm is not used since it is considerably higher than that of Strock (1936), who gives 2 ppm, and that of Pinson, Ahrens, and Franck (1953), who give <0.3 ppm. The value for carbonates is an upper limit, and the value of carbonate deep-sea cores is based on the assumption that even the purest pelagic calcareous cores have approximately 10 per cent clay fraction which contributes the lithium.

Beryllium: The data for granitic and basaltic rocks are taken from Sandell (1952). Merrill, Honda, and Arnold (1958) report 3.3 ppm for G-1 standard granite and 0.68 ppm for W-1 standard diabase. The nepheline syenite value is from Borodin (1956). This is lower than the concentrations given by Goldschmidt (1954) and Holser *et al.* (1951). Merrill *et al.* (1960) have analyzed four pelagic clay cores from the Pacific and one from the Atlantic and find very small variations in the beryllium concentration. Their average of 2.6 ppm is used here. Other data appearing in the literature for pelagic clays range from 1.1 ppm (Goel *et al.*, 1957) to 8 ppm (Tatsumoto, 1957). Since the beryllium concentrations of the Atlantic and Pacific pelagic sediments are not different, although the Atlantic and Pacific have different accumulation rates, we assume that the beryllium is closely associated with the clay minerals. Hence we have assumed that shales will have the same composition as pelagic clays rather than the 6 ppm reported by Goldschmidt (1954).

Goldschmidt's data seem high for this element in all rock types compared to the current data. The sandstone, carbonate, and carbonate deep-sea sediment data are lacking, but probably the abundance in each rock type is of the order of tenths of parts per million.

Boron: The ultrabasic, basaltic, granitic, and syenitic values are from Harder (1959a; 1959b). The granitic rocks present some problems of interpretation. Sahama's (*See* Rankama and Sahama, 1950) low values (3–10 ppm) for Fennoscandian rocks may be compared to Wasserstein's (1951) values for some South African granites which run up to 150 ppm. Okada (1955; 1956) found boron concentrations in Japanese granitic rocks ranging from 1 to 160 ppm. Since boron is a highly mobile element during metamorphic and igneous activity, the wide range of values may be expected. Granitic rocks from roof areas of intrusive rocks and granitic migmatites generally have higher concentrations of boron. Degens, Williams, and Keith (1957) and Harder give an average value for shales of 100 ppm. The deep-sea clay value is the average of the boron content of Pacific clays (Goldberg and Arrhenius, 1958) and Atlantic clays analyzed by Harder (1959b). The carbonate deep-sea sediment value is based on a few analyses of Atlantic material made by Harder, and the sandstone and carbonate rock values are also his.

Nitrogen: There are two current sets of determinations of the nitrogen content of some igneous rocks. F. Wlotzka (1960, Ph.D. thesis, Göttingen Univ.) reports about 30 ppm for basaltic rocks and 20 ppm for granitic rocks. R. S. Scalan (1959, Ph.D. thesis, Univ. of Arkansas), in studying the isotope geochemistry of nitrogen, determined the composition of a number of ultrabasic (average 6 ppm) and basaltic (average 17 ppm) rocks. Because of the wide range of values within each rock type we have chosen a value of 20 ppm for each igneous rock except for ultrabasic rocks, for which Scalan's average of 6 ppm is used, and syenites, for which Wlotska's average of 30 ppm N is used. Both investigators indicate that the main form of the nitrogen is as the NH_4^+ ion.

Since sediments have greatly variable nitrogen concentrations, mainly a function of the organic content of the sediment, these estimates are not included in the table.

Fluorine: Most of the values in Table 2 are from Koritnig (1951) as modified in the following cases by information from other workers. R. H. Seraphim (1951, Ph.D. thesis, Mass. Inst. of Technology) and Kokubu (1956) list 820 ppm and 830 ppm respectively for granitic rocks they analyzed; this agrees closely with Koritnig's value. On the other hand Kokubu (most of whose rocks were Japanese) found a low value of 280 ppm for basaltic rocks, whereas Seraphim reported a value of 540 ppm, which is higher than Koritnig's. Koritnig's value of 520 ppm for granodioritic rocks is used, although the average of alkali granitic and dioritic values of other authors leads to a higher value. The syenite value is the average of Koritnig's (950 ppm) and Seraphim's (1480 ppm) values. The carbonate value is the average of Koritnig's limestone and dolomite analyses. Kokubu reports considerably lower values for limestones (100 ppm). The values for deep-sea sediments are taken from Seraphim. They are based only on Atlantic Ocean sediments. Shepherd's (1940) figures on sediments from the Pacific (clay, 660 ppm) seem too low.

Sodium: The igneous-rock data except basalt are from Nockolds (1954), using the averages for alkali granite (his Table 1, column III), granodiorite (Table 2, column III), peridotite (Table 9, column I), and alkali syenite (Table 3, column IV). The basaltic value is an average of Green and Poldervaart's (1955) compiled mean tholeiitic and mean olivine basaltic rock. The sedimentary-rock data are Clarke's (1924). The deep-sea sediments provide some difficulty since all the cores are rich in sodium chloride derived from interstitial sea water. Goldberg and Arrhenius (1958) present compelling reasons for accepting the bulk composition of the core, including the interstitial salts, as representative of the sediment, and this is done in the table. The data for pelagic clays are from Goldberg and Arrhenius (1958). The data for the carbonate deep-sea cores are more difficult to obtain. Broecker, Turekian, and Heezen (1958) report an average of 5 per cent NaCl in dry, unleached carbonate core material. This corresponds to a sodium concentration of around 20,000 ppm and a chlorine concentration of 30,000 ppm. The highest-carbonate core reported by Goldberg and Arrhenius (1958) has 16,000 ppm Na.

Magnesium: Igneous-rock data are from Nockolds (1954) and Green and Poldevaart (1955), as above. Sedimentary-rock data are from Clarke (1924). The pelagic-clay value is from Clarke (1924) and Goldberg and Arrhenius (1958). Carbonate deep-sea-core data are from P. J. Wangersky (1958, Ph.D. thesis, Yale Univ.) and Turekian and Feely (1956), who agree very well for Atlantic Equatorial cores.

Aluminum and silicon: Igneous-rock data are from Nockolds (1954) and Green and Poldevaart (1955) as above; sedimentary-rock data from Clarke (1924); pelagic clay from Goldberg and Arrhenius (1958); and carbonate deep-sea-core data from the analysis of Atlantic Equatorial Core A180–74 by P. J. Wangersky (1958, Ph.D. thesis, Yale Univ.).

Phosphorus: The igneous-rock data are from Nockolds (1954) and Green and Poldevaart (1955) as described above. The sandstone and carbonate-rock data are from Koritnig (1951). The shale value is the average previously reported by Wedepohl (1960).

Correns (1937) reports 1500 ppm for Atlantic pelagic clays, which is probably a minimum for these sediments. He also found that clay-free calcareous sediments from the Atlantic had about 350 ppm phosphorus. We use his values for deep-sea sediments.

Sulfur: Because of the various possible forms of sulfur incorporation in geological materials, it is difficult to assess the significance of the various data reported in the literature on this element. The earliest paper giving a large amount of data on sulfur in igneous rocks is by Tröger (1934) and is that used in the compilation by Rankama and Sahama (1950) and others. Sandell and Goldich (1943) report three values for sulfur in Minnesota rocks ("granite," "diorite," and "diabase"), which have a range of 200 to 400 ppm with no obvious relationship to rock type, and two diabases from New England with a value of 1200 ppm. Ricke (1960, in press) reports about 270 ppm S for granites and 250 ppm S for basalts. He found that olivine contains about 30 ppm sulfur, but since ultrabasic rocks have a variable sulfide component this number cannot be used with certainty. Ricke also reports 400 ppm S for granodioritic rocks and 440 ppm S for syenites. Although one of us (Wedepohl) feels that these numbers represent the abundance of sulfur in the various igneous-rock types, we have assigned a common value for all "igneous" rock types, *viz.* 300 ppm S, because it may be that the variations within the rock types in a wider sampling would exceed that between units. One of us (Turekian) believes that this value based on Ricke's data probably has only order of magnitude reliability, but even then it is lower than some of Tröger's values.

The information on sediments and sedimentary rocks is in no better shape. Clarke (1924) reports an average value of 2600 ppm for shales, whereas Ricke (in press) gets an average of 2200 ppm for his sampling. Higher values have been reported by Tourtelot (1957) for the Pierre shale (5500 ppm) and by other authors (including Minami, 1935a; Vinogradov and Ronov, 1956) for carbonaceous shales. We choose the average of Clarke's and Ricke's values for all the sedimentary-rock types. Information on the sulfur concentration of deep-sea sediments is from Edgington and Byers (1942). Ricke got essentially the same value for pelagic clays. The sulfur concentration is obviously that of sea-salt contribution to the sediment.

Chlorine: Correns (1956) has recently compiled the available data on the halogens.

The ultrabasic value is the average of the anhydrous dunite analysis by Kuroda and Sandell (1954). These authors give a wide range of values for igneous rocks with averages all about 200 ppm for the various rock types, except syenitic rocks. We have used the data of Behne (1953), however, for all the rock types except the ultrabasic and syenitic. The deep-sea-sediment data are contingent on the arguments presented under sodium. However, the clay fraction probably has some sodium in excess of the stoichiometric amount necessary to balance the chloride. Behne reports 21,000 ppm chlorine for pelagic clays. The same value is assumed for the carbonate sediments.

Potassium: We have chosen the low average value of Holyk and Ahrens (1953) for ultrabasic rocks. Nockolds (1954) gives an average of about 2000 ppm K, but this may either include mica or feldspar-rich ultrabasic rocks such as kimberlite or include analyses erroneously high in potassium. The remaining igneous-rock data are from Nockolds (1954) and Green and Poldervaart (1955); sedimentary-rock data are from Clarke (1924). The pelagic-clay value is from Goldberg and Arrhenius (1958). The deep-sea carbonate value is based on the assumption that the potassium is in the 10 per cent clay fraction plus about 400 ppm K in the soluble salts.

Calcium: Igneous-rock data are from Nockolds (1954) and Green and Poldervaart (1955); sedimentary-rock data from Clarke (1924), whose sandstone average may be high; pelagic-clay data from Goldberg and Arrhenius (1958); carbonate deep-sea-sediment data from Turekian and Feely (1956) and P. J. Wangersky (1958, Ph.D. thesis, Yale Univ.) who have similar results on Atlantic Equatorial cores.

Scandium: The ultrabasic value is from Pinson, Ahrens, and Franck (1953). Both Nockolds and Allen (1956) and Ahrens (1954) report mean values in basaltic rocks of about 30 ppm. The data for low-calcium and high-calcium granitic rocks are from Ahrens (1954). He reports a value of 11 ppm for granites. If these granites can be regarded as a one-to-one mixture of low-calcium and high-calcium granitic rocks, as seems likely, and if the Sc is greater by a factor of two in the more calcic granitic rocks than in the low-calcium granitic rocks, then low-calcium granitic rocks have 7 ppm and high-calcium granitic rocks have 14 ppm Sc; Sahama (1945) reports 1 ppm Sc for Finnish granites and Hügi (1956) 12 ppm Sc for Swiss granites. The Sc content of syenitic rocks given is that of Sahama (1945) for Finnish rocks which compares with the analysis of an Arkansas nepheline syenite (Gordon and Murata, 1952). The shale value is from Wedepohl (1960); it compares with that of Shaw (1954) for the Littleton formation primarily. The pelagic-clay value is the average of Pacific and Atlantic values from Goldberg and Arrhenius (1958) and Wedepohl (1960) respectively. The carbonate deep-sea-core value is based on a 10 per cent red-clay fraction contributing the Sc. The value for sandstones is Sahama's (1945) quartzite average, and that for limestones is guessed at, assuming that they contain approximately 10 per cent clay.

Titanium: The igneous-rock data are from Nockolds (1954) and Green and Poldervaart (1955). Sandstone and carbonate-rock data are from Clarke (1924). The shale value is the average used by Wedepohl (1960). The pelagic-clay value is the average of the figures given by Wedepohl (1960) and Goldberg and Arrhenius (1958), and the deep-sea carbonate sediment value is from P. J. Wangersky (1958, Ph.D. thesis, Yale Univ.).

Vanadium: The ultrabasic value is derived from the data of Ross, Foster, and Myers (1954), who list values for vanadium in separated minerals from ultrabasic rocks. Using a ratio of 60 per cent olivine, 20 per cent enstatite, 10 per cent chrome diopside, and 10 per cent plagioclase we arrive at 40 ppm V. The value for basaltic rocks is from an average of all basaltic rocks (72) analyzed by Nockolds and Allen (1956). This figure corresponds with a one-to-one average of tholeiitic basalts (330 ppm V) and olivine basalts (140 ppm V) from unpublished results of Wedepohl. The granitic values are derived from Ahrens (1954), using the same assumptions as those used to derive the scandium numbers. Hügi (1956) gets 80 ppm V for granitic rocks of the Aare-massiv. For syenitic rocks Sahama (1945) reports 30 ppm V; Butler (1954) got less than 10 ppm in one sample. Gordon and Murata (1952) list a value of 47 ppm for an Arkansas nepheline syenite. We choose 30 ppm for this rock type.

The shale value is from Wedepohl (1960); it corresponds with Jost's (1932) and Shaw's (1954). Degens, Williams, and Keith (1957) report a lower value for Carboniferous shales of Pennsylvania (44 ppm). The data for sandstones and limestones are from Goldschmidt (1954), who quotes the data of Jost primarily. The limestone value agrees with the average of eight British limestones analyzed by Hirst and Nicholls (1958). The pelagic-clay value is from Goldberg and Arrhenius (1958) and Wedepohl (1960). The carbonate deep-sea-sediment value lies between 1 and 3 ppm V (Wedepohl, 1955); hence we choose an average of 2 ppm.

Chromium: The ultrabasic value for chromium is derived from the data in Ross, Foster, and Myers (1954). These authors give chromium values for separated minerals from ultrabasic rocks. There is not much variation for any one mineral type. We again use the arbitrarily defined ultrabasic rock of the following mineralogic composition: 60 per cent olivine, 20 per cent enstatite, 10 per cent chrome diopside, and 10 per cent plagioclase. The resulting value of 1600 ppm Cr may be too low if chromite is a very important accessory. A single analysis of a dunite by activation analysis reported by Turekian and Carr (1960), however, confirms this low value. The basalt value is from Turekian (1956). Fröhlich (in press) reports 70 ppm for tholeiitic basalt and 280 ppm for olivine basalt. The low-calcium granitic value is from Turekian and Carr (1960) based on neutron activation analyzed rocks. The high-calcium value has been changed from our previous 27 ppm Cr reported in the paper just cited to 22 ppm Cr as the result of additional work to be published soon. These numbers are lower than those of Ahrens (1954). The syenitic rock value is from Gordon and Murata (1952) and Butler (1954). The shale value is an average of the data of Shaw (1954), Fröhlich (in press), and Turekian (unpublished). Fröhlich reports an average of 15 ppm Cr for 98 limestones, whereas Turekian and Carr (in press) find an average of 11 ppm for three carbonate rocks analyzed by neutron activation and Hirst and Nicholls (1958) report an average of 8 ppm for eight British limestones by a spectrographic technique. We use the average of these three sets of data, 11 ppm Cr. The sandstone value of 35 ppm Cr is the average of Fröhlich's 53 sandstone and quartzite samples. Turekian and Carr (in press) report an average of 7 ppm Cr for two determinations by neutron activation. The pelagic-clay value is from Goldberg and Arrhenius (1958) and Fröhlich (1959), and the carbonate deep-sea-sediment value is from Turekian and Feely (1956).

Manganese: The igneous-rock data are from Nockolds (1954) and Green and Poldervaart (1955). The shale value is the average of the values reported by Shaw (1954), Tourtelot (1957), and Wedepohl (1960). Ostrom (1957) reports an average of 1400 ppm Mn for Carboniferous limestone samples from Illinois, and Runnels and Schleicher (1956) report an average of 850 ppm Mn for some Kansas limestones. We use these two values to arrive at an average of 1100 ppm Mn, which is higher than most previous estimates. The sandstone order-of-magnitude value is a guess. The pelagic-clay value is from Goldberg and Arrhenius (1958) and Wedepohl (1960), and the carbonate deep-sea-sediment value is from P. J. Wangersky (1958, Ph.D. thesis, Yale Univ.). Both Correns (1937) and Wedepohl (1955) report that the clay-free deep-sea carbonate tests contain about 200 ppm Mn.

Iron: The igneous-rock data are from Nockolds (1954) and Green and Poldervaart (1955); the sedimentary-rock data are from Clarke (1924); the pelagic-clay value is from Goldberg and Arrhenius (1958); and the carbonate deep-sea-sediment value is from P. J. Wangersky (1958, Ph.D. thesis, Yale Univ.).

Cobalt: Most of the values are from Carr and Turekian (in press), who used a combined neutron-activation and spectrographic technique to analyze a large number of specimens. The ultrabasic value is similar to the value obtained from the weighted average of ultrabasic mineral analyses by Ross, Foster, and Myers (1954) in the manner described under chromium. The basaltic-rock value agrees with the average of 72 basaltic rocks by Nockolds and Allen (1956), Ahrens' (1954) value for North American rocks, and Smales, Mapper, and Wood's (1957) value for oceanic islands. From Sandell and Goldich's (1943) data, 13 low-calcium granitic rocks give an average of 2.7 ppm, whereas two high-calcium granitic rocks give an average of 5.8 ppm. The syenite value is a guess based on Gordon and Murata's (1952) data. The shale value is similar to that of Shaw (1954). Hirst and Nicholls (1958) find an average of 10 ppm for eight British limestones, which we consider too high. The pelagic-clay value is an average of high values for the Pacific and low values for the Atlantic (Goldberg and Arrhenius, 1958; Smales, Mapper, and Wood, 1957; Hutchinson *et al.*, 1955; Wedepohl, 1960). If the carbonate deep-sea-sediment value is based on a 90 per cent $CaCO_3$ Atlantic Equatorial core, a calculation from the data of Smales, Mapper, and Wood (1957) on a 67 per cent $CaCO_3$ Atlantic Equatorial core containing an average of 11 ppm Co will give 4 ppm, which compares with the value of 6 ppm obtained by Carr and Turekian (in press) for deep-sea carbonate sediments.

Nickel: The ultrabasic value was gotten in the manner described under chromium from the data of Ross, Foster, and Myers (1954). The basaltic value is from Turekian (1956). The granitic-rock values are derived from Sandell and Goldich's (1943) data on 13 low-calcium granitic rocks and two high-calcium rocks. The syenite value is a guess based on the few scattered data on this rock type (Sahama, 1945; Butler, 1954; Gordon and Murata, 1952). The shale value is the intermediate between Shaw's (1954) average of 64 ppm and Turekian and Carr's (1960) average of 71 ppm. The sandstone value is from Sahama's (1945) data on Finnish quartzites. Hirst and Nicholls (1958) report an average of 27 ppm Ni in eight limestones. Runnels and Schleicher (1956) report 10 ppm for some limestone from Kansas, and Wedepohl reports (unpublished) 25 ppm on a limestone composite made by Goldschmidt. A value of 20 ppm is chosen for limestones considering these data. The nickel values in pelagic-clay and carbonate deep-sea sediments are based on the same type of argument used for cobalt, and the values derived are from the same sources.

Copper: The ultrabasic value is based on a dunite from St. Paul's Rock in the Atlantic Ocean analyzed by Smales, Mapper, and Wood (1957) by neutron activation. Two peridotites of Morita (1955) have Cu up to 20 ppm. The basalt value is from Turekian (1956) and corresponds with that of Morita for Japanese rocks. The granitic values are derived from several scattered sources and represent the best estimate possible from the manner in which the data are reported. The sources are: Sandell and Goldich (1943), North American granitic rocks; Sugawara and Morita (1950) and Kuroda (1957), Japanese granitic rocks; and Smales (1955), analysis of G-1 granite. The syenite value is a guess.

The shale value is the average of six sets of data: Shaw (1954), Littleton formation, Devonian, 18 ppm; Degens, Williams, and Keith (1957), Carboniferous shales of Pennsylvania, 73 ppm; Turekian (unpublished), Fox Hills formation, Cretaceous, 18 ppm; Sugawara and Morita (1950), Mesozoic of Japan, 55 ppm, Paleozoic of Japan, 40 ppm, and Paleozoic of Europe, 65 ppm—all composites. Heide and Singer (1950) report 105 ppm for the Röt shale of Jena. No data are available for sandstones. The × indicates the probable order of magnitude for sandstones. The limestone value is from three composites (93 samples) of German limestones of Paleozoic and Mesozoic age (Wedepohl, 1955) averaging 2 ppm Cu and from data on the calcareous portions of rocks from the Hanover mining district, New Mexico, reported by Barnes (1957) with 5 ppm Cu. Heide and Singer (1950) report 5 ppm for the Muschelkalk limestone of Jena.

The deep-sea-clay and -carbonate data are from the same sources as cobalt and nickel, and the same method of calculation is used.

Zinc: The igneous-rock data are from Wedepohl (1953 and unpublished), Sandell and Goldich (1943), Morita (1955), and Tauson and Pevtsova (1955), and agree in general with each other quite well. The syenite value is from

Morita. The shale value is from Wedepohl (1960). Sugawara and Morita (1950) report an average of 110 ppm on the same composites used in the copper determination; Heide and Singer (1950) report a value of 103 ppm for the Röt shale of Jena, and Barnes (1957) reports 70 ppm for limeless shales near Hanover, New Mexico. The sandstone value is from Wedepohl (1953), and the limestone value is the average of Wedepohl's and Barnes' data. The pelagic-clay value is from Wedepohl (1960), and that for the deep-sea carbonate is from unpublished data by the same author.

Gallium: Sandell (1949) reports 1 ppm Ga for ultrabasic rocks, whereas Borisenok and Saukov (1960) report an average of 2 ppm. We have used the average of these two values. The data of the different workers on the Ga concentration of the other igneous rocks agree on the whole, but subtle differences exist. For basaltic rocks Borisenok and Saukov report 15 ppm Ga, and C. K. Bell (1953, Ph.D. thesis, Mass. Inst. of Technology) reports 17 ppm Ga, whereas Fleischer's (1955) average of a large number of data from different workers on rocks ranging in 45–55 per cent SiO_2 is 20 ppm Ga. We choose the average value of 17 ppm Ga for basalts. For high-calcium granitic rocks Borisenok and Saukov report 16 ppm, whereas Bell reports 17 ppm and Fleischer reports 20 ppm as an average of rocks ranging from 55–65 per cent SiO_2. We use a value of 17 which is similar to the basaltic value. The low-calcium granitic rock values range from 16.5 ppm (Fleischer's average for rocks with greater than 65 per cent SiO_2) to Bell's 17 ppm, to Borisenok and Saukov's 19 ppm. We choose 17 ppm Ga for this rock type. The syenitic rocks range from 20 ppm (Bell) to 40 ppm (Borisenok and Saukov), and we choose a value of 30 ppm.

The shale value is from Bell, Shaw (1954), and Wedepohl (1960), who find the same average value. Bell reports an average of 14 ppm Ga for four sandstones and 6 ppm for a quartzite, giving an average of 12 ppm. The limestone value and the carbonate deep-sea core value are from estimates in Goldschmidt (1954). Borisenok and Saukov report 10–30 ppm Ga for "marine oozes." The pelagic-clay value is from Goldberg and Arrhenius (1958) and Wedepohl (1960).

Germanium: The data are from El Wardani (1957) and Onishi (1956), who generally agree. El Wardani gives about 1.2 ppm for shales, whereas Onishi (1956) gives 2 ppm. We have chosen an intermediate value. The limestone and carbonate deep-sea-sediment values are calculated on the basis of 10 per cent clay fraction. Pure *Globigerina* tests have 0.0 ppm Ge (El Wardani, 1958). The pelagic-clay average is that of El Wardani; Onishi reported 1.6 ppm Ge.

Arsenic: The data for arsenic are all from Onishi and Sandell (1955a). They report that silicic volcanic rocks and serpentines have about 4 ppm As, which is considerably higher than the value for the usual igneous-rock types. Correns (1937) reports 7 ppm As for six samples of Atlantic pelagic clay.

Selenium: The values of all units except the sediments are calculated from the sulfur abundances using a S to Se ratio of 6000, reported by Goldschmidt and Strock (1935) and Goldschmidt (1954), and have order of magnitude of significance only. The shale value is from Minami (1935a). Sandstone and limestone values are those of Goldschmidt and Strock (1935). The deep-sea-sediment values are from Edgington and Byers (1942).

Bromine: The data are all from Behne (1953). Assuming that all the bromine of the deep-sea sediments is in the sea salt (*Globigerina* shell sample $\leqslant$ 1 ppm Br) for the deep-sea carbonate, we have also used Behne's pelagic clay value.

Rubidium: The ultrabasic value is calculated to give a Rb/K ratio the same as in basalts. All the other igneous-rock values and the shale and sandstone values are from Horstman (1957). Isotope-dilution analyses of composite basalts and granitic rocks by Gast (1960) give very close to the same values. The carbonate deep-sea-sediment value is from Smales and Salmon (1955) and Horstman (1957), and the pelagic-clay value is from Wedepohl (1960) and Horstman (1957) and an extrapolation of Smales and Salmon's (1955) data on deep-sea-carbonate-sediment samples with varying amounts of clay.

Strontium: The ultrabasic value is based on the data of Pinson, Ahrens, and Franck (1953); the pelagic-clay value is from Goldberg and Arrhenius (1958) and Wedepohl (1960) for carbonate-free sediment. All other values are from Turekian and Kulp (1956).

Yttrium: The data for yttrium will influence the values for the rare-earth elements, since little or no information is available for most of the rare-earth elements in the common rock types.

The ultrabasic yttrium value is not known but is probably of the order of tenths of a part per million. The basaltic value is from 72 basaltic rocks reported by Nockolds and Allen (1956). A confirmatory unpublished value for a one-to-one average of olivine basalts and tholeiitic basalts is 25 ppm Y (Wedepohl). The granitic values are from Fleischer's (1955) compilation, omitting the data of Laboratory #4 of his tables. The values are the average of the maximum and the minimum values he reports. Wedepohl (unpublished) gets 43 ppm Y for 17 German granites and G-1. The syenite value is an average of Wedepohl's 22 nepheline syenites and Butler's (1954) value for a Norwegian quartz-free syenite having 20 ppm Y. Gordon and Murata (1952) report a value of 130 ppm for an Arkansas nepheline syenite. The shale value is from Minami's (1935b) data. Wedepohl (1960) reports about the same figure. The sandstone value is a guess. Sahama (1945) reports a low value of 2 ppm for quartzite, but his figures for granites (<10 ppm Y) and syenites (<10 ppm Y) are also low. The reason such a high value was chosen is because most resistate deposits must contain a considerable amount of resistant rare-earth minerals. One can compare yttrium in this sense with zirconium, for which data are available. If we assume that the ratio of yttrium in sandstones relative to shales is the same as for zirconium, we get 40 ppm Y. Wedepohl's unpublished result for three limestone composites (93 samples) is 30 ppm Y. The pelagic-clay value is from Goldberg and Arrhenius (1958) and Wedepohl (1960). The carbonate deep-sea-sediment value is that of Wedepohl's unpublished data on the Atlantic.

Zirconium and hafnium: The data for all rock types except the deep-sea clays are from Degenhardt (1957). His values generally agree with those of other workers. The pelagic-clay value is from Goldberg and Arrhenius (1958) and Wedepohl (1960).

Very little information on the hafnium abundance in common rocks is available. We can, however, use the coherence of hafnium and zirconium as a method of estimating the hafnium content of rocks from the zirconium content. The Zr/Hf ratio varies in zirconium with the rock type. If zircon and the mafic minerals are the main carriers of both the zirconium and hafnium, and if the Zr/Hf ratio of coexisting zircon and the mafic minerals is the same, then a method of approximation is available to us. Gottfried, Waring, and Worthing (1956) and Kosterin, Zuev, and Shevaleevskii (1958) have determined the Zr/Hf ratio of zircon from various rock types. The only difference in the two sets of data is in syenitic rocks where Gottfried, Waring, and Worthing report a higher ratio. Table 1 gives an estimate of the hafnium content of the various rock types based on the Degenhardt and Kosterin, Zuev, and Shevaleevskii data.

Table 1.—Estimation of Hafnium Concentrations in "Igneous" Rocks

	ppm Zr (in rock) (Degenhardt)	Zr/Hf (in zircons) (Kosterin, Zuev, and Shevaleevskii)	ppm Hf (in rock)
Ultrabasic rocks	45	70	0.6
Gabbro	140	70	2.0
Granodiorite	140	60	2.3
Granite	175	45	3.9
Syenite	500	45	11.1
(Sedimentary rocks Zr/Hf = 58)			

Cooley *et al.* (1953) provide data which give a Zr/Hf average ratio of 44, indicating perhaps that most of their zirconium numbers were of granitic or syenitic affinity.

Niobium and tantalum: The igneous-rock data of Rankama (1944; 1948) generally agree with those of Znamenski (1957) except for the high-calcium granitic rocks. For these Rankama reports 3.6 ppm Nb and 0.7 ppm Ta for six Scandinavian dioritic rocks. Znamenski gets an average of 20 ppm Nb and 3.6 ppm Ta for this rock type, and we shall use his values. Grimaldi (1960) reports 22 ppm Nb for standard granite G-1 and 9.6 ppm Nb for standard diabase W-1. The sedimentary-rock and deep-sea-sediment data are from Rankama.

Molybdenum: The igneous-rock values are the averages of the data on each rock type reported by Kuroda and Sandell (1954) and Vinogradov, Vainshtein, and Pavlenko (1958). The latter's values, determined spectrographically on Russian rocks, are generally higher (except for ultrabasic rocks) than Kuroda and Sandell's, determined colorimetrically. Ishimori (1951) reports a value of 0.9 ppm Mo for the average of 10 Japanese basalts, which is comparable to the low value Kuroda and Sandell derived for basaltic rocks.

The sedimentary-rock data are from Kuroda and Sandell (1954). They also report 3 ppm Mo for both carbonate and clay deep-sea sediments. Goldberg and Arrhenius (1958), however, report 45 ppm for East Pacific pelagic-clay samples, and Wedepohl (1960) reports 9 ppm for Atlantic pelagic-clay samples. We use the average of these two last values, although we cannot explain the discrepancy with Kuroda and Sandell. We use Kuroda and Sandell's carbonate deep-sea sediment value, however.

Palladium: The few new data available are from Vincent and Smales (1956), who determined palladium by neutron activation. The granitic-rock values are probably of the order of magnitude indicated.

Silver: All the silver data, where numbers are listed, are from Hamaguchi and Kuroda (1959), who analyzed primarily Japanese rocks. The unpublished data of A. Kvalheim quoted by Goldschmidt (1954) appear to be too low. The high values for diabases from Ontario reported by Fairbairn, Ahrens, and Gorfinkle (1953) are probably characteristic of that region only and not applicable generally.

Cadmium: No data could be found for ultrabasic rocks, but the order of magnitude listed is probably correct. The igneous-rock data are from Sandell and Goldich (1943). Preuss (1940) got 0.2 ppm Cd for a granite composite and 0.3 ppm Cd for a shale composite. The deep-sea-sediment data are calculated from Mullin and Riley (1956). Their average of recent calcium carbonate shells is 0.035 ppm which we use for the limestone value although this is undoubtedly a lower limit since other contributing phases in a normal limestone have not been considered.

Indium: The data are from Shaw (1952b). However, there are some uncertainties here. The high-calcium granitic rocks have a value much lower than either the low-calcium granitic rocks or the basaltic rocks. Wager, Smit, and Irving (1958) report neutron-activation values for indium in W-1 standard diabase and the chill zone from the Skaergaard complex, Greenland, as 0.064 and 0.058 ppm respectively. These numbers are lower than the values chosen for the table.

Tin: The tin data are primarily from Onishi and Sandell (1957). The high-calcium granitic rocks were arbitrarily assigned a value of 1.5 ppm. Degens, Williams, and Keith (1957) give 3.2 ppm for the value of their Carboniferous shales, and Wedepohl (unpublished) finds a value of 5 ppm for shales. The value of Onishi and Sandell for shales (11 ppm) has been averaged with the above authors' to give the value in the table.

Antimony: The data are all from Onishi and Sandell (1955b). These authors were not completely satisfied with their results and claim they should be taken tentatively. In the absence of any later information these are the best estimates available.

Iodine: The estimates for all the rock types except the deep-sea-sediment data are based on the monograph "Geochemistry of Iodine" (Chilean Iodine Educational Bureau, 1956). The deep-sea-sediment data are based on the chlorine content of these sediments as inferred above and the I/Cl ratio of the sea (= 2.27 x 10^{-6}). These values may be too low, since there is a correlation of organic content of shales and iodine, so some of the iodine may be enriched in sediments relative to the sea.

Cesium: The cesium concentrations in ultrabasic rocks, limestones, and sandstones are not known except that they are all probably less than 1 ppm (Horstman, 1957). The granitic value is calculated from Gast (1960), who analyzed two granitic composites. From the values he obtained for Li and Sr, it appears that the composites could be resolved into one part low-calcium to one part high-calcium granitic rock with the assumed values listed to give the observed value of 3.2 ppm. Horstman (1957) reports 1 ppm Cs as an average of a composite of 66 samples. The syenite value is from the average of three syenitic rocks from East Greenland analyzed by Liebenberg (1956). The shale value is from Horstman. Canney's (1952) average seems to be rather high. The deep-sea data are from Smales and Salmon (1955). They report a value of 0.4 ppm for 90 per cent calcium carbonate sediment increasing to 1.5 ppm for the portion of the core analyzed which has 80 per cent $CaCO_3$. By extrapolation to 0 per cent calcium carbonate, a value of about 6 ppm is obtained. This compares with Horstman's (1957) value for a pelagic-clay composite. The basaltic value is the average of cesium values determined by Gast (1960) on three basalt composites by isotope dilution. Cabell and Smales' (1957) value for W-1 standard diabase (1.08 ppm Cs) agrees, whereas their value for the Skaergaard chilled marginal gabbro (0.10 ppm Cs) is low.

Barium: The value used for ultrabasic rocks is a single activation analysis of a dunite made by Hamaguchi, Reed, and Turkevich (1957); it is considerably lower than the 6 ppm reported by Pinson, Ahrens, and Franck (1953). Von Engelhardt's (1936) figures for olivine scatter around 1 ppm. Gast (1960) reports an average of 333 ppm for three basalt composites analyzed by isotope dilution. Hamaguchi, Reed, and Turkevich (1957) get 310 ppm for a single activation analysis of a Hawaiian basalt. The basaltic value from Nockolds and Allen (1956) for 72 basaltic rocks is 180 ppm, considerably lower. The granitic values are calculated from Gast's (1960) average granitic value of 620 ppm as described under cesium. The syenite value is the average of the values of von Engelhardt (1936) and of Sahama (1945). The shale value is the average of data from five different studies: Degens, Williams, and Keith (1957), Carboniferous shales, 450 ppm Ba; Tourtelot (1957), Pierre (Cretaceous) shale, 720 ppm Ba; Macpherson (1958), Precambrian graywackes, argillites, and low-grade schists, 440 ppm Ba; Shaw (1957), Littleton formation (Devonian) pelitic rocks, 580 ppm; and Wedepohl (1960) Japanese and European shales, 700 ppm. The limestone value is based on modern molluscan shells (Turekian and Armstrong, 1960). The sandstone value is a guess. Quartz generally has very low barium, but the presence of heavy minerals and $BaSO_4$ cement will raise the figure. We have assumed that von Engelhardt's values of 170 ppm Ba for sandstones and 120 ppm Ba for limestones are too high. The value for deep-sea clays from the Atlantic is 700 ppm (Wedepohl, 1960) and from the Pacific 4000 ppm (Goldberg and Arrhenius, 1958). The average of these values is used. The Pacific has a strong barium sulfate component either dispersed or in the form of concretions (Goldberg and Arrhenius, 1958). The carbonate deep-sea-sediment value is an unpublished result for four "*Globigerina* ooze" cores from the Atlantic (Wedepohl).

Lanthanum: The ultrabasic value is a guess. The basalt value is that for Ontario diabase from Fairbairn, Ahrens, and Gorfinkle (1953). For granites, Nockolds and Allen (1953), Sahama (1945), and Ahrens (1954) report about the same averages, around 55 ppm La. The granodiorite average is from Nockolds and Allen (1953). The same authors report (1954) 95 ppm La in trachytes, whereas Sahama (1945) got 50 ppm in syenites. An intermediate figure is used. Nepheline syenites are again much higher (Gordon and Murata, 1952).

Wedepohl checked Minami's (1935b) La determinations and found his shale averages too low (this concerns only the La values of his report, however). Wedepohl (1960) reports 92 ppm La as an average of shales, which we have used. The deep-sea-clay value is again a one-to-one average of that for Pacific (Goldberg and Arrhenius, 1958): 130 ppm, and Atlantic samples (Wedepohl, 1960) : 98 ppm. For the carbonate deep-sea-sediment, 10 per cent of the clay value is assumed.

Other rare-earth elements: The other rare-earth values for most of the rock types are based on the assumption that the ratio of each of the rare-earth elements to yttrium is the same as it is in shales as determined by Minami (1935b). Data on Ce, Pr, Nd, Sm, Eu, Gd, Tb, Dy, Er, and Yb in granites are reported by Sahama (1945). Except for a low cerium value of Sahama, there is a good agreement with our computed values. In pelagic clays from the Pacific, 100 ppm Nd and 12 ppm Yb could be estimated (Wedepohl, unpublished), also in close correspondence to our prediction. A few small deviations from our values result if one uses the considerations of Masuda (1957) as a base for the computations.

Tungsten: The ultrabasic value is from Vinogradov, Vainshtein, and Pavlenko (1958). The basaltic, granitic, and syenitic values are intermediate between the averages of these authors and those of Sandell (1946). In all but the syenitic rocks Sandell's values are lower. Jeffery (1959) reports 10 ppm for the average of alkali rocks from Uganda. We consider this too high for a general average for syenitic rocks. His average for granites, however, (undistinguished as to low or high calcium), 1.4 ppm, is comparable to the value we have chosen. The shale and sandstone values are the analyses made by Vinogradov, Vainshtein, and Pavlenko of composites of several thousand samples of these rock types prepared by Ronov. The limestone value is the average of seven analyses on African limestones by Jeffery. Unfortunately no data are as yet available for deep-sea sediments, and so order of magnitude guesses have been made.

Gold: The only recent data are neutron-activation determinations by Vincent and Crocket (1960) and Crocket, Vincent, and Wager (1958) on some ultrabasic rocks, basaltic rocks, and standard granite G-1. The values for these igneous-rock types are from their data. It is assumed that the gold content of all other rocks will be of the same order of magnitude, although Clarke (1924) reported 0.03 ppm Au for sandstones and 0.005–0.009 ppm for limestones.

Mercury: The values for the igneous rocks where any are listed and shales are averages of the determination of Stock and Cucuel (1934) and Preuss (1940) on the same composites of German rocks prepared by Goldschmidt. The two sets of values agree fairly well. The limestone value is the average of the determinations on the Muschelkalk by Stock and Cucuel (1934) (one analysis, 0.033 ppm Hg) and Heide and Böhm (1957) (average of several specimens, 0.048 ppm Hg). The latter authors also report 0.19 ppm for the underlying red shale ("Röt") near Jena. The sandstone value is from a single analysis by Stock and Cucuel. The other values are order of magnitude guesses.

Thallium: The data are from Shaw (1952a), Ishimori and Takashima (1955), and Preuss (1940). The reported value for ultrabasic rocks and syenites is from Shaw, that for basalts is the average of Shaw's (0.13 ppm), Ishimori's (0.3 ppm), and Preuss' (0.3 ppm) data. The granodiorite value is intermediate between Shaw's (0.43 ppm) and Ishimori's (1.0 ppm). For a composite of German granites, Preuss got 3 ppm. Shaw reports 3.1 ppm as an average for granites and Ishimori 0.9 ppm for Japanese granites, resulting in an average of 2.3 ppm Tl. Preuss and Ishimori get the same value for the same composite of European carbonaceous shales, 2 ppm Tl; Shaw reports a shale average of about 0.8 ppm. We use the average of these two. Canney (1952) reports a value of about 0.4 ppm Tl for shales. For Pacific pelagic clay Shaw reports 1.2 ppm Tl, whereas Atlantic clay has 0.42 ppm Tl. Reed, Kigoshi, and Turkevich (1958) report a value of 0.94 ppm Tl for a perthite from a granite and of 0.07 ppm Tl for a basalt using neutron activation. These numbers are slightly lower than Shaw's.

Lead: The ultrabasic value is based on the range ($\sim$0.1 to 0.01 ppm) reported by Tilton and Reed (1960). The rest of the data are primarily from Wedepohl (1956). The Atlantic pelagic clays have a value of 45 ppm (Wedepohl, 1960), the Pacific clays a value of 110 ppm. Goldberg and Arrhenius (1958) got 140 ppm for the Pacific. Hence again there are differences in the chemistry of the sediments of the two oceans. The average of the two is used. The carbonate deep-sea-sediment value is 10 per cent of the average pelagic-clay value as before. Turekian and Feely (1956) report a mean value of 4 ppm for an Atlantic Equatorial carbonate core. The granitic-rock data are confirmed by Ahrens (1954) for North American rocks of low-calcium and high-calcium granitic composition. Gordon and Murata (1952) report a value of 7 ppm for an Arkansas nepheline syenite. Shaw (1954) lists a value of 16 ppm for pelitic rocks, which compares with Wedepohl's data. Degens, Williams, and Keith (1957) on the other hand find 35 ppm for Carboniferous shales of Pennsylvania. Heide and Lerz (1955) report a value of 21 ppm for the Röt shale near Jena and 7.9 ppm for the Muschelkalk limestone.

Bismuth: Data for granites and shales are from Preuss (1940). Reed, Kigoshi, and Turkevich (1958), as a byproduct of their work on meteorites, have published Bi values for a perthite from a granite and a basalt (from the Snake River region, U.S.). These numbers are included in Table 2 on the premise that some idea of the possible value for the abundance of Bi in a rock type may be better than no idea. There are other values in the literature, but they all appear high. Preuss (1940), for example, reports 2 ppm Bi for a composite of German granites and 1 ppm Bi for shales. Brooks, Ahrens, and Taylor (1960) report a wide range of values for a variety of rocks in a preliminary report.

Thorium and uranium: The ultrabasic value for thorium is derived from the uranium value (which is used for this rock type) of a single dunite by Hamaguchi, Reed, and Turkevich (1957) and assuming a Th/U ratio of 4. These low values have also been found for chondrites. The basaltic and syenitic values are from Evans and Goodman (1941). The granite values are from Whitfield, Rogers, and Adams (1959). The shale and limestone values are from Adams and Weaver (1958) and the sandstone value from Murray and Adams (1958). The uranium value for deep-sea-clay sediments is derived from Starik *et al.* (1958). On a clay core from the southern part of the Indian Ocean they find an average of 1.3 ppm U.

For a core with about 40 per cent $CaCO_3$ these workers found the same value for uranium and a high value for thorium (13.5 ppm). Others have found very low concentrations of uranium in the carbonate fraction ($\ll$1 ppm U, W. S. Broecker, personal communication) indicating that the uranium value for average carbonate deep-sea sediments is the order of magnitude indicated in Table 2 rather than the high value mentioned above. Picciotto and Wilgain (1954) report an average of about 5 ppm Th for a Central Pacific pelagic-clay core. The average between this and the higher value obtained by Starik and his coworkers on Indian Ocean sediments serves as our choice for the abundance of thorium in pelagic clays. The carbonate deep-sea-sediment values for Th from the literature are widely divergent, and so we indicate only an order of magnitude estimate.

(1955)
ale near
k lime-

ales are
Turke-
vork on
s for a
om the
bers are
at some
lance of
no idea.
are, but
for ex-
osite of
shales.
eport a
cks in a

sic value
m value
a single
rkevich
4. These
ondrites.
m Evans
lues are
(1959).
n Adams
ne value
uranium
derived
ore from
ean they

t $CaCo_3$
alue for
um (13.5
concen-
fraction
nal com-
um value
nts is the
2 rather
Picciotto
of about
lagic-clay
he higher
orkers on
ur choice
gic clays.
alues for
livergent,
nagnitude

Table 2.—Distribution of the Elements in the Earth's Crust

(Expressed in parts per million)*

		"Igneous" Rocks					Sedimentary Rocks			Deep-Sea Sediments	
		Ultrabasic	Basaltic Rocks	Granitic Rocks High Calcium	Granitic Rocks Low Calcium	Syenites	Shales	Sandstones	Carbonates	Carbonate	Clay
1 Hydrogen	H	A	A	A	A	A	A	A	A	A	A
2 Helium	He	B	B	B	B	B	B	B	B	B	B
3 Lithium	Li	0.X	17.	24.	40.	28.	66.	15.	5.	5.	57.
4 Beryllium	Be	0.X	1.	2.	3.	1.	3.	0.X	0.X	0.X	2.6
5 Boron	B	3.	5.	9.	10.	9.	100.	35.	20.	55.	230.
6 Carbon	C	A	A	A	A	A	A	A	A	A	A
7 Nitrogen	N	6.	20.	20.	20.	30.	A	A	A	A	A
8 Oxygen	O	A	A	A	A	A	A	A	A	A	A
9 Fluorine	F	100.	400.	520.	850.	1200.	740.	270.	330.	540.	1300.
10 Neon	Ne	B	B	B	B	B	B	B	B	B	B
11 Sodium	Na	4200.	18,000.	28,400.	25,800.	40,400.	9600.	3300.	400.	20,000.	40,000.
12 Magnesium	Mg	204,000.	46,000.	9400.	1600.	5800.	15,000.	7000.	47,000.	4000.	21,000.
13 Aluminum	Al	20,000.	78,000.	82,000.	72,000.	88,000.	80,000.	25,000.	4200.	20,000.	84,000
14 Silicon	Si	205,000.	230,000.	314,000.	347,000.	291,000.	73,000.	368,000.	24,000.	32,000.	250,000.
15 Phosphorus	P	220.	1100.	920.	600.	800.	700.	170.	400.	350.	1500.
16 Sulfur	S	300.	300.	300.	300.	300.	2400.	240.	1200.	1300.	1300.
17 Chlorine	Cl	85.	60.	130.	200.	520.	180.	10.	150.	21,000.	21,000.
18 Argon	Ar	B	B	B	B	B	B	B	B	B	B
19 Potassium	K	40	8300	25,200.	42,000.	48,000.	26,600.	10,700.	2700.	2900.	25,000.
20 Calcium	Ca	25,000.	76,000.	25,300.	5100.	18,000.	22,100.	39,100.	302,300.	312,400.	29,000.
21 Scandium	Sc	15.	30.	14.	7.	3.	13.	1.	1.	2.	19.
22 Titanium	Ti	300.	13,800.	3400.	1200.	3500.	4600.	1500.	400.	770.	4600.
23 Vanadium	V	40.	250.	88.	44.	30.	130.	20.	20.	20.	120.
24 Chromium	Cr	1600.	170.	22.	4.1	2.	90.	35.	11.	11.	90.
25 Manganese	Mn	1620.	1500.	540.	390.	850.	850.	X0.	1100.	1000.	6700.
26 Iron	Fe	94,300.	86,500.	29,600.	14,200.	36,700.	47,200.	9800.	3800.	9000.	65,000.
27 Cobalt	Co	150.	48.	7.	1.0	1.	19.	0.3	0.1	7.	74.
28 Nickel	Ni	2000.	130.	15.	4.5	4.	68.	2.	20.	30.	225.
29 Copper	Cu	10.	87.	30.	10.	5.	45.	X.	4.	30.	250.
30 Zinc	Zn	50.	105.	60.	39.	130.	95.	16.	20.	35.	165.
31 Gallium	Ga	1.5	17.	17.	17.	30.	19.	12.	4.	13.	20.
32 Germanium	Ge	1.5	1.3	1.3	1.3	1.	1.6	0.8	0.2	0.2	2.
33 Arsenic	As	1.	2.	1.9	1.5	1.4	13.	1.	1.	1.	13.
34 Selenium	Se	0.05	0.05	0.05	0.05	0.05	0.6	0.05	0.08	0.17	0.17
35 Bromine	Br	1.	3.6	4.5	1.3	2.7	4.	1.	6.2	70.	70.
36 Krypton	Kr	B	B	B	B	B	B	B	B	B	B
37 Rubidium	Rb	0.2	30.	110.	170.	110.	140.	60.	3.	10.	110.
38 Strontium	Sr	1.	465.	440.	100.	200.	300.	20.	610.	2000.	180.
39 Yttrium	Y	0.X	21.	35.	40.	20.	26.	40.	30.	42.	90.
40 Zirconium	Zr	45.	140.	140.	175.	500.	160.	220.	19.	20.	150.
41 Niobium	Nb	16.	19.	20.	21.	35.	11.	0.0X	0.3	4.6	14.
42 Molybdenum	Mo	0.3	1.5	1.0	1.3	0.6	2.6	0.2	0.4	3.	27.
43 Technetium	Tc	C	C	C	C	C	C	C	C	C	C
44 Ruthenium	Ru	D	D	D	D	D	D	D	D	D	D
45 Rhodium	Rh	D	D	D	D	D	D	D	D	D	D
46 Palladium	Pd	0.12	0.02	0.00X	0.00X	D	D	D	D	D	D
47 Silver	Ag	0.06	0.11	0.051	0.037	0.0X	0.07	0.0X	0.0X	0.0X	0.11
48 Cadmium	Cd	0.X	0.22	0.13	0.13	0.13	0.3	0.0X	0.035	0.0X	0.42
49 Indium	In	0.01	0.22	0.0X	0.26	0.0X	0.1	0.0X	0.0X	0.0X	0.08
50 Tin	Sn	0.5	1.5	1.5	3.	X.	6.0	0.X	0.X	0.X	1.5
51 Antimony	Sb	0.1	0.2	0.2	0.2	0.X	1.5	0.0X	0.2	0.15	1.0
52 Tellurium	Te	D	D	D	D	D	D	D	D	D	D
53 Iodine	I	0.5	0.5	0.5	0.5	0.5	2.2	1.7	1.2	0.05	0.05
54 Xenon	Xe	B	B	B	B	B	B	B	B	B	B
55 Cesium	Cs	0.X	1.1	2.	4.	0.6	5.	0.X	0.X	0.4	6.
56 Barium	Ba	0.4	330.	420.	840.	1600.	580.	X0.	10.	190.	2300.
57 Lanthanum	La	0.X	15.	45.	55.	70.	92.	30.	X.	10.	115.
58 Cerium	Ce	0.X	48.	81.	92.	161.	59.	92.	11.5	35.	345.
59 Praseodymium	Pr	0.X	4.6	7.7	8.8	15.	5.6	8.8	1.1	3.3	33.
60 Neodymium	Nd	0.X	20.	33.	37.	65.	24.	37.	4.7	14.	140.
61 Promethium	Pm	C	C	C	C	C	C	C	C	C	C
62 Samarium	Sm	0.X	5.3	8.8	10.	18.	6.4	10.	1.3	3.8	38.
63 Europium	Eu	0.X	.8	1.4	1.6	2.8	1.0	1.6	0.2	0.6	6.
64 Gadolinium	Gd	0.X	5.3	8.8	10.	18.	6.4	10.	1.3	3.8	38.
65 Terbium	Tb	0.X	.8	1.4	1.6	2.8	1.0	1.6	0.2	0.6	6.
66 Dysprosium	Dy	0.X	3.8	6.3	7.2	13.	4.6	7.2	0.9	2.7	27.
67 Holmium	Ho	0.X	1.1	1.8	2.0	3.5	1.2	2.0	0.3	0.8	7.5
68 Erbium	Er	0.X	2.1	3.5	4.0	7.0	2.5	4.0	0.5	1.5	15.
69 Thulium	Tm	0.X	0.2	0.3	0.3	0.6	0.2	0.3	0.04	0.1	1.2
70 Ytterbium	Yb	0.X	2.1	3.5	4.0	7.0	2.6	4.0	0.5	1.5	15.
71 Lutetium	Lu	0.X	0.6	1.1	1.2	2.1	0.7	1.2	0.2	0.5	4.5
72 Hafnium	Hf	0.6	2.0	2.3	3.9	11.	2.8	3.9	0.3	0.41	4.1
73 Tantalum	Ta	1.0	1.1	3.6	4.2	2.1	0.8	0.0X	0.0X	0.0X	0.X
74 Tungsten	W	0.77	0.7	1.3	2.2	1.3	1.8	1.6	0.6	0.X	X.
75 Rhenium	Re	D	D	D	D	D	D	D	D	D	D

36 Krypton	Kr	B	B	B	B	B	B	B	B	B	B
37 Rubidium	Rb	0.2	30.	110.	170.	110.	140.	60.	3.	10.	110.
38 Strontium	Sr	1.	465.	440.	100.	200.	300.	20.	610.	2000.	180.
39 Yttrium	Y	0.X	21.	35.	40.	20.	26.	40.	30.	42.	90.
40 Zirconium	Zr	45.	140.	140.	175.	500.	160.	220.	19.	20.	150.
41 Niobium	Nb	16.	19.	20.	21.	35.	11.	0.0X	0.3	4.6	14.
42 Molybdenum	Mo	0.3	1.5	1.0	1.3	0.6	2.6	0.2	0.4	3.	27.
43 Technetium	Tc	C	C	C	C	C	C	C	C	C	C
44 Ruthenium	Ru	D	D	D	D	D	D	D	D	D	D
45 Rhodium	Rh	D	D	D	D	D	D	D	D	D	D
46 Palladium	Pd	0.12	0.02	0.00X	0.00X	D	D	D	D	D	D
47 Silver	Ag	0.06	0.11	0.051	0.037	0.0X	0.07	0.0X	0.0X	0.0X	0.11
48 Cadmium	Cd	0.X	0.22	0.13	0.13	0.13	0.3	0.0X	0.035	0.0X	0.42
49 Indium	In	0.01	0.22	0.0X	0.26	0.0X	0.1	0.0X	0.0X	0.0X	0.08
50 Tin	Sn	0.5	1.5	1.5	3.	X.	6.0	0.X	0.X	0.X	1.5
51 Antimony	Sb	0.1	0.2	0.2	0.2	0.X	1.5	0.0X	0.2	0.15	1.0
52 Tellurium	Te	D	D	D	D	D	D	D	D	D	D
53 Iodine	I	0.5	0.5	0.5	0.5	0.5	2.2	1.7	1.2	0.05	0.05
54 Xenon	Xe	B	B	B	B	B	B	B	B	B	B
55 Cesium	Cs	0.X	1.1	2.	4.	0.6	5.	0.X	0.X	0.4	6.
56 Barium	Ba	0.4	330.	420.	840.	1600.	580.	X0.	10.	190.	2300.
57 Lanthanum	La	0.X	15.	45.	55.	70.	92.	30.	X.	10.	115.
58 Cerium	Ce	0.X	48.	81.	92.	161.	59.	92.	11.5	35.	345.
59 Praseodymium	Pr	0.X	4.6	7.7	8.8	15.	5.6	8.8	1.1	3.3	33.
60 Neodymium	Nd	0.X	20.	33.	37.	65.	24.	37.	4.7	14.	140.
61 Promethium	Pm	C	C	C	C	C	C	C	C	C	C
62 Samarium	Sm	0.X	5.3	8.8	10.	18.	6.4	10.	1.3	3.8	38.
63 Europium	Eu	0.X	.8	1.4	1.6	2.8	1.0	1.6	0.2	0.6	6.
64 Gadolinium	Gd	0.X	5.3	8.8	10.	18.	6.4	10.	1.3	3.8	38.
65 Terbium	Tb	0.X	.8	1.4	1.6	2.8	1.0	1.6	0.2	0.6	6.
66 Dysprosium	Dy	0.X	3.8	6.3	7.2	13.	4.6	7.2	0.9	2.7	27.
67 Holmium	Ho	0.X	1.1	1.8	2.0	3.5	1.2	2.0	0.3	0.8	7.5
68 Erbium	Er	0.X	2.1	3.5	4.0	7.0	2.5	4.0	0.5	1.5	15.
69 Thulium	Tm	0.X	0.2	0.3	0.3	0.6	0.2	0.3	0.04	0.1	1.2
70 Ytterbium	Yb	0.X	2.1	3.5	4.0	7.0	2.6	4.0	0.5	1.5	15.
71 Lutetium	Lu	0.X	0.6	1.1	1.2	2.1	0.7	1.2	0.2	0.5	4.5
72 Hafnium	Hf	0.6	2.0	2.3	3.9	11.	2.8	3.9	0.3	0.41	4.1
73 Tantalum	Ta	1.0	1.1	3.6	4.2	2.1	0.8	0.0X	0.0X	0.0X	0.X
74 Tungsten	W	0.77	0.7	1.3	2.2	1.3	1.8	1.6	0.6	0.X	X.
75 Rhenium	Re	D	D	D	D	D	D	D	D	D	D
76 Osmium	Os	D	D	D	D	D	D	D	D	D	D
77 Iridium	Ir	D	D	D	D	D	D	D	D	D	D
78 Platinum	Pt	D	D	D	D	D	D	D	D	D	D
79 Gold	Au	0.006	0.004	0.004	0.004	0.00X	0.00X	0.00X	0.00X	0.00X	0.00X
80 Mercury	Hg	0.0X	0.09	0.08	0.08	0.0X	0.4	0.03	0.04	0.0X	0.X
81 Thallium	Tl	0.06	0.21	0.72	2.3	1.4	1.4	0.82	0.0X	0.16	0.8
82 Lead	Pb	1.	6.	15.	19.	12.	20.	7.	9.	9.	80.
83 Bismuth	Bi	D	0.007	D	0.01	D	D	D	D	D	D
84 Polonium	Po	E	E	E	E	E	E	E	E	E	E
85 Astatine	At	E	E	E	E	E	E	E	E	E	E
86 Radon	Rn	E	E	E	E	E	E	E	E	E	E
87 Francium	Fr	E	E	E	E	E	E	E	E	E	E
88 Radium	Ra	E	E	E	E	E	E	E	E	E	E
89 Actinium	Ac	E	E	E	E	E	E	E	E	E	E
90 Thorium	Th	0.004	4.	8.5	17.	13.	12.	1.7	1.7	X.	7.
91 Protactinium	Pa	E	E	E	E	E	E	E	E	E	E
92 Uranium	U	0.001	1.	3.0	3.0	3.0	3.7	0.45	2.2	0.X	1.3
93 Neptunium	Np	F	F	F	F	F	F	F	F	F	F
94 Plutonium	Pu	F	F	F	F	F	F	F	F	F	F

* In some cases, only order of magnitude estimates could be made. These are indicated by the symbol X.

A: These elements are the basic constituents of the biosphere, hydrosphere, and atmosphere. Oxygen is also the most important element of the lithosphere, whereas carbon is important in sedimentary rock.

B: The rare gases occur in the atmosphere in the following amounts (volume per cent): He, 0.00052; Ne, 0.0018; A, 0.93; Kr, 0.0001; Xe, 0.000008. He is produced by radioactive decay of U and Th but is also lost to outer space. A^{40} is produced by the radioactive potassium 40 and is the major isotope of argon in the atmosphere.

The argon and helium contents of rocks will vary with their age owing to the effect of radioactive decay.

The estimated rare-gas contents of igneous rocks are (in cc per gm of rock): He, 6×10^{-5}; Ne, 7.7×10^{-8}; A, 2.2×10^{-5}; Kr, 4.2×10^{-9}; Xe, 3.4×10^{-10}.

C: These elements do not occur naturally in the Earth's crust.

D: The data for these elements are missing or unreliable.

E: All these elements are present as radioactive nuclides in the decay schemes of U and Th.

F: These elements occur naturally only as a consequence of neutron capture by uranium.

TURKEKIAN AND WEDEPOHL, TABLE 2

Geological Society of America Bulletin, volume 72

Adams
ess
p.
Ahrens
p.
Barnes
str
Behne,
v.
Borisk
Co
Borodi
be
Broeck
to
Brooks
ro
p.
Butler,
Os
Cabell,
an
Canney
sec
Carr, N
Chilea
Clarke,
Cooley
sp
Corren
De
—— 19
S.
Crocke
ba
Degenl
Ge
Degens
m
Pe
Edging
Ne
Pr
El Wa
—— 1
Ac
Engelh
Evans,
49
Fairbai
Ge
Fleisch
Su

REFERENCES CITED

Adams, J. A. S., and Weaver, C. E., 1958, Thorium-to-uranium ratios as indicators of sedimentary processes: Example of concept of geochemical facies: Am. Assoc. Petroleum Geologists Bull., v. 42, p. 387–430

Ahrens, L. H., 1954, The lognormal distribution of the elements: Geochim. Cosmochim. Acta, v. 5, p. 49–73

Barnes, H. L., 1957, Trace-element distribution in shales near Hanover, New Mexico, mining area (Abstract): Geol. Soc. America Bull., v. 68, p. 1699

Behne, W., 1953, Untersuchungen zur Geochemie des Chlor und Brom: Geochim. Cosmochim. Acta v. 3, p. 186–214

Boriskenok, L. A., and Saukov, A. A., 1960, Geochemical cycle of gallium: XXI Internat. Geol. Congress, Copenhagen, Part I, p. 96–105

Borodin, L. S., 1956, On the distribution of beryllium in the Khibina alkalic massif and on the clarke of beryllium in nepheline syenites: Doklady Akad. Nauk SSSR, v. 109, p. 811

Broecker, W. S., Turekian, K. K., and Heezen, B. C., 1958, The relation of deep sea sedimentation rates to variations in climate: Am. Jour. Sci., v. 256, p. 503–517

Brooks, R. R., Ahrens, L. H., and Taylor, S. R., 1960, The determination of trace elements in silicate rocks by a combined spectrochemical-anion exchange technique: Geochim. Cosmochim. Acta, v. 18, p. 162–175

Butler, J. R., 1954, The geochemistry and mineralogy of rock weathering. (2) The Nordmarka area, Oslo: Geochim. Cosmochim. Acta, v. 6, p. 268–281

Cabell, M. J., and Smales, A. A., 1957, The determination of rubidium and caesium in rocks, minerals and meteorites by neutron-activation analysis: Analyst, v. 82, p. 390–405

Canney, F. C., 1952, Some aspects of the geochemistry of potassium, rubidium, cesium, and thallium in sediments (Abstract): Geol. Soc. America Bull., v. 63, p. 1238

Carr, M. H., and Turekian, K. K., in press, The geochemistry of cobalt: Geochim. Cosmochim. Acta

Chilean Iodine Educational Bureau, 1956, Geochemistry of Iodine: London, Stone House, 150 p.

Clarke, F. W., 1924, Data of geochemistry: U. S. Geol. Survey Bull. 770, 841 p.

Cooley, R. A., Martin, A. V., Feldman, C., and Gillespie, J., 1953, The Hf to Zr abundance ratio and specific radioactivity of some ores: Geochem. Cosmochim. Acta, v. 3, p. 30–33

Correns, C. W., 1937, Die Sedimente des äquatorialen Atlantischen Ozeans. 2: Wiss. Ergebnisse d. Deutschen Atlant. Expedition Meteor 1925–27, v. III/3, Berlin

—— 1956, The geochemistry of the halogens, p. 183–234 *in* Ahrens, L. H., Rankama, K., and Runcorn, S. K., Physics and chemistry of the Earth, volume 1: London, Pergamon Press, 317 p.

Crocket, J. H., Vincent, E. A., and Wager, L. R., 1958, The distribution of gold in some basic and ultrabasic igneous rocks and minerals: Geochim. Cosmochim. Acta, v. 14, p. 153–154

Degenhardt, H., 1957, Untersuchungen zur geochemischen Verteilung des Zirconiums in der Lithosphäre: Geochim. Cosmochim. Acta, v. 11, p. 279–309

Degens, E. T., Williams, E. G., and Keith, M. L., 1957, Environmental studies of Carboniferous sediments, part 1: Geochemical criteria for differentiating marine and fresh water shales: Am. Assoc. Petroleum Geologists Bull., v. 41, p. 2427–2455

Edgington, G., and Byers, H. G., 1942, Geology and biology of North Atlantic deep-sea cores between Newfoundland and Ireland. Part 9: Selenium content and chemical analyses: U. S. Geol. Survey Prof. Paper 196-F, p. 151–155

El Wardani, S. A., 1957, On the geochemistry of germanium: Geochim. Cosmochim. Acta, v. 13, p. 5–19

—— 1958, Marine geochemistry and the origin of Pacific pelagic clay minerals: Geochim. Cosmochim. Acta, v. 15, p. 237–254

Engelhardt, W. von, 1936, Die Geochemie des Barium: Chemie d. Erde, v. 10, p. 187–246

Evans, R. D., and Goodman, C., 1941, Radioactivity of rocks: Geol. Soc. America Bull., v. 52, p. 459–490

Fairbairn, H. W., Ahrens, L. H., and Gorfinkle, G., 1953, Minor element content of Ontario diabase: Geochim. Cosmochim. Acta, v. 3, p. 34–46

Fleischer, M., 1953, Recent estimates of the abundances of the elements in the Earth's crust: U. S. Geol. Survey Circ. 285, 7 p.

Fleischer, M., 1955, Estimates of the abundances of some chemical elements and their reliability, p. 145–154 *in* Poldervaart, Arie, *Editor*, Crust of the Earth: Geol. Soc. America Special Paper 62, 762 p.

Fröhlich, F., in press, Beitrag zur Geochemie des Chroms: Geochim. Cosmochim. Acta

Gast, P. W., 1960, Limitations on the composition of the upper mantle: Jour. Geophys. Research, v. 65, p. 1287–1297

Goel, P. S., Kharkar, D. P., Lal, D., Narsappaya, N., Peters, B., and Yatirajam, V., 1957, The beryllium-10 concentration in deep-sea sediments: Deep-Sea Research, v. 4, p. 202–210

Goldberg, E. D., and Arrhenius, G.O.S., 1958, Chemistry of Pacific pelagic sediments: Geochim. Cosmochim. Acta, v. 13, p. 183–212

Goldschmidt, V. M., 1954, Geochemistry: Oxford, Clarendon Press, 730 p.

Goldschmidt, V. M., and Strock, L. W., 1935, Zur Geochemie des Selens II: Nachr. Ges. Wiss. Göttingen Math.-Phys. Kl. IV., v. 1, p. 123–143

Gordon, M., and Murata, K. J., 1952, Minor elements in Arkansas bauxite: Econ. Geology, v. 47, p. 169–179

Gottfried, D., Waring, C. L., and Worthing, H. W., 1956, Hafnium content, hafnium to zirconium ratio, and radioactivity of zircon from igneous rocks (Abstract): Geol. Soc. America Bull., v. 67, p. 1700

Green, J., 1959, Geochemical table of the elements for 1959: Geol. Soc. America Bull., v. 70, p. 1127–1184

Green, J., and Poldervaart, A., 1955, Some basaltic provinces: Geochim. Cosmochim. Acta, v. 7, p. 177–188

Grimaldi, F. S., 1960, Determination of niobium in the parts per million range in rocks: Anal. Chem., v. 32, p. 119–121

Hamaguchi, H., and Kuroda, R., 1959, Silver content of igneous rocks: Geochim. Cosmochim. Acta, v. 17, p. 44–52

Hamaguchi, H., Reed, G. W., and Turkevich, A., 1957, Uranium and barium in stone meteorites: Geochim. Cosmochim. Acta, v. 12, p. 337–347

Harder, H., 1959a, Beitrag zur Geochemie des Bors. I. Bor in Mineralen und Magmatischen Gesteinen Nachr.: Akad. Wiss. Göttingen, II. Math.-phys. Kl., v. 5 p. 67–122

—— 1959b, Beitrag zur Geochemie des Bors. II. Bor in Sedmenten: Akad. Wiss. Göttingen, II. Math.-phys. Kl., v. 6, p. 123–183

Heide, F., and Böhm, G., 1957, Geochemie des Quecksilbers: Chemie d. Erde, v. 19, p. 198–204

Heide, F., and Lerz, H., 1955, Zur Geochemie des Bleies: Chemie d. Erde, v. 17, p. 217–222

Heide, F., and Singer, E., 1950, Zur Geochemie des Cu und Zn: Der Naturwiss., v. 37, p. 541–542

Hirst, D. M., and Nicholls, G. D., 1958, Techniques in sedimentary geochemistry: (1) Separation of the detrital and non-detrital fractions of limestones: Jour. Sed. Petrology, v. 28, p. 468–481

Holser, W. T., Warner, L. A., Wilmarth, V. R., and Cameron, E. N., 1951, Notes on the geochemistry of beryllium (Abstract): Geol. Soc. America Bull., v. 62, p. 1450–1451

Holyk, W., and Ahrens, L. H., 1953, Potassium in ultramafic rocks: Geochim. Cosmochim. Acta, v. 4, p. 241–250

Horstman, E. L., 1957, The distribution of lithium, rubidium and caesium in igneous and sedimentary rocks: Geochim. Cosmochim. Acta, v. 12, p. 1–28

Hügi, T., 1956, Vergleichende petrologische und geochemische Untersuchungen an Graniten des Aarmassivs: Beitr. Geol. karte Schweiz., Neue Folge 94, 86 p.

Hutchinson, G. E., Benoit, R. J., Cotter, W. B., and Wangersky, P. J., 1955, On the nickel. cobalt, and copper contents of deep-sea sediments: Nat. Acad. Sci. Proc., v. 41, p. 160–162

Ishimori, T., 1951, Gehalt an Molybdän in japanischen vulkanischen Gesteinen: Bull. Chem. Soc. Japan, v. 25, p. 251–252

Ishimori, T., and Takashima, Y., 1955, Thallium content of Japanese igneous rocks: Kyushu Univ. Faculty Sci. Mem., ser. C., Chemistry, v. 2, p. 65–74

Jeffery, P. G., 1959, The geochemistry of tungsten, with special reference to the rocks of the Uganda Protectorate: Geochim. Cosmochim. Acta, v. 16, p. 278–295

Jost, K., 1932, Über den Vanadiumgehalt der Sedimentgesteine und sedimentären Lagerstätten: Chemie d. Erde, v. 7, p. 177–290

Kay, M., 1951, North American geosynclines: Geol. Soc. America Mem. 48, 143 p.

Kokubu, N., 1956, Fluorine in rocks: Kyushu Univ., Faculty Sci. Mem., ser. C., Chemistry, v. 2, p. 95–149

Koritnig, S., 1951, Ein Beitrag zur Geochemie des Fluor: Geochim. Cosmochim. Acta, v. 1, p. 89–116

Kosterin, A. V., Zuev, V. N., and Shevaleevaskii, I. D., 1958, Zr/Hf ratio in zircons in some igneous rocks of Northern Kirgizia: Geochemistry (USSR), English ed. (Geochemical Society) no. 1, p. 116–119

Kuroda, P. K., and Sandell, E. B., 1954, Geochemistry of molybdenum: Geochim. Cosmochim. Acta, v. 6, p. 35–63

Kuroda, R., 1957, Geochemical investigations of granite: Jour. Chem. Soc. Japan, Pure Chem. Sec., v. 78, p. 141

Liebenberg, C. J., 1956, The spectrochemical determination of Cs in igneous rocks, using a chemical concentration procedure: Geochim. Cosmochim. Acta, v. 10, p. 196

Macpherson, H. G., 1958, A chemical and petrographic study of Pre-Cambrian sediments: Geochim. Cosmochim. Acta, v. 14, p. 73–92

Mason, B., 1958, Principles of geochemistry: 2d ed., New York, John Wiley, 310 p.

Masuda, A., 1957, Simple regularity in the variation of relative abundances of rare earth elements: Jour. Earth Sciences, Nagoya Univ., v. 5, p. 125–134

Merrill, J. R., Honda, M., and Arnold, J. R., 1958, Beryllium geochemistry and beryllium-10 age determination: Proc. 2d United Nations Internat. Conf. Peaceful Uses of Atomic Energy, Geneva, v. 2, p. 251–254

Merrill, J. R., Lyden, E. F. X., Honda, M., and Arnold, J. R., 1960, The sedimentary geochemistry of the beryllium isotopes: Geochim. Cosmochim. Acta, v. 18, p. 108–129

Minami, E., 1935a, Selen-Gehalte von europäischen und japanischen Tonschiefern: Nacher. Ges. Wiss. Göttingen, Math.-phys. Kl. IV, v. 1, p. 143–145

—— 1935b, Gehalte an seltenen Erden in europäischen und japanischen Tonschiefern: Nachr. Ges. Wiss. Göttingen, Math.-phys. Kl. IV, v. 1, p. 155–170

Morita, Y., 1955, Distribution of copper and zinc in various phases of the earth materials: Jour. Earth Sciences, Nagoya Univ., v. 3, p. 33

Mullin, J. B., and Riley, J. P., 1956, The occurrence of cadmium in seawater and in marine organisms and sediments: Jour. Marine Research, v. 15, p. 103–122

Murray, E. G., and Adams, J. A. S., 1958, Thorium, uranium and potassium in some sandstones: Geochim. Cosmochim. Acta, v. 13, p. 260–269

Nockolds, S. R., 1954, Average chemical composition of some igneous rocks: Geol. Soc. America Bull., v. 65, p. 1007–1032

Nockolds, S. R., and Allen, R., 1953, The geochemistry of some igneous rock series. Part I: Geochim. Cosmochim. Acta, v. 4, p. 105–142

—— 1956, The geochemistry of some igneous rock series. Part III: Geochim. Cosmochim. Acta, v. 9, p. 34–77

Okada, S., 1955, Chemical composition of Japanese granitic rocks in regard to petrographic provinces. Part III: Science Rep. Tokyo Kyoiko Daigacu, Sec. C, v. 4, p. 163–184

—— 1956, Chemical composition of Japanese granitic rocks in regard to petrographic provinces. Part IV: Science Rep. Tokyo Kyoiko Daigacu, Sec. C., v. 5, p. 25

Onishi, H., 1956, Geochemistry of germanium: Bull. Chem. Soc. Japan, v. 29, p. 686–694

Onishi, H., and Sandell, E. B., 1955a, Geochemistry of arsenic: Geochim. Cosmochim. Acta, v. 7, p. 1–33

—— 1955b, Notes on the geochemistry of antimony: Geochim. Cosmochim. Acta, v. 8, p. 213–221

—— 1957, Meteoritic and terrestrial abundance of tin: Geochim. Cosmochim. Acta, v. 12, p. 262–270

Ostrom, M. E., 1957, Trace elements in Illinois Pennsylvanian limestones: Illinois State Geol. Surv. Circ. 243, 34p.

Ottemann, J., 1940, Untersuchungen von Spurenelementen, insbesondere Zinn, *in* Tiefengesteinen und einigen gesteinsbildenden Mineralien des Harzes: Z. angew. Mineralogie, v. 3, p. 142–169

Petterson, H., and Rotschi, H., 1952, The nickel content of deep sea deposits: Geochim. Cosmochim. Acta, v. 2, p. 81–90

Picciotto, E., and Wilgain, S., 1954, Thorium determination in deep-sea sediments: Nature, v. 173, p. 632–633

Pinson, W. H., Ahrens, L. H., and Franck, M. L., 1953, The abundances of Li, Sc, Sr, Ba and Zr in chondrites and ultrabasic rocks: Geochim. Cosmochim. Acta, v. 4, p. 251–260

Preuss, E., 1940, Beiträge zur spektralanalytischen Methodik. II. Bestimmung von Zn, Cd, Hg, In, Tl, Ge, Sn, Pb, Sb und Bi durch fraktionierte Destillation: Z. angew. Mineralogie, v. 3, p. 8–20

Rankama, K., 1944, On the geochemistry of tantalum: Bull. de Comm. geol. Finlande no. 133, 78 p.

—— 1948, On the geochemistry of niobium: Ann. Acad. Scient. Fennicae A III, no. 13, 57 p.

Rankama, K., and Sahama, Th., 1950, Geochemistry: Chicago, Univ. of Chicago Press, 912 p.

Reed, G. W., Kigoshi, K., and Turkevich, A., 1958, Activation analysis for heavy elements in stone meteorites: Proc. 2d United Nations Internat. Conf. Peaceful Uses of Atomic Energy, Geneva, v. 28, p. 486–490

Ricke, W., in press, Ein Beitrag zur Geochemie des Schwefels: Geochim. Cosmochim. Acta

Ross, C. S., Foster, M. D., and Myers, A. T., 1954, Origin of dunites and of olivine-rich inclusions in basaltic rocks: Am. Mineralogist, v. 39, p. 693–737

Runnels, R. T., and Schleicher, J. A., 1956, Chemical composition of Eastern Kansas limestones: State Geol. Survey Kansas Bull. 119, pt. 3, p. 81–103

Sahama, T. G., 1945, Spurenelemente der Gesteine im südlichen Finnisch-Lappland: Bull. de Comm. Geol. Finlande no. 135

Sandell, E. B., 1946, Abundance of tungsten in igneous rocks: Am. Jour. Sci., v. 244, p. 643–648

—— 1949, The Ga content of igneous rocks: Am. Jour. Sci., v. 247, p. 40–48

—— 1952, The beryllium content of igneous rocks: Geochim. Cosmochim. Acta, v. 2, p. 211–216

Sandell, E. B., and Goldich, S. S., 1943, The rarer metallic constituents of some American igneous rocks: I, II: Jour. Geology, v. 51, p. 99–115, 167–189

Shaw, D. M., 1952a, The geochemistry of thallium: Geochim. Cosmochim. Acta, v. 2, p. 118–154

—— 1952b, The geochemistry of indium: Geochim. Cosmochim. Acta, v. 2, p. 185–206

—— 1954, Trace elements in pelitic rocks I, II: Geol. Soc. America Bull., v. 65, p. 1151–1166, 1167–1182

—— 1957, Some aspects of the determination of barium in silcate rocks: Spectrochim. Acta, v. 10, p. 125–127

Shepherd, E. S., 1940, Note on the fluorine content of rocks and ocean bottom samples: Am. Jour. Sci., v. 238, p. 117–128

Smales, A. A., 1955, Some trace-element determinations in G-1 and W-1 by neutron activation: Geochim. Cosmochim. Acta, v. 8, p. 300

Smales, A. A., and Salmon, L., 1955, Determination by radioactivation of small amounts of urbidium and caesium in sea-water and related materials of geochemical interest: Analyst, v. 80, p. 37–50

Smales, A. A., Mapper, D., and Wood, A. J., 1957, The determination, by radioactivation, of small quantities of nickel, cobalt, and copper in rocks, marine sediments and meteorites: Analyst, v. 82, p. 75–88

Starik, I. E., Kuznetsov, Y. V., Grashchenko, S. M., and Trenklikh, M. S., 1958, The ionium method of determination of marine sediments: Geochemistry (USSR), English ed. (Geochemical Society), no. 1, p. 1–15

Stock, A., and Cucuel, F., 1934, Die Verbreitung des Quecksilbers: Naturwiss., v. 22–24, p. 390–393

Strock, L. W., 1936, Zur Geochemie des Lithiums: Nachr. Ges. Wiss. Göttingen Math.-Phys. Kl. IV, v. 1, p. 171–204

Sugawara, K., and Morita, Y., 1950, On the revision of the Clarke numbers of copper and zinc: Mikrochemie, v. 36/37, p. 1093–1099

Tatsumoto, M., 1957, Chemical investigations of deep sea deposits (nos. 21–26): Ni, Co, Cu, Zn, Sn, Pb, Be content of deep sea deposits: Jour. Chem. Soc. Japan, v. 77, p. 1637, v. 78, p. 38, 42, 405, 409, 502 (in Japanese)

Tauson, L. W., and Pevtsova, L. A., 1955, On the relationship of the distribution of lead and zinc in the rocks of the Caledonian granite complex of Susamyr (Central-Tienshan): Doklady Acad. Nauk, USSR, v. 103, p. 1069–1072

Tilton, G. R., and Reed, G. W., 1960, Concentration of lead in ultramafic rocks by neutron activation analysis (Abstract): Jour. Geophys. Research, v. 65, p. 2529

Tourtelot, H. A., 1957, Chemical composition of the Pierre shale and equivalent rocks of Late Cretaceous age, Great Plains region (Abstract): Geol. Soc. America Bull., v. 68, p. 1806

Troger, E., 1934, Der Gehalt an selteneren Elementen bei Eruptivgesteinen: Chemie d. Erde, v. 9, p. 286–310

Turekian, K. K., 1956, The abundance of Cu, Ni, and Cr in basaltic rocks (Abstract): Am. Geophys. Union Trans., v. 37, p. 361

— 1960, Elements (geochemical distribution), *in* Encyclopedia of Science and Technology, v. 4: New York, McGraw-Hill Book Co., p. 549–552

Turekian, K. K., and Armstrong, R. L., in press, Magnesium, strontium, and barium concentrations and calcite-aragonite ratios of some recent molluscan shells: Jour. Marine Res.

Turekian, K. K., and Carr, M. H., 1960, The geochemistries of chromium, cobalt, and nickel: XXI Internat. Geol. Congress, Copenhagen, Part I, p. 14–26.

Turekian, K. K. and Carr, M. H., in press, Chromium, cobalt and strontium in some Bureau of Standards rock reference samples: Geochim. Cosmochim. Acta

Turekian, K. K., and Feely, H. W., 1956, Variations in the abundance of trace elements in a eupelagic Atlantic core (Abstract): Geol. Soc. America Bull., v. 67, p. 1739

Turekian, K. K., and Kulp, J. L., 1956, The geochemistry of strontium: Geochim. Cosmochim. Acta, v. 10, p. 245–296

Vincent, E. A., and Crocket, J. H., 1960, Studies in the geochemistry of gold—II: Geochim. Cosmochim. Acta, v. 18, p. 143–148

Vincent, E. A., and Smales, A. A., 1956, The determination of palladium and gold in igneous rocks by radioactivation analysis: Geochim. Cosmochim. Acta, v. 9, p. 154–160

Vinogradov, A. P., 1956, The regularity of distribution of chemical elements in the Earth's crust: Geokhimiya, p. 1–52 (A.E.R.E. Lib/Trans. 795; 1957)

Vinogradov, A. P., and Ronov, A. B., 1956, Composition of sedimentary rocks of the Russian platform in connection with the history of its tectonic movements: Geochemistry (USSR), no. 6, p. 3–24

Vinogradov, A. P., Vainshtein, E. E., and Pavlenko, L. I., 1958, Tungsten and molybdenum in igneous rocks: Geochemistry (USSR), English ed. (Geochemical Society), no. 5, p. 497–509

Wager, L. R., Smit, J. van R., and Irving, H., 1958, Indium content of rocks and minerals from the Skaergaard intrustion, East Greenland: Geochim. Cosmochim. Acta, v. 13, p. 81–86

Wasserstein, B., 1951, South African granites and their boron content: Geochim. Cosmochim. Acta, v. 1, p. 329–338

Weber, J. N., 1960, Geochemistry of graywackes and shales: Science, v. 131, p. 664–665

Wedepohl, K. H., 1953, Untersuchungen zur Geochemie des Zinks: Geochim. Cosmochim. Acta, v. 3, p. 93–142

— 1955, Schwermetallgehalte der Kalkgerüste einiger mariner Organismen: Nachr. Akad. Wiss. Göttingen Math.-Phys. Kl. 5, p. 79

— 1956, Untersuchungen zur Geochemie des Bleis: Geochim. Cosmochim. Acta, v. 10, p. 69–148

— 1960, Spurenanalytische Untersuchungen an Tiefseetonen aus dem Atlantik: Geochim. Cosmochim. Acta, v. 18, p. 200–231

Whitfield, J. M., Rogers, J. J. W., and Adams, J. A. S., 1959, The relationship between the petrology and the thorium and uranium contents of some granitic rocks: Geochim. Cosmochim. Acta, v. 17, p. 248–271

Znamensky, E. B., 1957, On the average contents of niobium and tantalum in igneous rocks and the crust of the earth: Geochemistry (USSR), No. 8, p. 730

Manuscript Received by the Secretary of the Society, January 21, 1959

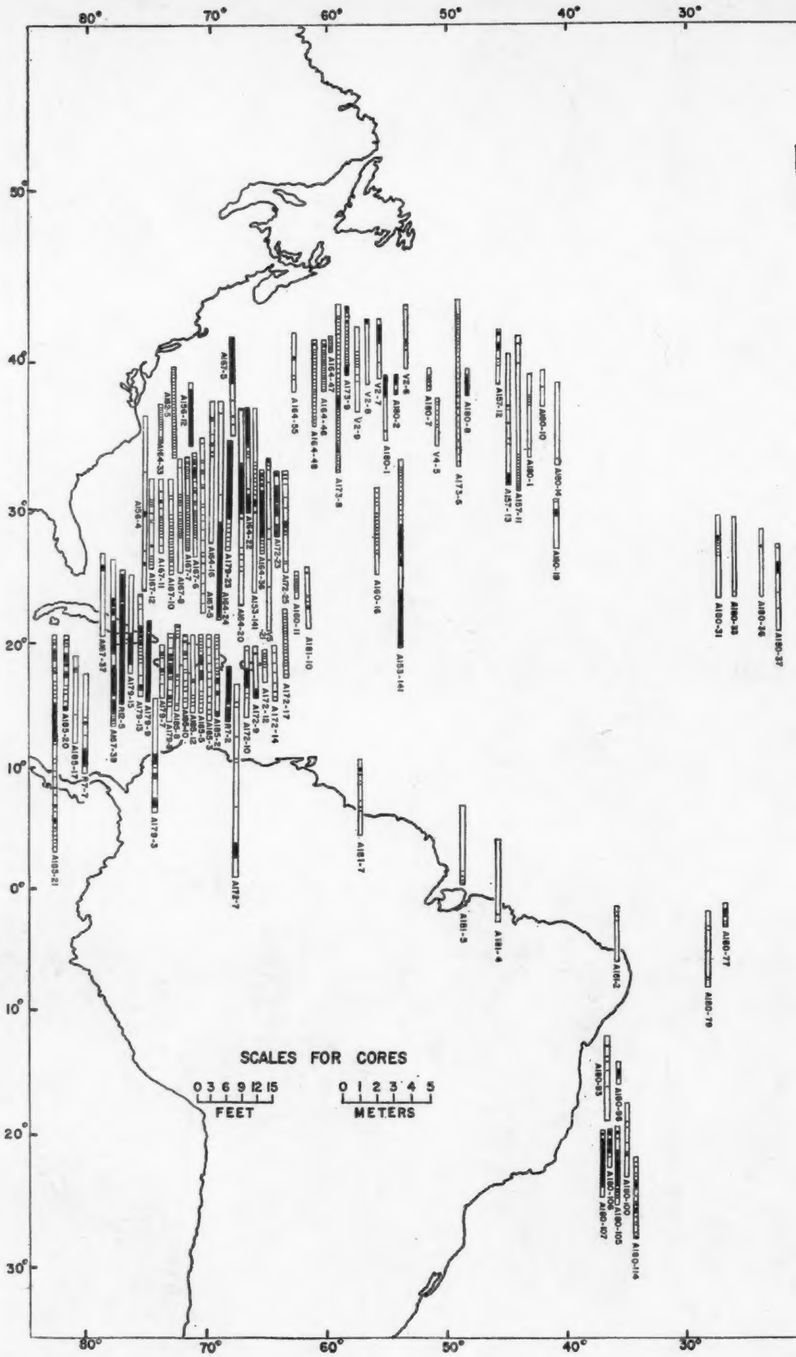

A

The top of the column is the approximate location of the core station. A black zone denotes sanc
a thin sand or silt layer; an open zone indicates lutite.

DISTRIBUTION OF SEDIMENTS IN CORES CONTAININC

ERICSON *ET AL.*, PLATE 1

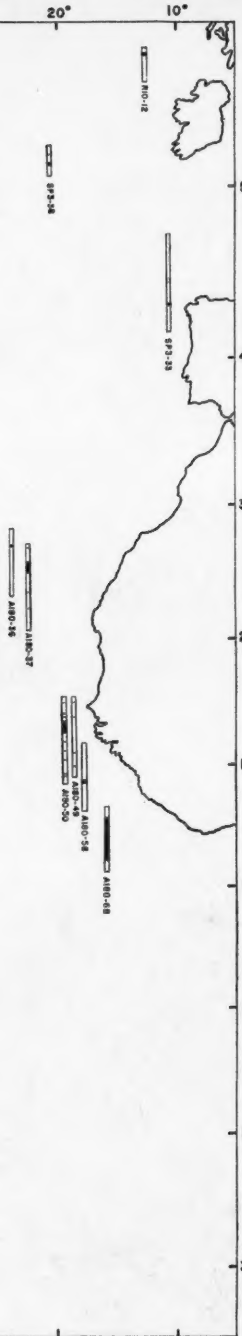

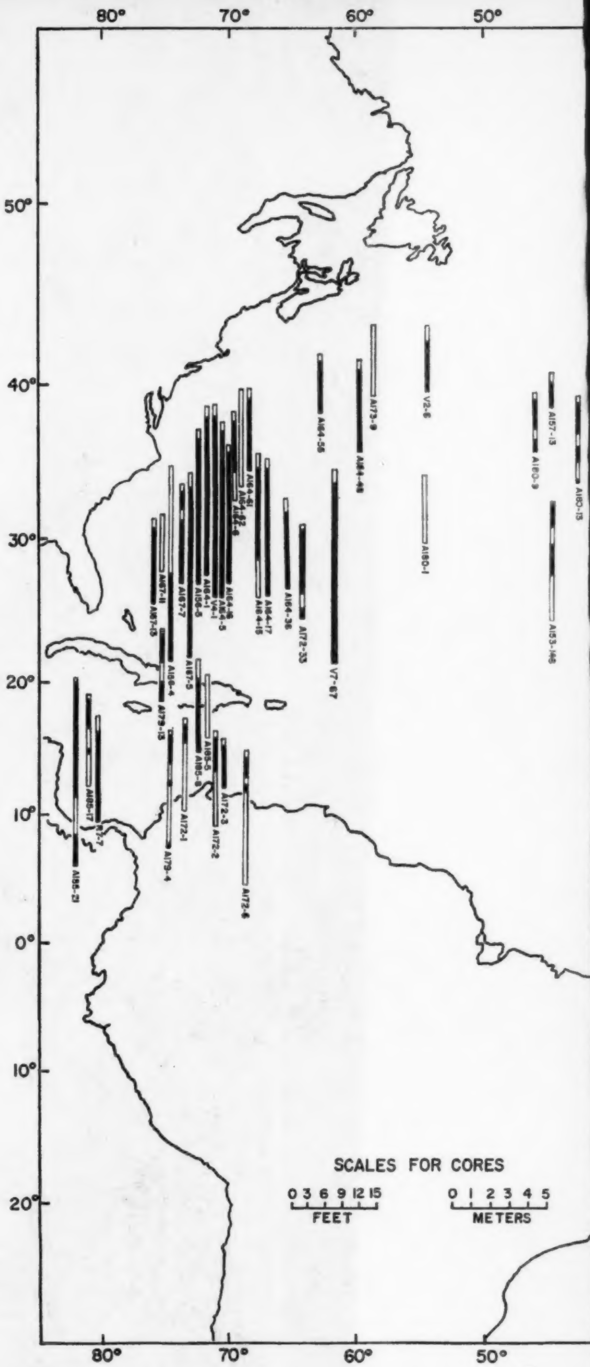

B

es sand and/or silt; a line denotes

The top of the column is the approximate location of the core station. are: the Postglacial (open); the Last Glacial 2–3 (black); the interstad the Last Interglacial (open). All stages shown are considered to be c planktonic Foraminifera and lithology of all the cores and on radioca selected samples from selected cores.

NING SAND AND SILT LAYERS (DIAGRAM A) AND DISTRIBUTION OF THE CLIMATIC STAGES OF

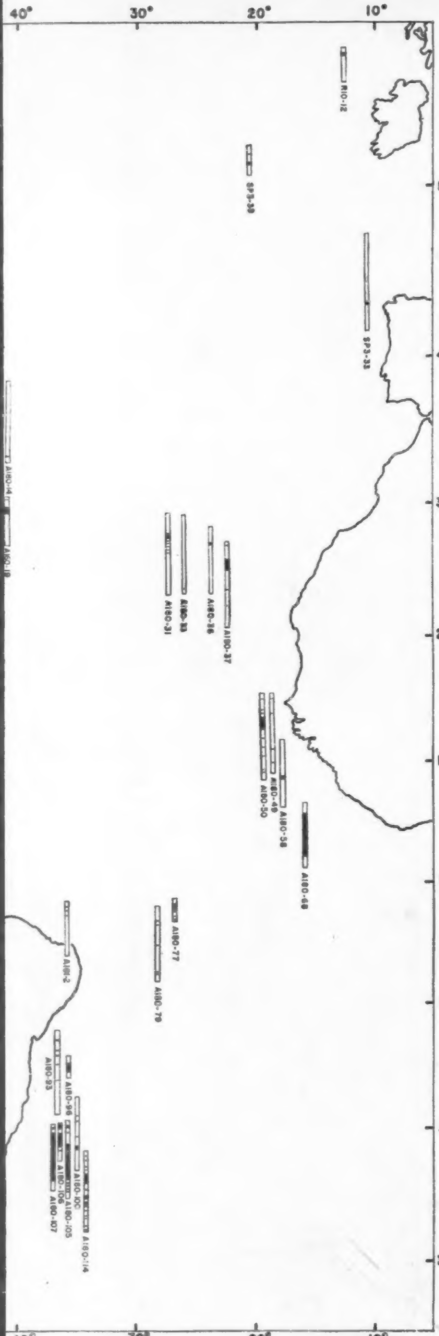

n. A black zone denotes sand and/or silt; a line denotes

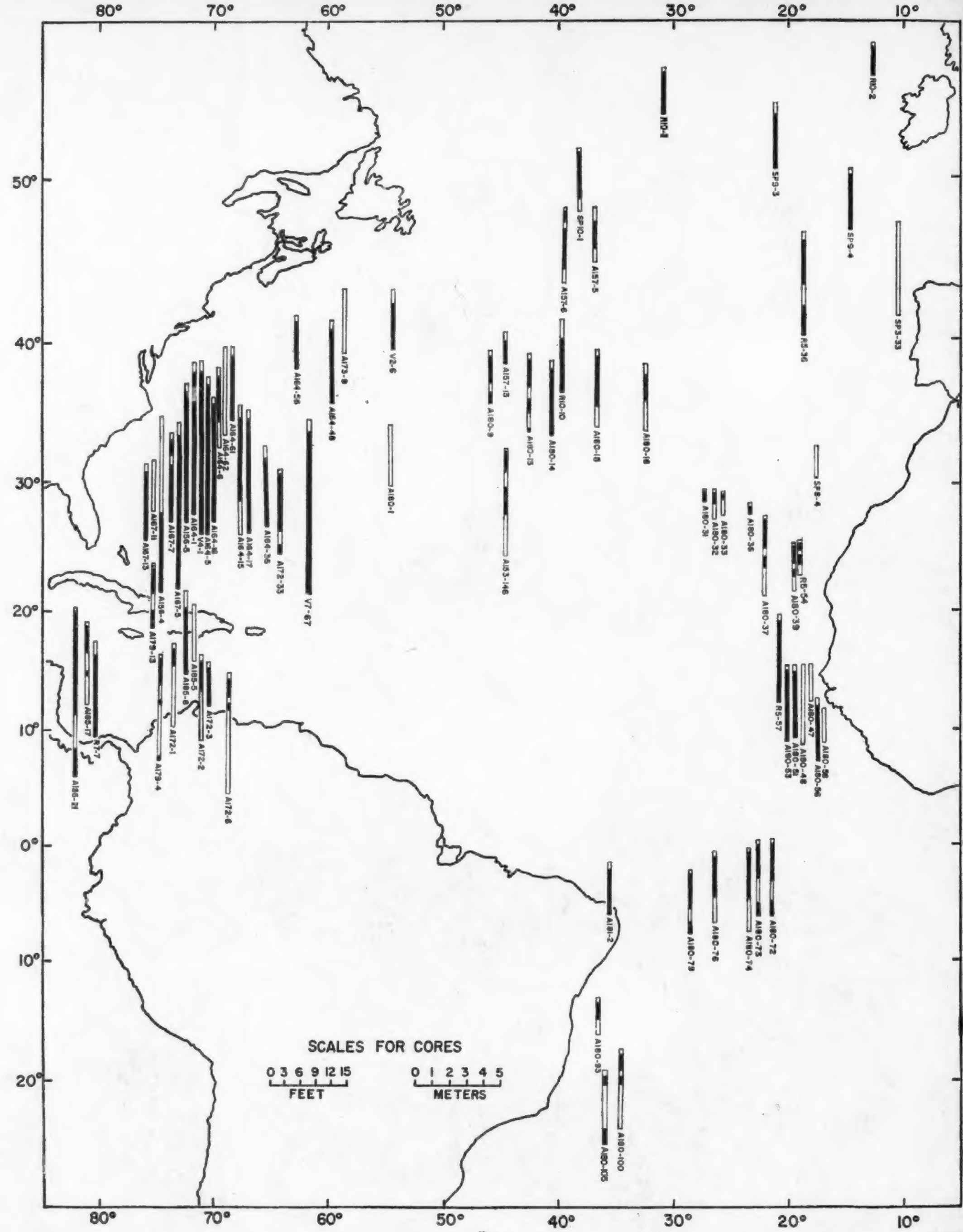

B

The top of the column is the approximate location of the core station. Beginning from the top of the columns the stages indicated are: the Postglacial (open); the Last Glacial 2–3 (black); the interstadial of the Last Glaciation (open); the Last Glacial 1 (black); the Last Interglacial (open). All stages shown are considered to be complete. Interpretations are based on investigations of the planktonic Foraminifera and lithology of all the cores and on radiocarbon dates, isotopic temperatures, and grain-size analyses of selected samples from selected cores.

IN CORES CONTAINING SAND AND SILT LAYERS (DIAGRAM A) AND DISTRIBUTION OF THE CLIMATIC STAGES OF THE CORES (DIAGRAM B)

DAVID B. ERICSON
MAURICE EWING
GOESTA WOLLIN
BRUCE C. HEEZEN

Lamont Geological Observatory (Columbia Univ.), Palisades, N. Y.

Atlantic Deep-Sea Sediment Cores

Abstract: Studies of lithology, particle-size distributions, and micropaleontology and chemical analyses of 221 Atlantic and Caribbean deep-sea cores lead to new conceptions of processes of sedimentation, rates of sediment accumulation, Pleistocene chronology, and pre-Pleistocene history of the Atlantic Basin.

Anomalous layers of sand, silt, and lutite occur widely in the deep basins of the Atlantic. Evidence for deposition of these layers by turbidity currents is as follows: (1) the layers occur in submarine canyons, in deltalike features at the terminal ends of canyons, in basins and depressions, never on isolated rises; (2) they are interbedded with late Pleistocene sediments of abyssal facies; (3) they are well-sorted and commonly graded; and (4) they commonly contain organic remains of shallow-water origin.

Late Pleistocene slumping of compacted Neogene sediments along the banks of the Hudson Submarine Canyon at depths exceeding 3000 m indicates deepening of the canyon by erosion by turbidity currents.

Variations in the planktonic Foraminifera in 108 of the cores and extrapolation of rates of sediment accumulation determined by 37 radiocarbon dates in 10 cores show that the last period of climate comparable with the present ended about 60,000 years ago. A faunal change indicating climatic amelioration, probably corresponding to the beginning of postglacial time, occurred about 11,000 years ago. Cross-correlations by micropaleontological methods establish the continuity of the climatic record deduced from the planktonic Foraminifera. Study of variation in the Planktonic Foraminifera leads to a different Pleistocene chronology from that proposed by Emiliani (1955).

Cross-correlations of faunal zones and radiocarbon dates show that rates of continuous sediment accumulation, as opposed to turbidity-current deposition, range from 0.5 cm to 274.4 cm in 1000 years, depending upon bottom configuration. Cross-correlations by means of changes in coiling direction of planktonic Foraminifera give relative rates of sediment accumulation beyond the range of the radiocarbon method of dating.

Forty one of the cores contain pre-Pleistocene sediments. The oldest sediment is Upper Cretaceous. Foraminifera and discoasters indicate the ages. Absence of sediment older than Late Cretaceous and thickness, 800–1000 m, of sediment in the Atlantic Basin as determined by seismic methods suggest that a large-scale reorganization of the Atlantic Basin took place in the Mesozoic.

CONTENTS

Geological Society of America Bulletin, v. 72, p. 193–286, 50 figs., 3 pls., February 1961

Figure

Plate Facing

Table

INTRODUCTION

Since 1947, Maurice Ewing and his associates have taken more than 2000 deep-sea sediment cores during 45 cruises in the North and South Atlantic, Caribbean, Gulf of Mexico, and Mediterranean. This collection, stored at the Lamont Geological Observatory of Columbia University, also includes some cores taken by ships of the U. S. Hydrographic Office, using coring gear supplied by Lamont.

The laboratory treatment of the cores has been influenced by various circumstances. One has been the quantity of material. Some minimal description of each core has been needed in the planning of subsequent coring campaigns. This has compelled us to resist the temptation to concentrate on any one group of cores or any single aspect. Nor have we entirely neglected any cores with the thought that we could study them later when there might be more time.

The reconnaissance approach which the conditions necessitated has proven advantageous in certain ways. It has enabled us to return to areas of particular interest provided with information obtained from cores taken on previous expeditions and to test hypotheses by coring at stations which were most likely to yield crucial information. Furthermore, rapid survey of all the cores has permitted selection of the best material for more intensive study. This has been particularly important in the micropaleontological work. Cores giving most promise of containing long unbroken records of past climatic changes have been and are being studied in detail.

Ericson and Wollin (1956a; 1956b) have published articles giving numerical data from a few cores, but these have focused on individual cores and have failed to emphasize the abundance of material investigated at Lamont and the consequent statistical weight of the evidence. The 221 sediment cores described here have been selected from 548 cores from the Atlantic and Caribbean. Since the numerical results of the investigation of the Foraminifera alone amount to more than 50,000 values, synoptical presentation of the data is necessary. For this reason graphical representation of variables in the cores has been substituted to a large extent for tables.

ACKNOWLEDGMENTS

We gratefully acknowledge the help of Janet Wollin, who ably assisted in every part of the laboratory investigation.

We also express our sincere appreciation to Allan Bé, Albert Bally, Arnold Finck, Robert Menzies, K. K. Wang, William Wiles, and other members of the Lamont Geological Observatory staff, too numerous to mention by name, who directly or indirectly contributed to this study.

Walter Bucher's enthusiastic interest in all phases of the investigation has been an invaluable source of encouragement for which we are warmly grateful.

It is a pleasant duty to express our thanks to Horace Richards, who identified the mollusks in a core from the Hudson Submarine Canyon.

We are grateful to J. Laurence Kulp, Wallace S. Broecker, and Hans Suess for radiocarbon age determinations.

We express our thanks to Alfred Loeblich who examined the Cretaceous Foraminifera from the Blake Plateau, to William Riedel who examined the Radiolaria in numerous cores, to M. N. Bramlette who gave us valuable help with the discoasters, and to Hans Bolli who determined the ages of some of the older assemblages of Foraminifera.

We are grateful to R. G. Smalley and to the La Habra Laboratory of the California Research Corporation for an important series of spectrochemical analyses.

We are grateful to H. H. Hess, P. F. Kerr, and J. T. Fyles for the classification of a sample of igneous rock from Bermuda.

The Office of Naval Research and the National Science Foundation (research grants NSF-G763, G4174, and G6540) have supported a large part of the laboratory work.

PART I: LITHOLOGY AND PROCESSES OF DEPOSITION

Method of Taking Cores

The cores were taken with a coring device which combines the principle of the piston coring tube developed by Kullenberg (1947; 1955) with that of the free-fall coring tube of Hvorslev and Stetson (1946). The advantages of this type of coring apparatus, which makes use of hydrostatic pressure to overcome friction between sediment and the inner wall of the tube, have been discussed by Kullenberg (1947) and by Ericson and Wollin (1956a). The cores recovered are much longer than those obtained by corers without a piston and are undistorted. In corers without a piston, the sedimentary section is shortened because an increasingly large part of the sediment is squeezed aside as friction between sediment and the inner wall of the coring tube builds up. Cores so taken may give a false impression of the sediment section *in situ* because layers of sediment of firm consistency are recovered rather than more plastic layers. Such cores are worthless in the study of variation in rate of sediment accumulation. Good evidence that cores taken with the piston corer are not shortened by squeezing is provided by burrows, some unfilled, which retain their undistorted circular cross section in the lower parts of long cores. This evidence indicates that when correlatable zones differ in thickness from core to core it is because of a real difference in rate of accumulation rather than changes in the section due to the coring process.

The coring tube is made up of 20-foot (6.1-m) lengths of standard steel tubing of 2½-inch (63.5-mm) inside diameter and one-eighth of an inch wall thickness. Use of this standard commercial tubing in place of the specially made (very expensive) tapered tube of the Hvorslev-Stetson apparatus is advantageous because a fairly large reserve of tubing can be kept on board on each cruise without prohibitive expense. As a result, many cores of older sediment were obtained by lowering the coring apparatus even when the fathometer record indicated that hard bottom might be encountered with consequent damage to the tube.

The coring apparatus is connected to the trawl wire by a release mechanism essentially similar to that developed by Hvorslev and Stetson. It is actuated by a lever about 1.5 m (5 feet) long, from the end of which hangs a line and lead weight, or trigger weight. The trigger weight hangs from 3 to 4.5 m (10–15 feet) below the lower end of the coring tube. Since the coring tube is released when the trigger weight touches bottom, the free fall equals the length of the line, or 3 to 4.5 m. A lead weight of between 1000 and 2000 pounds attached to the upper part of the tube adds to the kinetic energy of the falling tube.

A Fiege fitting is attached to the outboard end of the trawl wire and a piston is bolted to the end of the wire. The piston, provided with three leather cups, is of the type used in conventional water-well pumps. When the apparatus is lowered, the piston is at the bottom of the tube. The trawl wire from the piston extends up through the coring tube, through the release mechanism, and to the A-frame and winch. At a point in the tube near the bottom of the main weight, there is a constriction through which a bumper attached to the Fiege cannot pass. When the apparatus is raised, the bumper comes in contact with the constriction, whereupon the entire apparatus is lifted. Because the constriction impedes the flow of water during rapid ascent of the piston in the pipe, there are ports just below it to permit some water to escape.

A self-tightening clamp known as the come-along is used to attach the release mechanism to the trawl wire. The advantage of this device is that it can be loosened after having been hauled up to the A-frame and made fast. Thus the wire is free to slide through the come-along while the main weight with the tube is hauled up.

The trigger weight is provided with a short coring tube fitted with a plastic liner. The cores taken by the trigger-weight corer, usually no more than 30 cm long, may be kept upright in their liners until they reach the laboratory. In this way a sample of the uppermost layer of sediment, an invaluable reference datum, is preserved in an undisturbed condition.

In theory the long coring tube should sink into the sediment until the constriction near the top of the tube has come into contact with the bumper on the Fiege which is held stationary by the trawl wire. In practice the coring tube frequently comes to rest before contact has been made. When this happens the piston must be pulled up in the tube before the apparatus can be raised. The great hydrostatic pressure developed in this way causes sediment to flow into the tube. Fortunately sediment which enters the tube by flowing takes on a characteristic vertical structure which clearly distinguishes it from sediment cored *in situ*.

Since the Ewing corer is not provided with a liner, the cores must be extruded on board so that the tubing may be re-used. This is done by pulling the tube by means of a rope led to one of the ship's winches against a plunger and rod which is held stationary. The core is received on a strip of heavy impervious paper, which is then wrapped around the core; the edges of the paper are stapled. The wrapped sections of core are then put into 10-foot (3-m) lengths of galvanized gutter pipe, the ends of which are closed with tin caps held in place and sealed with friction tape. In this way cores may be kept on board ship for several months without serious loss of water.

Preparation and Sampling of Cores

At the laboratory the cores are taken out of the gutter pipes, unwrapped, and split or sliced lengthwise into halves. The most satisfactory tool is a kitchen knife. If kept clean, the knife leaves an unsmeared, or little-smeared, surface. Details of structure such as fine bedding and burrows are visible after splitting. Thick beds of well-sorted sand even when wet tend to crumble as the halves fall apart after passage of the knife. Fairly stiff aluminum foil, molded against both sides of the sandy section before splitting, supports the material and facilitates its transfer to a tray.

The split cores are stored in galvanized trays 245 cm long and slightly wider than the core diameter. The core sections in the trays dry in time. This is not entirely disadvantageous. Texture variations, particularly grading or gradual decrease in particle size upward within a single bed, become conspicuous on drying. Grading in beds containing much material of clay size is not ordinarily visible while the sediment is wet. However, the shrinkage of such a sediment on drying is proportional to the ratio of clay particles to finely divided quartz. In consequence a core section containing a graded layer when thoroughly dry tapers smoothly from the base where the proportion of quartz silt is large and there is little shrinkage to the top where clay, with correspondingly great shrinkage, predominates (Ewing, Ericson, and Heezen, 1958).

If a core is of particular interest, a quarter section is preserved in 120-cm lengths of pyrex tubing of 40-mm diameter, the ends of which are closed with rubber stoppers. In this way the original water content is retained indefinitely without refrigeration, shrinkage is eliminated, and color change is reduced to a minimum. Growth of molds and bacteria is inhibited by the addition of 2–3 ml of formaldehyde in the tube. Core sections so preserved are invaluable for reference during the microscopic and chemical study of samples taken from the remaining three-quarters which are stored in the metal trays at room temperature. The pyrex remains clear and permits visual examination of the sediment even with a low-power hand lens without removal of the core from the tube.

The cores are photographed, and descriptions of their gross lithology are written immediately after the cores have been put into their trays. After the cores are split, color changes may take place very rapidly. For example, a dark-gray lutite with inky-black hydrotroilite mottling will change to tan with rusty mottling within an hour after exposure to air. To avoid errors in description because of oxidation of hydrotroilite staining, it is desirable to note the distribution of hydrotroilite while the core is being split.

Samples for coarse fraction ($> 74\mu$) are taken while the cores are moist. The samples, 1–2 cm thick, are taken from only one-quarter of the total section at intervals of 10 cm in the upper 50 cm. If, from the lithology, it seems probable that the sediment has been deposited slowly without interference by slumping or turbidity-current deposition, the 10-cm interval is maintained throughout; otherwise samples below 50-cm are taken at 50-cm intervals or wherever the lithology changes.

By this procedure half of the core is left intact for future reference, and about nineteen-twentieths of the other half remains available for further study. This economy of material has yielded valuable returns. In many cases radiocarbon dating has been possible only because an abundance of material remained in the core trays after study of coarse fraction and logging of the foraminiferal zones.

In sampling, a reasonable degree of cleanliness must be observed to avoid contamination of the samples. The most serious source of contamination is the outer smear, 2 or 3 mm thick, which results from frictional drag between the core and the inner wall of the coring tube. All trace of this smear is removed as the samples are taken.

The samples, after having been dried at 105° C., are weighed to the nearest tenth gram and washed on a 200-mesh stainless-steel sieve which retains particles coarser than 74 μ in diameter. The fine fraction is discarded unless there is some special reason to examine it for coccoliths, diatoms, or discoasters. The coarse fractions are dried and weighed to the nearest tenth gram, and the weights are reduced to percentages of original sample weights. These weights and percentages are recorded in the permanent notes on the various cores. The coarse fractions are stored in 5-ml glass vials.

Salt content is not taken into account in determination of the percentage of coarse fraction. This introduces an error, but one which is probably no greater than that due to incomplete washing. Inevitably some fine sediment remains attached to the particles of the coarse fraction, particularly when it is composed largely of the tests of Foraminifera. In view of these inherent errors, the weighings are made on a rough triple-beam balance, and the percentages are rounded off to the nearest unit. In spite of this imprecision the percentage of coarse fraction is a useful parameter. Its significance is discussed in this paper.

In theory a size separation at the 62-μ level might seem to be preferable since by general agreement the dividing line between silt and very fine sand has been drawn at 0.0625 mm. We used the 74-μ level of separation for ex-

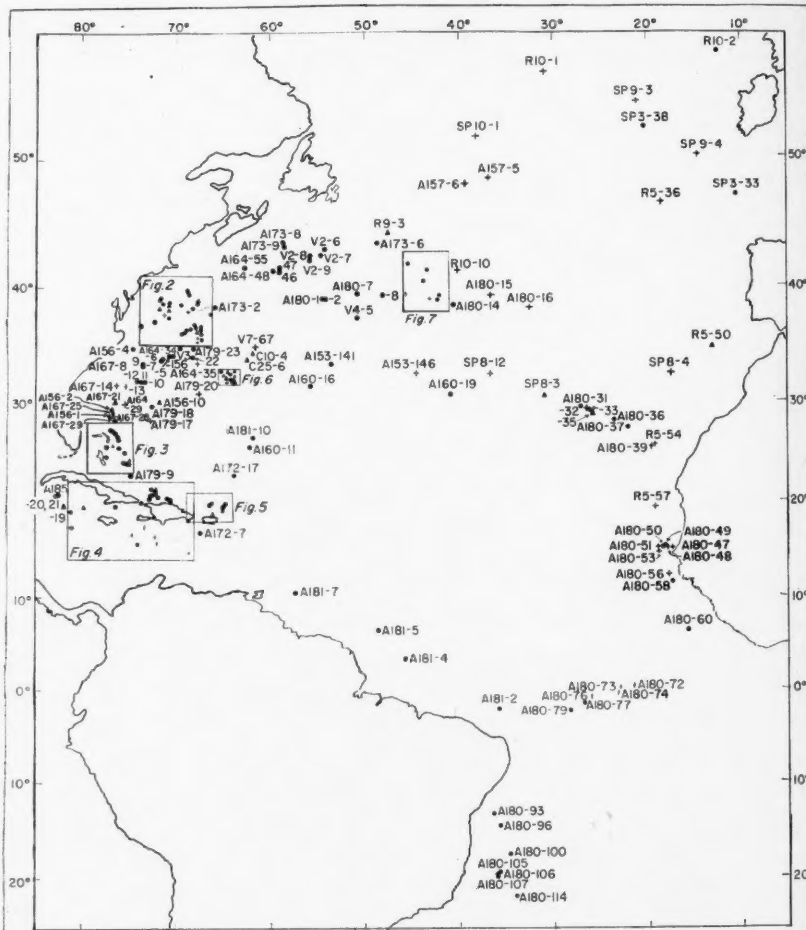

Figure 1. Locations of Cores. *See* Figures 2–7 for core numbers within insets. A dot indicates a core containing quartz- or calcareous-sand and/or -silt layers; a cross, a core without sand or silt layers; a triangle, a core with sediments older than Pleistocene.

pediency. The 62-μ bronze gauze would be prohibitively expensive because of the short life of such material under the severe conditions of use at Lamont. In contrast, replacement discs of 200-mesh stainless-steel gauze are inexpensive and easily obtainable from suppliers of equipment to the laboratories of petroleum companies.

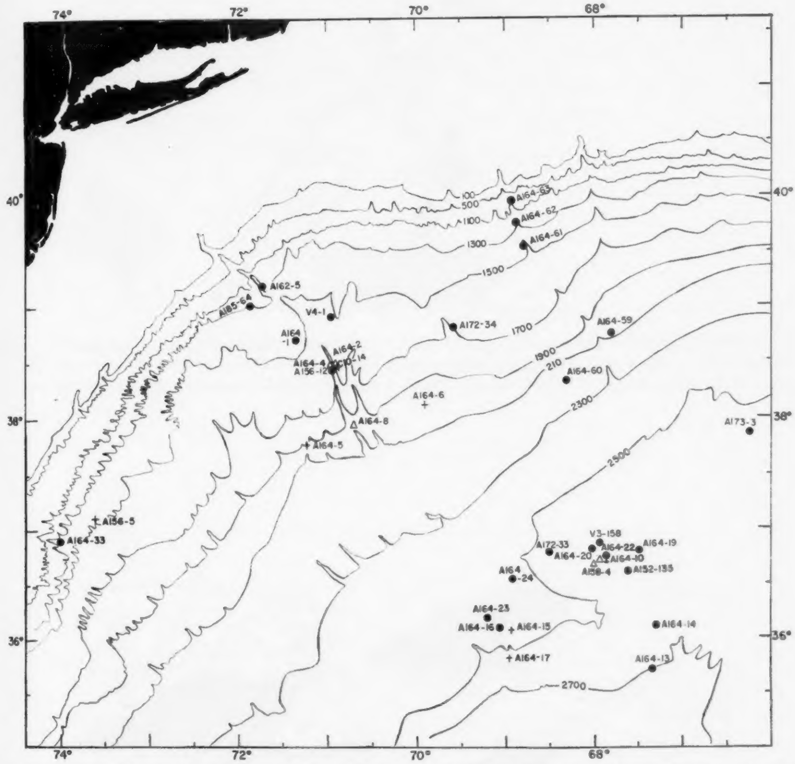

Figure 2. Topography and Locations of Cores from the Hudson Submarine Canyon Region. *See* Figure 1 for location. Contours in fathoms. A dot denotes a core containing quartz-sand and/or -silt layers; a cross, a core without sand or silt layers; a triangle, a core with sediment older than Pleistocene.

Core Locations and Physiographic Settings

Figure 1 shows the locations and numbers of cores included in this report. The letter before a core number indicates the research vessel by which the core was taken: A stands for ATLANTIS and C for CARYN, research vessels of the Woods Hole Oceanographic Institution, V for VEMA, research vessel of the Lamont Geological Observatory, R for REHOBOTH and SP for SAN PABLO, both ships of the U. S. Hydrographic Office. The number directly following the letter is the number of the cruise, and the number following the hyphen is the number of the particular station at which the core was taken.

Figures 2–7 show the locations of the cores with respect to the bottom topography of the following regions: Hudson Submarine Canyon, Bahamas, Western Caribbean, Puerto Rico Trench, Bermuda, and the Northwest Atlantic Mid-Ocean Canyon. Figure 8 shows the distribution of the various kinds of sediments in the cores.

Table 1 gives the latitudes and longitudes of the coring stations, depths of water, lengths of cores, and the physiographic settings of the core stations according to the Heezen, Tharp,

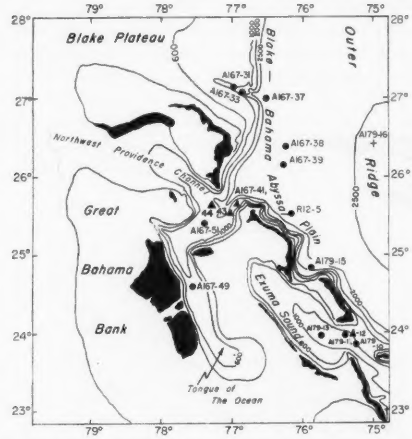

Figure 3. Topography and Locations of Cores from the Bahama Islands Region. *See* Figure 1 for location. Contours in fathoms. A dot indicates a core containing calcareous-sand and/or -silt layers; a cross, a core without sand or silt layers; a triangle, a core with sediment older than Pleistocene.

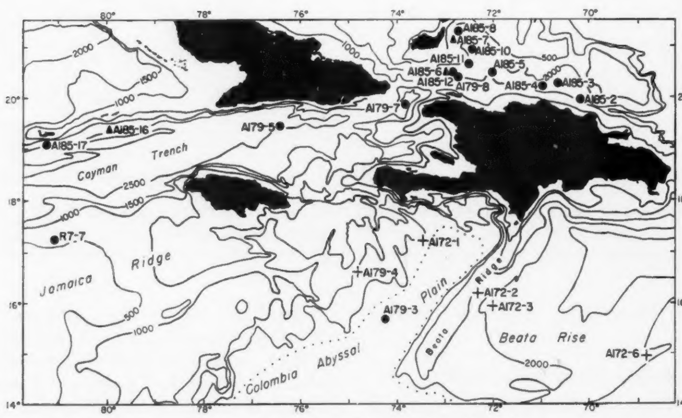

Figure 4. Topography and Locations of Cores from the Western Caribbean. *See* Figure 1 for location. Contours in fathoms. A dot denotes a core containing calcareous-sand and/or -silt layers (except for core A179–3, which contains quartz-sand and -silt layers); a cross denotes a core without sand or silt layers; a triangle, a core with sediment older than Pleistocene.

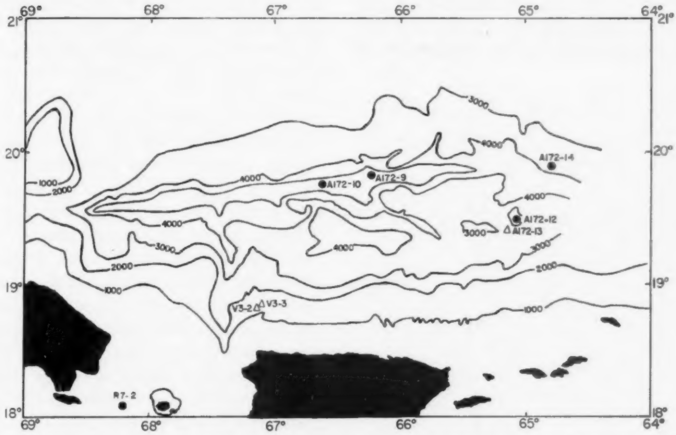

Figure 5. Topography and Locations of Cores from the Puerto Rico Trench Region. *See* Figure 1 for location. Contours in fathoms. A dot indicates a core containing calcareous-sand and/or -silt layers (except for cores A172–12 and A172–14 which contain quartz silt); a triangle, a core with sediment older than Pleistocene.

Figure 6. Topography and Locations of Cores from the Bermuda Region. *See* Figure 1 for location. Contours in fathoms. A dot denotes a core containing calcareous-sand and/or -silt layers; a triangle, a core with sediment older than Pleistocene.

and Ewing (1959) classification of deep-sea physiographic provinces as shown in Figure 10.

Plate 1A shows the locations and distribution of sediments in cores containing sand and silt layers, and Figure 9 shows the topography of

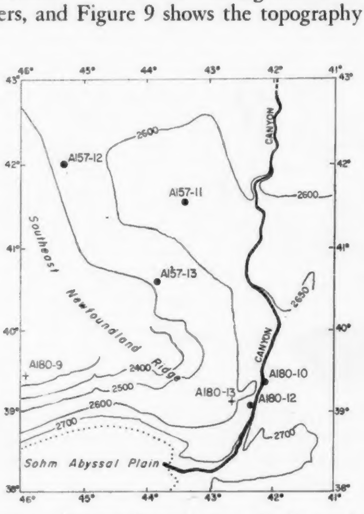

Figure 7. Topography and Locations of Cores from the Northwest Atlantic Mid-Ocean Canyon Region. *See* Figure 1 for location. Contours in fathoms. A dot indicates a core containing quartz-sand and/or -silt layers; a cross, a core without sand or silt layers.

the Hudson Submarine Canyon region with graphic logs of the cores.

Lithology of Pleistocene Cores

Applying the same program of detailed study to every core would waste time and money. We have found it helpful to make a preliminary, mainly visual, description of each core. Because important color changes take place in some sediments within an hour after splitting, it is desirable to write the preliminary descriptions with a minimum of delay, in terms which do not require more knowledge of mineral, chemical, or particle-size properties than can be obtained with a hand lens and some dilute hydrochloric acid.

In general, our endeavor has been to describe as objectively as possible but not necessarily to classify. Early in the investigation, attempts were made to use the accepted classification of deep-sea sediments. Conformity in this respect appeared to be desirable if only for the sake of brevity. We concede that it may seem naïve to call a certain sediment "light-tan (12C5 −)[1] thoroughly burrow-mottled abundantly foraminiferal lutite" when we could call the material *Globigerina* ooze. But does the definition of *Globigerina* ooze include burrow mottling? Presumably not, although the presence or absence of burrow mottling is important evidence of the process by which the sediment was laid down. On the other hand, having briefly described the sediment, do we gain anything by appending to the description the tag *Globigerina* ooze? We think not.

In short, it is not our intention to replace the old classification of deep-sea sediments with one of our own. If we do not use the terms red clay, *Globigerina* ooze, blue mud, and others, it is because in this particular investigation such terms do not serve our purpose. When much more is known about deep-sea sediments, it may be possible to elaborate a really satisfactory classification and nomenclature which will not stultify our understanding of depositional processes.

COLOR: The Maerz and Paul (1930) Color Dictionary has been used when particular precision has been desirable for recording colors. However, matching colors of the sediments with the color plates is time consuming, particularly if the layer of sediment is mottled or shows continuous color gradation from bottom to top. Furthermore, in order to make the colors as recorded in the lithological logs intelligible without constant reference to the Color Dictionary, it is necessary to add to the number of the color square in the dictionary an approximate description using common color names. These verbal descriptions are in themselves sufficiently precise for most purposes. For example, color differences are useful in distinguishing layers of slow continuous accumulation from layers deposited by turbidity currents. In cores from deep stations, many layers deposited by turbidity currents are gray and contrast with the interbedded brown lutite of abyssal facies. Here the simple words brown and gray are enough; it is doubtful if more precise definition of the colors could help us to a better understanding of the depositional processes involved.

A finer distinction is needed when reddish-

[1] (12C5−) refers to plate, column, and row of a color square in the Color Dictionary of Maerz and Paul (1930). The minus sign following the number means that the color of the sediment was slightly lighter than the color square.

brown lutite is cored at stations where "red clay" might be expected. The reddish-brown lutite is more nearly red than the truly abyssal "red clay," which is in fact brown. Here again other evidence to be presented shows that such possible source of some of the reddish-brown lutite layers interbedded with sediments of normal deep-water facies.

Hydrotroilite, an amorphous monosulfide of iron, $FeS.nH_2O$, occurs in some cores as in-

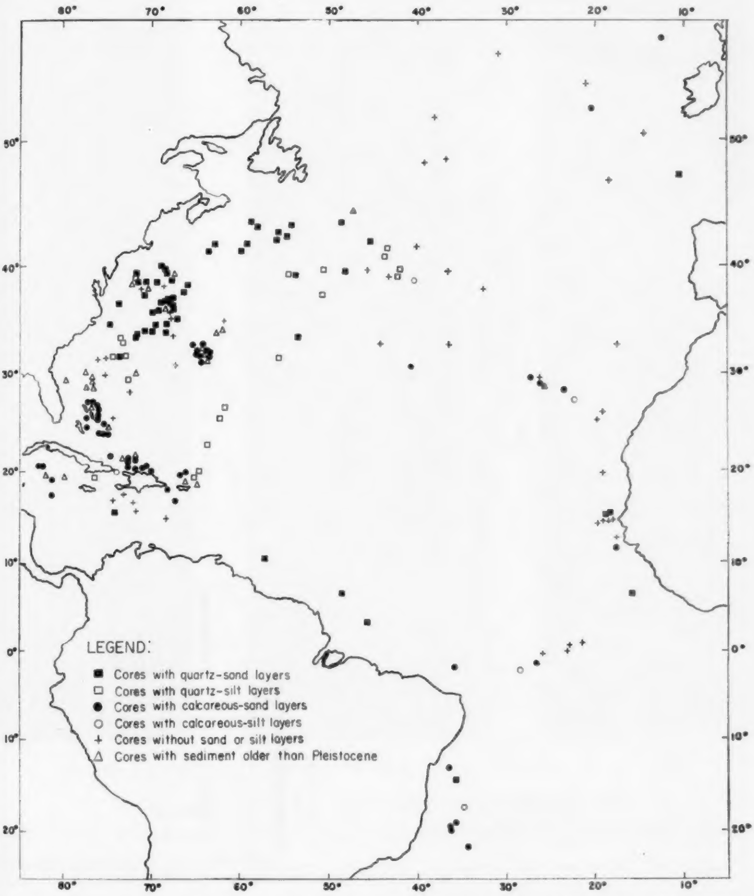

Figure 8. Locations and Distribution of Sediments in the Cores. Many of the cores which contain sand layers also contain silt layers.

reddish-brown lutite layers, like the gray layers previously mentioned, have been deposited by turbidity currents; the reddish color is probably due to subaerial oxidation during an earlier depositional cycle. Off the northeastern coast of North America the Triassic Newark series is a tensely black to dark-gray staining either fairly evenly disseminated or as speckling or irregular blotches. This colloidal sulfide in contact with air rapidly decomposes through oxidation of the iron. The reaction, strikingly apparent in the rapid color change from dark gray or inky black to rusty brown, distinguishes hydrotroilite from black speckling due to micronodules of iron-manganese oxide.

None of the cores described has hydrotroilite hydrotroilite. Presumably its formation depends upon the generation of hydrogen sulfide by anaerobic bacteria which take over several decimeters below the sediment surface after

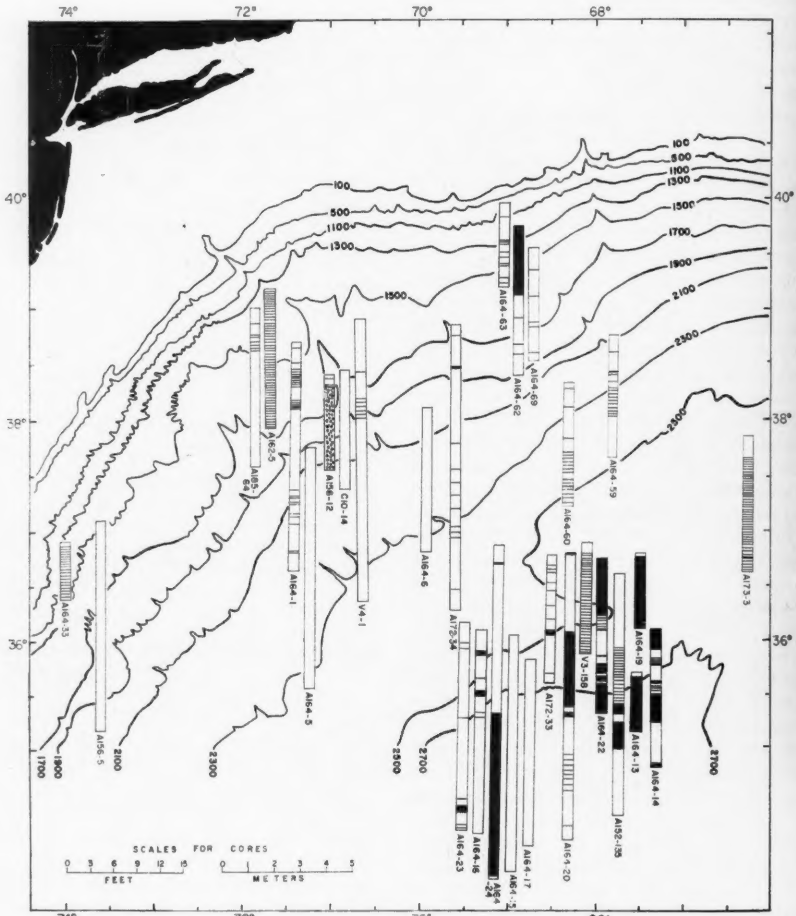

Figure 9. Topography of the Hudson Submarine Canyon Region and Columns of the Cores. Contours in fathoms. The top of the column is the approximate location of the core station. A black zone indicates quartz-sand and /or -silt, a line indicates a thin quartz-sand or -silt layer; an open zone indicates lutite. The dotted zone in core A156–12 denotes gravel.

in the upper few decimeters. Furthermore, benthic Foraminifera and burrow mottling throughout many of the cores containing hydrotroilite show that stagnation of bottom water is not necessary for the formation of the oxygen dissolved in the interstitial water has been exhausted by aerobic bacteria. Although anaerobic sulfate-reducing bacteria may be responsible for the generation of hydrogen sulfide in some cases, the rather common

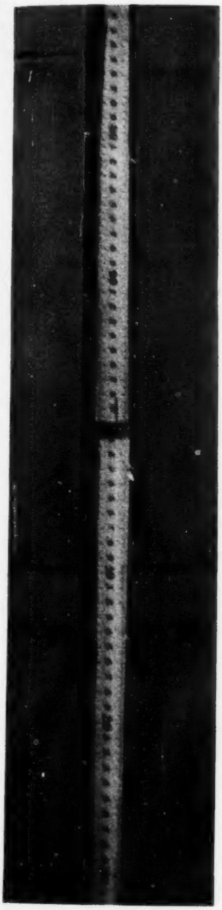

Figure 1

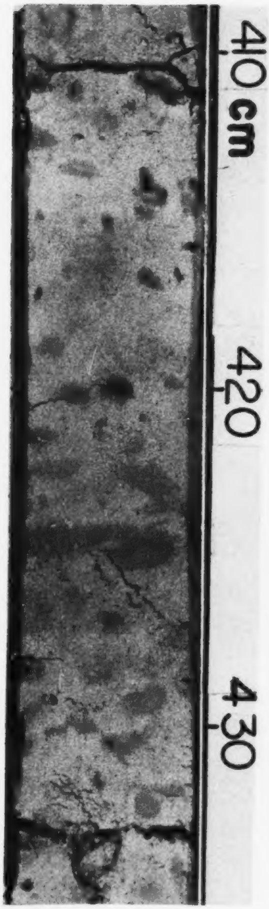

Figure 2

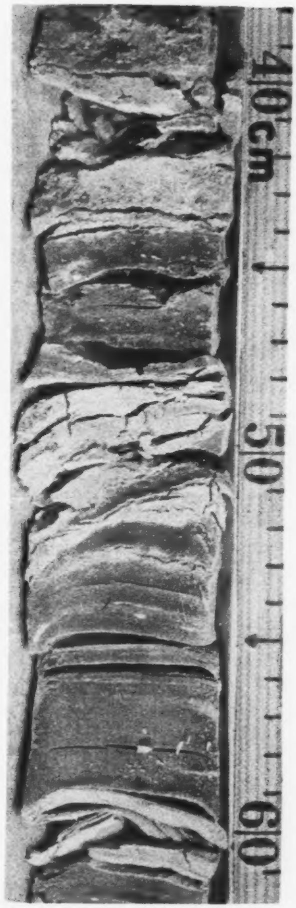

Figure 3

CORES SHOWING DIAGNOSTIC CHARACTERISTICS

Figure 1.—Core A167-5. Gray lutite with black hydrotroilite staining. The photograph was taken within less than half an hour after the core was split.

Figure 2.—Foraminiferal lutite with burrow mottling

Figure 3.—Thin bedding owing to a succession of small turbidity currents in the absence of mud feeders

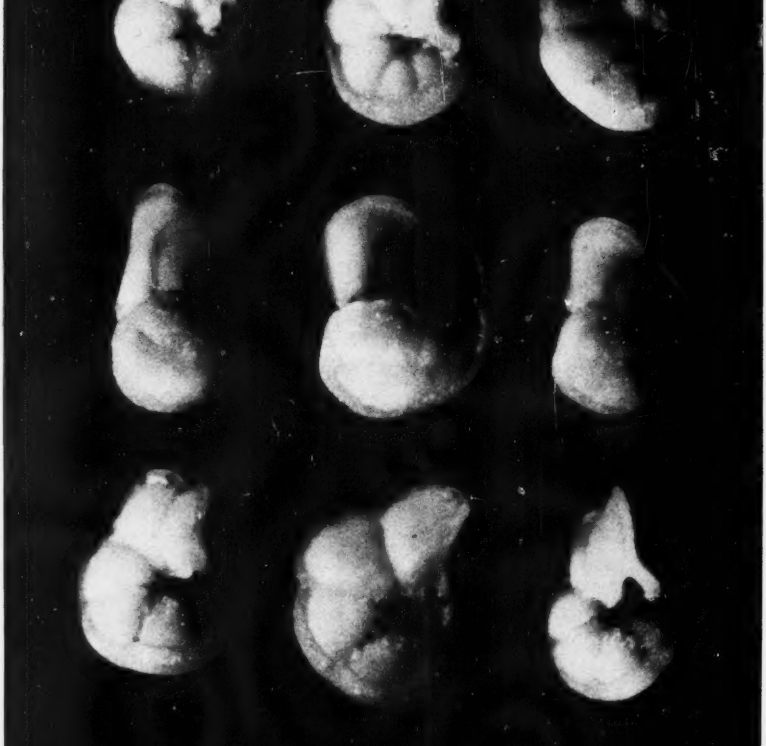

GLOBOROTALIA MENARDII FLEXUOSA (KOCH)

From zone (x) at 300 cm in core A172-7 (*See* Fig. 37). Note extreme thickening of keel and rough texture of earlier chambers because of the coarsely crystalline calcite layer.

association of organic matter, particularly plant detritus, and abundant hydrotroilite suggests that much hydrogen sulfide is produced by heterotrophic bacteria acting upon organic substances such as proteins. Thus organic matter entrained by turbidity currents and deposited with the lutite fraction may well account for the common appearance of hydrotroilite staining in the upper fine-grained parts of graded layers. It is also significant that the marcasite in the Neogene clays of the Hudson Submarine Canyon region, described later in this report, occurs in the form of fecal pellets and as fillings of diatom frustules. Very probably this marcasite is due to reorganization of hydrotroilite originally precipitated through the interaction of iron salts and hydrogen sulfide generated by anaerobic bacteria working on organic substances containing sulfur remaining in the fecal pellets and diatom frustules.

In the past some kinds of sediments containing hydrotroilite have been classified as blue muds. Water-saturated dark-gray or nearly black sediments may appear to have a bluish tinge when seen on shipboard under a blue sky, but in the laboratory the sediments containing hydrotroilite are gray of various shades or black. Accordingly we have not used the term blue mud in describing the cores.

Figure 1 of Plate 2 shows hydrotroilite staining in core A167–5.

BURROW MOTTLING: Mottling due to burrowing by mud-feeding animals is a reliable criterion by which sediments of slow particle-by-particle accumulation may be distinguished from layers of catastrophic deposition. Figure 2 of Plate 2 shows typical burrow mottling in a core from the Equatorial Atlantic.

The complete absence of burrow mottling from the lower parts of graded layers, even if they are composed of fine sediment, is probably due to the sudden deposition of several decimeters or even meters of sediment. When mud feeders recolonize the disaster area they confine their burrowing to the upper part of the recently deposited layer. Frequently they introduce some sediment of slow accumulation into the upper part of the underlying layer of turbidity-current deposition. When the two sediments differ in color, as is common, the mottling is particularly conspicuous.

Such burrow mottling below abrupt color changes shows that normal mud feeders rarely penetrate much more than about 10 cm below the water-sediment interface and that really significant mixing of sediment by burrowers is confined to the uppermost 5 cm. Although isolated burrows extending down to as much as 50 cm below color changes have been observed, these are far too rare to have any significant mixing effect.

The role of mud feeders in the vertical scattering of volcanic glass shards presumably due to a single explosive eruption has been fully discussed by Bramlette and Bradley (1940, p. 22) in their description of a suite of cores from the North Atlantic.

Arrhenius (1952, p. 86), in his classic study of sediment cores from the East Pacific, summarizes the significance of burrowing as follows: "The occurrence of digging structures, more or less visible, may thus be taken as a characteristic of normal pelagic deposits. The lack of such structures indicates abnormal conditions, probably a very high rate of deposition."

BEDDING: Evidently thin sharply defined bedding can become a part of the geological record only in the absence of mud feeders or similar bottom dwellers capable of stirring the upper several centimeters of the ocean floor. The necessary desertion of the bottom environment could arise from nonaeration of bottom water. As yet the cores show no clear evidence of nonaeration in the North Atlantic during the Pleistocene. On the contrary, much evidence indicates that during the late Pleistocene, stagnation of bottom water did not take place on any broad scale.

All evidence indicates that the bottom environment from time to time has been made intolerable to the larger members of the benthic population by catastrophes in the form of floods of turbid water. Sharply defined bedding resulting from catastrophic deposition is common in the North Atlantic. We exclude from "sharply defined" all changes which include a transition zone as much as 1 cm thick. As a rule the lithological changes which can be attributed to climatic change on the evidence of the planktonic Foraminifera are marked by transition zones from 5 to 10 cm thick. In contrast, the contacts at the bases of layers which we regard as turbidity-current deposits are without trace of transition. On drying, the cores commonly break at these sharply defined contacts.

Figure 3 of Plate 2 shows such thin bedding.

TEXTURE: In this paper the particle-size classification of the Wentworth grade scale (Wentworth, 1922) has been used in a slightly modified form.

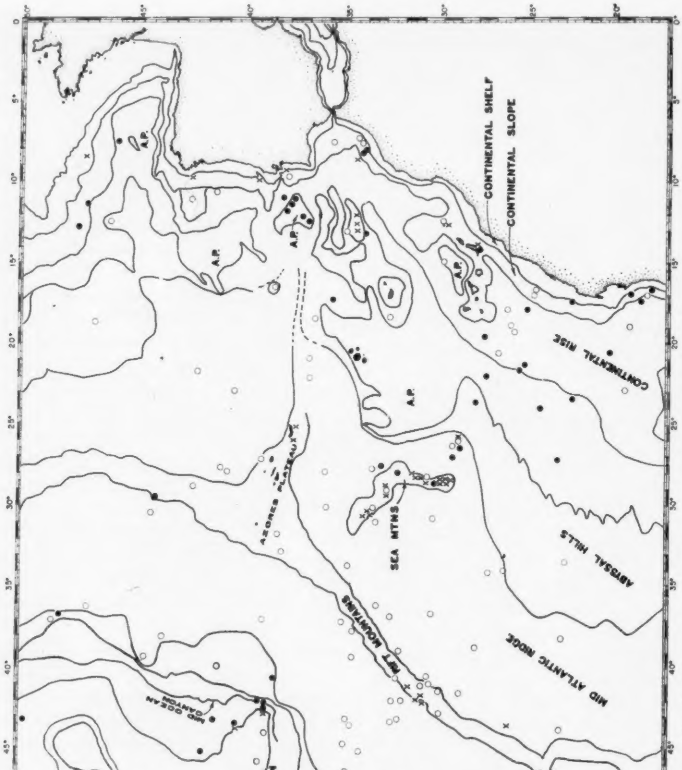

Figure 10. Physiographic Provinces of the North Atlantic. After Heezen, Tharp, and Ewing (1959).

TABLE 1.—LOCATIONS, DEPTHS, AND LENGTHS OF CORES

Core	Latitude	Longitude	Depth (M)	Depth (Fms)	Length (Cm)
A152–135	36°31′ N.	67°31′ W.	4845	2650	910
Abyssal plain near mouth of deep-sea fan of Hudson Submarine Canyon*					
A153–141	33°26′ N.	53°48′ W.	5350	2925	1025
South-central part of Sohm Abyssal Plain*					
A153–146	33°43′ N.	44°45′ W.	4050	2215	623
Upper Step Province of northwest flank of Mid-Atlantic Ridge†					
A156–1	28°36′ N.	77°10′ W.	1005	550	443
Blake Plateau**					
A156–2	29°12′ N.	76°49′ W.	2140	1170	566
Blake Escarpment**					
A156–4	34°49′ N.	74°41′ W.	3100	1695	1006
Upper continental rise east-southeast of Cape Hatteras, North Carolina*					
A156–5	37°07′ N.	73°37′ W.	2500	1370	792
Upper continental rise near base of continental slope off Cape Charles, Virginia†					
A156–10	39°25′ N.	71°53′ W.	1400	765	243
Continental slope northeast of Hudson Submarine Canyon**					
A156–12	38°23′ N.	70°57′ W.	3470	1900	365
Bed of Hudson Submarine Canyon*					
A157–5	48°35′ N.	36°51′ W.	4500	2460	320
Lower Step Province, west flank of Mid-Atlantic Ridge†					
A157–6	48°03′ N.	39°20′ W.	4500	2460	441
Abyssal hills east of northwest Atlantic Mid-Ocean Canyon†					
A157–11	41°34′ N.	43°24′ W.	4775	2610	858
Newfoundland Abyssal Plain*					
A157–12	42°00′ N.	45°22′ W.	4680	2560	301
A157–13	40°34′ N.	43°51′ W.	4680	2560	720
Lower continental rise east of the Grand Banks*					
A158–4	36°41′ N.	67°59′ W.	3940	2155	565
Steep slope of Caryn Peak in abyssal plain west of Bermuda Rise**					
A160–11	25°34′ N.	62°11′ W.	5725	3130	150
Eastern part of Nares Abyssal Plain*					
A160–16	31°19′ N.	55°48′ W.	5390	2945	486
Southern part of Sohm Abyssal Plain*					
A160–19	30°32′ N.	40°57′ W.	3310	1810	270
High Fractured Plateau east of crest of Mid-Atlantic Ridge*					
A162–5	39°10′ N.	71°46′ W.	2120	1160	530
Northeast wall of Hudson Submarine Canyon near foot of continental slope*					
A164–1	38°44′ N.	71°23′ W.	2780	1520	869
Southwest bank of Hudson Submarine Canyon on upper continental rise*					
A164–2	38°27′ N.	70°55′ W.	3475	1700	106
A164–4	38°12′ N.	70°51′ W.	3330	1820	103
East wall of Hudson Submarine Canyon**					
A164–5	37°46′ N.	71°14′ W.	3330	1820	816
A164–6	38°08′ N.	69°51′ W.	3675	2010	540
Near Hudson Canyon on gentle upper continental rise into which canyon has been cut†					
A164–8	37°56′ N.	70°44′ W.	3825	2090	61
Wall of Hudson Submarine Canyon**					
A164–10	36°43′ N.	67°56′ W.	3550	1940	253
Steep slope of Caryn Peak**					

* Pleistocene core containing sand and silt layers
† Pleistocene core without sand and silt layers
** Pre-Pleistocene core

TABLE 1.—*Continued*

Core	Latitude	Longitude	Depth (M)	Depth (Fms)	Length (Cm)
A164-13	35°43′ N.	67°20′ W.	4940	2700	225
A164-14	36°06′ N.	67°19′ W.	4810	2630	518
Abyssal plain off mouth of deep-sea fan of Hudson Submarine Canyon*					
A164-15	36°08′ N.	68°55′ W.	4480	2450	897
Lower continental rise southeast of deep-sea fan of Hudson Submarine Canyon†					
A164-16	36°08′ N.	69°08′ W.	4480	2450	774
Deep-sea fan of Hudson Submarine Canyon*					
A164-17	35°47′ N.	68°56′ W.	4665	2550	706
Lower continental rise southeast of deep-sea fan of Hudson Submarine Canyon†					
A164-19	36°45′ N.	67°23′ W.	4845	2650	285
A164-20	36°47′ N.	68°04′ W.	4845	2650	1087
A164-22	36°44′ N.	67°52′ W.	4790	2620	580
Abyssal plain off mouth of deep-sea fan of Hudson Submarine Canyon**					
A164-23	36°13′ N.	69°24′ W.	4370	2390	790
A164-24	36°29′ N.	69°00′ W.	4390	2400	1275
Deep-sea fan of Hudson Submarine Canyon*					
A164-25	32°13′ N.	64°31′ W.	2955	1570	360
A164-26	32°01′ N.	64°58′ W.	2700	1480	63
Bermuda Pedestal**					
A164-29	29°45′ N.	75°21′ W.	4480	2450	372
Lower part of Blake Escarpment†					
A164-30	30°04′ N.	76°57′ W.	1120	590	819
Blake Plateau**					
A164-33	36°54′ N.	73°58′ W.	2505	1370	316
Upper continental rise off Cape Charles*					
A164-34	34°57′ N.	69°44′ W.	5030	2750	234
Lower continental-rise hills due east of Cape Hatteras*					
A164-35	33°30′ N.	67°48′ W.	4975	2720	402
Western part of Bermuda Rise northwest of Bermuda Islands†					
A164-36	32°43′ N.	65°16′ W.	4515	2470	467
Bermuda Apron northwest of Bermuda Islands*					
A164-38	32°00′ N.	64°16′ W.	4250	2325	173
Bermuda Apron southeast of Bermuda Islands*					
A164-46	41°24′ N.	59°02′ W.	4775	2610	281
A164-47	41°43′ N.	59°00′ W.	4720	2580	71
A164-48	41°35′ N.	59°53′ W.	4665	2550	483
Near base of lower continental rise south of Nova Scotia*					
A164-55	41°47′ N.	62°55′ W.	3330	1820	325
Upper continental rise east of Browns Bank, Nova Scotia*					
A164-59	38°42′ N.	67°52′ W.	3970	2170	464
A164-60	38°20′ N.	68°25′ W.	4005	2190	465
Lower continental rise in vicinity of Hydrographer Submarine Canyon*					
A164-61	39°32′ N.	68°47′ W.	2650	1450	428
A164-62	39°45′ N.	68°53′ W.	2270	1240	565
A164-63	39°56′ N.	68°58′ W.	1790	980	320
In Hydrographer Submarine Canyon on upper continental rise*					
A167-5	34°09′ N.	70°51′ W.	5120	2800	964
A167-6	33°59′ N.	71°31′ W.	5010	2740	565
A167-7	33°53′ N.	71°44′ W.	5030	2750	520
Lower continental-rise hills off Cape Hatteras*					

* Pleistocene core containing sand and silt layers
† Pleistocene core without sand and silt layers
** Pre-Pleistocene core

TABLE 1.—*Continued*

Core	Latitude	Longitude	Depth (M)	Depth (Fms)	Length (Cm)
A167-8	33°13′ N.	73°39′ W.	4645	2540	630
A167-9	33°14′ N.	73°41′ W.	4645	2540	320
Lower continental rise about 300 km southeast of Cape Hatteras*					
A167-10	31°47′ N.	73°24′ W.	5030	2750	517
At lower continental rise-Hatteras Abyssal Plain boundary northeast of Blake Plateau*					
A167-11	31°48′ N.	73°58′ W.	4865	2660	401
A167-12	31°50′ N.	74°21′ W.	4700	2570	488
Lower continental-rise hills northeast of Blake Plateau*					
A167-13	31°39′ N.	75°21′ W.	2880	1575	450
A167-14	31°28′ N.	76°28′ W.	2635	1440	467
Outer ridge northeast of Blake Plateau†					
A167-21	29°49′ N.	76°35′ W.	1455	795	365
A167-25	28°52′ N.	76°47′ W.	1745	955	175
Blake Escarpment**					
A167-28	28°42′ N.	76°46′ W.	1260	690	415
Blake Plateau**					
A167-29	28°26′ N.	76°40′ W.	1730	945	435
Blake Escarpment**					
A167-31	27°04′ N.	76°51′ W.	3550	1940	360
Bed of Great Abaco Canyon north of Great Abaco Island, Bahamas*					
A167-33	27°06′ N.	77°00′ W.	2215	1210	132
South wall of Great Abaco Canyon*					
A167-37	26°59′ N.	76°31′ W.	4755	2600	447
Blake-Bahama Abyssal Plain at base of Blake Escarpment*					
A167-38	26°23′ N.	76°14′ W.	4625	2530	262
A167-39	26°09′ N.	76°16′ W.	4625	2530	914
Blake-Bahama Abyssal Plain east of Great Abaco Island, Bahamas*					
A167-41	25°39′ N.	76°56′ W.	3110	1700	488
A167-43	25°27′ N.	77°03′ W.	2605	1410	510
Wall of Northeast Providence Channel Canyon**					
A167-44	25°39′ N.	77°21′ W.	2560	1360	475
Wall of Northwest Providence Channel Canyon**					
A167-49	24°36′ N.	77°34′ W.	1735	950	370
Nearly flat floor near center of the Tongue of the Ocean, Bahamas*					
A167-51	25°23′ N.	77°24′ W.	3385	1850	255
Floor of Northwest Providence Channel Canyon, Bahamas*					
A172-1	17°14′ N.	73°28′ W.	4150	2270	488
Side of a knoll rising 180 m above 4150-m floor of Colombia Abyssal Plain†					
A172-2	16°12′ N.	72°19′ W.	3070	1680	493
Terracelike feature east of crest of Beata Ridge†					
A172-3	15°56′ N.	72°02′ W.	3340	1825	563
East flank of Beata Ridge†					
A172-6	14°59′ N.	68°51′ W.	4160	2275	935
Gentle slope of eastern part of Beata Ridge†					
A172-7	16°55′ N.	67°30′ W.	4885	2670	1067
Smooth floor of Dominican Trench south of Mona Passage*					
A172-9	19°48′ N.	66°11′ W.	7955	4350	280
A172-10	19°45′ N.	66°37′ W.	7955	4350	397
Flat floor of Puerto Rico (Trench) Abyssal Plain*					
A172-12	19°28′ N.	65°04′ W.	6630	3625	178
South scarp of Puerto Rico Trench*					
A172-13	19°24′ N.	65°07′ W.	6400	3500	98
East slope of a seamount on northern wall of Puerto Rico Trench**					

TABLE 1.—*Continued*

Core	Latitude	Longitude	Depth (M)	Depth (Fms)	Length (Cm)
A172–14	19°54′ N.	64°48′ W.	7130	3900	300
Near base of north wall of Puerto Rico Trench*					
A172–17	22°46′ N.	63°58′ W.	5610	3070	378
South-central part of Nares Abyssal Plain*					
A172–21	31°49′ N.	63°52′ W.	4500	2460	270
A172–22	31°55′ N.	64°00′ W.	4480	2450	80
A172–23	31°57′ N.	64°04′ W.	4350	2380	355
A172–25	31°58′ N.	64°20′ W.	4135	2260	560
Bermuda Apron southeast of Bermuda*					
A172–33	36°43′ N.	68°32′ W.	4700	2570	490
Deep-sea fan of Hudson Submarine Canyon*					
A172–34	38°43′ N.	69°40′ W.	3090	1690	1092
Upper continental rise northeast of Hudson Submarine Canyon*					
A173–2	38°30′ N.	66°01′ W.	4480	2450	870
A173–3	37°49′ N.	66°22′ W.	4410	2575	515
Lower continental rise south of Georges Bank*					
A173–6	43°38′ N.	48°22′ W.	3110	1700	915
Upper continental rise east of the Grand Banks*					
A173–8	43°40′ N.	58°46′ W.	2725	1490	1025
Lower part of "Gully" submarine canyon on continental slope east of Sable Island*					
A173–9	43°27′ N.	58°34′ W.	3245	1775	374
Lower part of "Gully" submarine canyon on upper continental rise*					
A179–3	15°40′ N.	74°13′ W.	4095	2240	630
Northeastern part of Colombia Abyssal Plain*					
A179–4	16°36′ N.	74°48′ W.	2965	1620	690
Jamaica Ridge southeast of Albatross Bank†					
A179–5	19°30′ N.	76°26′ W.	4390	2400	329
South slope of Cayman Trench*					
A179–7	19°55′ N.	73°50′ W.	2925	1600	300
Eastern end of Cayman Trench south of Windward Passage*					
A179–8	20°28′ N.	72°49′ W.	4060	2220	485
Hispaniola-Caicos Abyssal Plain northeast of Windward Passage*					
A179–9	22°43′ N.	74°53′ W.	2470	1350	440
Floor of sill between Long Island and Crooked Island, Bahamas*					
A179–10	23°48′ N.	75°15′ W.	2325	1270	260
A179–11	23°56′ N.	75°25′ W.	2175	1190	490
Floor of submarine canyon leading south through mouth of Exuma Sound*					
A179–12	24°02′ N.	75°22′ W.	1720	940	460
South slope of Cat Island at the mouth of Exuma Sound**					
A179–13	23°56′ N.	75°45′ W.	1850	1010	550
Flat floor of Exuma Sound*					
A179–15	24°48′ N.	75°55′ W.	3110	1700	560
Continental slope east of Eleuthera Islands*					
A179–16	26°24′ N.	74°59′ W.	4500	2460	490
A179–17	28°00′ N.	73°47′ W.	4390	2400	540
Outer ridge east of Bahamas†					
A179–18	29°29′ N.	72°45′ W.	4620	2525	490
Eastern flank of outer ridge east of Blake Plateau*					
A179–20	30°47′ N.	67°40′ W.	4995	2730	365
Bermuda Plateau section of Bermuda Rise southeast of Bermuda Islands†					

* Pleistocene core containing sand and silt layers
† Pleistocene core without sand and silt layers
** Pre-Pleistocene core

TABLE 1.—*Continued*

Core	Latitude	Longitude	Depth (M)	Depth (Fms)	Length (Cm)
A179-22	34°07′ N.	68°20′ W.	5120	2800	188
Northern edge of Hatteras Abyssal Plain between Bermuda and New York†					
A179-23	34°56′ N.	68°14′ W.	5050	2760	610
Abyssal gap between deep-sea fan of Hudson Submarine Canyon Abyssal Plain†					
A180-1	39°07′ N.	54°32′ W.	5190	2840	360
A180-2	39°06′ N.	54°11′ W.	5190	2840	100
A180-7	39°36′ N.	50°51′ W.	5285	2890	123
A180-8	39°23′ N.	48°10′ W.	5285	2890	144
North-central part of Sohm Abyssal Plain*					
A180-9	39°27′ N.	45°57′ W.	4060	2220	490
Southeast Newfoundland Ridge southeast of Grand Banks†					
A180-10	39°23′ N.	42°04′ W.	5030	2750	200
Flat bed of Northwest Atlantic Mid-Ocean Canyon*					
A180-12	39°05′ N.	42°20′ W.	5090	2710	460
On nearly flat western bank of Northwest Atlantic Mid-Ocean Canyon 90 m above bed*					
A180-13	39°08′ N.	42°39′ W.	4880	2590	445
Eastern end of Southeast Newfoundland Ridge†					
A180-14	38°41′ N.	40°40′ W.	5020	2650	445
Western edge of Abyssal Hills Province east of the southeast Newfoundland Abyssal Gap*					
A180-15	39°16′ N.	36°42′ W.	4610	2450	490
A180-16	38°21′ N.	32°29′ W.	2270	1240	367
Lower Step Province, western flank of Mid-Atlantic Ridge†					
A180-31	29°26′ N.	27°02′ W.	5250	2875	445
Abyssal hills west of Madeira Abyssal Plain*					
A180-32	29°07′ N.	26°15′ W.	5030	2750	420
Abyssal hills halfway between Mid-Atlantic Ridge and Canary Islands†					
A180-33	29°05′ N.	26°08′ W.	5200	2845	437
Abyssal hills west of Madeira Abyssal Plain*					
A180-35	28°56′ N.	25°45′ W.	5030	2750	476
Abyssal hills southeast of Meteor Bank**					
A180-36	28°04′ N.	23°36′ W.	4950	2705	368
A180-37	27°21′ N.	22°03′ W.	5000	2735	471
Abyssal hills west of Madeira Abyssal Plain*					
A180-39	25°50′ N.	19°18′ W.	3470	1895	368
Upper continental rise off Africa and southwest of Canary Islands†					
A180-47	15°19′ N.	17°55′ W.	2195	1200	453
Wall of "Fosse de Cayar" Submarine Canyon northwest of Cape Verde, Africa†					
A180-48	15°19′ N.	18°06′ W.	1450	795	530
Near bottom of "Fosse de Cayar" Submarine Canyon northwest of Cape Verde, Africa†					
A180-49	15°20′ N.	18°12′ W.	2745	1500	450
A180-50	15°18′ N.	18°19′ W.	2835	1550	480
In bed of "Fosse de Cayar" Submarine Canyon on upper continental rise, northwest of Cape Verde, Africa*					
A180-51	15°18′ N.	18°24′ W.	2835	1550	425
A180-53	15°10′ N.	18°26′ W.	2940	1610	490
A180-56	12°14′ N.	17°46′ W.	2595	1420	368
Upper continental rise in vicinity of Cape Verde, Africa†					
A180-58	11°40′ N.	17°35′ W.	2240	1225	368
In a Canyon off Portuguese Guinea*					
A180-68	06°37′ N.	15°56′ W.	4910	2685	365
Near base of continental rise off Sierra Leone*					
A180-72	00°35′ N.	21°47′ W.	3840	2100	472
A180-73	00°10′ N.	23°00′ W.	3750	2050	490
A180-74	00°03′ S.	24°10′ W.	3330	1820	480
Eastern flank of Mid-Atlantic Ridge near Equator†					

TABLE 1.—*Continued*

Core	Latitude	Longitude	Depth (M)	Depth (Fms)	Length (Cm)
A180-76	00°46′ S.	26°02′ W.	3510	1920	425
Western flank of Mid-Atlantic Ridge near Equator†					
A180-77	01°26′ S.	26°55′ W.	5010	2740	123
On southwest flank of Mid-Atlantic Ridge*					
A180-79	02°04′ S.	28°11′ W.	5100	2790	412
Abyssal hills between Mid-Atlantic Ridge and South America*					
A180-93	13°04′ S.	36°26′ W.	4115	2250	470
On continental rise off Porto do Salvador, Brazil*					
A180-96	14°31′ S.	35°53′ W.	4390	2400	120
Near bottom of canyon on continental rise east of Brazil*					
A180-100	17°28′ S.	34°58′ W.	4260	2330	406
On continental rise off Brazil*					
A180-105	19°10′ S.	35°59′ W.	3840	2100	435
A180-106	19°24′ S.	36°02′ W.	3935	2150	210
A180-107	19°39′ S.	36°04′ W.	4025	2200	368
In canyons off Abrolhos Bank*					
A180-114	21°52′ S.	34°07′ W.	4435	2425	440
On continental rise off Abrolhos Bank*					
A181-2	02°00′ S.	35°58′ W.	4025	2200	300
A181-4	03°32′ N.	45°52′ W.	3655	2000	445
A181-5	06°32′ N.	48°43′ W.	3865	2115	435
A181-7	10°33′ N.	57°20′ W.	3765	2060	425
On continental rise off South America between Cape São Roque and Trinidad*					
A181-10	26°24′ N.	61°56′ W.	5855	3200	325
Northeastern portion of Nares Abyssal Plain*					
A185-2	19°59′ N.	70°13′ W.	3895	2130	447
A185-3	20°17′ N.	70°42′ W.	4115	2250	470
A185-4	20°14′ N.	71°00′ W.	4050	2215	320
A185-5	20°31′ N.	72°03′ W.	4050	2215	425
Hispaniola-Caicos Abyssal Plain*					
A185-6	20°31′ N.	73°00′ W.	3420	1870	240
A185-7	21°07′ N.	72°51′ W.	2470	1350	555
Insular slope west of Great Inagua Island**					
A185-8	21°18′ N.	72°45′ W.	3740	2045	477
A185-10	20°55′ N.	72°28′ W.	4000	2185	403
Northwest edge of Hispaniola-Caicos Abyssal Plain*					
A185-11	20°39′ N.	72°33′ W.	4025	2200	200
A185-12	20°29′ N.	72°50′ W.	4035	2205	425
Southwest portion of Hispaniola-Caicos Abyssal Plain*					
A185-16	19°25′ N.	79°48′ W.	2980	1630	360
North wall of Cayman Trench south of Cayman Brac Island**					
A185-17	19°05′ N.	81°16′ W.	3350	1830	490
North wall of Cayman Trench south of Cayman Islands*					
A185-19	19°51′ N.	82°00′ W.	2160	1180	555
North slope of Cayman Ridge northwest of Grand Cayman Island**					
A185-20	20°41′ N.	82°34′ W.	4300	2350	412
A185-21	20°42′ N.	82°41′ W.	4205	2300	1200
Yucatan Abyssal Plain of Yucatan Basin southwest of Cuba*					
A185-64	39°01′ N.	71°56′ W.	2255	1230	600
Upper continental rise near foot of continental slope on southwest bank of Hudson Submarine Canyon*					

* Pleistocene core containing sand and silt layers

† Pleistocene core without sand and silt layers

** Pre-Pleistocene core

TABLE 1.—*Continued*

Core	Latitude	Longitude	Depth (M)	Depth (Fms)	Length (Cm)
C10-4	33°40′ N.	62°30′ W.	1550	845	357
	Near top of Muir Seamount**				
C10-7	32°20′ N.	64°34′ W.	1150	625	287
C10-10	32°19′ N.	64°36′ W.	1005	550	182
C10-11	32°14′ N.	64°32′ W.	2230	1220	198
	Bermuda Pedestal**				
C10-13	38°22′ N.	70°56′ W.	3570	1955	419
	Wall of Hudson Submarine Canyon on upper continental rise**				
C10-14	38°24′ N.	70°52′ W.	2980	1630	450
	East bank of Hudson Submarine Canyon on upper continental rise†				
C22-2	32°11′ N.	64°45′ W.	1940	1060	140
C22-5	32°17′ N.	64°38′ W.	1095	600	120
C22-6	32°16′ N.	64°35′ W.	1510	825	189
C25-5	32°43′ N.	64°34′ W.	1710	935	280
	Bermuda Pedestal**				
C25-6	33°47′ N.	62°39′ W.	2360	1290	35
	West of crest of Muir Seamount**				
R5-36	46°55′ N.	18°35′ W.	4500	2460	620
	Lower Step Province, eastern flank of Mid-Atlantic Ridge southwest of Ireland†				
R5-50	34°58′ N.	13°11′ W.	1940	1060	168
	Southwestern slope of Ampere Bank, a seamount between Cape St. Vincent and Madeira**				
R5-54	25°52′ N.	19°03′ W.	3295	1800	388
	Upper continental rise southwest of Canary Islands†				
R5-57	19°40′ N.	19°06′ W.	2945	1610	515
	Upper continental rise off Mauritania, Africa†				
R7-2	18°06′ N.	68°11′ W.	2220	1215	300
	Continental slope south of Mona Passage between Puerto Rico and Hispaniola*				
R7-7	17°13′ N.	18°05′ W.	1245	680	545
	South Wall of Cayman Trench between Honduras and Jamaica*				
R9-3	44°33′ N.	47°33′ W.	3660	2000	365
	Upper continental rise east of Grand Banks**				
R10-1	56°47′ N.	31°00′ W.	2375	1300	305
	Eastern flank of Mid-Atlantic Ridge between Ireland and Cape Farvel, Greenland†				
R10-2	56°59′ N.	12°28′ W.	2305	1260	185
	Near foot of eastern slope of Rockall Bank in Rockall Channel northwest of Ireland*				
R10-10	41°24′ N.	40°06′ W.	4755	2600	415
	Near Western edge of Abyssal Hills Province in Newfoundland Basin†				
R12-5	25°34′ N.	76°12′ W.	4810	2630	735
	Blake-Bahama Abyssal Plain east of Eleuthera Island*				
SP3-33	47°11′ N.	11°25′ W.	4610	2520	545
	Near lower continental rise—Biscay Abyssal Plain boundary*				
SP3-38	52°06′ N.	20°21′ W.	3730	2040	169
	Abyssal gap southwest of Rockall Bank*				
SP8-3	30°24′ N.	30°47′ W.	4445	2430	55
	East flank of Mid-Atlantic Ridge west of Great Meteor Bank south of Azores**				
SP8-4	32°49′ N.	18°31′ W.	3365	1840	183
	Madeira Rise west of Madeira Island†				
SP8-12	32°37′ N.	36°46′ W.	3250	1775	185
	Upper Step Province, eastern flank of Mid-Atlantic Ridge southwest of Azores†				
SP9-3	53°53′ N.	21°06′ W.	2745	1500	375
	On Rockall rise east of Ireland†				
SP9-4	50°02′ N.	14°46′ W.	4205	2300	460
	Upper continental rise southwest of Ireland†				

TABLE 1.—*Continued*

Core	Latitude	Longitude	Depth (M)	Depth (Fms)	Length (Cm)
SP10-1	51°23′ N.	38°04′ W.	3695	2020	375
Lower Step Province western flank of the Mid-Atlantic Ridge northeast of Flemish Cap†					
V2-6	43°12′ N.	54°16′ W.	4205	2300	345
V2-7	42°47′ N.	54°47′ W.	4535	2480	330
V2-8	42°43′ N.	55°55′ W.	4115	2250	360
V2-9	42°28′ N.	54°54′ W.	4570	2500	470
Lower continental rise south of Newfoundland*					
V3-2	18°49′ N.	67°09′ W.	1830	998	459
V3-3	18°51′ N.	67°07′ W.	2595	1420	368
South wall of Puerto Rico Trench**					
V3-156	34°14′ N.	70°31′ W.	5140	2811	490
North end of Hatteras Abyssal Plain*					
V3-158	36°48′ N.	67°56′ W.	4775	2611	420
Abyssal plain off mouth of deep-sea fan of Hudson submarine Canyon*					
V4-1	38°53′ N.	70°55′ W.	2815	1541	1070
Upper continental rise northeast of Hudson Submarine Canyon*					
V4-5	37°22′ N.	50°58′ W.	5245	2868	262
Eastern arm of Sohm Abyssal Plain south of Grand Banks*					
V5-14	32°19′ N.	64°27′ W.	2305	1260	170
Bermuda Pedestal**					
V5-21	32°48′ N.	64°17′ W.	4245	2321	980
Bermuda Apron northeast of Bermuda Islands*					
V7-67	34°40′ N.	61°27′ W.	4180	2285	1205
Northeastern part of Bermuda Rise, northeast of Muir Seamount					

* Pleistocene core containing sand and silt layers
† Pleistocene core without sand and silt layers
** Pre-Pleistocene core

The term clay has not been used to designate a grade size because it has a definite mineralogical implication. Instead the term lutite has been applied to those sediments in which an important fraction consists of particles smaller than 0.004 mm. Particles of silt size are common, and in some instances the median diameter falls within the silt grade. The important distinction is that the sorting is poor and the proportion of fine material is large enough to mask particles of silt size, thus giving the sediment a smooth or even slick quality. In contrast the sediments which we have called silts are well sorted. Silts normally occur either as winnowed sediments on topographical highs exposed to gentle current scour or as parts of graded layers deposited by turbidity currents in depressions. In spite of the overlapping ranges of median diameters, the distinction between lutite and silt is useful and can be made easily with a hand lens.

The ranges of grade size used in this paper are as follows:

Silt: particle diameters 0.004–0.0625 mm
Fine sand: particles 0.0625–0.25 mm
Medium sand: particles 0.25–0.5 mm
Coarse sand: particles 0.5–2 mm
Granules: particles 2–4 mm.

Silts and sands are further classified as quartz sands and calcareous sands depending upon whether the dominant mineral is quartz or a calcium carbonate mineral. In the latter case, most of the material is of organic origin, not uncommonly with a fairly large proportion of comminuted calcareous algae, particularly *Halimeda* sp. Some calcareous sands have been found on topographical rises, presumably owing to the winnowing effect of gentle current scour which restricts accumulation of the finer grades. Winnowed sands are easily distinguished from sediments deposited by turbidity currents. Sorting is poor since all particles larger than a certain grade remain in place. Grading is absent, and transported remains of organisms of shallow-water environment are nowhere present. Of the sand and silt layers in the cores which belong to the class *Pleistocene cores containing sand and silt layers*, none is considered to have resulted from winnowing.

The term graded layer denotes a layer with relatively coarse material which grades upward into finer sediment. In most thin horizontal sections of graded layers, there is obvious particle-size sorting, particularly if the sediment is homogeneous in mineral composition. If it is not homogeneous, large particles of low-density material may occur together with finely divided denser material. For example, some silts in graded layers contain particles of plant detritus more than 1 mm in diameter. Almost invariably the basal boundaries of graded layers are sharply defined. If the layer grades upward into silt or lutite, the top is commonly indefinite and blends into the overlying sediment. In most cases the blurring of upper contacts of graded layers is due to mixing by mud feeders which thoroughly churn the upper few centimeters of the ocean floor but are unable to reach the basal contacts or are discouraged by increasing coarseness lower down in the layers. The significance of graded bedding has been discussed by Kuenen and Migliorini (1950), Kuenen and Menard (1952), and Kuenen (1953).

A layer of sand or silt is called nongraded when there is no appreciable change in average particle size from top to bottom.

PARTICLE-SIZE DISTRIBUTION IN THE GRADED LAYERS: Table 2 gives quartile and median diameters in microns, quartile deviations ($QD\phi$), and values of skewness ($SKq\phi$) of 84 sediment samples from graded layers.

The first step in the mechanical analysis of the samples was a separation into coarse and fine fractions by washing on a 74-μ sieve. Next the coarse fractions were dried and sieved. The size interval between sieves was one-quarter phi unit. Wherever the weight of the coarse fraction equaled or exceeded 75 per cent of the dry weight of the original sediment sample, the quartile diameters in the phi units could be obtained at once from the cumulative curve of percentages by weight of the grade sizes in phi units plotted on arithmetic graph paper. Where the coarse fraction was less than 75 per cent of the original sample weight, it was necessary to analyze the fine fraction by the pipette method (Krumbein and Pettijohn, 1938) in order to obtain a value for the third quartile.

The quartile deviation ($QD\phi$) and skewness ($SKq\phi$) were obtained from the quartiles by means of the following relationships:

$$QD\phi = \tfrac{1}{2}(Q_3\phi - Q_1\phi)$$
$$SKq\phi = \tfrac{1}{2}(Q_1\phi + Q_3\phi - 2Md\phi)$$

in which $Q_1\phi$ and $Q_3\phi$ are the first and third quartiles and $Md\phi$ is the median diameter in phi units (Krumbein and Pettijohn, 1938).

Figures 11 to 15 show the positions of the graded layers in the cores which were sampled for size analysis and the levels within the layers from which the samples were taken. Median diameters in microns shown beside the points sampled show the particle-size grading or increase in particle size downward within the individual layers.

Table 2 shows the prevalence of good sorting by the values of the $QD\phi$. Among the 84 core samples only 5 have quartile deviations which exceed unity, and of these none exceeds 1.23.

The quartile skewness, $SKq\phi$, is a measure of the asymmetry of the curve of particle-size distribution. Evidently if the curve is perfectly symmetrical, $SKq\phi$ is equal to zero. If spread of particle sizes is greater on the fine side of the median diameter, $SKq\phi$ has a positive value; in the reverse case its value is negative.

The dominance of positive skewness among the values shown in Table 2 may result from the composite nature of the samples. The greater spread of particle sizes on the fine side of the median diameter, as indicated by the positive skewness, may be due to the vertical gradation of particle sizes within the thickness of sediment sampled.

However, we surmise that positive skewness results from transportation and deposition. It is not improbable on theoretical grounds that the material in suspension in a turbidity current is skewed in the positive direction. This would follow from the fact that normally there should be no limit to the degree of fineness among the particles in suspension, whereas the degree of coarseness is strictly limited by the competency of the current at the particular point in its course. Obviously the material deposited at a particular point and instant will not be representative of the total mass of sediment in suspension, but the fact remains that although no material coarser than a certain upper limit can be deposited, at least some finer material

TABLE 2.—SIZE-FRACTION ANALYSES OF GRADED LAYERS

"Sample cm" indicates position of sample in cm from top of core.

Core	Sample cm	Q_1* (μ)	Md† (μ)	Q_3** (μ)	$QD\phi$††	$Skg\phi$***
A156-4	535	270	170	70	0.99	+0.29
A156-4	550	410	270	160	0.66	+0.09
A164-1	77	320	260	210	0.29	+0.03
A164-1	80	330	280	210	0.29	+0.06
A164-13	40	190	115	80	0.65	0.00
A164-13	220	230	165	115	0.50	0.00
A164-14	Top	180	140	90	0.50	+0.23
A164-14	65	370	280	190	0.46	+0.04
A164-14	250	110	65	44	0.65	−0.05
A164-14	352	280	210	150	0.45	+0.03
A164-22	Top	350	250	140	0.64	+0.14
A164-22	100	400	280	180	0.60	+0.05
A164-22	380	200	150	120	0.34	−0.01
A164-22	390	290	210	150	0.45	+0.03
A164-23	698	210	140	95	0.58	+0.05
A164-23	721	400	280	200	0.52	+0.03
A164-24	665	120	90	75	0.34	−0.01
A164-24	800	130	100	70	0.08	+0.03
A164-24	920	150	110	90	0.43	+0.03
A164-24	1240	210	150	100	0.53	+0.05
A164-24	1265	250	170	130	0.45	−0.10
A164-36	78	250	160	100	0.65	0.00
A164-36	92	400	300	200	0.50	+0.09
A164-36	231	350	260	120	0.77	+0.80
A164-36	380	980	650	220	1.15	+0.47
A164-38	Top	80	62	44	0.45	+0.05
A164-38	173	980	660	500	0.56	−0.07
A164-59	139	110	80	55	0.54	+0.10
A164-59	144	175	120	100	0.41	+0.02
A164-62	30	220	150	115	0.48	−0.13
A164-62	140	370	240	160	0.60	−0.05
A164-62	250	510	330	210	0.70	0.00
A167-39	435	290	220	140	0.51	+0.06
A167-39	524	620	490	310	0.54	+0.14
A172-22	25	240	180	130	0.42	+0.05
A172-22	77	400	280	220	0.43	−0.06
A179-3	560	160	120	70	0.53	+0.19
A179-3	602	200	140	80	0.63	+0.20
A179-7	32	300	170	120	0.64	−0.14
A179-7	38	310	210	150	0.53	−0.01
A179-7	66	210	110	60	0.87	+0.15
A179-7	74	200	130	80	0.64	+0.04
A179-9	Top	220	140	90	0.71	+0.04
A179-9	45	260	160	90	0.73	+0.06
A179-9	70	290	230	160	0.44	+0.08
A179-9	290	520	280	160	0.92	−0.14
A179-23	Top	250	170	120	0.5	0.00
A179-23	430	300	220	150	0.52	+0.03

* First quartile diameter
† Median diameter
** Third quartile diameter
†† Quartile deviation
*** Skewness

TABLE 2.—*Continued*

Core	Sample cm	Q_1* (μ)	Md† (μ)	Q_3** (μ)	$QD\phi$††	$Skg\phi$***
A180–1	Top	64	52	35	0.43	0.00
A180–1	71	74	62	48	0.35	−0.05
A180–2	Top	52	36	20	0.73	+0.17
A180–2	30	54	40	25	0.60	+0.10
A180–2	65	86	54	32	0.75	+0.05
A180–58	205	180	100	33	1.23	+1.34
A180–58	216	320	170	70	1.05	+0.21
A180–68	60	200	160	100	0.43	+0.08
A180–68	195	200	170	130	0.29	+0.04
A180–107	60	200	140	100	0.54	+0.07
A180–107	120	420	300	190	0.59	+0.09
A180–107	305	660	860	330	1.09	+0.31
A185–2	237	140	100	60	0.60	+0.09
A185–2	255	170	120	90	0.57	+0.04
A185–2	264	560	430	320	0.43	0.00
A185–5	145	260	160	90	0.82	+0.08
A185–5	158	640	440	290	0.58	+0.09
A185–12	377	350	230	150	0.63	+0.03
A185–12	387	400	260	170	0.59	+0.07
A185–21	415	160	120	90	0.45	+0.03
A185–21	500	230	170	130	0.43	−0.03
A185–21	570	350	250	160	0.55	+0.03
R7–2	Top	150	100	76	0.50	0.00
R7–2	100	350	250	190	0.45	−0.05
R7–2	205	560	400	310	0.45	−0.05
R7–2	215	500	350	280	0.43	−0.08
R7–2	300	720	500	360	0.55	0.00
R10–2	35	250	180	150	0.32	−0.10
R10–2	51	250	210	160	0.35	+0.04
R12–5	180	740	460	190	0.97	+0.31
R12–5	400	900	800	500	0.59	+0.12
R12–5	735	700	950	800	0.45	−0.03
V2–7	70	140	110	90	0.35	0.00
V2–7	135	160	130	110	0.26	−0.04
V4–1	198	220	130	42	1.12	+0.36
V4–1	200	520	400	200	0.74	+0.29

will certainly be trapped between the coarser particles. The fairly consistent positive skewness of the size distributions listed in Table 2 may be an additional means of distinguishing between deposits laid down by turbidity currents and sand and silt layers due to winnowing by deep-current scour. It must be emphasized that we do not suppose that well-sorted winnowed layers arise through removal of fine material from unsorted sediments after deposition. No doubt a sufficiently strong current could stir up the top several millimeters of an unsorted sediment and thereby produce a thin layer of lag material, but the very presence of this lag deposit would prevent further winnowing. To account for winnowed layers having thicknesses of 10 or more cm it is necessary to suppose that accumulation has taken place under the influence of a continuous or nearly continuous current which has prevented accumulation of particles below a certain grade size. Accumulation under such conditions should be extremely slow. Paleontological evidence and manganese oxide speckling on particles in winnowed layers both suggest that this is indeed the case. Thus the winnowing process would tend to prevent the accumulation of particles smaller than a certain limit, depending upon the velocity of the current, but it could not impose any limit in the coarser direction. Thus barnacle plates, quartz granules rafted by seaweeds, otoliths, and similar relatively large particles tend to be concentrated in winnowed layers and should affect the shape of the particle size-distribution curve appreciably.

A disturbing factor is variation in density among the particles carried along by a turbidity current. An extreme case, already cited, is the accumulation of coarse particles of plant detritus with quartz silt. This association is not common, but less extreme degrees of hydraulic density variation are. Examples are the association of relatively large shells of pteropods or Foraminifera with fine quartz sand. Presumably any method of mechanical analysis which corrected for this disturbing factor would accentuate the good sorting already found by sieve analyses.

COARSE FRACTION ($>74\mu$): Sediment samples

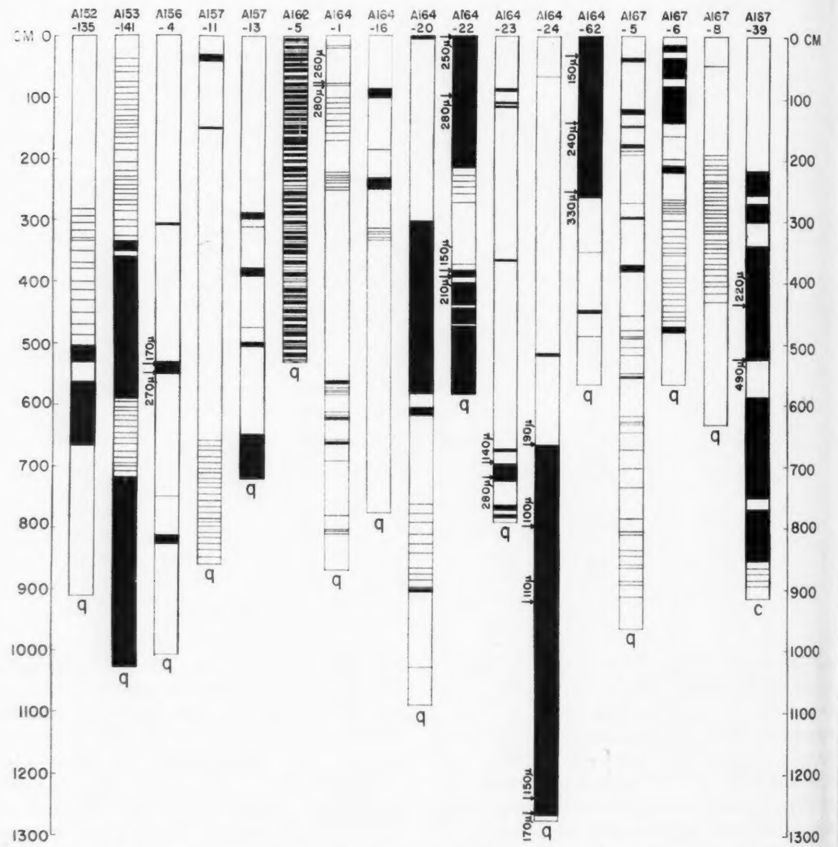

Figure 11. Pleistocene Cores Containing Sand and/or Silt Layers. *See* Figure 1 and Table 1 for core locations. Black zones indicate sand and/or silt; a line indicates a thin sand or silt layer; an open zone indicates lutite. The figures in microns show the median grain size of the sand or silt at the points referred to by arrows. A *q* at the bottom of a column indicates that the core contains quartz-sand and/or -silt layers; a *c* at the bottom of a column indicates that the core contains calcareous-sand and/or -silt layers.

intended for the study of Foraminifera are prepared by washing on a 74-μ sieve. In order to obtain as much information as possible it has been customary at Lamont to weigh the dry sediment samples before washing, to weigh the coarse fraction after washing, and to record the ratios of the weights as percentages of coarse fraction. Curves of variation in percentage of coarse fraction in selected cores are shown in Figures 16–21. Although percentages of coarse fraction do not take the place of complete mechanical analyses, they do provide valuable evidence as to processes and environments of deposition.

Cores A180-47, 48, 51, 53, and 56 (Fig. 19) from the vicinity of Cape Verde, French West Africa, are examples of sediments from an area receiving much finely divided terrigenous material. In these sediments of rapid accumulation the coarse fraction rarely exceeds 2 per cent. Farther from the continents the coarse fraction, largely composed of the tests of planktonic Foraminifera, accounts for an increasingly greater percentage of the sediment, as is shown in cores A179–4, A180–72, 73, 74, and 76 (Fig. 20).

At depths greater than 5000 m the percentage of coarse fraction decreases markedly because of solution of the tests of the planktonic Foraminifera. In normal abyssal brown lutites

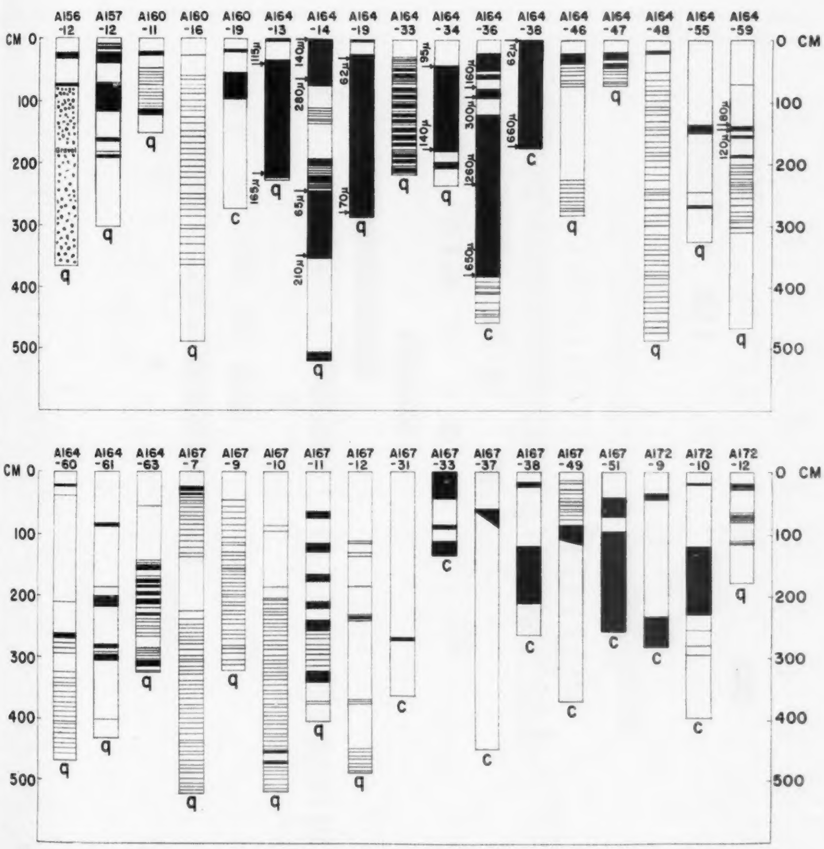

Figure 12. Pleistocene Cores Containing Sand and/or Silt Layers. *See* subcaption of Figure 11. Dotted zone in Core A156–12 denotes gravel.

or "red clays" the coarse fraction is less than 1 per cent as a rule. In such sediments it consists of little else than micronodules of manganese oxide, minute teeth of fish, and usually a few bronzite chondrules and meteoritic spherules.

Percentages of coarse fraction are useful in distinguishing between sediments of slow continuous accumulation and interbedded layers of catastrophic deposition by turbidity currents. Turbidity-current deposition may be suspected wherever the percentage of coarse fraction changes abruptly. A gradual decrease in coarse fraction from the bottom to top of a single layer is satisfactory evidence of grading which may be obtained without making several time-consuming mechanical analyses. Figures 16, 17, and 18 show variations in percentage of coarse fraction in cores containing layers deposited by turbidity currents.

WATER CONTENT AND COMPACTION: Most of the cores are extruded from the coring tubes on board ship and are brought back to the laboratory wrapped in thin sheets of plastic or in heavy paper treated to be impermeable. Since an appreciable amount of water is probably lost at the time of extrusion or later because of imperfect wrapping, no measurements of water content have been made on such cores.

A few water-content measurements have been made on cores which were received at the laboratory in the original coring pipes well sealed at the ends. The samples for water content were taken immediately after extrusion of the cores at the laboratory. The samples, taken from the cores with a brass cylinder and plunger about 1 cm in diameter, were extruded into weighing bottles. After the stoppered bottles were weighed, they were opened, the samples were dried at 105°C., and they were

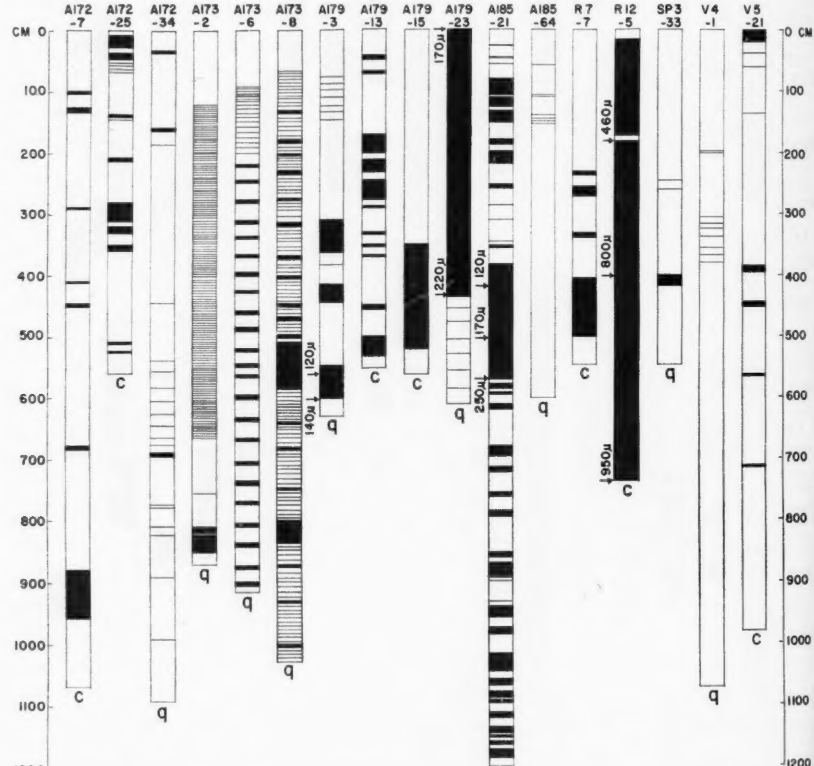

Figure 13. Pleistocene Cores Containing Sand and/or Silt Layers. *See* subcaption of Figure 11.

weighed again. Finally the cylindrical samples were broken open in order to make sure that they included no air pockets. The water contents have been calculated as percentage by volume of water in the original volume of sediment samples. Salt content of the interstitial water has been disregarded, and consequently the porosities are too low by the amount of salt weighed with the dry sediment. However, as relative values, the measurements should be accurate.

Except for a rather poorly defined increase in density or compaction between the top and about 1 m, there is no clearly defined trend toward greater compaction with depth of sediment. Probably the erratic variations from level to level are due to variations in proportion of clay minerals to finely divided quartz and calcite, rather than to variations in compaction *per se*.

Depth, cm	Per cent water by volume	Density of water-saturated sediment
R12-1: Position: 20°49′ N., 69°26′ W. Depth: 3660 m		
7	54	1.61
37	68	1.48
82	57	1.82
133	64	1.60
150	48	1.88
186	58	1.72
199	45	1.68
248	47	1.95
R12-2: Position: 20°20′ N., 68°40′ W. Depth: 2800 m		
35	69	1.64
48	67	1.62
73	66	1.67

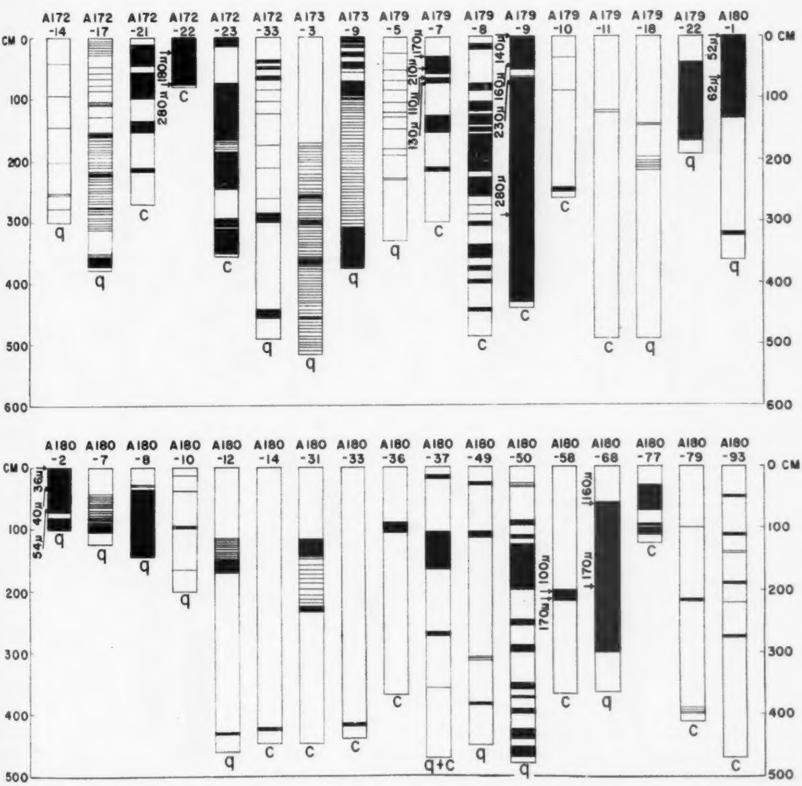

Figure 14. Pleistocene Cores Containing Sand and/or Silt Layers. *See* subcaption of Figure 11.

Depth, cm	Per cent water by volume	Density of water-saturated sediment
R12–4: Position: 25°47′ N., 75°43′ W. Depth: 4700 m		
Top	62	1.32
62	66	1.35
100	74	1.36
242	68	1.43
400	67	1.55
600	75	1.36
900	68	1.48
1000	75	1.31
SP12–12: Position: 18°48′ N., 65°58′ W. Depth: 2195 m		
Top	71	1.62
50	66	1.65
90	62	1.74
150	61	1.74
200	62	1.73
250	64	1.73
300	63	1.74
335	61	1.79

AREAL DISTRIBUTION OF THE VARIOUS KINDS OF SEDIMENTS: Figure 8 shows the locations of the cores and indicates which Pleistocene cores contain layers of quartz sand and silt, calcareous sand and silt, or no sand or silt. Also distinguished are those cores which contain sediments older than Pleistocene.

Plate 1A shows positions of sand layers, silt layers, and lutite in most of the cores together with the core locations.

Figure 9 shows diagrams of the cores obtained from the area of the Hudson Submarine Canyon together with the local bottom topography.

Sequences of sand layers, silt layers, and lutite layers in all cores containing coarse sediments are diagrammed in Figures 11–15. Median particle-size diameters in microns at various levels in the cores are also given in the diagrams. Lateral discontinuity of the sand and silt layers is evident from the lack of correlation between the cores. No theory which fails

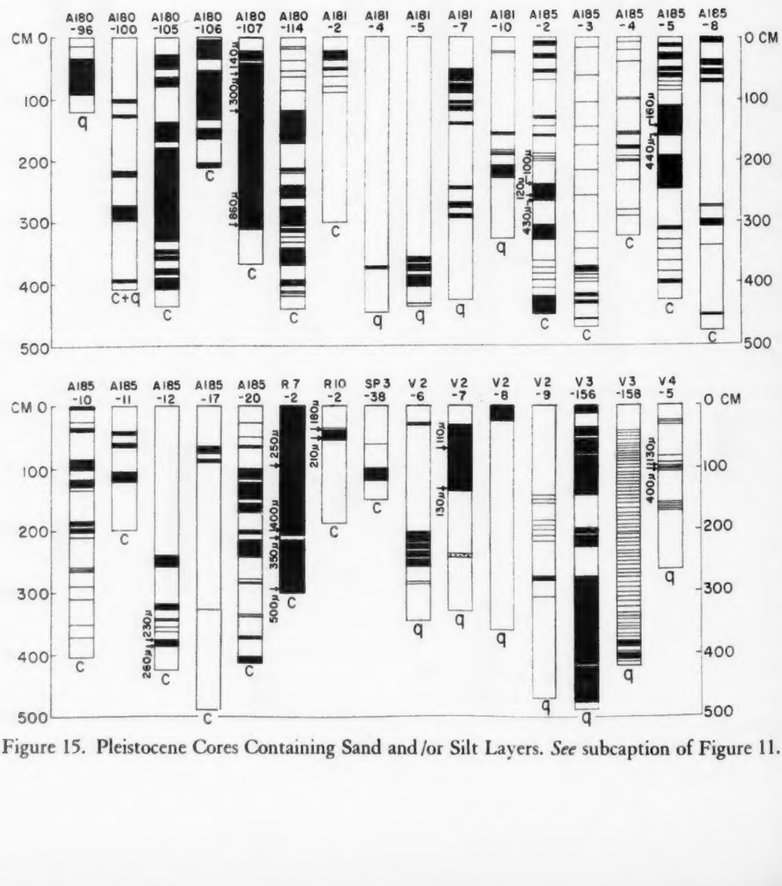

Figure 15. Pleistocene Cores Containing Sand and/or Silt Layers. *See* subcaption of Figure 11.

to explain the restricted areal extent of the individual graded layers and the fact that the interbedded sediment is in most cases unmistakably of abyssal facies can be given serious consideration.

Glacial marine sediment has not been indicated in the figures for sake of simplicity and because this facies is of minor importance among the cores described in this report. The term was first applied by Philippi (1910) to deposits adjacent to the ice front in Antarctica consisting dominantly of clastic material, including coarse sand and pebbles of various igneous and metamorphic rocks. The outstanding characteristic of the facies is its complete absence of particle-size sorting; this distinguishes such sediments from layers deposited by turbidity currents.

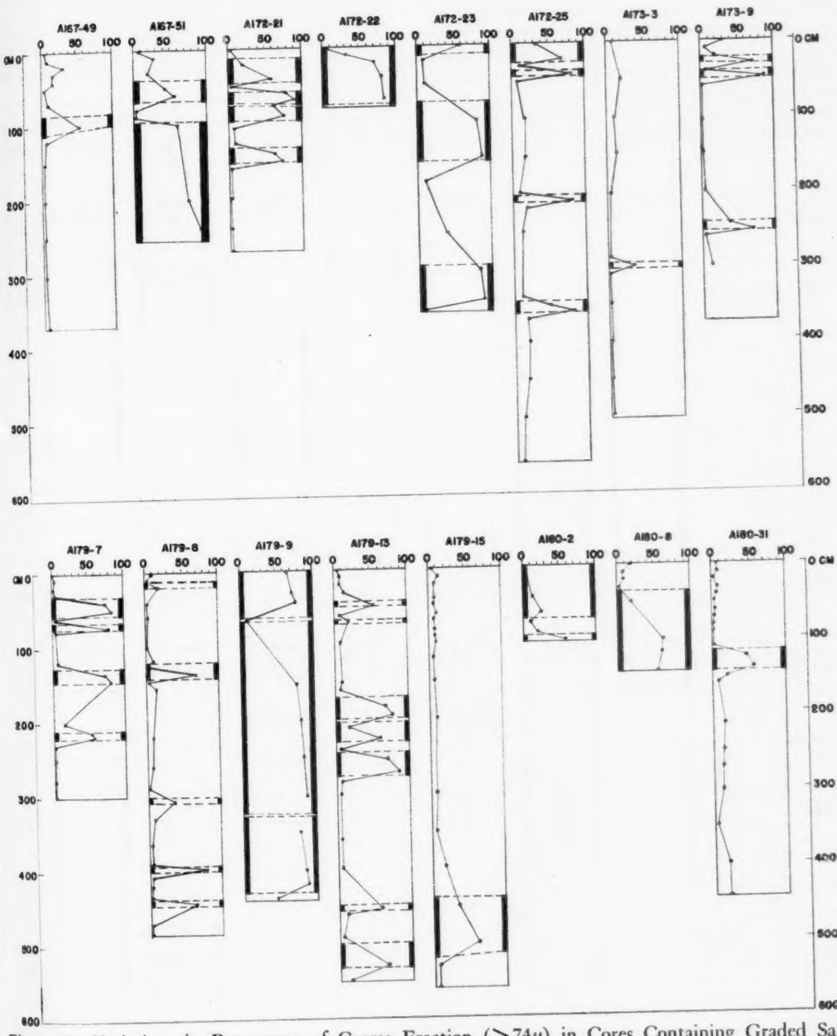

Figure 16. Variations in Percentage of Coarse Fraction ($>74\mu$) in Cores Containing Graded Sand Layers. Black boxes at the sides of core diagrams denote graded layers; dashed lines show tops and bottoms of layers. *See* Figure 1 and Table 1 for locations of cores.

SPECTROCHEMICAL ANALYSES: Table 3 gives results of spectrochemical analyses of top samples from 105 of the cores included in this paper. Dr. R. G. Smalley, who made the analyses, has commented on the accuracy of the values as follows.

"The samples range in type from siliceous and highly argillaceous sediments to nearly pure carbonates. Because of the wide range of sediment type and because single determinations only were made, the usual accuracy of $\pm 10\%$ of the amount present may not have been attained for certain element ranges. In particular, reliability of the SiO_2 analyses decreases above about 40% concentration and values over fifty are reported simply as greater than fifty. Al_2O_3 above 15% and TiO_2 above 1.0% tend to be less reproducible, in the same manner as SiO_2, with accuracies more nearly in the range of $\pm 20\%$ of the amount present."

Figure 22 shows the interdependence between SiO_2 and TiO_2, and Figure 23 shows that between CaO and SrO.

CALCIUM CARBONATE: Carbonate in selected samples from the cores has been determined at Lamont by the alkalimeter method. This method depends upon loss of carbon dioxide upon addition of dilute hydrochloric acid to the sample which is weighed before and after treatment. Thus the substance actually determined is carbon dioxide. In order to make our data comparable with previously published data, the results have been reported as "calcium carbonate". The method of analysis

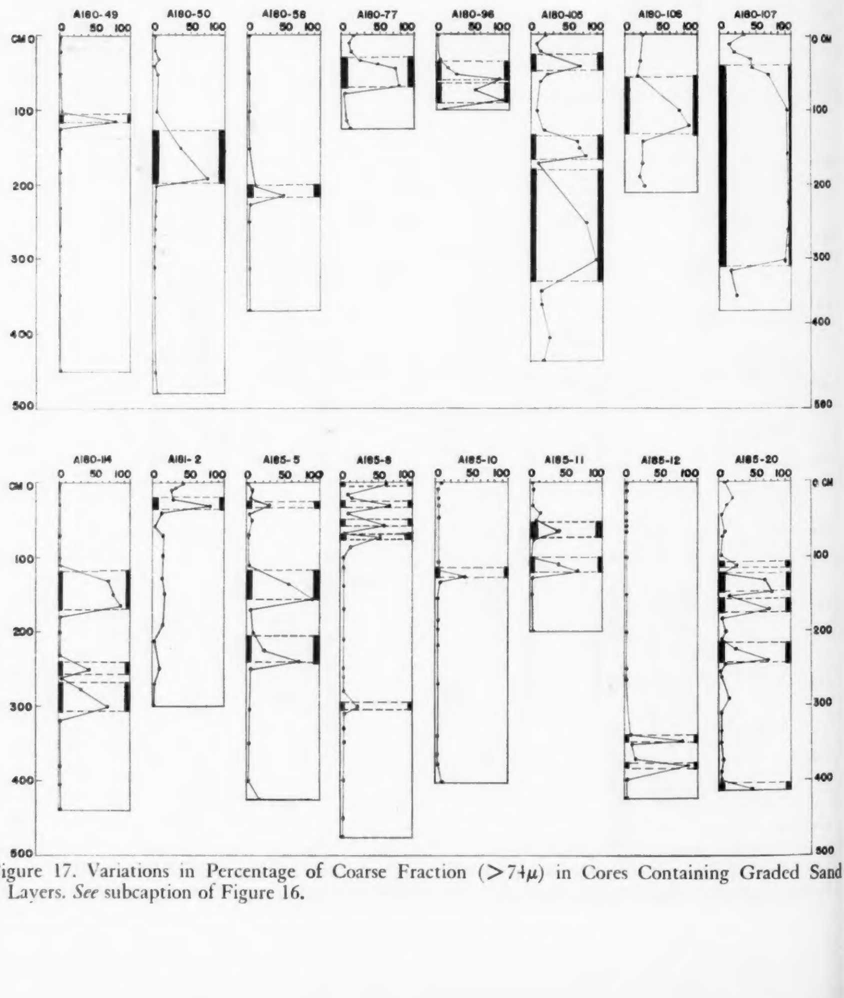

Figure 17. Variations in Percentage of Coarse Fraction ($>74\mu$) in Cores Containing Graded Sand Layers. *See* subcaption of Figure 16.

is not particularly exact, but it is reasonably rapid, does not require expensive apparatus, and has been adequate to show the important distinction in carbonate content between layers of abyssal brown lutite and interbedded gray lutites of turbidity-current deposition. Table 4 gives the results of the carbonate determinations.

In the last few years isotopic analyses of carbonate in sediments have been used to date samples and to determine paleotemperatures. For temperature determinations by the oxygen-isotope method the tests of planktonic Foraminifera have been used on the assumption that all the carbonate of the tests has been secreted in the photic zone. In view of the crucial importance of this assumption in the oxygen-isotope method, we will re-examine its validity.

The tests of planktonic Foraminifera caught in plankton nets towed in the photic zone differ markedly from most of those found in sediment samples. The surfaces of the tests from plankton samples are smooth and without apparent crystallinity even under high magnification. In contrast, many of the tests of certain species

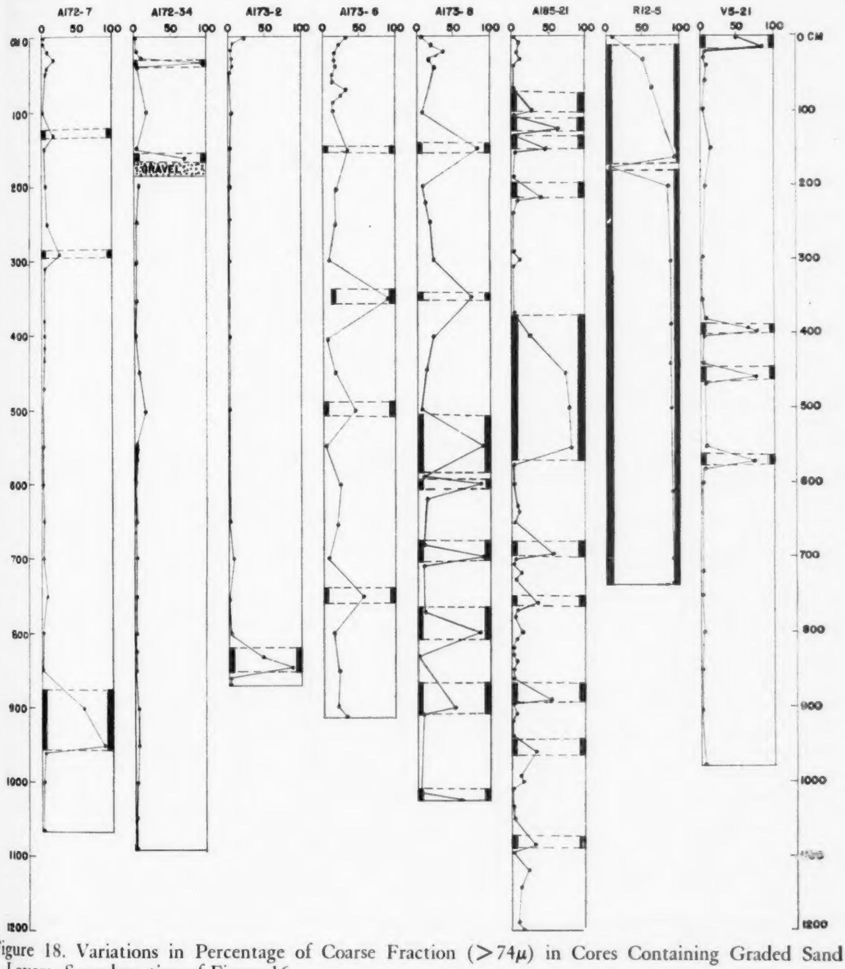

Figure 18. Variations in Percentage of Coarse Fraction ($>74\mu$) in Cores Containing Graded Sand Layers. See subcaption of Figure 16.

in the sediments have a sugary texture due to glittering faces of minute calcite crystals. Murray and Phillippi (1908) attributed it to recrystallization on the ocean bottom; Revelle (1944) and Phleger, Parker, and Peirson (1953) have also ascribed it to recrystallization. We cannot agree, however, that recrystallization is involved.

Examination of tests naturally broken or broken with a needle shows that the sugary surface is due to a discrete layer of calcite crystals which may be chipped off; the original surface of the test is smooth and entirely similar to that of specimens taken in plankton nets. Apparently no reorganization of the original shell has taken place. We must also reject the explanation that the calcite crust is due to inorganic precipitation of calcium car-

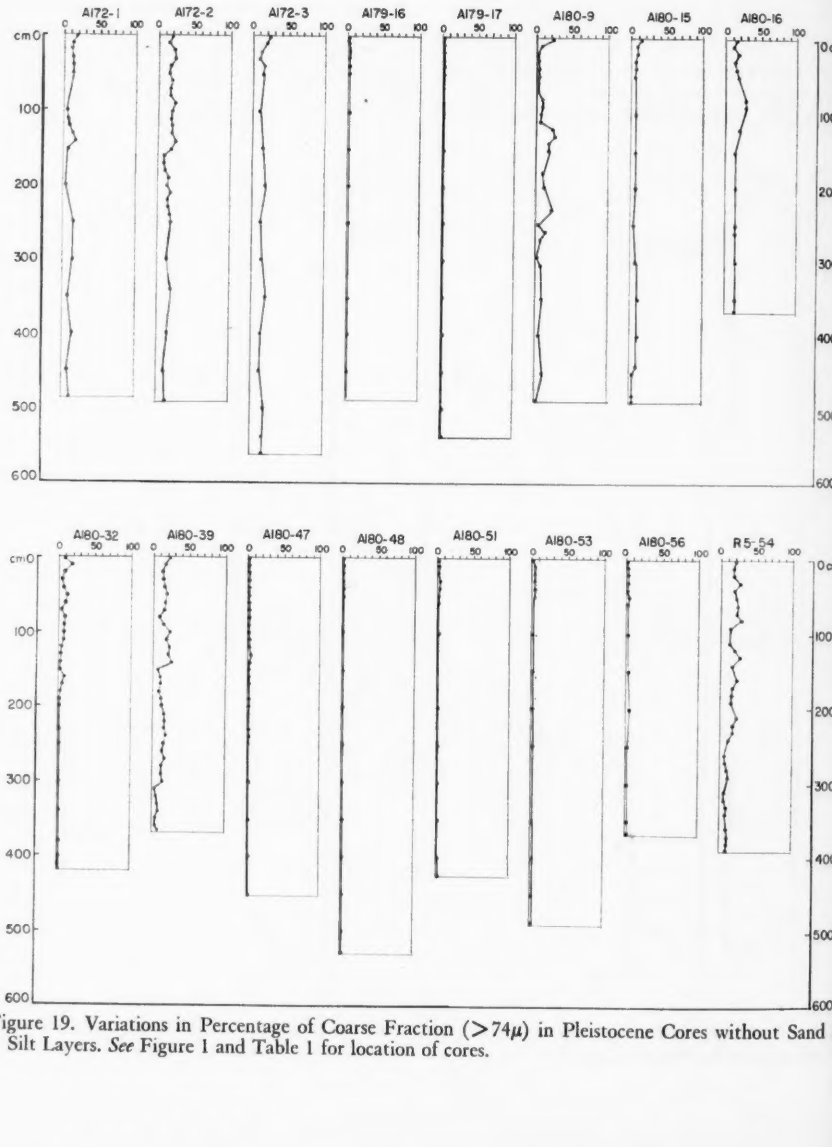

Figure 19. Variations in Percentage of Coarse Fraction (>74μ) in Pleistocene Cores without Sand or Silt Layers. *See* Figure 1 and Table 1 for location of cores.

bonate while the tests lie on the ocean bottom for the following reasons. None of the tests of benthic species is encrusted, although these species are invariably accompanied by heavily encrusted planktonic species. The crust is confined to the tests of certain planktonic species, whereas tests of other species are essentially free of it no matter where found. While the mature individuals in a sample are for the most part heavily encrusted, immature tests in the same sample are only thinly encrusted or more commonly not at all encrusted. The calcite crust is well developed at deep stations where there is every indication that the dominant process is solution, not precipitation of calcite. If the crust formed during diagenesis, it should be thicker on tests from samples from some depth below the sediment surface; however, the crust is as thick on tests from surface samples as from samples anywhere below.

The evidence proves that the calcite crust is not due to chemical precipitation on the ocean floor. Evidence will be adduced hereafter to show that the crystalline crust must be secreted during the life of the animal. Since the tests of Foraminifera caught in the photic zone do not have crystalline crusts, we conclude that the planktonic Foraminifera pass a part of their life cycle below the photic zone and there secrete an important part of their calcareous tests. This conclusion has an important bearing on the interpretation of

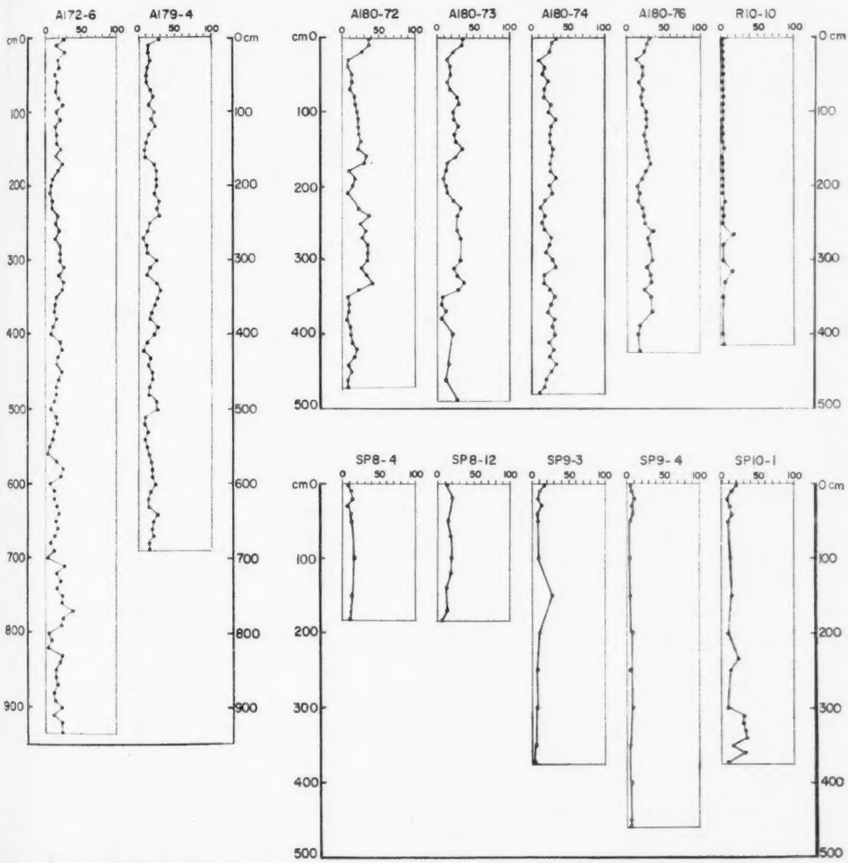

Figure 20. Variations in Percentage of Coarse Fraction ($>74\mu$) in Pleistocene Cores without Sand or Silt Layers. *See* Figure 1 and Table 1 for location of cores.

oxygen-isotope ratios in the tests of planktonic Foraminifera in terms of temperature of the photic zone.

Descriptions of Cores Containing Pre-Pleistocene Sediments

The detailed topography of the continental slopes, as revealed by the echo sounder, affords evidence that some process of erosion, similar to stream erosion, has been active on the slopes (Veatch and Smith, 1939). The recording echo sounder has made it possible to explore the bottom topography and attempt to sample selected features of the bottom such as the steep walls of submarine valleys where exposures of older sediments would be most likely to occur. In 1934 samples of older sediments were dredged from the Georges Bank canyons by the R–V ATLANTIS under the direction of Stetson (1936). Cushman (1936) concluded that the oldest Foraminifera in these sediments were Late Cretaceous. Subsequently Stetson took two cores on the continental slope southeast of New York using a Piggot corer. Cushman (1939) determined these sediments to be late Eocene on the evidence of the Foraminifera.

Phleger, Parker, and Peirson (1953) have reported a Miocene assemblage of planktonic Foraminifera from a core taken from 3577 m deep in the Equatorial Atlantic by workers

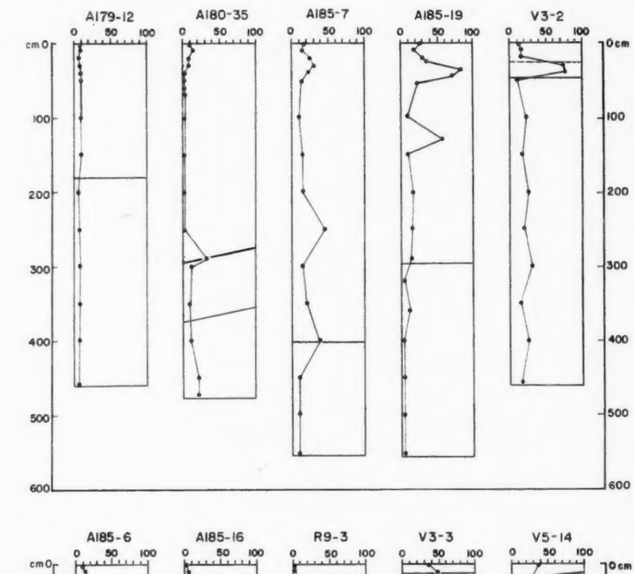

Figure 21. Variations in Percentage of Coarse Fraction (>74μ) in Cores Containing Sediments Older than Pleistocene. Sharply defined contacts are indicated by solid lines, gradational contacts by dashed lines. *See* Figure 1 and Table 1 for location of cores.

TABLE 3.—SPECTROCHEMICAL ANALYSES OF TOP SAMPLES OF DEEP-SEA CORES

Results in percentages. + indicates greater than, and − less than.
Analyses made by R. G. Smalley in La Habra Laboratory of The California Research Corporation.

Core	SiO_2	Al_2O_3	TiO_2	Fe_2O_3	MgO	CaO	Na_2O	K_2O	SrO	MnO	CuO	V_2O_5	BaO	Cr_2O_3	B_2O_3	PbO
A152–135	49.	13.	.64	5.5	3.4	12.	1.7	3.7	.034	.10	.006	.016	.044	.018	.08	.006
A153–141	42.	12.	.62	6.4	3.4	7.2	2.2	3.6	.008	.096	.006	.012	.038	.014	.08	.008
A153–146	23.	9.	.34	3.6	3.6	38.	1.8	2.2	.13	+.18	.012	.014	.070	.018	.08	.008
A156–4	44.	11.	.58	4.7	3.4	15.	2.3	2.8	..	.094	.003	.014	.038	.016	.08	.006
A156–5	40.	11.	.56	4.7	3.2	19.	2.4	3.0	..	.062	.005	.016	.052	.018	.08	.006
A156–12	45.	12.	.54	5.	3.6	17.	2.5	3.1	..	+.18	.006	.016	.050	.018	.08	.006
A157–5	38.	9.	.48	4.3	4.4	22.	2.9	2.8	..	.14	.008	.016	.046	.018	.09	.008
A157–6	31.	6.	.44	3.6	3.8	27.	1.6	1.7	.063	.14	.003	.010	.038	.014	.06	.006
A157–11	33.	8.	.46	4.2	4.4	31.	2.	2.3	.072	.15	.005	.016	.040	.016	.08	.006
A157–12	30.	8.	.46	3.8	4.8	29.	2.9	2.4	.071	.066	.006	.018	.038	.018	.08	.008
A160–11	+50.	11.	.58	5.2	2.8	3.2	1.7	3.2	−.005	+.18	.007	.012	.030	.012	.08	.010
A160–16	+50.	20.	.88	+6.5	4.	8.8	1.9	4.8	.018	.10	.004	.026	.054	.020	.09	.010
A160–19	2.	1.	.08	0.9	2.2	+45.	1.5	0.6	+.18	.12	.005	.010	.018	.014	.03	−.005
A162–5	+50.	11.	.56	5.	2.4	1.4	1.5	3.9	−.005	.056	.005	.014	.030	.012	.08	.006
A164–1	48.	12.	.54	6.	3.	20.	1.6	2.8	..	.092	.011	.016	.054	.016	.09	.006
A164–5	42.	11.	.58	4.6	4.	20.	+4.	3.2	..	+.18	.007	.022	.044	.020	.09	.010
A164–6	43.	11.	.56	4.6	3.4	18.	2.6	3.	..	+.18	.006	.016	.042	.018	.07	.010
A164–13	42.	11.	.52	4.9	3.2	13.	2.4	3.3	.041	.17	.007	.016	.034	.016	.08	.008
A164–14	+50.	2.2	.20	1.5	−0.4	3.8	0.6	0.8	−.005	.032	−.003	−.005	.010	−.01	.04	−.005
A164–15	41.	9.	.48	4.2	3.4	20.	2.1	2.5	..	+.18	.005	.012	.034	.016	.08	.006
A164–16	44.	10.	.50	4.1	3.	18.	2.	2.7	..	.14	.005	.012	.034	.016	.06	−.005
A164–17	45.	10.	.52	4.3	3.2	19.	1.8	2.5	..	.17	.005	.012	.034	.016	.07	.006
A164–19	+50.	13.	.76	6.3	3.2	7.	2.2	3.6	.012	.11	.007	.018	.040	.018	.08	.006
A164–20	43.	7.	.30	3.	2.	5.8	1.6	2.5	−.005	.044	−.003	−.005	.024	.012	.05	−.005
A164–22	+50.	2.	.04	1.3	−0.4	1.8	0.9	0.9	−.005	.040	−.003	−.005	.012	−.01	.04	−.005
A164–23	47.	12.	.62	4.8	3.	17.	2.2	3.1	..	+.18	.006	.016	.040	.18	.07	.006
A164–24	47.	13.	.74	6.	4.	14.	2.4	3.8	.045	.11	.009	.020	.046	.020	.09	.008
A164–29	36.	13.	.54	5.	3.4	19.	2.1	3.1	..	+.18	.010	.018	.034	.018	.08	.008
A164–33	44.	7.	.48	4.1	2.8	14.	2.	2.4	.038	.096	.003	.010	.038	.016	.06	−.005
A164–34	43.	12.	.58	4.8	2.8	9.6	1.5	3.2	.021	.18	.004	.012	.032	.012	.07	−.005
A164–35	35.	13.	.54	5.	3.8	27.	2.3	3.1		+.18	.012	.020	.036	.020	.08	.008
A164–36	13.	4.	.24	2.2	3.4	41.	1.4	1.2	+.18	.11	.005	.012	.020	.018	.05	−.005
A164–38	1.	0.9	.10	1.4	4.2	45.	0.7	0.2	+.18	.026	.003	−.005	.008	.012	.02	.006
A164–46	44.	10.	.54	4.5	4.	15.	3.3	3.1	..	.13	.005	.016	.038	.016	.09	.010
A164–47	42.	11.	.62	4.8	3.2	16.	1.7	3.1	..	.11	.005	.014	.038	.016	.06	−.005
A164–48	42.	11.	.58	4.8	4.	19.	2.7	3.1	..	+.18	.008	.018	.042	.018	.09	.008
A164–55	40.	11.	.52	5.	4.	19.	2.9	3.2	..	+.18	.005	.018	.056	.020	.09	.008
A164–59	42.	9.	.52	4.7	3.	11.	2.4	2.8	.025	.054	.005	.014	.036	.016	.08	.006
A164–60	+50.	13.	.70	5.8	2.8	5.	2.2	3.4	−.005	.068	.003	.012	.038	.014	.09	−.005

TABLE 3.—*Continued*

Core	SiO_2	Al_2O_3	TiO_2	Fe_2O_3	MgO	CaO	Na_2O	K_2O	SrO	MnO	CuO	V_2O_5	BaO	Cr_2O_3	B_2O_3	PbO
A164–61	44.	12.	.60	5.	3.2	15.	2.9	3.1	.054	+.18	.005	.018	.054	.018	.08	.008
A164–62	+50.	2.	.04	1.9	−0.4	4.8	0.6	0.8	−.005	.016	−.003	−.005	.008	−.01	.05	−.005
A164–63	48.	8.	.46	3.8	2.	8.	2.1	2.5	.013	.044	−.003	.006	.036	.014	.08	−.005
A167–5	46.	15.	.70	5.6	3.2	11.	2.4	3.5	.032	+.18	.006	.018	.038	.016	.08	.006
A167–6	44.	15.	.66	5.4	3.4	16.	2.1	3.1	..	.086	.005	.016	.036	.016	.08	.006
A167–7	42.	8.	.48	4.	2.2	9.8	1.7	2.2	.015	.10	+.003	.006	.026	.012	.07	−.005
A167–8	44.	16.	.72	5.7	4.	2.4	3.	3.4	.073	+.18	.009	.022	.042	.020	.10	.010
A167–9	48.	16.	.70	5.8	3.8	18.	1.7	3.2	..	+.18	.008	.020	.042	.018	.08	.006
A167–10	45.	16.	.74	5.6	3.4	12.	2.3	3.5	.040	+.18	.008	.018	.034	.016	.08	.006
A167–11	44.	16.	.74	5.9	4.2	15.	+4.	3.8	.060	+.18	.009	.026	.042	.020	.11	.012
A167–12	42.	16.	.74	6.4	4.	17.	3.3	3.6	.073	+.18	.010	.024	.040	.020	.09	.022
A167–13	40.	13.	.58	4.7	3.4	25.	2.3	2.6	..	+.18	.005	.018	.040	.020	.08	.006
A167–14	28.	11.	.48	3.8	3.	30.	1.8	2.	+.18	.14	.005	.016	.034	.020	.05	.006
A167–31	6.	3.	.16	1.7	3.2	43.	1.7	0.6	+.18	.080	.005	.012	.016	.018	.04	.018
A167–33	2.	1.	.08	0.7	3.2	45.	1.5	0.4	+.18	.022	.003	.008	.008	.014	.03	−.005
A167–37	25.	9.	.40	3.8	3.8	35.	2.4	1.9	.12	.15	.007	.018	.028	.020	.07	.008
A167–38	11.	3.	.20	1.7	2.4	42.	1.1	0.7	+.18	.090	.003	.008	.014	.016	.03	−.005
A167–39	16.	7.	.30	2.6	3.2	38.	1.3	1.4	+.18	.15	.006	.012	.020	.016	.06	.012
A167–49	0.4	0.4	.06	0.3	3.4	+45.	1.1	0.2	+.18	.016	−.003	.008	.008	.016	.02	−.005
A167–51	1.	1.	.04	0.6	3.2	45.	2.1	−0.4	+.18	.026	−.003	.006	.008	.014	.03	−.005
A172–1	26.	11.	.46	4.5	3.8	31.	2.3	1.2	.072	+.18	.009	.020	.020	.018	.07	.008
A172–2	14.	8.	.26	2.8	3.6	37.	3.3	1.3	.14	.14	.007	.020	.034	.020	.07	.018
A172–3	16.	9.	.28	3.	3.4	37.	3.7	1.4	.11	.13	.006	.020	.028	.018	.06	.008
A172–6	19.	11.	.32	3.3	3.	36.	3.	1.5	.092	.15	.004	.020	.022	.018	.07	.008
A172–7	32.	15.	.52	5.1	4.	27.	3.8	2.	..	+.18	.010	.028	.024	.020	.08	.008
A172–9	46.	19.	.74	7.2	3.4	1.2	2.5	3.7	−.005	+.18	.017	.024	.03	.018	.10	.008
A172–10	45.	19.	.72	7.	2.8	1.4	1.7	3.3	−.005	+.18	.015	.022	.028	.016	.08	.006
A172–12	41.	16.	.58	6.5	2.6	1.	1.7	2.9	−.005	+.18	.023	.018	.026	.014	.08	.006
A172–14	46.	18.	.70	7.1	3.2	2.8	2.6	3.1	.009	+.18	.019	.024	.028	.018	.09	.008
A172–17	45.	18.	.74	6.6	3.	2.2	2.2	4.6	.005	+.18	.009	.022	.034	.016	.08	.008
A172–21	28.	13.	.50	4.5	4.4	31.	4.5	3.1	.10	.17	.007	.024	.034	.020	.09	.010
A172–22	3.	1.	.04	0.6	3.4	+47.	1.6	0.4	+.18	.040	−.003	−.005	.006	.012	.03	−.005
A172–23	2.	0.9	.06	1.1	3.8	46.	1.7	0.3	+.18	.032	−.003	−.005	.006	.012	.03	−.005
A172–25	5.	3.	.14	1.6	3.8	46.	1.6	0.7	+.18	.058	−.003	.008	.014	.014	.04	−.005
A172–33	40.	9.	.44	3.9	3.	18.	2.	2.6	..	.16	.003	.012	.034	.014	.08	.006
A172–34	43.	13.	.56	5.5	3.8	16.	2.3	3.3	..	.10	.005	.018	.048	.016	.09	.006
A173–2	38.	9.	.46	3.8	3.2	23.	2.3	2.2	..	.15	.003	.010	.034	.014	.07	.006
A173–3	38.	9.	.46	3.8	2.6	17.	1.6	2.4	..	.13	−.003	.008	.030	.012	.06	−.005
A173–6	41.	7.	.28	3.1	3.	12.	1.9	2.2	.035	.042	−.003	−.005	.044	.010	.07	−.005
A173–8	46.	11.	.58	4.3	2.4	7.8	2.	3.	.023	.056	−.003	.008	.042	.016	.07	−.005
A173–9	+50.	2.	.04	1.3	−0.4	2.	0.5	0.9	−.005	.020	−.003	−.005	.012	−.01	.04	−.005
A179–3	39.	22.	.60	5.6	3.4	18.	3.	2.2	.067	+.18	.008	.036	.034	.018	.09	.010

A179–4	17.	9.	.28	3.1	3.4	37.	2.5	1.1	.12	+.18	.008	.018	.024	.018	.06	.008
A179–5	49.	18.	.68	7.6	3.8	4.2	2.4	1.8	.007	+.18	.015	.028	.018	.016	.08	.012
A179–7	42.	13.	.70	6.8	4.4	13.	1.9	1.6	.038	+.18	.009	.024	.018	.030	.08	.005
A179–8	38.	15.	.66	8.7	6.6	16.	1.7	1.	..	.10	.01	.030	.016	.078	.07	.005
A179–9	3.	1.	.04	1.1	3.4	+47.	1.4	0.2	+.18	.036	−.003	−.005	.006	.012	.03	−.005
A179–10	3.	1.	.06	0.7	4.	47.	1.8	0.2	+.18	.044	−.003	−.005	.008	.014	.02	−.005
A179–11	3.	1.	.08	0.6	4.2	+47.	1.	0.3	+.18	.054	−.003	.006	.014	.014	.03	−.005
A179–13	3.	1.	.08	0.7	4.4	+47.	2.	0.5	+.18	.064	−.003	.008	.010	.016	.04	.005
A179–15	2.	0.9	.06	0.5	4.8	47.	1.8	0.3	+.18	.032	−.003	.008	.006	.016	.03	−.005
A179–16	41.	18.	.66	5.7	4.	24.	2.6	3.6	..	+.18	.011	.024	.042	.020	.09	−.005
A179–17	44.	17.	.68	6.	4.4	24.	2.8	3.9	..	+.18	.009	.026	.044	.020	.10	.010
A179–18	45.	19.	.70	6.	4.	20.	2.2	3.9	..	+.18	.008	.024	.044	.020	.09	.008
A179–20	40.	19.	.66	5.8	3.8	25.	2.3	3.7	..	+.18	.011	.026	.042	.020	.09	.010
A179–22	42.	16.	.60	5.5	3.6	23.	2.	3.4	..	+.18	.007	.020	.038	.018	.08	.008
A179–23	+50.	3.	.08	1.5	−0.4	2.6	0.8	1.1	.006	.028	−.003	−.005	.012	−.01	.04	−.005
C10–14	42.	12.	.48	4.5	3.2	24.	1.5	2.7	..	.10	.003	.014	.048	.018	.05	.008
R5–57	33.	13.	.50	4.	3.4	31.	2.2	2.	.080	.056	.004	.016	.064	.02	.07	.014
R7–2	2.	0.4	−.02	0.6	4.4	46.	0.8	−0.1	+.18	.028	−.003	−.005	−.004	.010	.02	−.005
R7–7	7.	2.	.12	1.	3.8	44.	2.1	0.5	+.18	.042	−.003	.014	.02	.018	.03	.006
R10–10	38.	12.	.58	4.9	4.	15.	2.2	2.4	..	+.18	.003	.012	.042	.012	.06	−.005
SP3–38	16.	6.	.24	2.	2.	42.	1.2	1.1	.14	+.18	.004	.010	.058	.014	.04	−.005
SP9–3	34.	12.	.60	4.6	4.	30.	2.6	2.9	..	.15	.009	.022	.074	.020	.08	.024
SP9–4	26.	9.	.36	3.8	4.	37.	2.7	2.3	.12	.12	.015	.018	.058	.018	.08	.008
SP10–1	19.	6.	.28	3.2	3.	41.	1.9	1.4	.12	.13	−.003	.012	.038	.014	.06	.006

on the ALBATROSS of the Swedish Deep-Sea Expedition. Several other cores raised by the members of ALBATROSS scientific parties contained extinct species of Foraminifera, but the authors concluded that they were reworked.

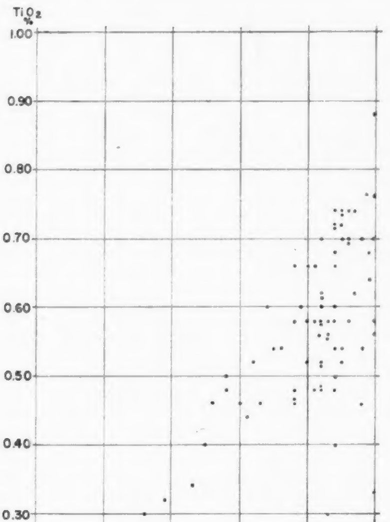

Figure 22. Relationship of TiO_2 Content to SiO_2 Content in Sediments in the Atlantic Ocean. Samples from the tops of 105 cores were analyzed. Most of the cores were obtained from the Western Atlantic.

Furon (1949, p. 1509) believes that rock fragments containing parts of unidentified trilobites dredged by the TALISMAN in 1883 came from outcrops of Paleozoic rocks on the ocean floor. The samples were raised from two points in the North Atlantic, the positions being: 42°19′ N., 21°17′ W. and 44°20′ N., 17°12′ W. Edwards (1883) had concluded that the pieces of shale containing the trilobite fragments had been transported by drifting ice during a Pleistocene glacial age. Furon insists that this could not have been the case because there is no north to south current in the region and because the warm Gulf Stream would have prevented ice from drifting so far south. However, core R5–36 in the Lamont collection, from 46°55′ N., 18°35′ W., not far north of the TALISMAN stations, contains material which unquestionably has been transported by drifting ice. The location is south of the North Atlantic Drift. Evidently the warm current was not an effective barrier to drifting ice at all times. More evidence from dredging and coring in the region should be obtained before the trilobites are accepted as evidence of outcrops of Paleozoic rocks on the floor of the Atlantic.

Figure 23. Relationship of SrO Content to CaO Content in Sediments in the Atlantic Ocean. Samples from the tops of 71 cores were analyzed. Most of the cores were obtained from the Western Atlantic.

Members of the Mid-Pacific Expedition of 1950 dredged and cored extensively on several guyots or flat-topped seamounts. The material

TABLE 4.—CALCIUM CARBONATE ANALYSES OF DEEP-SEA CORES
"Sample cm" indicates position of sample in cm from top of core.

Core	Sample cm	Per Cent $CaCO_3$
A152-135	Top	13.9
A152-135	9	30
A152-135	672	19
A153-141	Top	14.5
A153-141	117	23
A153-141	122	34
A153-146	Top	63.4
A156-1	Top	95
A156-1	300	92
A156-1	443	89
A156-2	Top	60.9
A156-2	5	88
A156-2	180	58
A156-2	250	44
A156-2	253	43
A156-4	Top	12.3
A156-5	Top	20.9
A156-10	Top	14.8
A156-12	Top	18.7
A157-5	Top	40.5
A157-6	Top	47
A157-11	Top	44.5
A157-12	Top	27.2
A157-13	Top	45.8
A158-4	Top	20.3
A158-4	510-520	98.6
A160-11	Top	20.7
A160-16	Top	18
A160-19	Top	77.2
A162-5	Top	1.0
A164-1	Top	31.5
A164-2	Top	1.3
A164-5	Top	32.4
A164-6	Top	34.4
A164-13	Top	21.0
A164-14	75	33
A164-17	275	4.6
A164-17	340	22.3
A164-17	525	23.0
A164-17	575	12.4
A164-24	Top	25.0
A164-24	120	4.5
A164-24	575	12.4
A167-7	Top	32.0
A167-7	142	44.0
A167-9	Top	28.9
A167-21	Top	73.2
A167-25	Top	55.6
A167-37	Top	56.4
A167-37	130	15.1
A172-1	Top	48.1
A172-1	124	34.6
A172-2	30	60.4
A172-2	250	56.3
A172-9	Top	0.2
A172-9	50	36.4
A172-10	Top	0.8
A172-10	50	36.9
A172-10	218	74.5
A172-10	300	0.3
A179-4	Top	77
A179-4	19-23	67
A179-4	30-40	50.7
A179-4	150-155	43.7
A179-4	260-264	49.6
A179-4	390	53.6
A179-4	440	48.8
A179-4	490	63.3
A179-4	540	46.4
A179-4	590	61.4
A179-4	640	59.7
A179-4	690	55
A179-15	98	85
A179-17	Top	30.9
A179-18	Top	27.3
A179-20	Top	34.0
A179-23	Top	29.3
A180-1	139-140	21
A180-39	Top	58
A180-39	75	37.6
A180-39	85	45.8
A180-39	125-129	59
A180-39	137-140	55.1
A180-39	235	48.3
A180-39	350	76
A180-47	90	11
A180-48	450	19
A180-72	335-336	75.3
A180-73	Top	66.1
A180-73	61-62	58
A180-73	90-91	76
A180-73	97-99	68
A180-73	177-178	53
A180-73	193-194	61
A180-73	291	62
A180-73	335-336	73.5
A180-76	336-337	79.6
A180-100	Top	31.6
A180-100	30	37.9
A180-100	70	33.4
C10-13	Top	24.09
C10-14	Top	34.7
R5-36	Top	77
R5-50	Top	69.5
R5-54	Top	53
R5-54	44-46	47.3
R5-54	47-49	52.5
R5-54	51-60	60.6
R5-54	64-69	63
R5-54	77-80	58
R5-54	260	54.3
R5-54	290	82.8
R5-54	350	76.0
R5-57	Top	42.1

TABLE 4.—*Continued*

Core	Sample cm	Per Cent $CaCO_3$
R10-10	Top	30
R10-10	60	34
R10-10	90	32
R10-10	110	22.8
R10-10	140	37.8
SP3-33	Top	13.3
SP3-38	Top	70.2

obtained includes Late Cretaceous corals and rudistids as well as indurated Paleocene and Eocene *Globigerina* oozes (Hamilton, 1956). Hamilton has concluded that the guyots were islands in Cretaceous time and were reduced by wave erosion to relatively flat banks on which the coral-rudistid fauna found lodgement. Later subsidence of the sea bottom has lowered the flat tops to depths between 1280 and 1605 m (700 and 900 fm). As yet no sediment older than Cretaceous has been obtained from the bottom of the Pacific.

About 1 out of every 10 cores in the Lamont collection contains pre-Pleistocene sediment. As in the Pacific cores, no sample older than Cretaceous has been found. A few pre-Pleistocene sediments have been very briefly described by Ericson, Ewing, and Heezen (1952). In the following section 41 selected cores are described in detail. The geographical positions, depths, and lengths of these cores are given in Table 1, topography and locations in Figures 1–6. Because of the close relationship between the submarine exposures and regional structure and topography, the cores have been grouped on a regional basis.

NORTH AMERICAN CONTINENTAL SLOPE AND RISE

A156–10. Depth 1400 m

Description	*Thickness (cm)*
Uniform dark-green lutite containing postglacial planktonic Foraminifera. Well-defined contact.	66
Silty dark-green marcasitic lutite. Foraminifera include *Nodogenerina georgiana* and *Plectofrondicularia basispinata*	177
	243

Remarks: The Foraminifera suggest that the silty lutite corresponds to the green silts of the Georges Bank canyon. Cushman (1936) concluded that these silts were late Pliocene or earliest Pleistocene. However, we think it rather improbable that this silty lutite, and other occurrences described hereafter, can be Pleistocene, as the lithology and fauna differ strikingly from those of sediments of known Pleistocene age cored elsewhere in the Atlantic. The silty lutite could be broken only by hammering a knife blade into it. Hardness is due to compaction, not cementation. Samples put into water readily break down to mud, and coccoliths show no secondary calcite deposition.

A164–2. Depth 3475 m

Description	*Thickness (cm)*
Postglacial sediment (occurs only in depressions in top surface)	
Greenish-brown oxidized zone	10
Green lutite with abundant marcasite. Foraminifera similar to those in core A156–10.	35
Rusty-green lutite containing partially oxidized marcasite. Foraminifera include admixed Pleistocene species.	61
	106

Remarks: Unoxidized sediment above 45 cm is probably a slab of rock from the canyon wall which has slid down over a talus of partially oxidized green marcasitic clay with interstitial Pleistocene sediment.

A164–4. Depth 3330 m

Description	*Thickness (cm)*
A few Pleistocene Foraminifera occur in depressions in upper surface.	
Oxidized zone of yellowish-green lutite	27
Uniform dark-green marcasitic lutite containing *Nodosaria* sp. cf. *N. tosta*, *Uvigerina auberiana*, *Sphaeroidinella multiloba*, *Globorotalia fijiensis*, and *Discoaster brouweri* Tan as emended by Bramlette and Riedel (1954).	76
	103

Remarks: The fauna indicates Neogene, and probably Miocene age. The thick oxidized zone shows long exposure to aerated water. Evidently current scour or periodic slumping has prevented accumulation of a protecting layer of Pleistocene sediment. Below the oxidized zone marcasite is common as replaced coprolites and as minute discs, presumably fillings of diatom frustules which have subsequently been dissolved.

A164–8. Depth 3825 m

Description	*Thickness (cm)*
Oxidized zone; yellowish-green lutite	6
Uniform dark-green marcasitic lutite with Foraminifera, Radiolaria, discoasters	55
	61

Remarks: Very similar to cores A164–2 and A164–4. W. R. Riedel (Personal communication) concluded that the Radiolaria are very late Miocene or possibly early Pliocene.

C10–13. Depth 3570 m

Description	*Thickness (cm)*
Layers of Pleistocene foraminiferal lutite, redeposited green clay, and graded sands	142
Zone of slump emplacement; pebble-size fragments of green lutite in a sandy clay matrix containing Pleistocene Foraminifera and older reworked species	28
Uniform green marcasitic lutite. ***Globorotalia miocenica***, ***Plectofrondicularia basispinata***, and ***Nodosaria*** sp. cf. ***N. tosta*** indicate Neogene age.	249
	419

Remarks: Absence of an oxidized zone shows that the Neogene clay was covered soon after exposure. Since the overlying layers contain late Pleistocene Foraminifera, removal of original overburden occurred in the late Pleistocene.

R9–3. Depth 3660 m

Description	*Thickness (cm)*
Dark-gray lutite	40
Glacial marine, that is, granules and pebble-size fragments of igneous and metamorphic rocks in gray-lutite matrix. Well-defined contact without manganese oxide at base.	310
Green marcasitic lutite. Absence of the normal Pleistocene Foraminifera and presence of ***Nodogenerina georgiana*** suggest that this corresponds to the green silts of the Georges Bank canyons. Discoasters absent.	15
	365

Remarks: The green lutite is much firmer than the overlying sediment, apparently because of compaction under a former sediment cover and not cementation. Preservation of coccoliths shows that no solution or redeposition of calcium carbonate has taken place. Absence of oxidation of marcasite at the contact indicates that sediment accumulation recommenced soon after the green lutite was uncovered during the last glacial age. Figure 21 shows variation in percentage of coarse fraction ($>74\mu$). The coarse fraction of the green lutite consists of the tests of Foraminifera, abundant particles of marcasite, and finely divided quartz. Glauconite is absent. The iron sulfide suggests accumulation under anaerobic conditions; however, benthic Foraminifera are common in this and other samples of Neogene green lutite from the Hudson Canyon region, and accordingly the bottom water must have contained oxygen. Presumably aerobic bacteria in the interstitial water depleted the oxygen at some level below the water-sediment interface, after which anaerobic species generated hydrogen sulfide (Beerstecher, 1954) and precipitated hydrotroilite, which changed to marcasite during diagenesis (Twenhofel, 1950).

Blake Plateau

A156–1. Depth 1005 m

Description	*Thickness (cm)*
Incoherent calcareous sand composed of tests of planktonic Foraminifera and pteropods.	30
Clay-size fraction becomes more prominent. Below 60 cm winnowed layers of foraminiferal tests with little fine interstitial sediment are numerous.	190
Very gradual increase in percentage of clay-size fraction.	223
	443

Remarks: There is no evidence of loss of sediment by slumping anywhere in the core. ***Globorotalia miocenica***, ***G. multicamerata***, ***Sphaeroidinella multiloba***, ***Globoquandrina altispira***, ***Orbulina suturalis***, and ***Rectuvigerina optima*** occur below 220 cm. Hans Bolli (Personal communication) considers this assemblage to be late Miocene. Between 130 and 200 cm Miocene species are rare. Above 130 cm only Plio-Pleistocene species are present. The faunal succession from upper Miocene to typically post-glacial material in the top few centimeters in the absence of any well-defined contact or abrupt lithological change is noteworthy. The explanation may lie in a near balance between sediment accumulation and removal of sediment by current scour. Under such conditions net accumulation could be extremely slow. Particularly interesting and suggestive is the evidence of gradual increase in the winnowing effect with time, perhaps in consequence of gradual change in local bottom topography or as a result of increase in velocity of oceanic circulation.

A156–2. Depth 2140 m

Description	*Thickness (cm)*
Very fine sand composed of tests of planktonic Foraminifera and pteropods. Parameters of particle-size distribution are: $QD\phi = 1.5$, $SKg\phi = +0.4$, median diameter $= 90\mu$. Carbonate content is 88 per cent. The good sorting and high percentage of carbonate are probably due to winnowing action of current scour sufficient to prevent accumulation of fine terrigenous material.	15

Very light-gray calcilutite. The contact surface with the overlying sand has an apparent dip of 18° and is grooved parallel to the dip. It is free of manganese oxide. Burrows filled with the overlying sediment penetrate the calcilutite to a depth of a few centimeters. The particle-size distribution parameters are: $QD\phi = 2.4$, $SKg\phi = +0.5$, median diameter $= 4\mu$. The curve of particle-size distribution is bimodal, indicating absence of current scour to prevent accumulation of fine terrigenous material and coccoliths. The carbonate content ranges from 40 to 63 per cent. 551

566

Remarks: According to Hans Bolli (Personal communication) the Foraminifera of the calcilutite compare well with the assemblage in the *Globigerina ciperoensis* zone of the late or middle Oligocene Cipero formation of Trinidad. Abundant discoasters support this conclusion. Firmness of the calcilutite indicates compaction by former sediment cover. There is no cementation by secondary calcite deposition.

A164–30. Depth 1120 m

Description	*Thickness* (*cm*)
Sand largely composed of tests of Pleistocene planktonic Foraminifera. Basal contact sharply defined.	155
Oxidized zone; light-brown calcilutite	4
Light-gray calcilutite. *Globoquadrina altispira*, *G. venezuelana*, *Globorotalia multicamerata*, *G. miocenica*, *Orbulina suturalis*, and abundant discoasters indicate Miocene age.	660
	819

Remarks: Absence of manganese oxide at 155 cm indicates resumption of sediment accumulation soon after exposure of the Miocene lutite. Contrast between the texture of the Miocene lutite and that of the Pleistocene sand shows that a marked change in conditions of deposition has occurred since Miocene time.

A167–21. Depth 1455 m

Description	*Thickness* (*cm*)
Uniform light-cream calcilutite. A layer about half a mm thick of manganese oxide covers the surface of the calcilutite. Burrows filled with Pleistocene foraminiferal lutite penetrate to 28 cm below the top. Carbonate content is 70 per cent.	365

Remarks: Hans Bolli (Personal communication) concludes that the planktonic species of Foraminifera compare well with those of the upper Eocene Hospital Hill marl and Mount Moriah formation of Trinidad. Coccoliths and late Eocene discoasters are very abundant. The perfect preservation of these minute calcareous plates indicates that there was no solution or redeposition of calcium carbonate.

Although some postglacial sediment may have been lost from the top in bringing the core on board ship, it is unlikely that the thickness could have exceeded a few centimeters. The manganese oxide on the calcilutite surface suggests slow to zero sedimentation during a long time probably because of vigorous current scour.

A167–25. Depth 1745 m

Description	*Thickness* (*cm*)
Traces of Pleistocene sediment in small depressions in top of core. No manganese oxide. Oxidized zone; olive-green slightly sandy lutite.	16
Dark grayish-green slightly sandy lutite. Carbonate content at 75 cm is 56 per cent. At 80 cm, parameters of particle-size distribution are: $QD\phi = 3.3$, $SKq\phi = 0.2$, median diameter $= 6\mu$.	159
	175

Remarks: Firmness indicates compaction under a former overburden. The fine fraction shows no cementation. The sediment readily absorbs water and breaks down to mud. According to A. R. Loeblich (Personal communication) the Foraminifera are Cenomanian and a little younger than the surface Washita in Texas and Oklahoma.

A167–28. Depth 1260 m

Description	*Thickness* (*cm*)
Tan calcareous sand largely composed of tests of Pleistocene planktonic Foraminifera. Well-defined basal contact.	70
Light-gray foraminiferal lutite	345
	415

Remarks: Globorotalia miocenica is abundant in the light-gray lutite. Another species of *Globorotalia* is similar to *G. menardii* but differs from the Pleistocene form in its dextral coiling, in its small size, and in its more gradual increase in chamber size. Until the stratigraphic range of *G. miocenica* is better known, this core cannot be classified more closely than as Neogene.

A167–29. Depth 1730 m

Description	*Thickness* (*cm*)
Thin layers and lenses of calcareous sand composed of tests of planktonic Foraminifera alternating with layers of calcareous lutite. The dominant species are Pleistocene, but all samples contain a few reworked older species. Gradational change at base.	330
Abundantly foraminiferal calcilutite	105
	435

Remarks: The Foraminifera below 330 cm are Neogene. The absence of a sharply defined contact and the coarse texture suggest very slow sediment accumulation in the presence of current scour of varying intensity, rather than catastrophic removal of a part of the section by slumping. If so, this core may contain an unbroken sedimentary record commencing at some time in the Pliocene, if not Miocene. However, paleontological examination of samples from the core shows that the record is too blurred by reworking, by extreme abbreviation of the section, and perhaps by the stirring action of bottom dwellers, to be decipherable except in the broadest terms.

Bahama Islands Region

A167–41. Depth 3110 m

Description	*Thickness* (*cm*)
Unsorted sand composed of tests of Pleistocene planktonic Foraminifera. Sharply defined basal contact without manganese oxide.	215
Oxidized zone; brownish-gray foraminiferal lutite	35
Greenish-gray foraminiferal lutite with hydrotroilite and a trace of marcasite. *Globorotalia fijiensis*, *Globoquadrina altispira*, *Biorbulina bilobata*, and discoasters show that age is Neogene.	238
	488

Remarks: The Neogene sediment has been compacted but not cemented.

A167–43. Depth 2605 m

Description	*Thickness* (*cm*)
Light-tan lutite containing postglacial Foraminifera. Sharply defined basal contact with manganese oxide staining.	60
Soft very light-gray calcilutite. No discoasters. Probably early Pleistocene. Base marked by abrupt color change.	88
Nearly white calcilutite very gradually changing to light gray and below 400 cm to bluish green with much hydrotroilite and marcasite.	362
	510

Remarks: Dextral coiling of *Globorotalia menardii* and the presence of *Globoquadrina altispira*, *Biorbulina bilobata*, and discoasters show that the calcilutite below 148 cm is Neogene. Firmness of the Neogene sediment indicates compaction by former overburden. It is uncemented.

A167–44. Depth 2560 m

Description	*Thickness* (*cm*)
Pleistocene foraminiferal lutite. Well-defined basal contact without manganese oxide.	110
"Weathered" calcilutite. Rusty speckling indicates oxidation of hydrotroilite.	120
Very light-green calcilutite with much hydrotroilite staining	245
	475

Remarks: Abundant Foraminifera and discoasters show that the calcilutite below 110 cm is Neogene. Sediment firmly compacted but not cemented.

A179–12. Depth 1720 m

Description	*Thickness* (*cm*)
Pleistocene foraminiferal lutite. Well-defined basal contact without manganese oxide	180
Uniform white calcilutite. *Globorotalia miocenica*, *Globoquadrina* sp., *Globigerina grimsdalei*, *Sphaeroidinella* sp. cf. *S. seminulina*, and very abundant discoasters indicate Neogene, probably late Miocene, age.	280
	460

Remarks: The Neogene sediment is firmly compacted but not cemented. Figure 21 shows variation in coarse fraction ($>74\mu$).

Cuba, Hispaniola, and Puerto Rico Region

A172–13. Depth 6400 m

Description	*Thickness* (*cm*)
Foraminiferal lutite in various shades of green with lenses of calcareous sand composed of tests of Foraminifera. Well-defined bedding absent. Particles of serpentine containing finely divided magnetite are common in the coarse fraction. Manganese oxide is absent from top of core.	98

Remarks: The coarse material is in part of shallow-water origin (Bryozoa, particles of *Halimeda*, *Amphistegina chipolensis*). Lensy structure and absence of grading indicate concentration of coarse material by current scour rather than by turbidity-current transportation. This implies subsidence since Miocene time.

A185–6. Depth 3420 m

Description	*Thickness* (*cm*)
Dark-brown foraminiferal lutite containing postglacial planktonic Foraminifera	25
Poorly sorted muddy calcareous sand. Well-defined basal contact without manganese oxide	10
Khaki foraminiferal lutite. *Globorotalia miocenica*, *Globoquadrina venezuelana*, *G. altispira*, *Globigerina dubia*, and abundant discoasters indicate Miocene age.	205
	240

Remarks: Figure 21 shows variation in percentage of coarse fraction.

A185–7. Depth 2470 m

Description	*Thickness (cm)*
Pleistocene foraminiferal lutite. Well-defined basal contact	403
Light-brown foraminiferal lutite. *Globorotalia miocenica, Globoquadrina altispira,* and *Discoaster brouweri* Tan as emended by Bramlette and Riedel (1954) indicate Miocene age.	152
	555

Remarks: Figure 21 shows variation in percentage of coarse fraction.

A185–16. Depth 2980 m

Description	*Thickness (cm).*
Pleistocene foraminiferal lutite. Sharply defined basal contact without manganese oxide.	290
Light-tan abundantly foraminiferal lutite containing *Globigerina grimsdalei, Bulimina jarvisi, Globoquadrina* sp. According to M. N. Bramlette (Personal communication) the discoasters are late Oligocene.	70
	360

Remarks: The contact at 290 cm has an apparent dip of 40°. Grooving is parallel to the dip. Figure 21 shows variation in percentage of coarse fraction.

A185–19. Depth 2160 m

Description	*Thickness (cm)*
Pleistocene light-tan foraminiferal lutite. A breccia of angular fragments of the underlying sediment forms a 10-cm zone at the base.	300
Light-tan calcilutite containing Miocene Foraminifera and discoasters which M. N. Bramlette (Personal communication) considers to be early Miocene.	255
	555

Remarks: Change in conditions of deposition is indicated by contrast between percentages of coarse fraction in the Pleistocene and Miocene sections. Figure 21 shows the curve of variation of coarse fraction.

V3–2. Depth 1830 m

Description	*Thickness (cm)*
Pleistocene dark-brown lutite	26
Sand consisting largely of Pleistocene Foraminifera and pteropod shells. Sharply defined basal contact without manganese oxide.	21
Uniform light-tan calcilutite. *Globorotalia multicamerata, G. miocenica, Globigerina dubia, Globoquadrina altispira, G. dehiscens,* and abundant discoasters show that the age is Miocene, probably late Miocene.	412
	459

Remarks: Figure 21 shows variation in percentage of coarse fraction.

V3–3. Depth 2595 m

Description	*Thickness (cm)*
Pleistocene dark-brown foraminiferal lutite	12
A series of overlapping mud flows including several abrupt color and texture changes. Well-defined basal contact	292
Very light-gray calcilutite. *Globorotalia miocenica, G. multicamerata,* and abundant discoasters indicate Neogene age.	64
	368

Remarks: Figure 21 shows variation in percentage of coarse fraction.

Bermuda Rise and Seamounts

C22–6. Depth 1510 m

Description	*Thickness (cm)*
Pleistocene light-tan foraminiferal lutite. Well-defined basal contact dipping 25°	31
Greenish-gray volcanic mud with abundant Foraminifera	158
	189

Remarks: The coarse fraction of the volcanic mud averages about 30 per cent and consists largely of mica, pyroxene, perovskite, garnet, magnetite, and "spiny" pyroxene. This mineral assemblage is essentially similar to that described by Young (1939) and Foreman (1951) in sediments from Bermuda and the nearby ocean floor. Ross, Miser, and Stephenson (1929) attribute the peculiar "spiny" form of the pyroxene crystals to solution etching. Preservation of the Foraminifera is poor because of secondary calcite on the tests. Hans Bolli (Personal communication) concluded that the assemblage compares well with the uppermost part of the *Globigerina ciperoensis* zone or the lowermost part of the *Globigerina dissimilis* zone of the late Oligocene Cipero formation of Trinidad. Uniform distribution of the Foraminifera in the volcanic mud and burrow mottling are evidence that the volcanic material was not deposited at the core stations directly as ash falls resulting from explosive vulcanism but that it was originally deposited on the ancient island and subsequently was redeposited during planation of the island. Thus the Foraminifera indicate the time of redeposition and not that of the original vulcanism. C22–2, depth 1940 m, C22–5, depth 1095 m, and V5–14, depth 2305 m, are similar to C22–6. The thicknesses of Pleistocene sediment in the three cores range from 17 to

33 cm. The planktonic Foraminifera show that in each case sediment accumulation commenced shortly before the end of the last period of cool climate. Alteration of the volcanic material varies from core to core. It is farthest advanced in C22–5, where the volcanic section consists of a smooth green clay with about 1 per cent coarse fraction. The relatively fresh condition of the Foraminifera in this clay is further evidence that the volcanic material was redeposited after alteration. Dip of the contact surface between the volcanic mud and the Pleistocene cover ranges from 15° to 25°. Figure 21 shows variation in percentage of coarse fraction in V5–14.

A164–25. Depth 2955 m

Description	*Thickness (cm)*
Light-brown lutite containing abundant fragments of white chalk and mixed Pleistocene and Neogene species of Foraminifera.	26
Uniform white chalk. Base marked by abrupt color change.	34
Very light-yellow calcilutite gradually changing to light tan below 100 cm.	300
	360

Remarks: Globoquadrina dehiscens, G. venezuelana, Siphonodosaria abyssorum, Almaena alanensis, and *Discoaster aster* Bramlette and Riedel in the calcilutite below the abrupt color change indicate Oligocene age.

A164–26. Depth 2780 m

Description	*Thickness (cm)*
Pleistocene unsorted calcareous sand with a few reworked Miocene species and fragments of coarsely crystalline igneous rock with adhering limestone. Particles of feldspar, mica, garnet, magnetite, pyroxene and perovskite present.	40
Indurated white calcarenite containing "spiny" pyroxene crystals. Foraminifera indicate Miocene age.	23
	63

Remarks: H. H. Hess, P. F. Kerr, and J. T. Fyles (Personal communication) have classified the igneous rock as an alkaline pyroxenite.

C10–7. Depth 1150 m

Description	*Thickness (cm)*
Calcilutite containing postglacial planktonic Foraminifera. Base marked by abrupt change in lithology.	25
Coarsely granular hard calcarenite	262
	287

Remarks: The calcarenite contains the usual Pleistocene Foraminifera and *Uvigerina flintii*. The benthic, relatively shallow-water forms, *Amphistegina lessoni* and *Asterigerina* sp., are markedly more abundant in the calcarenite. Pyroxene and particles of altered igneous rock are common in the calcarenite but absent from the postglacial lutite. *Uvigerina flintii* and evidence for distinctly different conditions of deposition suggest that the calcarenite is Pliocene.

C10–10. Depth 1005 m

Description	*Thickness (cm)*
White calcareous silt	130
Coarser texture. Remains of organisms of shallow-water environment, including *Amphistegina lessoni*, Bryozoa, and *Lithothamnion* sp., are common.	52
	182

Remarks: Globorotalia multicamerata, Orbulina suturalis, Globoquadrina sp., *Amphistegina chipolensis*, and discoasters show that the entire core is Miocene. Pyroxene crystals are common throughout, and particles of volcanic rock are common below 165 cm.

C10–11. Depth 2230 m

Description	*Thickness (cm)*
Except for traces of Pleistocene sediment at the top, the entire core is a firm light-brown calcilutite. The coarse fraction includes particles of volcanic rock, pyroxene, and altered mica, and micronodules of manganese oxide.	198

Remarks: Bulimina jarvisi, Nodosaria longiscata, Plectofrondicularia sp. cf. *P. spinifera, Gümbelina* sp., and abundant discoasters indicate Oligocene age.

C25–5. Depth 1710 m

Description	*Thickness (cm)*
Pleistocene foraminiferal lutite; 60 per cent is coarse fraction largely composed of tests of Foraminifera. Basal contact is gradational.	100
Similar foraminiferal lutite but with less coarse fraction. The Foraminifera are Miocene.	120
Foraminiferal lutite with 20 per cent coarse fraction containing Oligocene Foraminifera.	60
	280

Remarks: The absence of well-defined contacts suggests extremely slow sedimentation with gradual increase in effectiveness of current scour.

A158–4. Depth 3940 m

Description	*Thickness (cm)*
Pleistocene brown foraminiferal lutite. Base marked by abrupt lithological change.	73
Structureless tan calcareous lutite with Neogene discoasters.	388

Description	Thickness (cm)
Brown clay with abundant small calcite crystals and angular fragments of limestone.	104
	565

Remarks: Manganese oxide speckling on fracture surfaces of the limestone shows that it was not broken by the coring tube. Probably the limestone and the clay have slumped from the upper part of the seamount. The clay contains *Inoceramus* prisms but no diagnostic Foraminifera. Poorly preserved *Gümbelina* sp. in the limestone suggest that it is upper Cretaceous.

A164–10. Depth 3550 m

Description	*Thickness (cm)*
Pleistocene foraminiferal tan lutite with abundant limestone fragments and manganese oxide nodules. Gradational with underlying sediment.	100
Similar to the lutite but with Neogene Foraminifera, including *Siphonodosaria abyssorum*, *Globoquadrina venezuelana*, and *Ehrenbergina hystrix*. Limestone fragments become more abundant downward, the lowermost 50 cm being almost entirely composed of calcite crystals, limestone particles, and recrystallized echinoid fragments.	153
	253

Remarks: Reworked Late Cretaceous fossils are present throughout the core. These include small pieces of *Inoceramus* shells, *Globotruncana* sp., and echinoid fragments.

C10–4. Depth 1550 m

Description	*Thickness (cm)*
Unsorted Pleistocene biogenous sand	2
Manganese oxide	1
Light-tan foraminiferal calcilutite. Burrows filled with Pleistocene sediment penetrate to 40 cm. *Globorotalia praemenardii*, *Globoquadrina dehiscens*, *G. venezuelana*, *Orbulina suturalis*, *Rectuvigerina optima*, *Bulimina jarvisi*, and abundant discoasters indicate late Oligocene age.	354
	357

Remarks: Particle-size distribution parameters of the Pleistocene sediment are: $QD\phi = 1.1$, $SKG\phi = -0.2$, median diameter $= 225\mu$. The curve of particle sizes has a single mode. The particle-size distribution of the Oligocene sediment at 100 cm is bimodal and has the following parameters: $QD\phi = 2.4$, $SKg\phi = -0.1$, median diameter $= 25\mu$. The modes fall in the size range of foraminiferal tests and that of the coccoliths and discoasters, an indication that accumulation was uninfluenced by horizontal transportation, the particle-size composition of the sediment being determined by relative rates of productivity of the contributing organisms. Either there was no deep circulation at the time of its accumulation or the sediment originally accumulated on a plain and was raised to its present position by faulting. Firmness of the Oligocene sediment indicates compaction; there is no evidence of cementation.

C25–6. Depth 2360 m

Description	*Thickness (cm)*
Breccia of white calcilutite with interstitial Pleistocene brown lutite.	15
Pleistocene foraminiferal tan lutite	9
White calcilutite	11
	35

Remarks: Manganese oxide on fracture surfaces of calcilutite fragments in the breccia shows that breakage was not due to the coring tube. Foraminifera of the calcilutite are either Oligocene or Miocene.

R5–50. Depth 1940 m

Description	*Thickness (cm)*
Pleistocene tan foraminiferal lutite	9
Breccia of white calcilutite and limestone fragments	48
Nearly white foraminiferal calcilutite. *Globorotalia multicamerata*, *Rectuvigerina optima*, *Sphaeroidinella multiloba*, *Globoquadrina altispira*, and discoasters indicate Miocene age.	111
	168

Remarks: Manganese oxide on fragments in the breccia shows that fracturing was not due to the coring tube.

A180–35. Depth 5030 m

Description	*Thickness (cm)*
Pleistocene light-tan foraminiferal lutite	30
Tan lutite darkening to dark brown at 288 cm. Well-defined contact has 20 degree dip.	258
Manganese oxide	2
Light-tan lutite darkening to very dark brown below 340 cm. Well-defined contact at 367 cm dips about 20° and is parallel to the contact surface at 288 cm.	77
Dark-brown lutite containing abundant inclusions of light-tan lutite about 1 cm in diameter. The contact surface at 367 cm is coated with manganese oxide.	109
	476

Remarks: Neogene discoasters are abundant at 50 cm. The only other diagnostic fossil is a dextral *Globorotalia* sp. which is similar to *G. miocenica*. The coarse fraction below 367 cm consists of manganese micronodules, minute teeth, crystals of various volcanic minerals, particles of palagonite, and clay molds of Radiolaria from which the silica has been removed. Foraminifera are absent, and only a trace of calcium carbonate is present. The facies of the sediment below 30 cm is typical of that now found at depths exceeding 6000 m. This suggests local uplift of the ocean bottom by about 1000 m since Neogene time. Figure 21 shows variation in percentage of coarse fraction.

SP8-3. Depth 4445 m

Description	*Thickness (cm)*
Pleistocene very light-tan foraminiferal lutite	18
Zone of thin bedding and coarse texture due to concentration of tests of Foraminifera by current scour. Well-defined basal contact without manganese oxide	7
Very light-tan foraminiferal lutite. *Globorotalia miocenica* and *Globoquadrina* sp. indicate Neogene age.	30
	—
	55

Remarks: Change in conditions of deposition within the section below the contact is shown by increase in coarse fraction from 1 per cent at 50 cm to 11 per cent at 30 cm. *Globorotalia truncatulinoides* is absent at 50 cm and abundant at 30 cm.

Discussion of the Older Sediments

To those who maintain that even the deepest parts of submarine canyons are products of subaerial stream erosion, the occurrences of older sediments beneath little or no cover of Pleistocene sediment may seem to offer additional evidence of great changes of sea level during the Pleistocene. However, there is strong evidence against this interpretation. Cores from stations less deep than many of the occurrences of older sediments contain records of continuous sediment accumulation since the penultimate interglacial age. Furthermore, the restricted thickness of overlying sediment in some cores containing unconformities and the absence of any evidence of climatic change in the Foraminifera of the overlying sediment prove that at least some unconformities have had their origin in postglacial time and certainly at a time when pelagic sediment was accumulating at the shallower stations.

The possibility remains that some of these unconformities may have resulted from great vertical movements of relatively small areas of the ocean bottom. At present there is no general evidence by which this possibility can be excluded in every case. If the island of Barbados should sink so that the highest part came to lie 1000 m or more below sea level, it would become a seamount on which Eocene and Oligocene sediments of pelagic facies could be cored under essentially the same conditions that older sediments have been cored on the Muir Seamount.

This line of reasoning cannot, however, account for the older sediments along the walls of the Hudson Submarine Canyon at depths between 3000 and nearly 4000 m. Cores from the divides with their records of continuous accumulation of pelagic sediment during late Pleistocene time show that the canyons of the east coast of North America must have been under water at least during late Pleistocene time. It is improbable, to say the least, that conditions during the earlier Pleistocene were so radically different as to have made possible subaerial erosion where depths of water now measure several kilometers.

Shepard (1952) suggested that the original channels of submarine canyons were carved by stream erosion some time ago. To account for exposures of Cenozoic sediments along the canyon walls without the intervention of some kind of submarine erosion, he supposed that the walls of the canyons have been built up by normal sediment accumulation while filling of the original canyons has been prevented by turbidity currents, which he believes to be capable of removing wholly unconsolidated sediment. Accordingly Neogene sediments cored along the walls of the Hudson Submarine Canyon are now exposed simply because they have never been covered by more than a minor thickness of transient sediment periodically removed either by slumping or by large turbidity currents. If we knew no more about these Neogene sediments than their age, it would be difficult to refute this theory.

As pointed out in the descriptions of the individual cores, the Neogene clays are not cemented, but they are quite unlike Pleistocene sediments in their degree of compaction. We conclude from this that at some time in their history they have been covered by considerable sediment. But if the canyon floor has not been lowered since deposition of the Neogene clays, we are forced to conclude that the canyon walls must have been a good deal steeper than they now are. Yet the present rather gentle slopes of the canyon walls must be the steepest slopes stable in sediments having the mechanical properties of those making up the canyon walls. Thus the theory of Shepard leads to the paradox that to account for the compaction of the wall sediments, we must suppose that the walls were steeper before compaction and therefore at a time when the wall sediments must have been weaker than they now are.

A further objection to Shepard's theory is the evidence that even the compacted Neogene clays have slumped from time to time in the late Pleistocene, although according to the theory they ought to have reached stability shortly after accumulation. Evidence of this slumping is provided by core A164–2 in which a "slab" of Neogene clay overlies oxidized Neogene clay mixed with Pleistocene sediment and by core A156–12 from the canyon floor which contains lumps of the Neogene clay in a gravel of late Pleistocene age. In our opinion periodic lowering of the canyon floor by erosion with consequent steepening of the canyon walls is the only satisfactory explanation for instability of the Neogene clays.

Lastly Shepard admits that turbidity currents can keep submarine canyons free of accumulating sediment and talus from the walls. Is this not an admission that turbidity currents are capable of something strangely similar to erosion? Why not go one step farther and admit the possibility that turbidity currents can erode compacted but uncemented sediments?

We feel that the most acceptable theory of origin of the Hudson Submarine Canyon and the exposures of Neogene sediments along the walls is erosion by turbidity currents as proposed by Daly (1936) and supported by Kuenen (1950). Shepard and Emery (1941) have found that the wallrock of the upper parts of certain canyons off the coast of California is granite. It must be admitted that the erosion of granite does put a strain upon the turbidity-current theory. On the other hand, the granite outcrops in these canyons do not lie at great depths. In Monterey Canyon, for example, granite is found at 930 m (500 fm). It is doubtful if eustatic lowering of sea level by itself could have been sufficient to expose the canyon walls to subaerial erosion at a present depth of nearly 1 km, but a combination of lower sea level and former uplift of the coast as suggested by Shepard (1948) might very well have sufficed to expose the granite to stream erosion. But if erosion of granite strains the turbidity-current theory, erosion of the lower reaches of the Hudson Submarine Canyon strains the "glacial-control and marginal-warping hypothesis" to the breaking point, for here we are confronted by depths down to 4000 m. Still worse, in the Northwest Atlantic Mid-Ocean Canyon (Ewing *et al.*, 1953) erosion at 5000 m must be explained. Here again we must emphasize that in these canyons at great depths there is no evidence of erosion of anything harder than compacted, but unlithified clay.

Further suggestive evidence of erosion by turbidity currents is the great quantity of sand interbedded with Pleistocene sediments of deep-water facies in the deep-sea fan which lies beyond the canyon. The particles of upper Eocene chalk containing characteristic discoasters in some of the coarse sand layers are significant. This same chalk has been cored in the canyon near the foot of the continental slope. The conclusion is inescapable that some erosion of the chalk took place as the current which carried the sand passed down the canyon.

We submit that erosion by turbidity currents is only one of the possible processes which has given rise to submarine unconformities. Elsewhere than in the canyons there is evidence that sediment cover has been removed by slumping. Probably most submarine exposures of old sediments are revealed by slumping.

In some cases direct evidence of movement of former overburden is visible on the contact surface as grooves parallel to the direction of dip of the surface. Such evidence of slumping has been found in cores taken on the continental slope, along the edge of the Blake Plateau, on the southern slope of the Puerto Rico Trench, and the northern slope of the Bartlett Deep. In other cores where grooving is absent slumping may be reasonably inferred from the dip of the contact surface and the regional topography.

Shepard (1948) has reviewed theories of origin of the continental slope. He rejects the prevalent theory that the continental slope represents a foreset deltalike deposit, built out in front of the advancing edge of the continental shelf. He cites the presence of rock surfaces on the outer shelf and rock bottom in many places on continental slopes. He concludes that the slope is due to faulting rather than to downwarping on the evidence of Cretaceous sediments along the east coast of the United States which are truncated by the slope rather than being bent down. The occurrence of pre-Pleistocene sediments in cores from the continental slope supports Shepard's conclusion. Truncation of sediments by the surface of the slope is further supported by a photograph of an outcrop of Eocene sediment on the continental slope off the northeast coast of the United States by Northrop and Heezen (1951). The camera, designed by Ewing, was provided with a small coring tube which brought up a few centimeters of sediment from the outcrop.

Exposures of older sediments on the flanks of the Bermuda Rise and certain seamounts such as the Muir Seamount pose a question. Must we look for a different cause to explain these exposures? In general, evidence of turbidity-current activity in the Bermuda region is confined to graded deposits in a zone near the base of the rise. Between this zone and the Bermuda Islands is a broad area of exposures of older sediments. Truncation of the older sediments is suggested, although not proven because of lack of sufficient instances, by occurrence of the oldest sediments at the deepest stations with successively younger sediments at shallower depths. It would seem from this that the initial slope on which the sediments were deposited was less steep than that of the present flanks of the Bermuda Rise. The graded layers of the outer zone of deposition prove that turbidity currents have from time to time flowed down the flanks of the Rise, but it is hardly conceivable that the widespread exposures of old sediments could have resulted solely from turbidity-current erosion. The source area within which turbidity currents could be generated by the stirring effect of storm waves appears to be too small even when allowance is made for lower levels of the sea during glacial ages. More probably the exposures have resulted directly from slumping which in turn would give rise to turbidity currents, the latter, no doubt, being responsible for the graded layers cored far down on the flanks. We ascribe the instability of sediment masses on the flanks of the rise to tectonic steepening of the slope in late Cenozoic time.

Some evidence suggests that the Muir Seamount on the northeastern flank of the Bermuda Rise is an uptilted fault block. Older sediments have been cored on its top and on its flanks. The layer of recent sediment in core A150-1 from the top gives evidence of current scour in its coarseness and presence of manganese oxide.

In contrast, the underlying Eocene sediment in its fineness and bimodal particle-size distribution is characteristic of accumulation on a broad surface of little relief. It appears probable, therefore, that uplift of the seamount postdates the vulcanism of the Bermuda Rise and is a result of faulting in late Cenozoic time. Similar faulting concentric to the Bermuda Islands may have been responsible for steepening of the slope with consequent slumping of sediment cover within the zone of exposures of older sediments.

With the single doubtful exception of the shale fragments with trilobites discussed heretofore, no sediment older than Cretaceous has yet been found in the Atlantic or Pacific (Revelle *et al.*, 1955). When considered in connection with the remarkably thin layer of unconsolidated sediment in the two oceans, this takes on possible significance. According to seismic-refraction measurements by Raitt (1956), the thickness of unconsolidated sediment in the Pacific ranges between 0.17 km and 1.0 km, the average being a little less than 0.5 km. Revelle *et al.* (1955) have remarked that this thickness seems to account for sediment accumulation only as far back as the Cretaceous, if it is assumed that the rate of accumulation in the Pacific has remained about the same as that determined for the past 14,000 years by Arrhenius, Kjellberg, and Libby (1951) from radiocarbon data.

Seismic measurements by Ewing, Sutton, and Officer (1954) show that the thickness of unconsolidated sediment in the Atlantic ranges between 500 and 1000 m. Here, as in the Pacific, the thickness of sediment cannot represent more than a small fraction of geological time, on the assumption that the rate of accumulation in the Atlantic has been somewhat faster than that in the Pacific. Because of the marginal trenches surrounding the Pacific, turbidity currents from the continental slopes are prevented from reaching the broad floor of the Pacific. There is no such barrier to turbidity currents in the Atlantic, a fact clearly demonstrated by the nature of the sediments cored in the deepest basins of the Atlantic. Very probably, therefore, the thickness, 1000 m, of sediment in the Atlantic represents about the same space of time as the 200 to 400 m in the Pacific.

Restricted thickness of unconsolidated sediment alone could mean nothing more than that the average rate of sediment accumulation during geological time had been much slower than it is at present. However, restricted thickness and apparent absence of any sediment older than Cretaceous together suggest that a large-scale reorganization of that part of the Earth's surface now occupied by the great ocean basins may have taken place during the latter part of the Mesozoic era.

Processes of Deposition

THE TWO CLASSES OF SEDIMENTS IN DEEP BASINS: Examination of hundreds of long deep-sea sediment cores from the North Atlantic has shown that there are two types of sediments in deep basins. One comprises types of sediment which are characteristic of deep environments. The other, found in many cores, usually interbedded with sediments of normal facies, comprises layers which differ strikingly in color, texture, and mineral and organic content. Many of these discordant layers are relatively coarse and contain remains of organisms characteristic of a shallow-water environment.

In the early days of oceanography these anomalous layers caused much speculation and led Philippi (1910) to postulate enormous vertical movements of the ocean bottom to explain their occurrence at great depths. Andrée (1920) devoted a chapter of his "Geologie des Meeresbodens" to discussion of their occurrence and possible modes of origin. However, there was no reason then to suppose that these anomalous sediments made up any important part of all sediment accumulating in the deep-ocean basins.

In 1947 an important suite of long cores was taken with a Kullenberg corer in the Atlantic by members of the ALBATROSS scientific party, who were on a worldwide oceanographic expedition under the direction of Hans Pettersson. Sand layers were found in several of these cores. Pettersson (1953) suggested that these may be turbidity-current deposits.

More than 2000 long cores raised by Ewing and coworkers in the Atlantic, Caribbean, Gulf of Mexico, and Mediterranean have proven that these anomalous sediments are widespread and that locally they make up the major part of the Pleistocene section in the deep basins.

It has, therefore, seemed desirable to recognize two classes of sediments, that is (1) those which have accumulated slowly and continuously, and (2) those deposited catastrophically by turbidity currents.

SEDIMENTS OF CONTINUOUS ACCUMULATION: The Pleistocene sediments of continuous accumulation in the cores discussed in this paper are composed essentially of mineral particles of silt and clay size, of coccoliths, or minute calcareous plates secreted by various species of Protista, and of the calcareous tests of planktonic Foraminifera. The proportion of calcareous to mineral elements varies with depth of water and proximity to the continents. On the continental slopes the calcareous fraction is diluted by fine terrigenous material. At stations more remote from the continents and where the depth of water exceeds 5000 m the calcareous element is much reduced by solution. Such abyssal sediments largely composed of clay-size particles and nearly devoid of the tests of planktonic Foraminifera are the "red clays" of Murray and Renard (1891). Typical "red clays" or brown lutites contain less than 1 per cent of material coarser than 74μ. This coarse fraction is highly characteristic and makes possible a clear distinction between brown lutites of truly abyssal facies and fine-grained sediments deposited at abyssal depths by turbidity currents. It consists of micronodules of manganese oxide. usually a few grains of quartz, minute teeth, chrondrules of bronzite, and "cosmic spherules" from outer space. Lutites deposited by turbidity currents contain no coarse material other than an occasional particle of plant detritus.

Because of the extremely slow rate of accumulation, many cores of brown lutite in the Lamont collection probably include the entire Pleistocene section. Unfortunately we have no way of distinguishing Pleistocene climatic zones in these cores. For this reason no core consisting solely of brown lutite has been described herein.

Although Foraminifera may be fairly abundant in sediments from depths between 5000 and 4000 m, many of the tests are fragile because of partial solution and break during washing. Hence, if the objective of coring is to obtain records of Pleistocene climatic changes, sediments from depths less than 4000 m should be chosen wherever possible.

If the climatic changes of the Pleistocene were of world-wide effect, the corresponding faunal zones in deep-sea sediments ought to be correlatable over long distances. Correlation among many cores from widely scattered stations in the Atlantic and Caribbean establishes the validity of the faunal zones shown in Figure 24. The figure also shows a generalized climatic curve based on variations in planktonic Foraminifera, a linear time scale, and a tentative correlation of the faunal zones with the generally accepted sequence of Pleistocene climatic events. Figures 25–37 show the climatic curves of individual cores.

Figure 25 shows curves of climatic variation deduced from the planktonic Foraminifera in three cores, A180–72, 73, and 76, raised in the Equatorial Atlantic from depths between 3000 and 4000 m. Table 1 gives the positions of these cores. Correlation of the faunal zones from core to core proves that sedimentation at these stations has not been interrupted by slumping, submarine erosion, or deposition by turbidity currents. The methods of faunal analysis by which the correlations have been made will be explained hereafter. Figure 20 shows the variation in percentage of coarse fraction of the three cores. A reasonably good correlation between the adjacent cores, A180–72 and 73, is apparent, and in A180–76 there is a suggestion of correlation. However, in A180–74, another core in this suite, the faunal zones of which correlate very well with those in the other three cores, there is no discernible correlation in variation of the coarse fraction. Evidently the percentage of 74-μ fraction is not a very reliable parameter by which to correlate over long distances. In these cores the coarse fraction consists for the most part of the tests of planktonic Foraminifera. The sediment is foraminiferal lutite with burrow mottling throughout (Pl. 2, fig. 2).

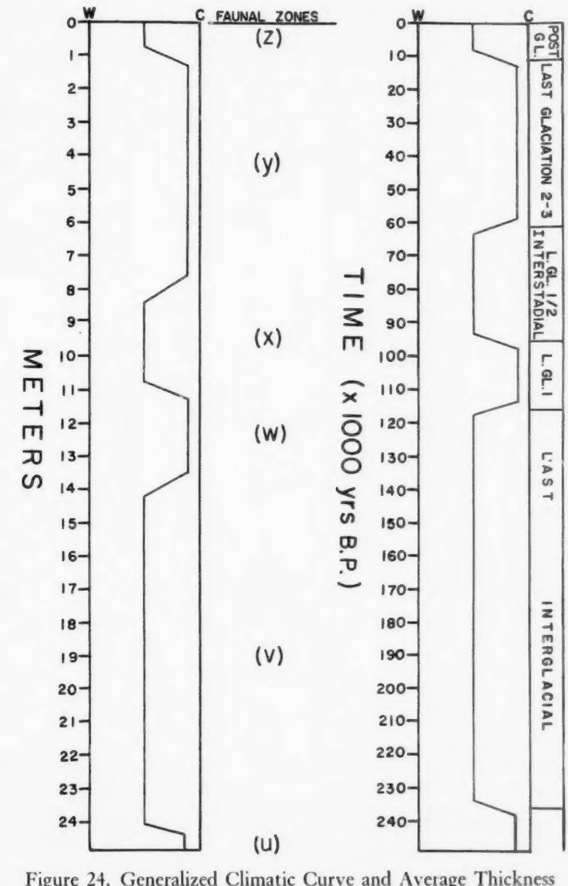

Figure 24. Generalized Climatic Curve and Average Thickness of Sediments in the Deep Atlantic and Caribbean, and Generalized Climatic Curve, Linear Time Scale, and Climatic Succession. Faunal zones u–z discussed in text.

In these cores the color of the sediments varies according to the climate, as shown by the Foraminifera. The zones of mild climate are brown, whereas those containing cool-water Foraminifera are shades of gray.

Another peculiarity of coloring is the cyclical nature of the upper gray zone. In the four cores this gray zone includes nine distinct layers or cycles, each marked by rather abrupt change from light to dark gray at the base followed by gradual lightening upward. Thicknesses of the cycles range from 15 to more than 30 cm. The zone of cool-water Foraminifera beneath the zone of warm-water Foraminifera or below 360 cm in core A180–72 includes a single cycle only.

Possibly the brown zones correspond to times of desiccation and the gray to pluvial phases in North Africa. The current system of the eastern North Atlantic is such that the major part of the terrigenous sediment reaching these stations probably came from the rivers of Northern Africa; these rivers during the pluvial phases may have brought quantities of plant detritus to the Atlantic. If so, the gray color of the sections corresponding to glacial ages may be due to carbonaceous pigment.

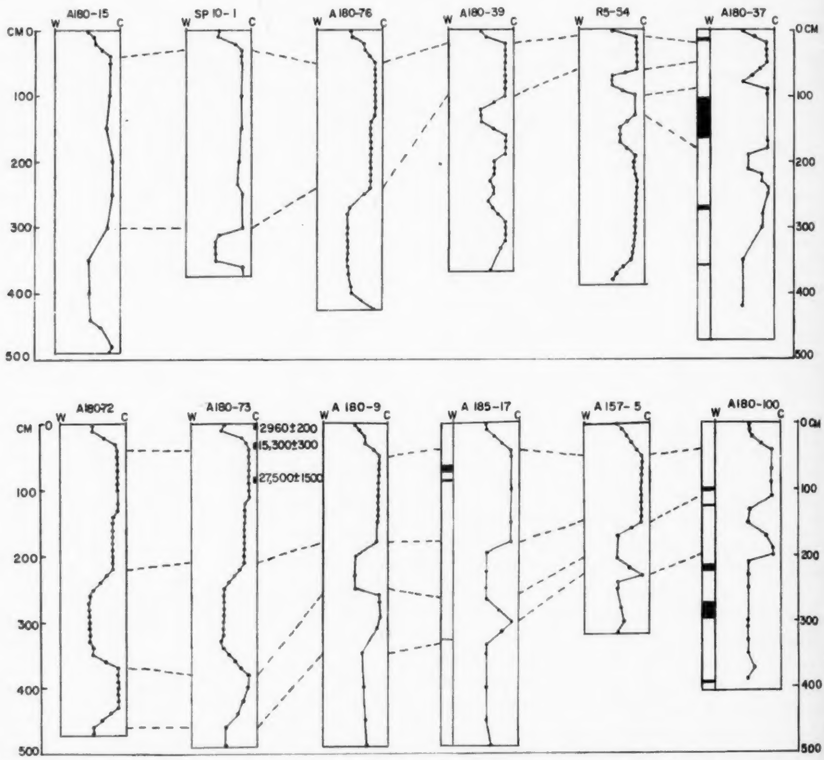

Figure 25. Climatic Curves Based on the Relative Numbers of Warm- and Cold-Water Planktonic Foraminifera. *See* Figure 1 and Table 1 for locations of cores. *W* indicates relatively warm climate and *C* relatively cold climate. Present climate is plotted on midpoint between *W* and *C*, and inferred past climate is plotted with respect to it. Dashed lines connect faunal and climatic changes believed to have been synchronous. Numbers to right of core are radiocarbon ages in years B. P. Sections of core used for dating are indicated by black boxes. Black denotes sand and silt; lines denote thin sand or silt layers; open zones indicate lutite. Cores without lithological columns consist of lutite only.

Color layers corresponding to climatic zones have not been found in the western Atlantic or Caribbean. For example cores A172–6 and A179–4 (Fig. 37) from the Caribbean contain corresponding faunal zones, but the sediment is brown throughout. It is unlikely that much sediment from Northern Africa would enter the Caribbean, whereas the northern part of South America, the major source of terrigenous sediment in the Caribbean, because of proximity to the equator, probably did not experience corresponding extremes of climate during the Pleistocene.

The cyclical layering of the upper gray zone remains unexplained, however. In their well-defined boundaries and gradual change upward from dark to light the layers superficially resemble layers deposited by turbidity currents. However, in other ways they are very different. For example, they lack particle-size sorting or grading. Foraminifera are evenly distributed from top to bottom. There is no concentration of burrow mottling in the upper parts. The layers correlate from core to core in spite of the wide separation of the stations and intervening bottom topography which would prevent any single turbidity current from reaching all four stations.

If the penultimate period of mild climate came to an end about 60,000 years ago (Fig. 24), the average time interval represented by each gray cycle must be on the order of 5000 to 6000 years. We are not aware of any known climatic cycle of about that period.

Two cores, A180–51 (Fig. 31) and 53 (Fig. 27), from stations northwest of Cape Verde, French West Africa, show similar cyclical layering, that is, an abrupt upward change from light to dark and a gradual change to light again. Here the cycles are thicker, with variation from half a meter to more than 1 m, as would be expectable at these relatively nearshore stations where accumulation of fine terrigenous sediment would be much more rapid. The rapid accumulation is shown by the uniformly small percentage of coarse fraction in both cores (Fig. 19). As is the case with the equatorial cores, all evidence is against turbidity-current deposition. Unfortunately neither core penetrates to what can be identified with certainty as the penultimate warm zone. Consequently, it is impossible to determine whether there is a layer-by-layer correlation between these Cape Verde cores and the Equatorial suite.

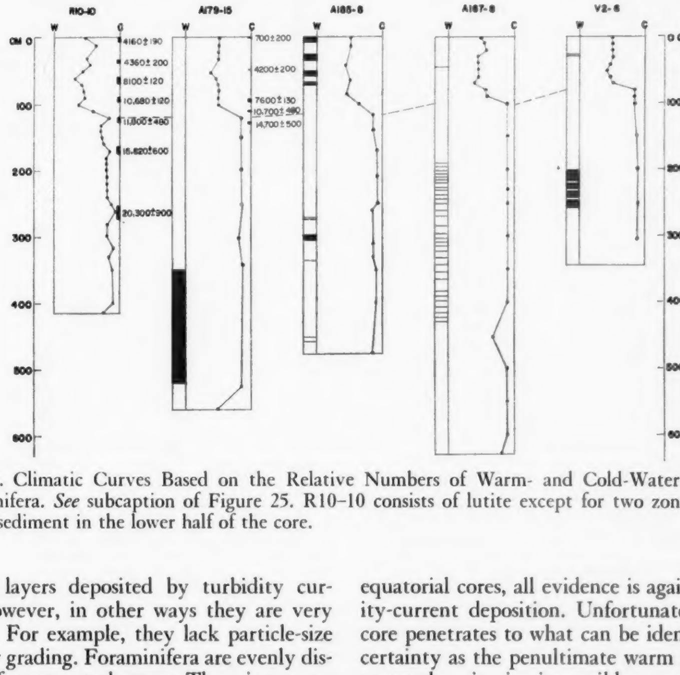

Figure 26. Climatic Curves Based on the Relative Numbers of Warm- and Cold-Water Planktonic Foraminifera. *See* subcaption of Figure 25. R10–10 consists of lutite except for two zones of glacial marine sediment in the lower half of the core.

Although rate of sediment accumulation is in general influenced by distance from the source of terrigenous material, irregularities of bottom topography may be the dominant influence locally. Core R10–10 is an interesting example of the probable effect of the topographical setting upon rate of accumulation. The position is given in Table 1. Although not quite in mid-ocean, it is nevertheless far removed from any source of abundant terrigenous sediment. The sequence of Foraminifera (Fig. 26) indicates the climatic change at the close of the last glacial age at a depth of about 100 cm. This implies a rate of accumulation not very different from that in core A179–15 (Fig. 26), which was raised not far from Eleuthera, Bahama Islands (Fig. 3), where rapid accumulation indicated by the Foraminifera is confirmed by the radiocarbon dates shown in Figure 26. In contrast, A180–14 (Fig. 27) from a station south of R10–10 contains evidence of the corresponding climatic change between 30 and 40 cm; A157–13 (Fig. 7) shows the climatic change at between 10 and 20 cm (Fig. 36). Because of the surprisingly rapid rate of accumulation and the interesting radiocarbon dates, the lithology of core R10–10 deserves attention.

The uppermost 10 cm of core R10–10 was badly disturbed during recovery and transportation. Mixing in this way may partly account for the anomalously old date of the uppermost sample, 4160 ± 190 years. From 10 cm to 175 cm the sediment is a slightly silty foraminiferal lutite in shades of gray and rose gray. There is no evidence of turbidity-current deposition or any abrupt change in lithology which might be indicative of emplacement of sediment by slumping or mud flow. The sequence of dates is in itself strong evidence that below the top 10 cm, deposition has been orderly. If slumping or mud flow had taken place, an anomalous sequence of old sediment over young would be almost inevitable. Below 175 cm the section is somewhat more variable. Shards of silicic volcanic glass are very abundant from 175 to 200 cm. From 210 to 220 cm, Radiolaria and diatoms are very abundant.

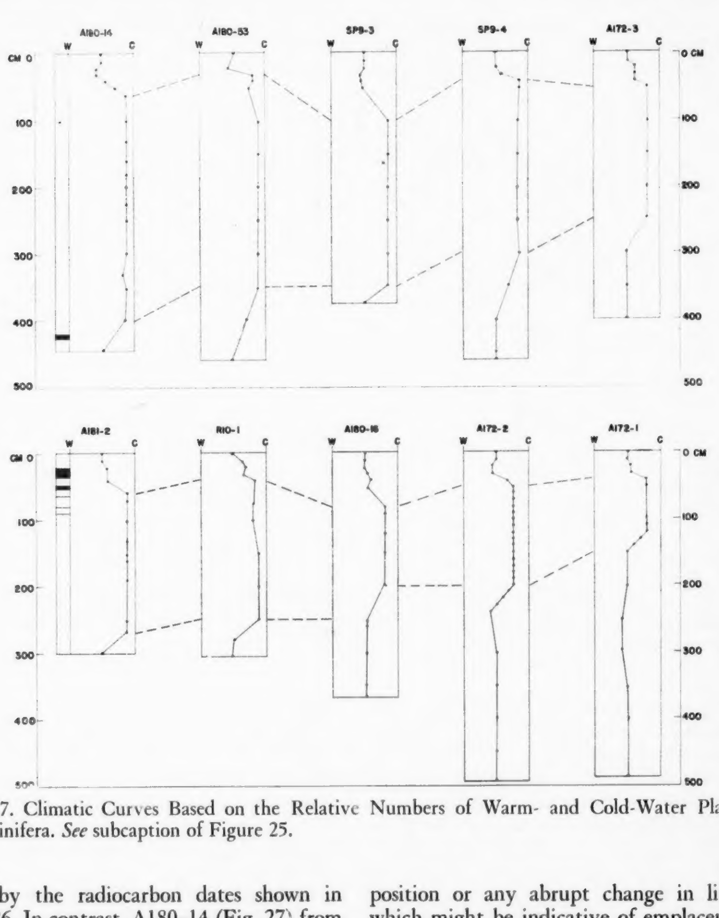

Figure 27. Climatic Curves Based on the Relative Numbers of Warm- and Cold-Water Planktonic Foraminifera. *See* subcaption of Figure 25.

Layers of glacial marine sediment occur between 250 and 265 cm and between 310 and 320 cm. The upper layer contains fragments of limestone and igneous rock up to 3 cm in diameter. Extremely rapid accumulation of this section is indicated by the date of 20,300 ± 900 years at 270 cm.

Figure 20 shows the variation in percentage of coarse fraction in core R10–10. From the curve it is evident that, except for the two samples from the glacial marine layers, the sediment in this core is remarkably fine for the depth of the station, a fact which is in agreement with the explanation for rapid accumulation by concentration of fine material by gentle current scour.

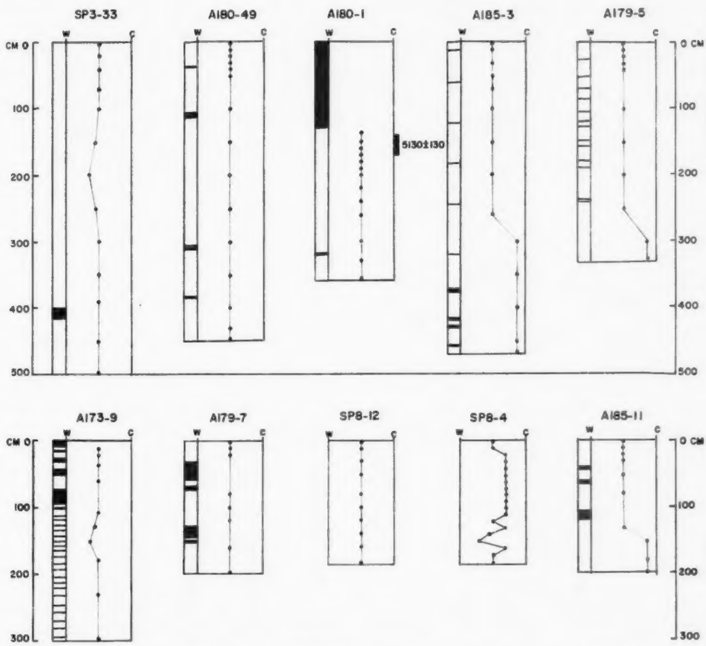

Figure 28. Climatic Curves Based on the Relative Numbers of Warm- and Cold-Water Planktonic Foraminifera. *See* subcaption of Figure 25.

This core was raised from the bottom of a depression which may act as a sediment trap. Unusual abundance of diatoms and Radiolaria throughout the core and particularly between 270 and 370 cm, the section of most rapid accumulation, suggests that this depression has been receiving fine material such as clay particles, coccoliths, diatoms, and Radiolaria from adjacent rises where gentle current scour has prevented their accumulation.

We conclude, therefore, that, except for the glacial marine layers, this core offers an example of rapid but orderly particle-by-particle sediment accumulation in a depression in which current scour has concentrated fine material of terrigenous and organic origin.

SEDIMENTS DEPOSITED BY TURBIDITY CURRENTS: In general, turbidity-current sediments differ from the layers of sediment due to particle-by-particle accumulation with which they are usually interbedded.

Many are strikingly coarse in comparison with normal abyssal sediment. They include layers of well-sorted silts and sands and in a few cases gravels.

Core A156–12 from the bed of the Hudson Submarine Canyon (Figs. 2, 9) 170 km southeast of the edge of the continental shelf and at a depth of 3470 m is an example of a core containing gravel. Figure 12 shows a graphic log of this core. The upper part to 75 cm consists of layers of foraminiferal lutite alternating with fine micaceous sand. From 75 cm to 100 cm there is fairly clean gravel containing molluscan shells and shell fragments; muddy gravel be- cording to Richards and Ruhle (1955), most of the mollusks present are species which are normally confined to shallow water. A few deep-water forms are also present, but even these have not been found previously at so

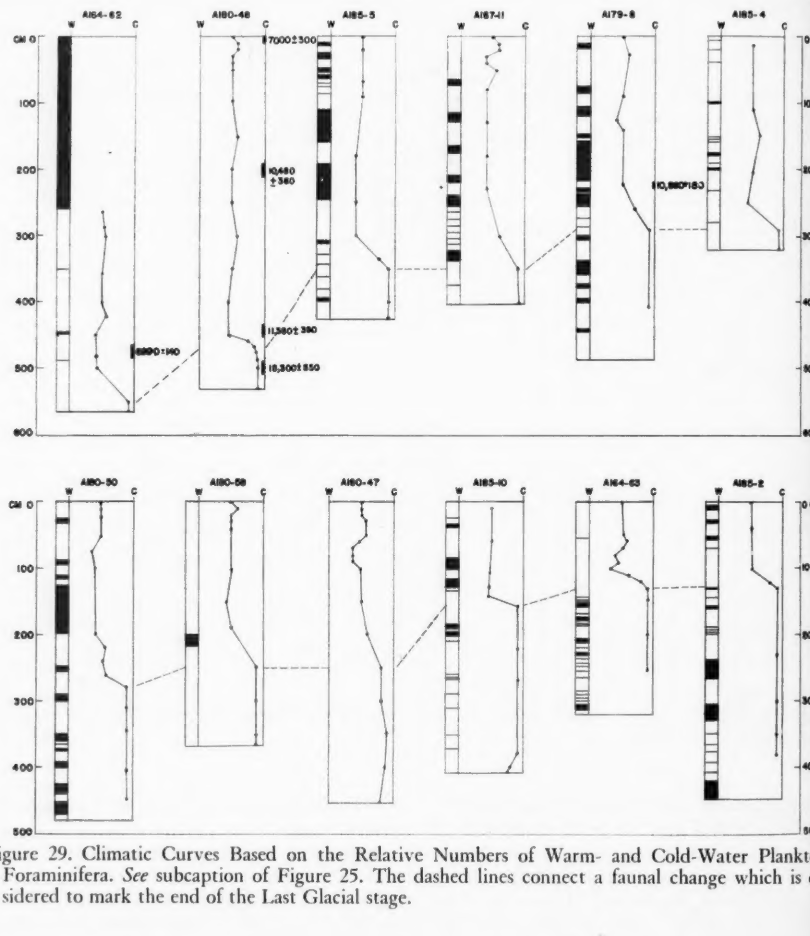

Figure 29. Climatic Curves Based on the Relative Numbers of Warm- and Cold-Water Planktonic Foraminifera. *See* subcaption of Figure 25. The dashed lines connect a faunal change which is considered to mark the end of the Last Glacial stage.

coming coarser downward extends from 100 cm to the bottom of the core at 365 cm. The pebbles, which reach a diameter of 2 cm, are composed of a variety of igneous, metamorphic, and sedimentary rocks including an Eocene chalk which has been cored near the foot of the continental slope (Northrop and Heezen, 1951) and Neogene green clay which has been cored at various points along the canyon walls. Ac-

great a depth as 3470 m. Richards and Ruhle conclude that the assemblage is characteristic of cold water and that Wisconsin age is substantiated by the presence of *Neptunea stonei.*

Another core, A164–38, containing material of gravel size, was raised from a depth of 4250 m at a station 55 km southeast of Bermuda (Figs. 6, 12). From the top, composed of calcareous silt, the particle size gradually increases downward. Well-sorted calcareous sand between 50 and 100 cm, containing much *Halimeda* detritus, is remarkably similar to the calcareous sands of Bermuda beaches. The material caught in the cutting edge of the coring tube below 173 cm includes shells and shell fragments with a few pebbles of limestone and igneous rock. The maximum diameter of the shells is 45 mm.

In typically graded layers there is complete gradation from well-sorted sand at the bottom to lutite devoid of any coarse fraction. Lutites of this kind commonly have a very high water content; they shrink greatly upon drying. Since settling of the finest material must be rather slow, completely graded layers are probably confined to stations where there is a fairly abrupt change in bottom gradient, as at the

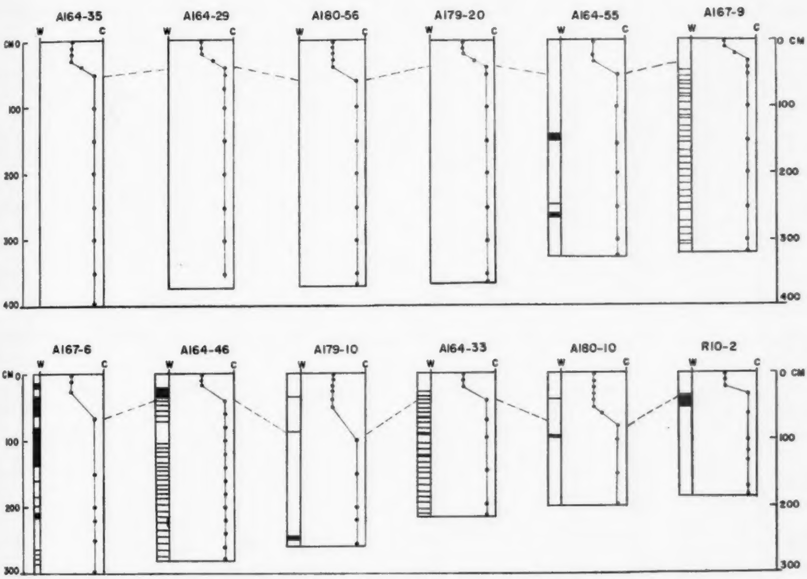

Figure 30. Climatic Curves Based on the Relative Numbers of Warm- and Cold-Water Planktonic Foraminifera. *See* subcaption of Figure 25. The dashed lines connect a faunal change which is considered to mark the end of the Last Glacial stage.

The absence of any appreciable layer of poorly sorted foraminiferal lutite on the calcareous silt at the top of the core indicates that the graded material of shallow-water origin must have been deposited relatively recently.

Another feature common in layers of sediment deposited from turbidity currents is grading, or gradual decrease in particle diameter from bottom to top of the individual layers. The importance of this feature has been emphasized by Kuenen and Migliorini (1950), who showed that grading is characteristic of sediments deposited by artificial turbidity currents. This experimental work provided a valuable clue to the origin of deep-sea sands.

margin of a basin, where ponding or backing up of the turbid water permits the settling out of the finest material. Examples of complete grading occur in core A179–8 from the margin of a basin north of Hispaniola (Pl. 1A). Figure 14 shows the graphic log of this core and indicates the positions of sand layers.

Another example of complete gradation occurs in core A172–10 taken on the flat floor of the Puerto Rico Trench at a depth of 7955 m. Figure 5 shows the position of the core, and Figure 12 shows the relationship between lutite and calcareous sand layers. The thick sand layer shown in Figure 12 is part of a graded layer extending from 28 cm below the top of the core to the base of the sand layer at 224 cm. The upper part of the graded layer is a gray-brown lutite of very smooth texture from which there is complete gradation downward into calcareous sand composed of the tests as against less than 1 per cent in the brown lutite. The sand indicates that the initial velocity of the current must have been fairly great. Rapid decrease in velocity, however, is indicated by the lutite of the upper part of the

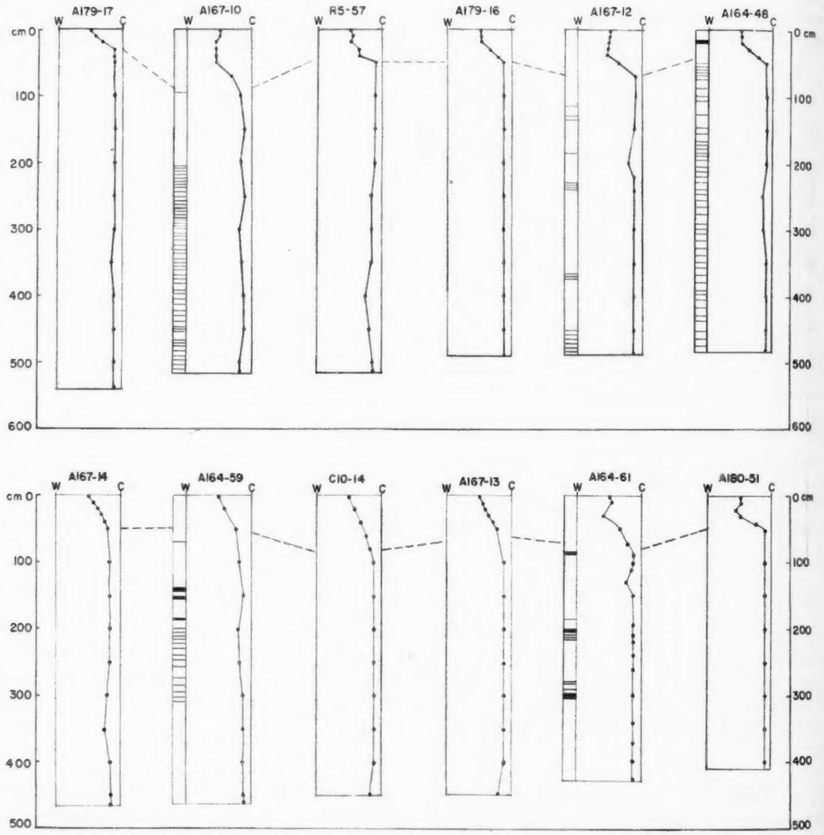

Figure 31. Climatic Curves Based on the Relative Numbers of Warm- and Cold-Water Planktonic Foraminifera. *See* subcaption of Figure 25. The dashed lines connect a faunal change which is considered to mark the end of the Last Glacial stage.

of Foraminifera and pteropods. Particles of a calcareous alga, *Halimeda* sp., and benthic species of Foraminifera of shallow-water environment are also present. In texture the lutite of the upper part is indistinguishable from the interbedded brown lutite of abyssal facies. The lutite of the upper part is distinct in color, however, and particularly in mineral composition, the carbonate content being 37 per cent layer which must have settled out of water nearly, if not quite, at rest. This suggests that a large part or all of the floor of the trench was flooded by turbid water.

On long slopes of fairly uniform gradient, such as the deep-sea fan of the Hudson Submarine Canyon (Fig. 2), sand layers having only a narrow range of particle sizes are common in the cores. Lutite is commonly absent from such layers, and grading of the sand is not readily discernible except by mechanical analyses. Layers of this kind occur in Core A164–14 (Figs. 2, 9), the graphic log of which is shown in Figure 12.

thermore, because of their low density, plant particles 1 mm or more in diameter may be transported and deposited in abundance with quartz silt. Finely divided dark to black organic matter is concentrated in places in the upper

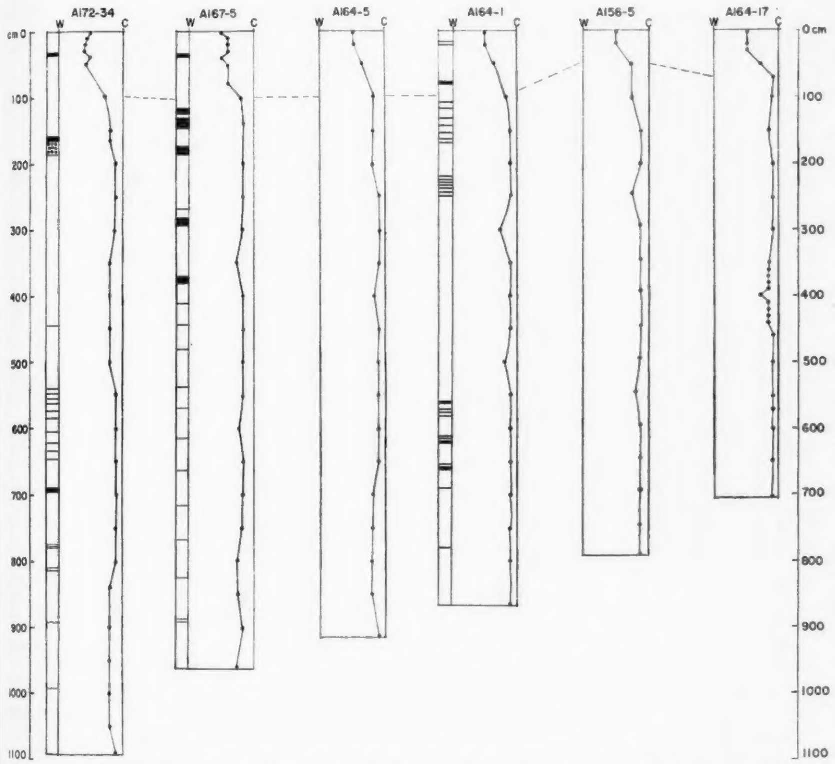

Figure 32. Climatic Curves Based on the Relative Numbers of Warm- and Cold-Water Planktonic Foraminifera. *See* subcaption to Figure 25. The dashed lines connect a faunal change which is considered to mark the end of the Last Glacial stage.

Much fine material is carried beyond the deep-sea fans of the continental rise, as evidenced by the common occurrence of gray calcareous lutite layers interbedded with abyssal brown lutite in cores from deep stations.

Shallow-water origin of at least a part of the coarse material in graded layers is proved by the presence of certain species of benthic Foraminifera, particles of calcareous algae, and by noncalcareous plant detritus. Noncalcareous plant detritus, because it is dark brown or nearly black, is particularly conspicuous. Furthermore, parts of graded layers, in which case there is gradual change upward from light to dark gray. The presence of abundant coarse particles of *Halimeda* in a graded layer proves conclusively that the coarse texture cannot have resulted from concentration of the coarse particles of a normal abyssal sediment through current scour.

On the other hand, the presence of material of shallow-water origin is not evidence of deposition in shallow water. Compelling evidence that these sediments were laid down in water of essentially the same depth as that which now covers them is the fact that with few exceptions they are interbedded with normal sediments of deep-water facies. Furthermore, their good particle-size sorting, regular deep, broad basins with nearly level floors. These layers are not found in cores taken on low isolated rises. Depth differences of only 200 or 300 m at depths between 4000 and 5000 m can make the difference between an almost

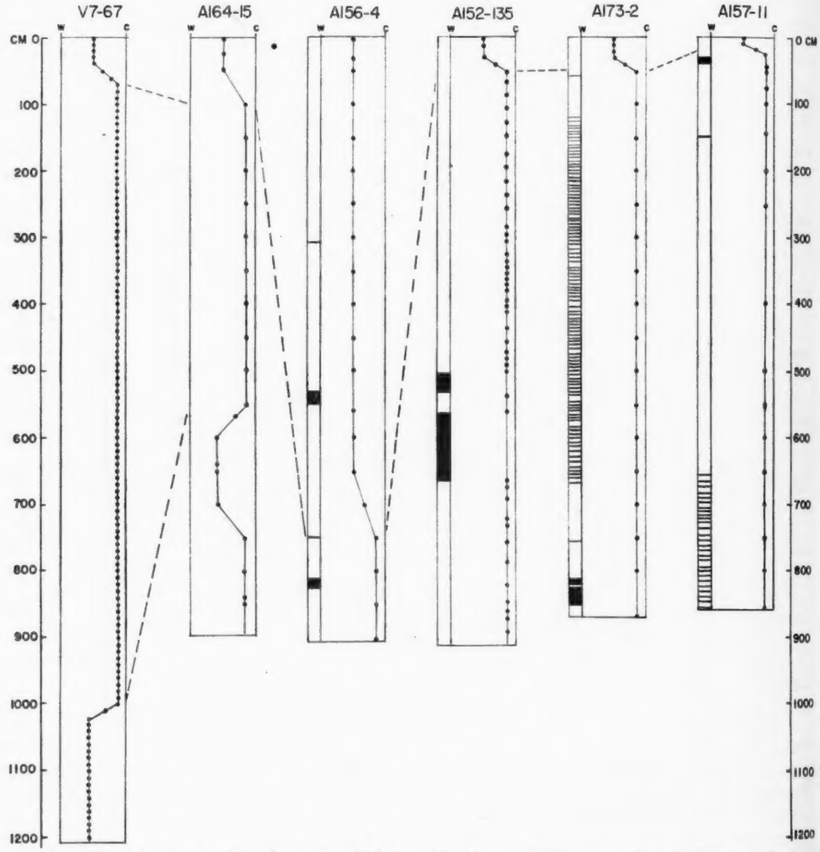

Figure 33. Climatic Curves Based on the Relative Numbers of Warm- and Cold-Water Planktonic Foraminifera. *See* subcaption to Figure 25.

bedding, and grading distinguish them from typical shallow-water deposits.

The areal distribution of these sediments with respect to ocean-bottom topography is significant. Graded layers of coarse sediment have been cored in submarine canyons, on gently sloping plains upon which submarine canyons open, and in deep trenches. The gray calcareous lutite layers occur particularly in continuous series of graded layers at one station and typical brown foraminiferal lutite with burrow mottling throughout the section at an adjacent station.

An important consequence of this localization of very different processes of deposition is great variation from place to place in rate of sediment accumulation depending upon bottom configuration. Use of the precision sonic depth recorder shows that the floors of deep oceanic depressions are commonly nearly level plains of extraordinary smoothness. This is in marked contrast with the rugged, much broken up topography of positive features such as the Bermuda Rise and Mid-Atlantic Ridge. This topographical contrast is most plausibly explained by the leveling effect of the rapid filling of depressions by turbidity currents.

Figure 2 shows the positions of cores from the region of the Hudson Submarine Canyon. Figure 9 shows the distribution of sand and silt layers in the cores. More detailed diagrams of cores A164–13, 14, and 19, A172–33, and V3–158 are shown in Figures 12, 14, and 15. With the possible exception of cores A164–13 and 19, correlation of sand layers from core to core is not evident. However, the stations are widely scattered. The most closely spaced stations, A164–20 (Fig. 11) and V3–158 (Fig. 15), are 13 km apart. Evidently the sands were not deposited by widely spreading sheet flow. This was hardly to be expected. The coarseness of many of the sands implies transportation by currents of greater velocity than could be attained by a thin layer of turbid water spread over a broad area. The distribution of sands and the topographical form of the fan can best be explained by supposing that the flow was channeled and that the channel or channels wandered from side to side across the fan.

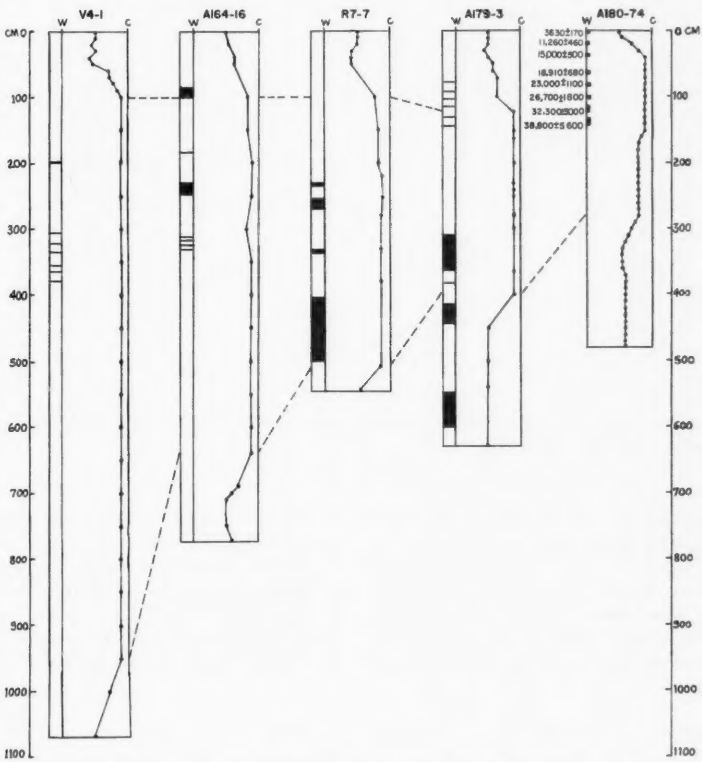

Figure 34. Climatic Curves Based on the Relative Numbers of Warm- and Cold-Water Planktonic Foraminifera. *See* subcaption of Figure 25.

However, given the right topographical setting there is no evident reason why turbid water flowing at low velocity should not spread

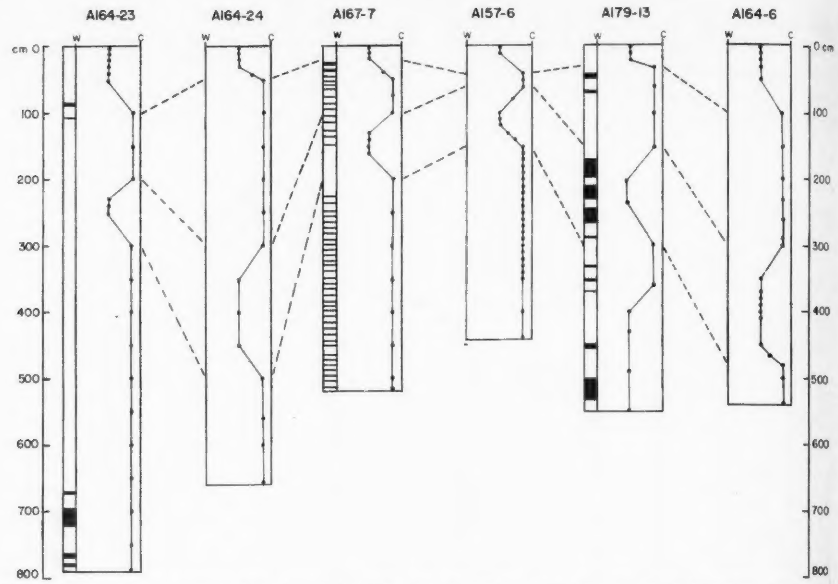

Figure 35. Climatic Curves Based on the Relative Numbers of Warm- and Cold-Water Planktonic Foraminifera. *See* subcaption of Figure 25.

over a wide area. This should happen whenever a large quantity of turbid water flows out on the nearly level floor of a basin. Evidence for such flooding of a broad area by turbid water occurs in the sediments of the Sigsbee Deep in the Gulf of Mexico. Here a number of easily identified graded layers extend over areas on the order of 3000 square miles. Under such circumstances low velocity of flow would be expectable, and this is borne out by the sediments themselves. Sands comparable with those of the deep-sea fan of the Hudson Submarine Canyon are absent from the graded layers of the Sigsbee Deep, which consist of thin basal

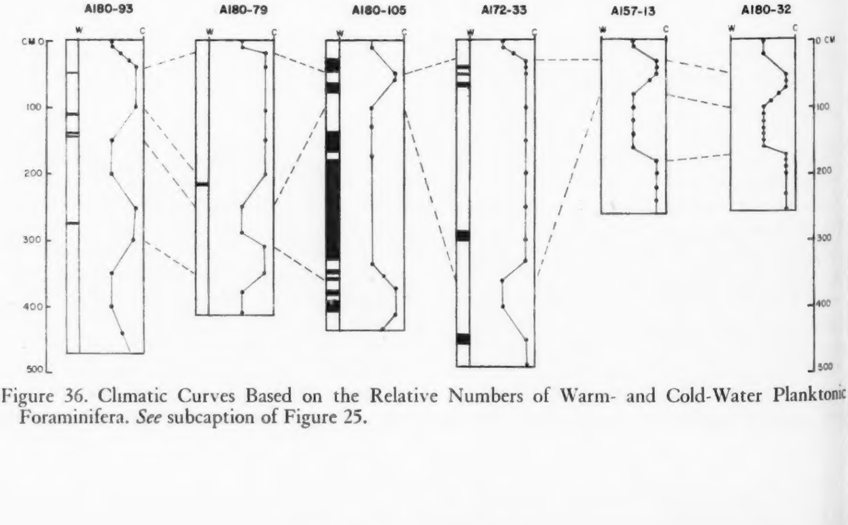

Figure 36. Climatic Curves Based on the Relative Numbers of Warm- and Cold-Water Planktonic Foraminifera. *See* subcaption of Figure 25.

layers of silt grading upward into relatively thick layers of gray lutite. The mass of turbid water must have been moving very slowly and may have been at rest when the finest sediment of these layers was settling. These sediments of coarse fraction, coiling direction of *Globorotalia truncatulinoides*, and climatic changes inferred from the planktonic Foraminifera. The samples for faunal analyses were taken from burrow-mottled layers of unsorted foraminif-

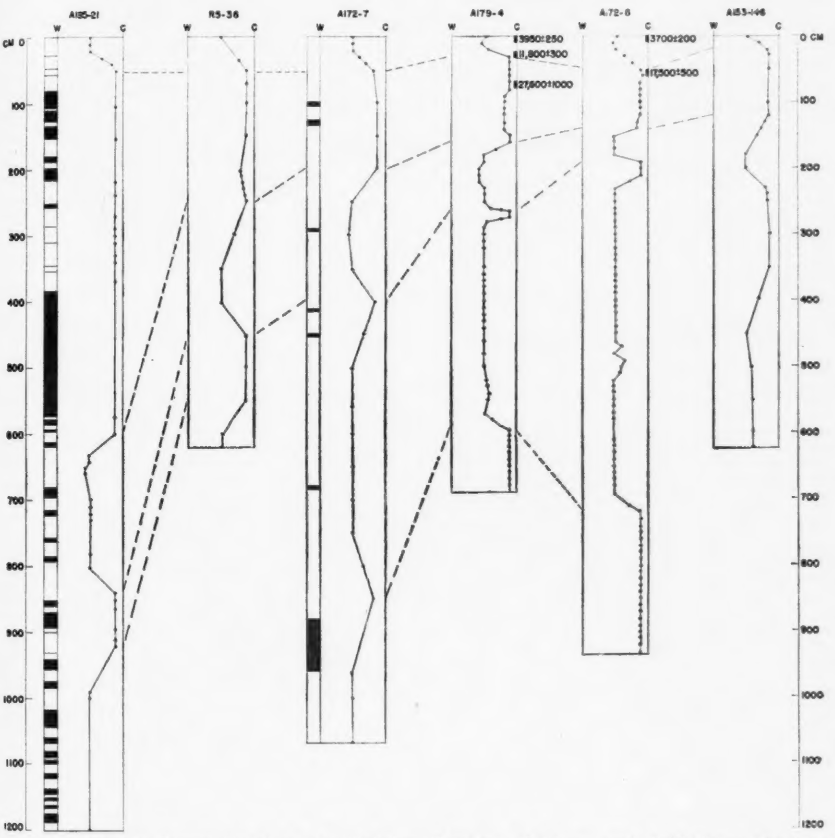

Figure 37. Climatic Curves Based on the Relative Numbers of Warm- and Cold-Water Planktonic Foraminifera. *See* subcaption of Figure 25.

are described and their significance discussed by Ewing, Ericson, and Heezen (1958).

A layer-by-layer correlation of graded sediments has been found in two cores, A185–20 and 21, from stations 19 km apart lying south of the western end of Cuba (Fig. 1). Figures 15 and 13 show the distribution of sand and silt layers in these cores. Figures 17 and 18 show their variations in percentage of coarse fraction. Figure 38 shows correlation by percentage

eral lutite lying between the graded layers. The sands and silts in these cores are for the most part calcareous with some admixture of plant detritus.

The mineral composition varies somewhat among sands and silts of graded layers in deep-sea cores. For the most part the coarse fractions are composed of quartz or calcareous particles of organic origin. Figure 8 shows the general areal distribution of the two kinds of sands.

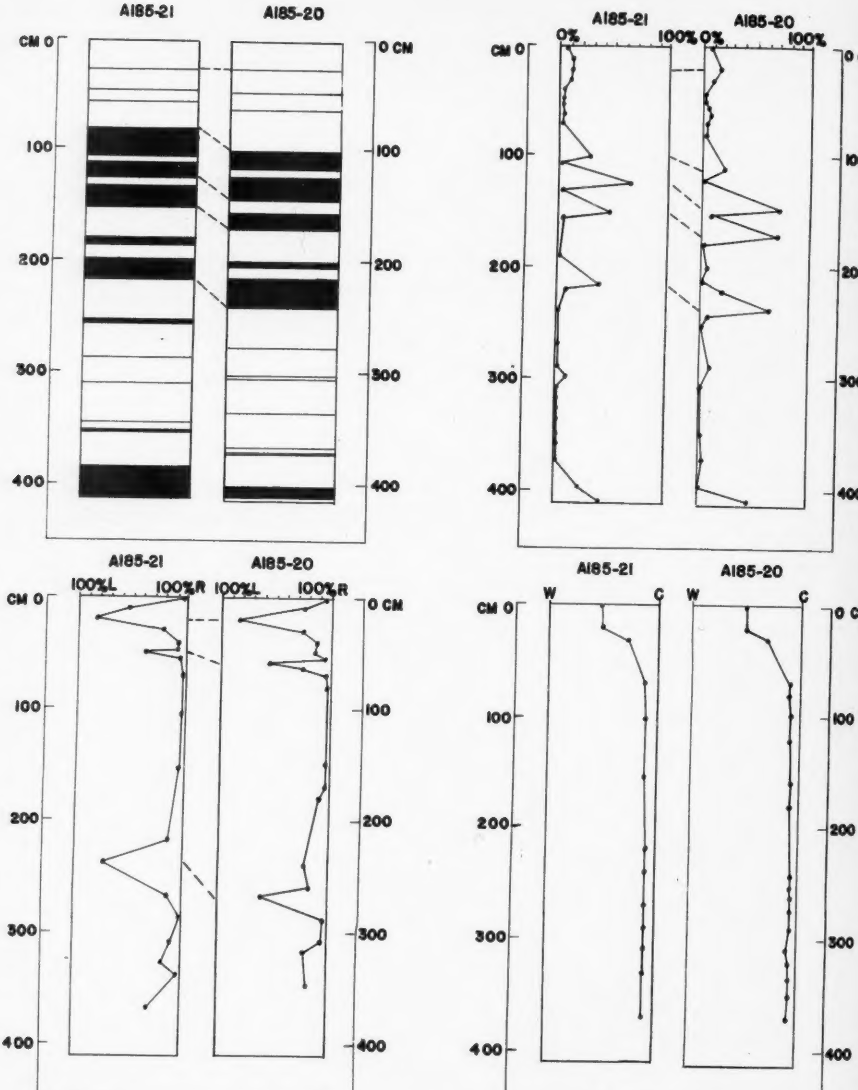

Figure 38. Correlation of Lithology, Variations in Coarse Fraction, Coiling Direction of *Globorotalia Truncatulinoides*, and Climatic Curves in Two Cores from Stations 6 Miles Apart and Approximately 50 Miles South of the Isle of Pines, Cuba. The two columns in the upper left-hand corner show lithology: black zones indicate calcareous sand and silt; lines indicate thin sand or silt layers; open zones indicate lutite. The curves in the upper right-hand corner are based on variations in percentage of coarse fraction $>74\mu$. The curves in the lower left-hand corner are based on the ratio in percentage between right- and left-coiling shells of *Globorotalia truncatulinoides:* L indicates left, R, right. The curves in the lower right-hand corner are based on the relative numbers of warm- and cold-water planktonic Foraminifera; *W* indicates relatively warm climate and *C* relatively cold climate. *See* Figure 1 and Table 1 for core locations.

Cores in which quartz is the dominant mineral are clustered in the region north of a line joining Cape Hatteras and Bermuda extending eastward almost to 45° West Longitude. In most of these cores quartz silts occur with the sands. However, the more easily transported silts are much more widely distributed than the quartz sands. Quartz silts without sand have been found between Puerto Rico and Bermuda, southeast of Cape Hatteras, and southeast of Newfoundland.

The calcareous sands occur predominantly around Bermuda and in the West Indies region. A general correspondence in mineral composition between the graded layers and the nearest shallow-water deposits is evident from Figure 8. Vast quantities of organic carbonate are produced in shallow water around Bermuda and in the West Indies.

Although quartz is the dominant mineral in the region north of Cape Hatteras, many other minerals and rock particles are abundant. Among these are species of feldspar, various micas, chert, glauconite, pyrite, limestone, gray and red shale, sandstone, coal, and particles of igneous and metamorphic rocks. In the Hudson Canyon region particles of Eocene chalk occur in some of the sands. These, although less than 1 mm in diameter, are easily identified by characteristic discoasters as coming from outcrops of Eocene chalk which have been cored at several stations on the continental slope in the vicinity of the Hudson Submarine Canyon (Cushman, 1939; Northrop and Heezen, 1951). In spite of their heterogeneous composition, these sands cannot be classified as graywackes or subgraywackes (Krumbein and Sloss, 1951) because of the strong dominance of quartz and good to excellent particle-size sorting.

The degree of rounding of sand grains varies greatly within single samples. This is particularly true of the larger grains, among which there is every gradation from angularity to good rounding, in some cases accompanied by frosting. Probably the well-rounded grains have passed through several cycles of erosion, abrasion, and redeposition. It is fairly certain that transportation by a Pleistocene turbidity current has not led to the rounding of the harder mineral particles. The well-preserved though fragile tests of Foraminifera which are common in graded layers indicate that transportation by turbidity currents does not entail much abrasion of sand-size particles.

In summary, the sands of the Hudson Canyon region are essentially similar in mineral composition and in diversity of degree of rounding to the coarse fraction of samples of unsorted sediment taken on the continental shelf by members of the Lamont Geological Observatory staff.

TURBIDITY CURRENTS AND THE ORIGIN OF PETROLEUM: The almost complete absence of hydrotroilite in the thoroughly burrow-mottled sediments of deep basins seems to indicate that the mud feeders devour so completely as to leave little or no nourishment for the heterotrophic bacteria. Apparently under normal conditions of slow and continuous sediment accumulation, complex organic substances are broken down into simple salts and carbon dioxide by scavengers. Because of this difficulty, students of the origin of petroleum have used the euxinic environment to explain the abundance of organic matter in some ancient sediments.

Vašíček (1953b) has advanced an alternative theory. In his view a turbidity current rushing down-slope should sweep up and carry along much organic matter, living or dead. With decrease in gradient the organic matter gathered up from the entire area traversed by the current will be deposited with the finer fractions of mineral matter. If the layer so formed is more than a few decimeters thick, much of it will be inaccessible to mud feeders. Some of this organic matter will be attacked by anaerobic bacteria, but it is at least possible that their action converts the heterogeneous organic substances into the various compounds which constitute petroleum (Beerstecher, 1954).

Furthermore, the well-sorted sands of the lower parts of graded layers are ideally suited to serve as reservoir rocks in view of their high porosity, permeability, and position between impermeable layers of clay.

Several pertinent observations from study of the cores are worth repeating: (1) burrowing is nearly always confined to the top 1 or 2 decimeters—the major part of thicker graded layers is unattacked by scavengers; (2) the fairly common occurrence of plant detritus in graded layers proves that organic matter can be transported and deposited by turbidity currents; and (3) hydrotroilite, commonly present in the clayey parts of graded layers, is indirect evidence of finely divided organic matter. We conclude that the possible role of turbidity currents in the concentration of organic matter, in preserving organic matter from scavengers, and in providing suitable reservoir rocks is worthy of further investigation. Passega (1954) has recognized the importance of this problem in petroleum exploration.

PART II. MICROPALEONTOLOGY AND PLEISTOCENE STRATIGRAPHY

Planktonic Foraminifera

Temperature variations in surface water of past times should be recorded in the succession of layers of bottom sediment as variations in relative frequencies of the species of planktonic Foraminifera most sensitive to temperature. To determine the temperature tolerances of the different species, we must know their present areal distributions in the oceans. The ideal method would be to chart occurrences of the living species collected with plankton nets, as Schott (1935) and Bé (1959) have done. Their charts unfortunately leave large areas of the Atlantic blank. Because of the expense of collecting plankton and the difficulty of separating the Foraminifera from the large volume of other planktonic organisms, these areas will probably remain blank for some time. In the meantime to obtain an over-all view of distributions in the North Atlantic and adjacent seas, we must rely upon occurrences of the tests in the uppermost layer of sediment. This method is open to some objections; the most serious is that the tests are subject to more or less solution depending upon the depth of water through which they must sink. For example, the bottom sediment of the Nares Abyssal Plain (Heezen, Tharp, and Ewing, 1959) southeast of Bermuda is "red clay" or brown lutite nearly devoid of Foraminifera. Elsewhere in shallower water, the tests show partial solution. The more fragile tests of some species may be nearly or entirely destroyed, with the result that the assemblage may appear to be dominated by some heavy-shelled form which was of minor importance. If the ecology of the planktonic Foraminifera were of primary interest, the foraminiferal assemblage in the uppermost layer of sediment would be of doubtful value. Our objective, however, is to use the assemblages in the deeper sediment layers to interpret oceanic climate. Thus it is probably more realistic to compare the thanatocoenoses of the older sediment layers with the thanatocoenose of the uppermost layer than to attempt to relate them all to the biocoenose now living in water thousands of meters above the bottom.

We have assumed that in the foregoing discussion the uppermost layer of sediment has been deposited in postglacial time and by slow particle-by-particle accumulation. Not uncommonly, however, the upper parts of cores have been deposited by turbidity currents. Such allochthonous layers are invariably sharply differentiated from normal sediment of slow accumulation, as has been noted.

Absence of the postglacial layer because of removal by slumping or erosion by turbidity currents may be more difficult to recognize. However, the Pleistocene faunal sequence in the North Atlantic helps to eliminate this source of confusion. For example, the zone corresponding to the last warm interstadial, when exposed at the surface, can be distinguished from Recent sediment by the presence of *Globorotalia menardii flexuosa* (Pl. 3) and *Globigerina hexagona*. This zone will be referred to hereafter as zone (x). (*See* Fig. 24.) A universally applicable test is the extent to which the faunal sequence in a given core correlates with the sequence in other cores from the same region and about the same depth. Any core which contains an anomalous assemblage of planktonic Foraminifera in the uppermost sediment layer must be regarded as incomplete in spite of lithological similarity with other cores.

Some of the uppermost sediment layer may be lost when the coring tube is brought on board ship. For this reason, whenever possible, top samples from trigger-weight cores, or pilot cores, have been used for study of the Recent foraminiferal assemblage. These trigger-weight cores are taken and stored in plastic liners which are kept upright until they reach the laboratory.

Charts showing the distribution of the important planktonic species in sediment samples from the Atlantic have been published by Schott (1935) and by Phleger, Parker, and Peirson (1953). Kane (1953) has investigated the correlation between distribution of planktonic species in sediments and mean annual surface temperatures in the North Atlantic.

The areal distributions of species deduced from their occurrence in top samples from cores in the Lamont collection agree with the charts by Phleger, Parker, and Peirson and support their conclusions regarding the significance of the species as indicators of climate.

The distribution of *Globorotalia menardii* is of particular interest because it and its subspecies are the most useful markers of climatic zones in the North Atlantic. In general, it is abundant only in the sediments which lie beneath the great clockwise current system of the

North Atlantic. It is, however, absent from the northeastern quadrant between the Azores and the Canary Islands, and it is poorly represented in the sediments of the Sargasso Sea. This cannot be due to solution of the tests, because many of the samples examined at Lamont were taken at relatively shallow stations on the flanks of the Mid-Atlantic Ridge and contain other species with fragile tests. Since the surface water of the Sargasso Sea is no cooler than the surrounding waters in which *Globorotalia menardii* is abundant, conditions other than temperature play some part in determining the geographical ranges of planktonic Foraminifera. Possibly the poor representation of the species in the Sargasso Sea is connected with the well-known infertility of this part of the Atlantic Ocean. In view of this, caution should be exercised in the interpretation of Pleistocene assemblages of planktonic Foraminifera in terms of surface-water temperatures. We favor, therefore, a broad approach to the problem of paleoclimates whereby patterns of distribution of sensitive species throughout the Atlantic are taken into account. For example, many widely scattered cores indicate that during the time of deposition of zone (x) (Fig. 24), most of the common species were distributed geographically just as they are now. This justifies the inference that during deposition of zone (x), oceanographic conditions in the Atlantic were much as they now are. This in turn implies similar climate and comparable temperatures of surface waters. On the other hand, the drastic change in species of planktonic Foraminifera in zone (y) (Fig. 24) implies a fairly considerable change in ecological conditions in general. Presumably lowered surface-water temperature was one of the changed conditions, but in view of other variables, which were almost certainly involved, it would seem rash to attempt to estimate the amount of temperature lowering in degrees Celsius.

Murray and Renard (1891, p. 59–61) observed that *Globorotalia menardii* was absent from sediments north of a line extending westward from the Canary Islands in the eastern North Atlantic, but that large specimens were abundant south of the boundary. This poses an interesting question: how does the population maintain itself south of the boundary in spite of the southward-setting Canaries current? Regardless of the weakness of the Canaries current, this species, quite without means of independent motion, should be swept southward and out of the region. Yet distribution of *Globorotalia menardii* in the tops of cores shows that the boundary has remained essentially stationary for fully 10,000 years.

Possibly the individuals pass only a part of their life cycle near the surface and as they approach maturity sink to some level where a current carries them north again. Apparently reproduction takes place at depth and the juvenile forms rise into the upper layers of water.

Many planktonic Foraminifera have been collected in plankton nets by members of the Lamont group. Those plankton samples collected only a few hundred meters below the surface have thin-walled tests with smooth surfaces which lack the crust of glittering calcite crystals present on the majority of tests in sediment samples.

As has been noted, the calcite layer found on the tests in sediment samples varies significantly in thickness from chamber to chamber, invariably being thickest on the earliest chamber of the last whorl and thinning on succeeding chambers. Only precipitation by some vital process of the animal itself can account for this consistent pattern of distribution of the crystalline calcite.

Although tests of Foraminifera collected with plankton nets near the ocean surface lack the crystalline layer, a few specimens from depths of several hundred meters had the typical layer. Among these was a single test of *Globorotalia menardii menardii* found by Bé in a plankton sample taken at lat. 12°51. N. and long. 77°22. W. between the surface and 380 m. Protoplasm within this test proved that its presence in the sample could not have been due to contamination by bottom sediment.

Wiseman and Todd (1959) have also observed the calcite layer on tests of *Globorotalia menardii menardii* and *G. menardii tumida* from plankton samples. On this evidence they have rejected the common view that the calcite layer is a secondary deposit formed after the death of the animal.

We believe that the organic nature of the calcite layer was first recognized by Rhumbler (1909, p. 109) but on different evidence as shown by the following translation:

"In *Globigerina pachyderma* the external layer of the test appears to be composed of conical or wedge-shaped calcareous units. These, because of their arrangement in a single compact layer, give the impression of a drusy crust due to crystallization from solution. However, decalcification of tests mounted in paraffin shows that simple precipitation has not taken place because each crystallike unit leaves a fairly copious intensely colored organic residue having exactly the same form as the original calcium carbonate."

Oddly enough this important observation seems to have been unnoticed by students of deep-sea sediments.

Arrhenius (1952, p. 88) has observed that tests with a crystalline crust are less corroded than those without it. This suggests that the crust may protect the thin and fragile tests of planktonic species against solution as the animals sink to greater depths and into more solvent water. If so, the unencrusted specimens caught in plankton nets in the upper 300 m of water are probably not mature. Presumably the final stages of development and, if so, reproduction take place at greater depth.

We have observed crystalline crusts on tests of *Globorotalia menardii menardii* and somewhat thicker and more coarsely crystalline crusts on *G. menardii tumida*, *G. truncatulinoides*, *Globigerina inflata*, *G. pachyderma*, *Globigerinoides sacculifera*, *G. conglobata*, and *Orbulina universa*. The tests of *Pulleniatina obliquiloculata* and *Globorotalia scitula* appear to be unencrusted.

The thickness of the crust as seen in cross section is in some cases several times that of the original test. Since the thickness diminishes toward the later chambers, the amount of calcium carbonate contributed by the crust is probably not much more than half of that in the whole shell. However, if most or all of the crust is added to the tests at fairly great depth, the reliability of the chemistry of the shell as an indicator of conditions in the euphotic zone is seriously impaired. We hope that deep plankton tows will provide more evidence on this important point.

Some evidence indicates that even at moderate depths there is selective destruction of tests. For example, *Hastigerina pelagica* is abundant in plankton samples collected in the northwest Atlantic by Menzies and his coworkers. It is absent or at most rare in bottom samples from this region. This species constructs a particularly fragile test which would be easily dissolved or destroyed by mud-feeding bottom dwellers.

Globigerinella aequilateralis is another species with a fragile test sensitive to solution or attrition. Although it is abundant in some sediment samples, evidence suggests that its presence or absence is due to variation in factors leading to destruction of the tests rather than to productivity of the organism or climatic variation. In samples in which other tests or broken fragments are without trace of solution the species may be abundant, but in samples in which other tests are chalky and broken it is consistently absent. Although it is of little use as an indicator of climate, its presence in a sample indicates that the other species there have not been subject to excessive solution or attrition.

In cores from water several thousand meters deep all gradations exist from perfect preservation in which even fragile forms are unbroken and small tests are glassy and transparent to samples in which hardly a test is unbroken and the fragments are chalky and corroded. Similar variation from sample to sample in long cores from the Atlantic was observed by Phleger, Parker, and Peirson (1953). Possible explanations are variation in the solvent power of the bottom water, variation in rate of accumulation of fine terrigenous material which would protect the tests by rapidly covering them, and variation in activity of mud-feeding animals. It is questionable from our observations whether climatic variation in itself has been the controlling factor. All degrees of preservation have been found in both glacial and interglacial stages of the cores.

As pointed out heretofore, turbidity currents may deposit calcareous layers containing uncorroded shells of Foraminifera and pteropods at great depths where such shells would normally be completely dissolved. However, such layers invariably show unmistakable evidence of their origin. In contrast, the layers containing uncorroded Foraminifera in the cores discussed here give every evidence of slow and uniform accumulation. Some cores which show much variation in degree of solution from layer to layer were taken at stations on isolated rises which presumably could not be reached by turbidity currents. We have given relatively little weight to samples consisting largely of broken and corroded tests in attempting to reconstruct the climatic record.

The following species and subspecies have been noted in the faunal analyses of samples:

Globorotalia menardii menardii (d'Orbigny)
G. menardii tumida (H. B. Brady)
G. menardii flexuosa (Koch)
G. hirsuta hirsuta (d'Orbigny)
G. hirsuta punctulata (d'Orbigny)
G. truncatulinoides (d'Orbigny)
G. scitula (H. B. Brady)
Globigerina inflata d'Orbigny
G. bulloides d'Orbigny
G. pachyderma (Ehrenberg)

G. eggeri Rhumbler
Globigerinoides rubra (d'Orbigny)
G. sacculifera (H. B. Brady)
G. conglobata (H. B. Brady)
Globigerinella aequilateralis (H. B. Brady)
Orbulina universa d'Orbigny
Pulleniatina obliquiloculata (Parker and Jones)
Sphaeroidinella dehiscens (Parker and Jones)

Most of these species have been figured and their taxonomy discussed by Phleger, Parker, and Peirson (1953) and by Loeblich and collaborators (1957).

In the postglacial zone or uppermost layer of sediment in the cores, *Globorotalia menardii* (d'Orbigny) and the form originally described by Brady as *Pulvinulina menardii* var. *tumida* are found together with a few individuals of intermediate form. The distribution is definitely bimodal with the extreme forms dominant over the intermediate forms. At lower levels in the cores, particularly in zone (x) (Fig. 24), a third form, described as *Pulvinulina tumida* var. *flexuosa* (Pl. 3) by Koch (1923), occurs in abundance. It is distinguished by deflection of the final chamber from the plane of the test. In extreme development the final chamber makes a right angle with the plane of the test, and the peripheral keel on the anterior margin of the final chamber is entirely suppressed. Within zone (x) the interrelationship between the three forms is complex and varies from level to level with intermediate forms in abundance at certain levels. Because of this complex interrelationship, Phleger, Parker, and Peirson (1953) in describing foraminiferal assemblages in lower sections of cores from the North Atlantic were unable to separate the groups satisfactorily and lumped them together as the *G. menardii-tumida* group. The intermediate forms indicate that there was gene flow throughout the population and that, therefore, the various groups were part of a single Mendelian population, or single species, *Globorotalia menardii* s. l. In the postglacial population the same thing holds true except that the relationship is less complex because of the absence of *G. menardii flexuosa* and a more clearly defined bimodal relationship between *G. menardii menardii* and *G. menardii tumida*. In view of this we treat all three forms as subspecies.

We are well aware of the "axiom" that subspecies cannot coexist. The underlying thought seems to be that interbreeding prevents the preservation of distinctive traits because of blending. According to this reasoning, after sufficient blending all members of a panmictic population ought to become virtually identical in "blood" and therefore in hereditary endowment. In view of the general acceptance in the western world of the gene theory of heredity, it is rather strange that this old misconception of the hereditary process should still be cited as an objection to the use of the race or subspecies category. Crossing within a Mendelian population cannot by itself eliminate any genotype from that population. Only selection can bring about elimination of genotypes. Presumably rigorous selection during the last ice age removed from the population the genes responsible for *G. menardii flexuosa*.

The association of the tests of planktonic organisms in a single sediment sample does not prove coexistence of the reproducing organisms. Emiliani (1954) has presented evidence from oxygen-isotope analyses that *G. menardii tumida* lives at a greater depth than *G. menardii menardii*. If so, the two races are not at present fully sympatric. The well-defined bimodality of the postglacial population may be a consequence of adaptation to layers of water having different temperatures.

We also regard *Globorotalia hirsuta* (d'Orbigny) and *G. punctulata* as subspecies because of similar intergradation. D'Orbigny published the name *Globigerina puncticulata* in 1826 as a *nomen nudum*. In 1832 Deshayes published a description of what he supposed to be the *Globigerina puncticulata* of d'Orbigny, but, as the following quotation (translated) from his description shows, he based his supposition on nothing more than that his specimen came from the same locality as d'Orbigny's and possessed surface markings suggestive of the trivial name *puncticulata*.

> "Having found this species in the sands of Rimini, we thought that it was the same as that which M. d'Orbigny had named *G. puncticulata*, since it came from the same locality and conformed well to the name."

Thus no authentic definition of d'Orbigny's *G. puncticulata* appeared in print until 1899 when Fornasini published d'Orbigny's original figure under the name *Globigerina punctulata*. Since a description of *Globorotalia hirsuta* had been published in 1839, it is by priority the nominate subspecies.

Methods of Faunal Analysis

Most other investigators of Pleistocene climatic changes in deep-sea cores have counted all tests of planktonic species in samples of convenient size and reduced the counts to percentages of the individual species in the total population of planktonic Foraminifera. This is a rigorous way of determining relative frequencies. It takes time and is in some respects wasteful in that much time is spent counting the eurythermal and usually very abundant species *Globigerinoides rubra*, *G. conglobata*, and *Orbulina universa*, although the percentages of these species are of little climatic significance except as a measure of total productivity.

ging the zones of *Globorotalia menardii*: valid correlations can be made without estimating the frequencies of the eurythermal species.

The rapidity of this method has enabled us to identify and correlate faunal zones in several hundred cores from widely scattered stations in the North Atlantic. The quantity of consistent data obtained has eliminated the possibility that the supposed faunal zones are merely chance concentrations of tests brought

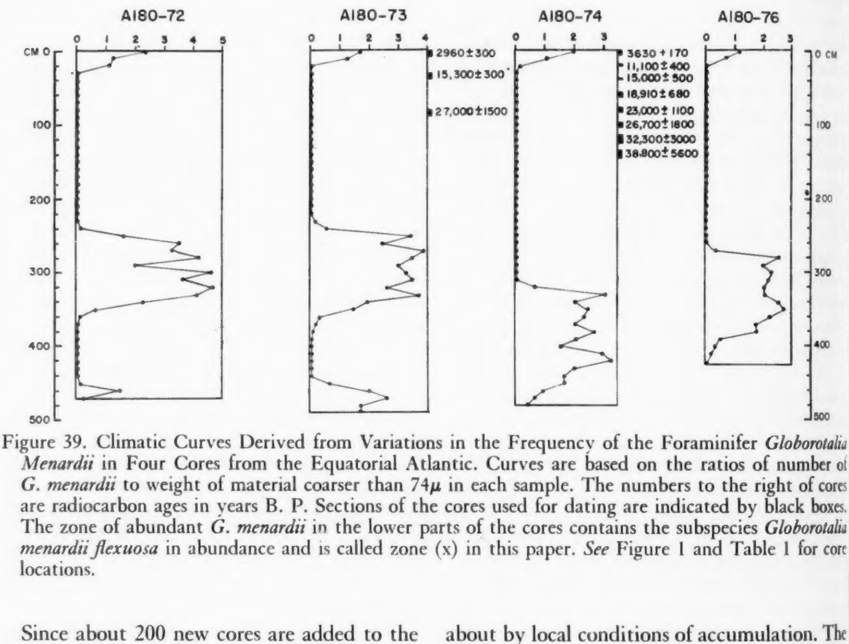

Figure 39. Climatic Curves Derived from Variations in the Frequency of the Foraminifer *Globorotalia Menardii* in Four Cores from the Equatorial Atlantic. Curves are based on the ratios of number of *G. menardii* to weight of material coarser than 74μ in each sample. The numbers to the right of cores are radiocarbon ages in years B. P. Sections of the cores used for dating are indicated by black boxes. The zone of abundant *G. menardii* in the lower parts of the cores contains the subspecies *Globorotalia menardii flexuosa* in abundance and is called zone (x) in this paper. *See* Figure 1 and Table 1 for core locations.

Since about 200 new cores are added to the Lamont collection each year, we were compelled to devise a more rapid method of study, if each core was to receive some attention. The following method was the result.

Sufficient washed material to cover a tray of 50 square cm is examined with a binocular microscope, and the frequencies of the important planktonic species are noted according to the following scale:

Rare (R): fewer than 6 tests
Frequent (F): 6–10 tests
Common (C): 11–24 tests
Abundant (A): 25–100 tests
Very abundant (VA): more than 100 tests

Estimates can be made in place of counts. The method is particularly suitable for log-

about by local conditions of accumulation. The method has also permitted selection from hundreds of cores those few which were most likely to contain reliable records of Pleistocene climates and which were best suited for more detailed study. The most serious fault of the method is its lack of sensitivity. It lumps together samples containing only 26 tests of a certain species with those containing 95 tests; similarly a sample containing 100 tests is given the same rating as one containing 600 or 1000.

In order to gain sensitivity without too serious a loss of time, Ericson and Wollin (1956b) devised the frequency-to-weight-ratio method. Its application is limited to cores in which the coarse fraction caught on the 74-μ sieve consists almost entirely of the tests of

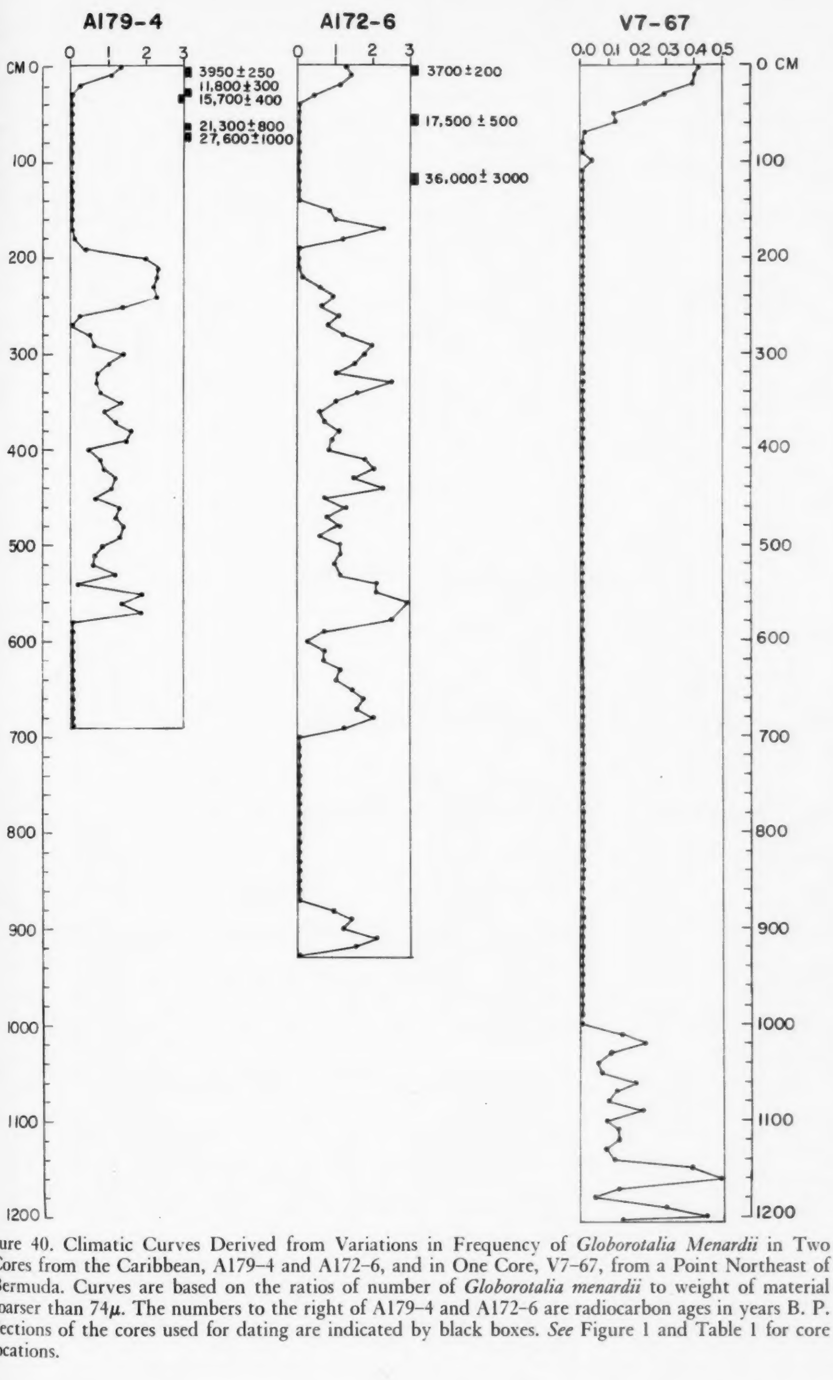

Figure 40. Climatic Curves Derived from Variations in Frequency of *Globorotalia Menardii* in Two Cores from the Caribbean, A179–4 and A172–6, and in One Core, V7–67, from a Point Northeast of Bermuda. Curves are based on the ratios of number of *Globorotalia menardii* to weight of material coarser than 74μ. The numbers to the right of A179–4 and A172–6 are radiocarbon ages in years B. P. Sections of the cores used for dating are indicated by black boxes. *See* Figure 1 and Table 1 for core locations.

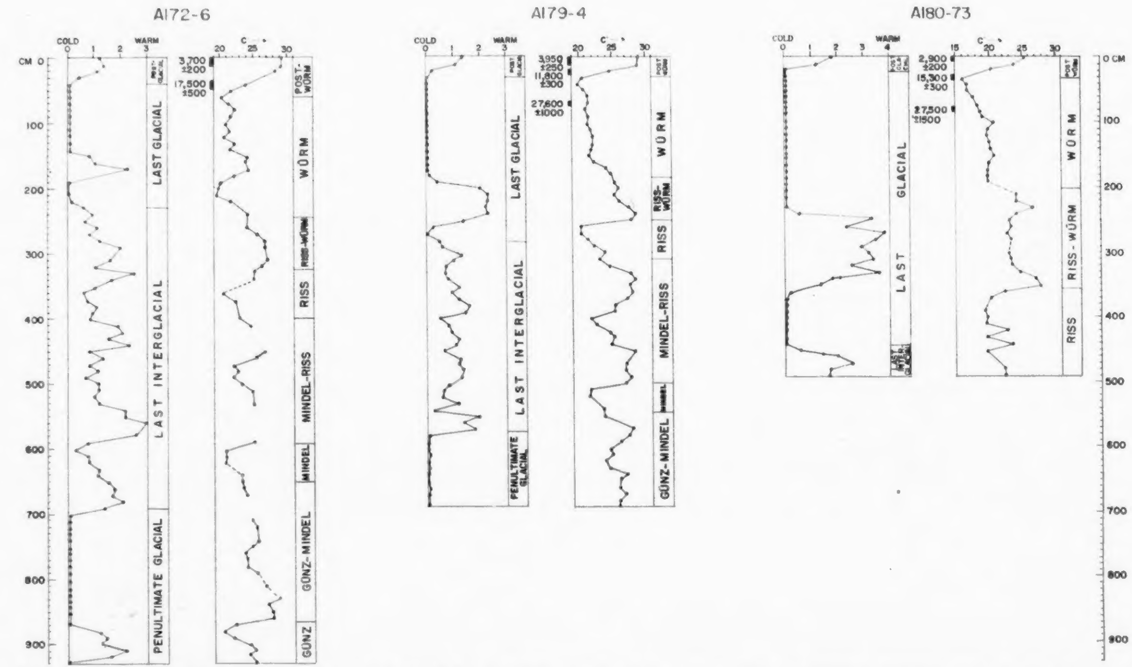

Figure 41. Comparison of Climatic Curves Derived from Variations in the Frequency of *Globorotalia Menardii* with Oxygen-Isotope Paleotemperature Curves. Of each pair of curves the curve to the right shows the isotopic temperatures obtained from the tests of *Globigerinoides sacculifera* with a Pleistocene chronology as interpreted by Emiliani (1955). The curves to the left are based on the ratios of the number of *Globorotalia menardii* to the weight of material coarser than 74μ in each sample. Between each pair of curves radiocarbon dates in years B. P. are given with black boxes indicating the core sections which were used for age determinations. *See* Figure 1 and Table 1 for core locations.

planktonic Foraminifera. Fortunately, the cores most likely to contain long uninterrupted records of climatic change are those in which the terrigenous fraction is almost entirely of lutite grade and the coarse fraction is composed essentially of the tests of planktonic Foraminifera. The method consists of counting the tests of single species or several climatically sensitive species and taking the ratio of the number of tests to the weight of the coarse fraction in milligrams or, in effect, to the weight of all planktonic Foraminifera in the sample. By means of the numbers obtained one can trace from sample to sample in a core the variation in frequency of a single species or group of species with respect to abundance of all species with reasonable precision. Variation in frequency of *Globorotalia menardii* as determined

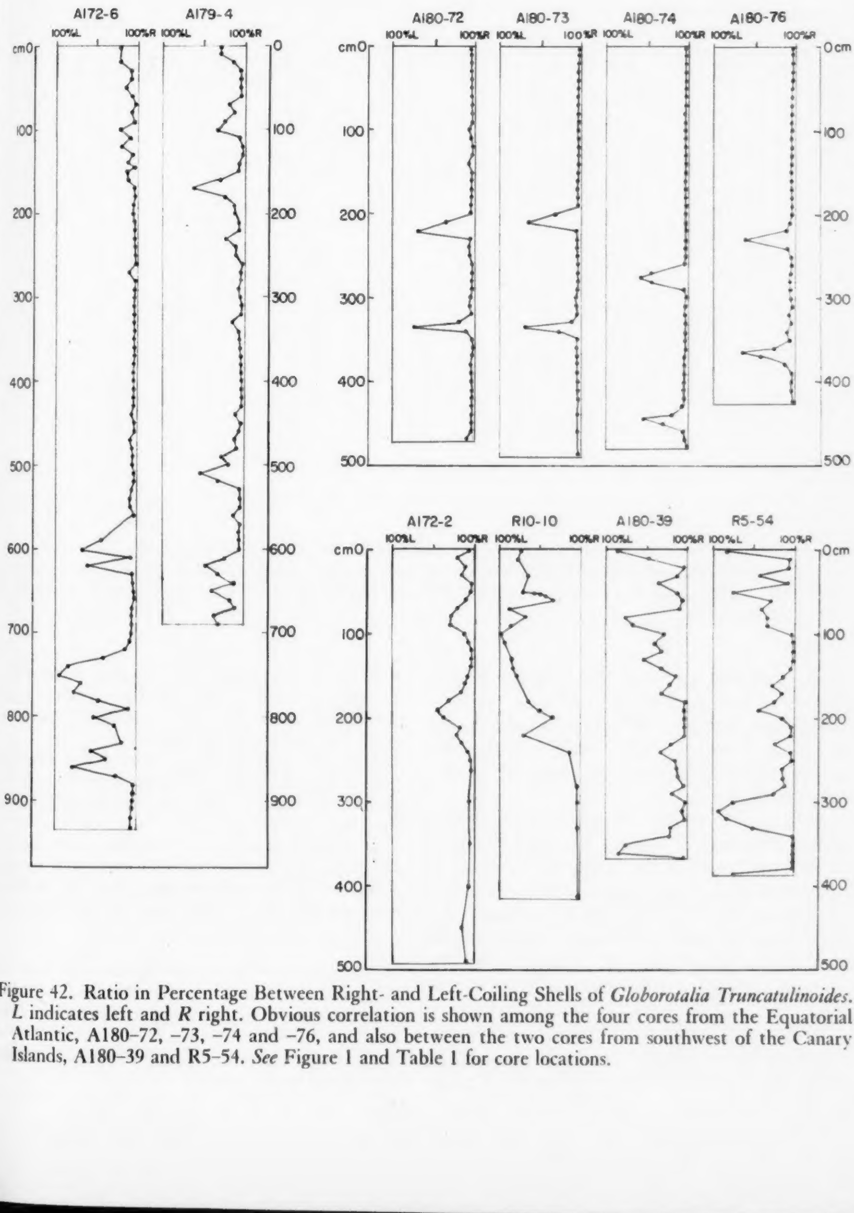

Figure 42. Ratio in Percentage Between Right- and Left-Coiling Shells of *Globorotalia Truncatulinoides*. *L* indicates left and *R* right. Obvious correlation is shown among the four cores from the Equatorial Atlantic, A180–72, –73, –74 and –76, and also between the two cores from southwest of the Canary Islands, A180–39 and R5–54. *See* Figure 1 and Table 1 for core locations.

by this method in several cores is shown in Figures 39, 40, and 41.

In addition, counts of left- and right-coiling tests of *Globorotalia truncatulinoides* have been made and recorded as percentages of tests coiling in the dominant direction in the total count of the species. This method and the results obtained have been discussed by Ericson and Wollin (1956a) and Ericson, Wollin, and Wollin (1954). It is especially useful as a precise species have been accompanied by sudden short-duration reversals of dominant coiling direction. Variations in ratios of right- and left-coiling tests of *G. truncatulinoides* in 15 cores are shown in Figures 42 and 43.

Faunal Zones

Study of the Foraminifera of cores from the Atlantic Ocean and connected seas shows that the following faunal zones are present (Fig. 24):

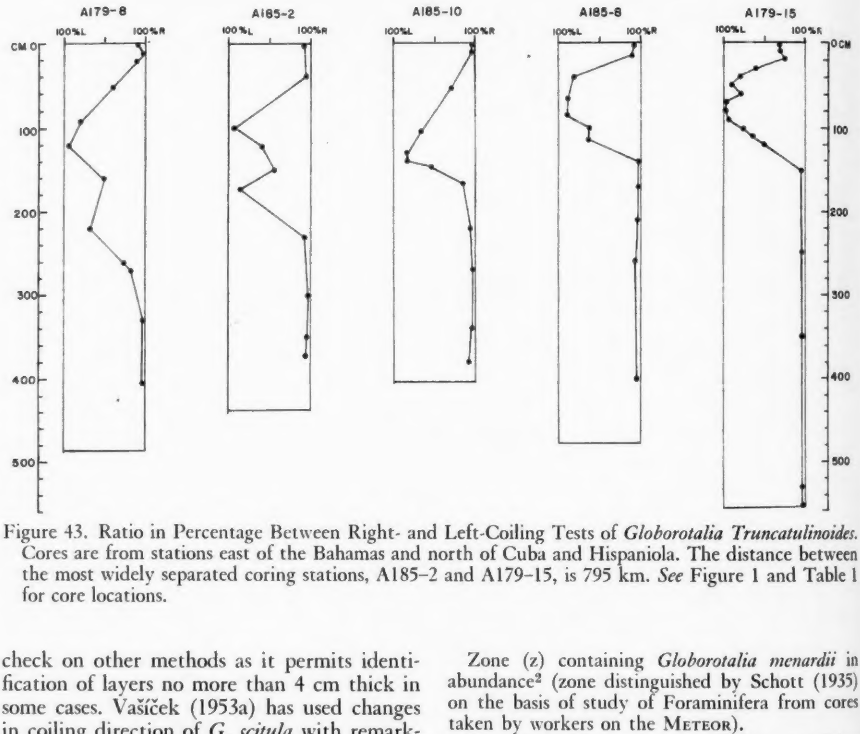

Figure 43. Ratio in Percentage Between Right- and Left-Coiling Tests of *Globorotalia Truncatulinoides*. Cores are from stations east of the Bahamas and north of Cuba and Hispaniola. The distance between the most widely separated coring stations, A185–2 and A179–15, is 795 km. *See* Figure 1 and Table 1 for core locations.

check on other methods as it permits identification of layers no more than 4 cm thick in some cases. Vašíček (1953a) has used changes in coiling direction of *G. scitula* with remarkable success in making stratigraphic correlations between oil wells.

Bolli (1950; 1951) has shown that a preferred direction of coiling has become fixed in the later stages of the evolutionary histories of certain planktonic species. Other evidence of this trend is afforded by the consistently high ratio of sinistral coiling in *Globorotalia menardii* in all regions in contrast with the variation in coiling from place to place in the relatively young species *G. truncatulinoides*.

Although the cause of change in coiling direction is not known, it appears that times of abrupt climatic change as indicated by other

Zone (z) containing *Globorotalia menardii* in abundance[2] (zone distinguished by Schott (1935) on the basis of study of Foraminifera from cores taken by workers on the METEOR).

Zone (y) without *G. menardii* but containing species now abundant in higher latitudes (distinguished by Schott, 1935: correlated by him with the Last Glacial Age).

Zone (x) containing *G. menardii* in abundance[2] (distinguished by Schott, 1935: correlated by him with the Last Interglacial Age). Both *G. menardii menardii* and *G. menardii flexuosa* are abundant

[2] Study of the cores in the Lamont collection has shown that the zones of *G. menardii* observed by Schott extend northward to the Canary Islands in the Eastern Atlantic and westward into the Caribbean, Gulf of Mexico, and through the straits of Florida northeastward almost to the Azores.

(the latter subspecies is apparently extinct in the North Atlantic), and *Globigerina hexagona*, described by Natland (1938) from the Pacific, occurs sparingly.

Zone (w), relatively thin, without *Globorotalia menardii* (representing a cooler period).

Zone (v) containing *G. menardii menardii* and *G. menardii flexuosa* in abundance. In most samples the latter subspecies is subordinate. This zone is thicker than either of the overlying zones containing *G. menardii* s. l.

Zone (u) without *G. menardii* (reached by only a few cores; represents a cooler period).

Plate 1B and Figures 44–48 show the relative thicknesses of the zones as they occur at stations in the Atlantic.

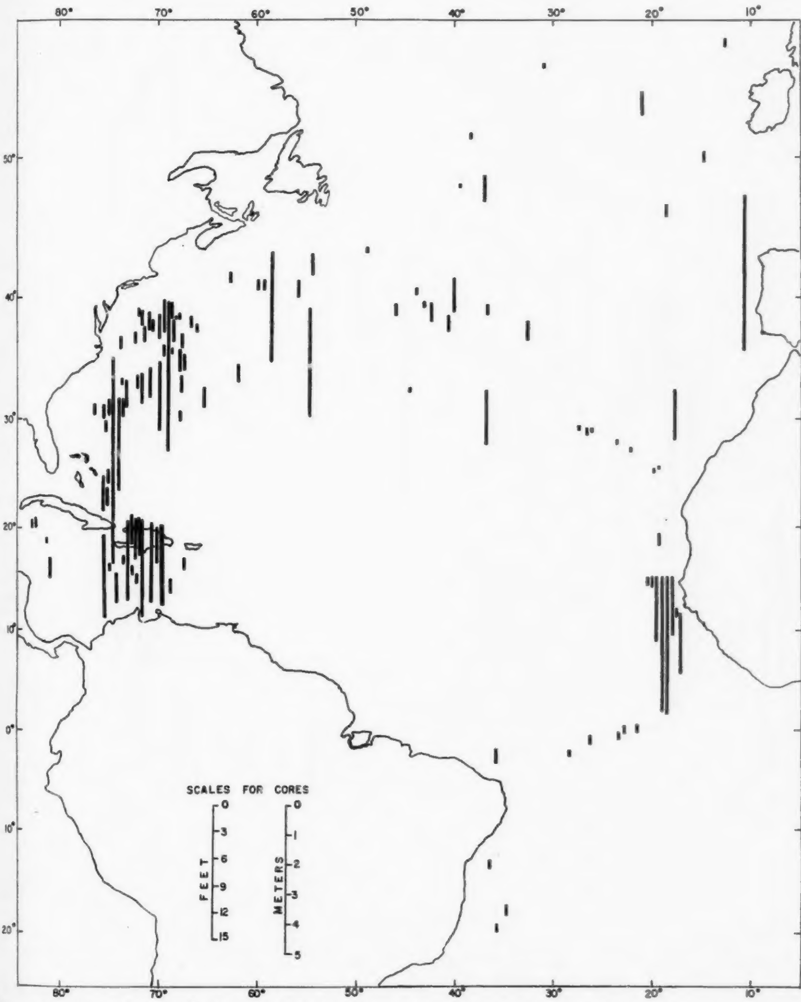

Figure 44. Distribution of the Postglacial Sections of the Cores. The top of the column is the approximate location of the core station. All sections shown are considered to be complete. Interpretations are based on investigations of the planktonic Foraminifera and lithology of all the cores and on radiocarbon dates, isotopic temperatures, and grain-size analyses of selected samples from selected cores.

Interpretation of Faunal Zones

Schott (1935) concluded that the appearance of *Globorotalia menardii* in abundance in the uppermost layer of sediment in cores from the Equatorial Atlantic marks the commencement of postglacial time and that the underlying layer without *Globorotalia menardii* represents deposition during the Last Glacial Age. We agree.

The position of zone (x) in the sequence of Pleistocene climatic changes as inferred from glacial deposits on the continents is less certain. Schott (1935) concluded that it was equivalent

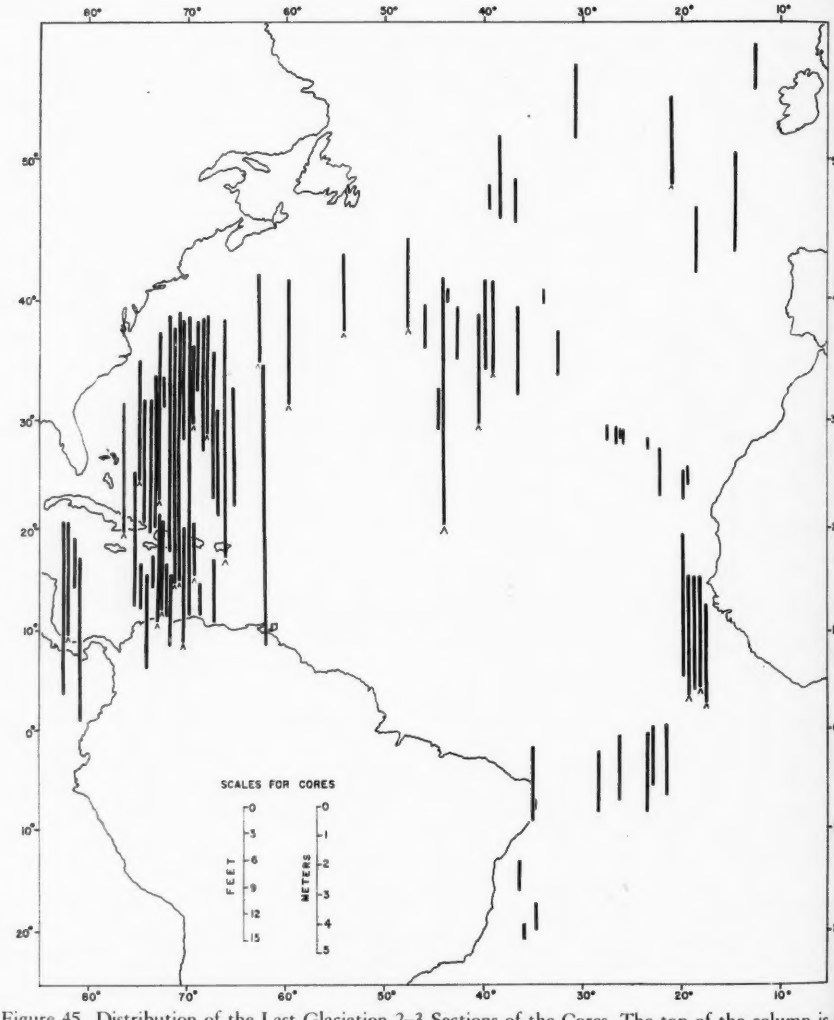

Figure 45. Distribution of the Last Glaciation 2–3 Sections of the Cores. The top of the column is the approximate location of the core station. An inverted V at the bottom of a column indicates that the section is not complete; all sections without it are considered to be complete. The interpretations are based on investigations of the planktonic Foraminifera and lithology of all the cores and on radiocarbon dates, isotopic temperatures, and grain-size analyses of selected samples from selected cores.

to the Last Interglacial. The cores taken by the METEOR did not penetrate to the base of zone (x), however, and consequently its thickness was unknown to Schott. The longer Lamont cores penetrate zone (x) and also pass through underlying zone (w), which represents a stage of cool climate.

It seems more probable to us that zone (x) represents an interstadial within the Last Glaciation. Zeuner (1954) indicates that climate during the first interstadial, or L.Gl. 1/2 according to his terminology, was temperate, in fact as temperate as that of postglacial time, whereas the climate of the second interstadial, L.Gl. 2/3, did not lead to a deglaciation comparable with that of the postglacial age. If so, the marine record should contain evidence of L.Gl. 1/2 but not necessarily of L.Gl. 2/3. If our correlation of zone (x) is correct, zone (y) must correspond to the Main

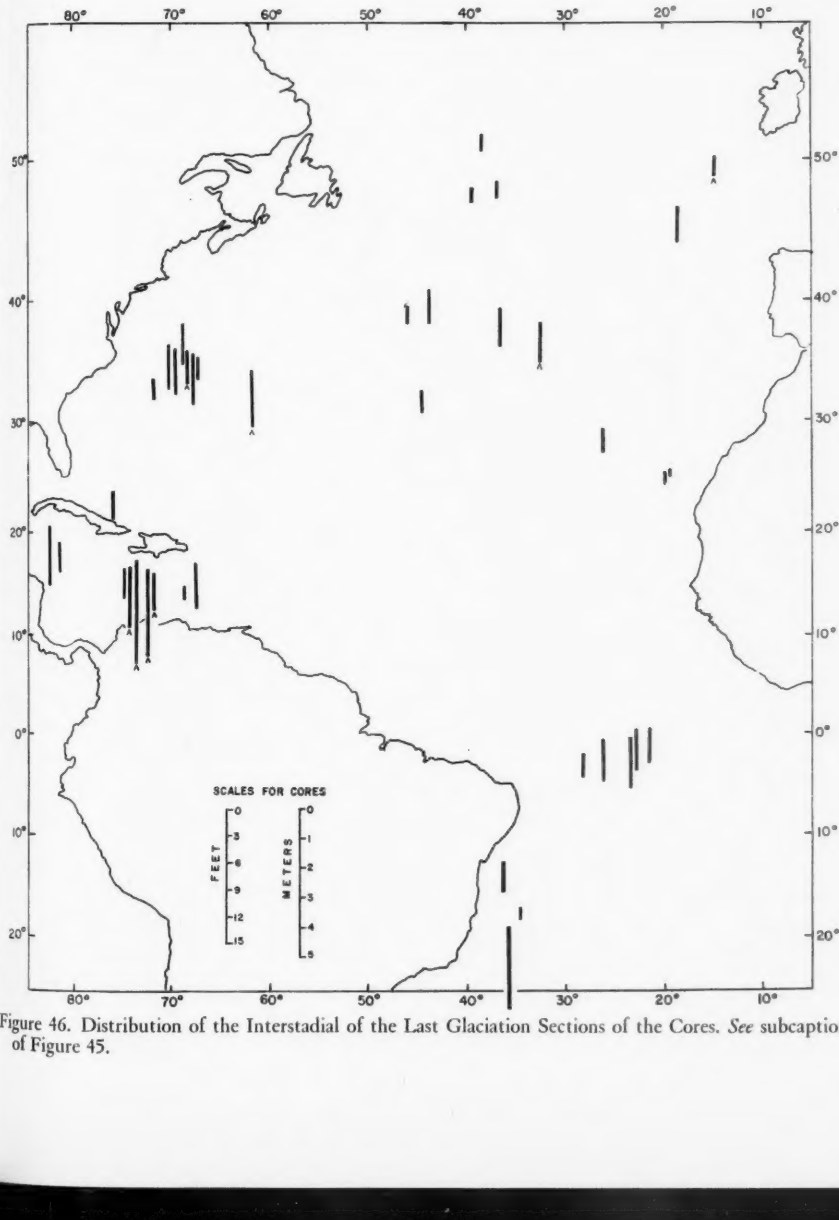

Figure 46. Distribution of the Interstadial of the Last Glaciation Sections of the Cores. *See* subcaption of Figure 45.

Würm of the alpine terminology, and therefore must include the three phases, L.Gl. 2, L.Gl. 2/3, and L.Gl. 3 of Zeuner's terminology. Hereafter we shall refer to this time interval as Last Glaciation 2–3 or L. Gl. 2–3.

A former objection to our interpretation of zone (x) was a series of radiocarbon dates of samples from peat deposits in Europe which were correlated with the L.Gl. 1/2. These seemed to show that this interstadial was much more recent than 50,000 years B. P. However, it now appears that the samples were contaminated. Tauber and de Vries (1958) have shown that the Brörup peat of Jutland is older than 50,000 B. P. Andersen (1957) correlates the Brörup peat deposit with the Götweig or Fellabrunn (Brandtner, 1954) interstadial which is equivalent to the L.Gl. 1/2 inter-

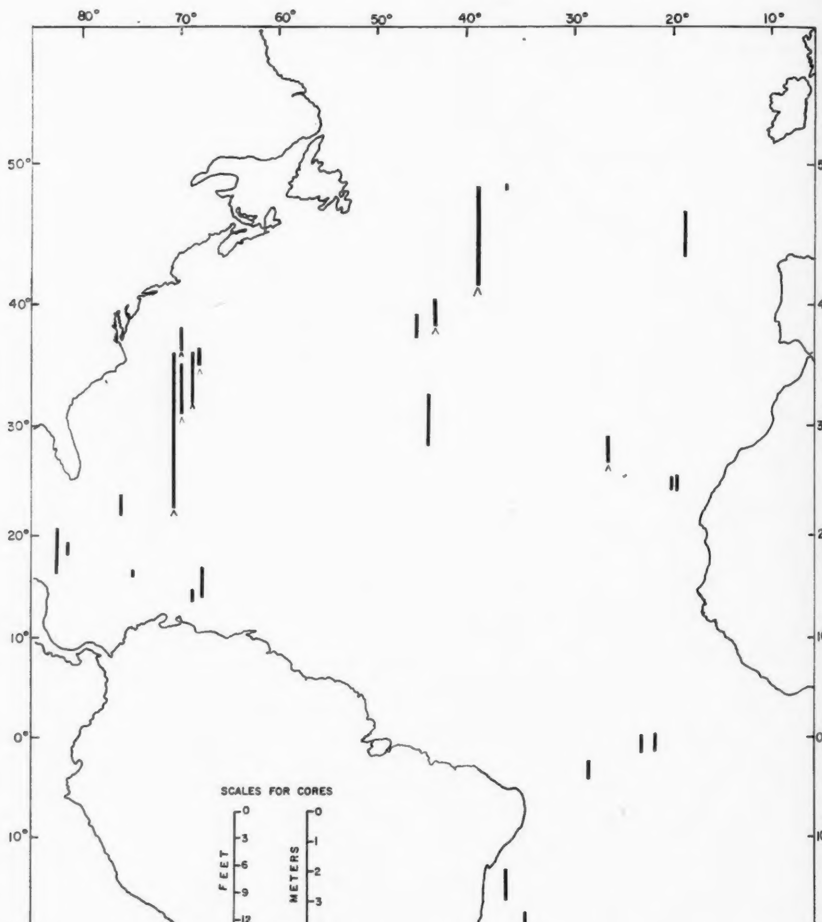

Figure 47. Distribution of the Last Glaciation 1 Sections of the Cores. *See* subcaption of Figure 45.

stadial. Tauber and de Vries (1958, p. 69) state that "after an extraction of humic acids none of the samples showed a significant activity." This means that the interstadial could well be 60,000 years old.

According to our tentative interpretation, zone (w) corresponds to the first cold phase of the Last Glaciation or to the Last Glaciation I of Zeuner, and zone (v) to the Last Interglacial. The general sequence is shown in Figure 24. Within the interval from 120,000 years B.P. to about 230,000 years B.P., there are several fluctuations in abundance of certain Foraminifera which are not shown in Figure 24. Presumably these record variations in climate, but on the evidence of the Foraminifera the climate was at no time as cool as it was directly before and after zone (x) time.

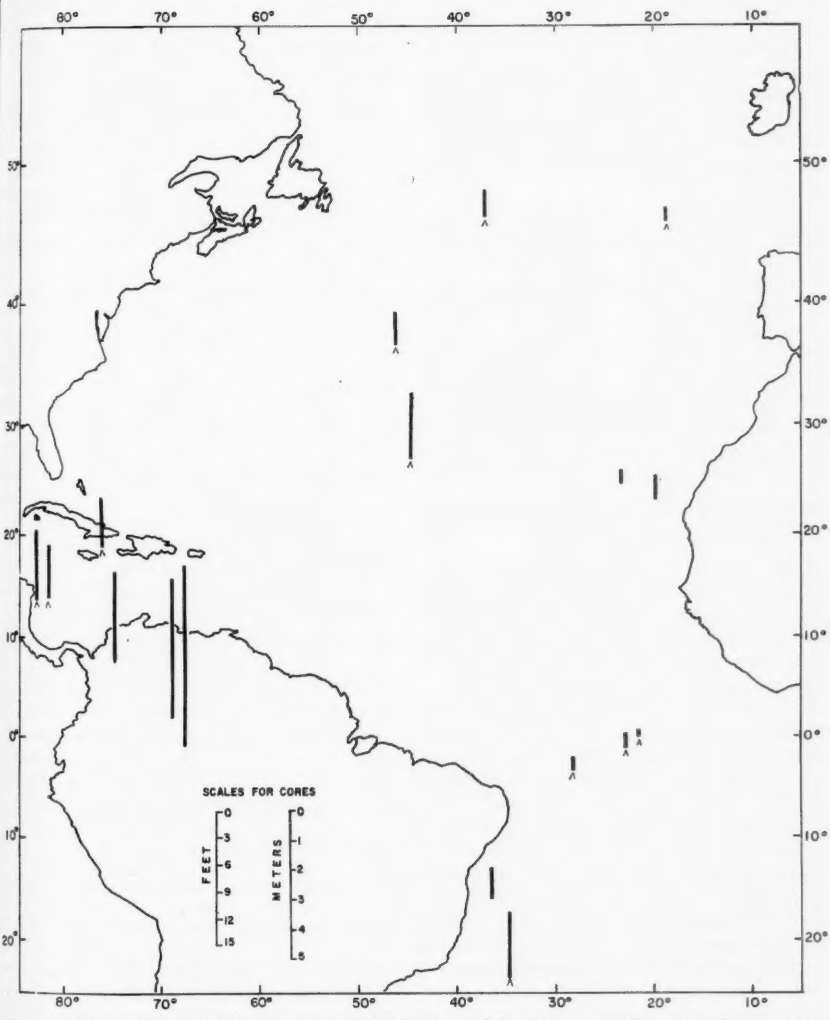

Figure 48. Distribution of the Last Interglacial Sections of the Cores. *See* subcaption of Figure 45.

We conclude, therefore, that the entire time interval comprises only the Last Interglacial, and that the faunal fluctuations represent no more than minor climatic variations superimposed upon a generally mild climate.

A few cores reach zone (u). This cool-climate zone (*Globorotalia menardii* is absent) by our interpretation corresponds to the latter part of the Penultimate Glaciation.

The interpretation given herein is at variance with that of Emiliani (1955), who bases his interpretation upon oxygen-isotope paleotemperatures. According to his view, the interval which by our interpretation corresponds to the Last Interglacial includes the Nebraskan and Kansan glacial ages and, therefore, the longer cores in the Lamont collection should include a complete record of the Pleistocene as known from glacial deposits on the continents.

At present with the cores available in the Lamont collection it is doubtful if a final decision can be made between these two interpretations. We hope that longer cores can be obtained. The relationship between bottom topography and processes of sedimentation is now fairly well understood. The difficulty is no longer in finding places on the ocean floor where accumulation has been continuous and uniform but to recover long cores including beyond reasonable doubt a sedimentary record of the entire Pleistocene.

Thicknesses of Sediments, Rates of Accumulation, and Late Pleistocene Chronology

Table 5 gives the thicknesses of the postglacial and Last Glaciation 2–3 stages in 108 cores and Last Glaciation 2/3 interstadial, Last Glaciation 1, and Last Interglacial stages in 36 cores. Figures 44–48 show the locations of measured sections and their thicknesses.

The different stages are distinguished by the relative abundances of cold- and warm-water species of Foraminifera in the 108 cores and by variations in frequency of *Globorotalia menardii*, isotopic temperatures, and radiocarbon dates of selected cores. Curves of climatic variation as inferred from relative numbers of warm- and cold-water planktonic Foraminifera are shown in Figures 25–37. The midpoint between the change from cold to warm or warm to cold in the curves is used as the boundary between the different stages.

Since estimations of the time intervals represented by the various zones in the cores depend upon extrapolation of rates of accumulation determined by radiocarbon dating of samples from the upper parts of the cores, we must consider to what extent apparent rates of accumulation may have been influenced by distortion due to the coring process itself. As has been noted, undisturbed burrow mottling indicates that there is no appreciable distortion in thicknesses of sediment layers in the coring process.

Since the range of the radiocarbon method extends well into the last ice age, the rates of accumulation used for extrapolation to deeper zones in the cores are averages of rates of accumulation under both glacial and postglacial conditions. However, the possibility remains that since the present climate is not fully interglacial, the rate of sediment accumulation during the past 10,000 years may not have been the same as during times of fully interglacial climate. At present, with no reliable method of dating the interglacial zones, there seems to be no objective way of resolving this question.

Evidence presented heretofore indicates that rates of accumulation may be greatly influenced by local configuration of the bottom and by current scour. Possible changes in deep circulation coupled with climatic changes of the Pleistocene might easily bring about fairly large local variations in rate of accumulation from zone to zone. An apparently effective way of eliminating this distorting factor from our estimations of time intervals would be to take the average rate of accumulation as determined by radiocarbon dates in many cores. This we have endeavored to do.

The micropaleontological study of the Foraminifera, the isotopic determinations, and the radiocarbon dating of cores A179–4 (Fig. 49), A179–8 (Fig. 29), A179–15 (Fig. 26), A180–73 (Fig. 49), A180–74 (Fig. 50), and R10–10 (Fig. 26) indicate that postglacial time began about 11,000 years ago. The total thickness of the postglacial sections (zone (z)) of the 108 cores in Table 5 is 10525 cm. The postglacial sections range from 5 cm to 700 cm and average $\frac{10525}{108}$ or 97 cm. The average rate of accumulation for postglacial time as shown by these cores is $\frac{97}{11}$ or 8.8 cm per thousand years. The rate of accumulation during postglacial time ranges from 0.5 cm to 63.6 cm per thousand years (Table 5). The rates of accumulation obtained from one radio-

TABLE 5.—THICKNESSES OF FAUNAL ZONES AND RATES OF ACCUMULATION OF ZONES (z) AND (y) IN 108 ATLANTIC AND CARIBBEAN DEEP-SEA CORES

Interpretations based on investigation of planktonic Foraminifera and lithology of all cores and on radiocarbon dates, isotopic temperatures, and grain-size analyses of selected samples from selected cores. Table 1 gives depth of water and locations of the cores. Figure 24 shows climatic interpretation of faunal zones.

Core	Thickness of Zone (z) (Cm)	Thickness of Zone (y) (Cm)	Rate of Accumulation of Zone (z) (Cm/1000 Years)	Rate of Accumulation of Zone (y) (Cm/1000 Years)	Thickness of Zone (x) (Cm)	Thickness of Zone (w) (Cm)	Thickness of Zone (v) (Cm)
A152-135	40	>870	3.6	>17.5	..	..	..
A153-146*	15	135	1.4	2.7	65	185	>223
A156-4	700	>306	63.6	>6.1	..	..	..
A156-5	35	>757	3.2	>15.1	..	..	..
A157-5*	30	135	2.7	2.7	55	15	>85
A157-6*	25	55	2.3	1.1	55	>305	..
A157-11	20	>840	1.8	>16.8	..	..	..
A157-13*	20	45	1.8	0.9	105	>90	..
A164-1	75	>794	6.8	>15.9	..	..	..
A164-5	70	>846	6.4	>16.9	..	..	..
A164-6*	75	275	6.8	5.5	140	>75	..
A164-15*	75	500	6.8	10.0	150	>172	..
A164-16*	75	600	6.8	12.0	>101	..	..
A164-17	50	>656	4.5	>7.1	..	..	..
A164-23*	75	140	6.8	2.8	60	>515	..
A164-24*	40	285	3.6	5.7	150	>185	..
A164-29	30	>342	2.7	>6.8	..	..	..
A164-33	30	>185	2.7	>3.7	..	..	..
A164-35	35	>367	3.2	>7.3	..	..	..
A164-46	30	>270	2.7	>5.4	..	..	..
A164-48	35	>448	3.2	>9.0	..	..	..
A164-55	40	>285	3.6	>5.7	..	..	..
A164-59	35	>429	3.2	>8.6	..	..	..
A164-61	50	>377	4.5	>7.5	..	..	..
A164-62	525	>40	47.7	>0.8	..	..	..
A164-63	115	>200	10.5	>4.0	..	..	..
A167-5	90	>874	8.2	>17.5	..	..	..
A167-6	45	>255	4.1	>5.1	..	..	..
A167-7*	35	80	3.2	1.6	..	..	..
A167-8	95	>535	8.6	>10.7	..	..	..
A167-9	20	>300	1.8	>6.0	..	..	..
A167-10	70	>447	6.4	>8.9	..	..	..
A167-11	320	>81	29.1	>1.6	..	..	..
A167-12	60	>428	5.5	>8.6	..	..	..
A167-13	40	>410	3.6	>8.2	..	..	..
A167-14	30	>437	2.7	>8.7	..	..	..
A172-1*	30	100	2.7	2.0	>358	..	..
A172-2*	35	170	3.2	3.4	>288	..	..
A172-3*	40	235	3.6	4.7	>125	..	..
A172-6*	35	110	3.2	2.2	40	35	480
A172-7*	35	190	3.2	3.8	150	75	350
A172-33*	20	325	1.8	6.5	80	>65	..
A172-34	75	>1017	6.8	>20.3	..	..	..
A173-2	40	>830	3.6	>16.6	..	..	..
A173-9	>300	..	>27.3		..	..	..
A179-3*	110	315	10.0	6.3	>205	..	..
A179-4*	25	145	2.3	2.9	95	20	300
A179-5	280	>50	25.5	>1.0	..	..	..
A179-7	>200	..	>18.0	..	..	..	..
A179-8	275	>210	25.0	>4.2	..	..	..
A179-10	75	>185	6.8	>3.7	..	..	..
A179-13*	25	150	2.3	3.0	90	115	>170

* Cores containing complete Last Glaciation 2–3 (zone (y)) sections

(z) represents postglacial sediment, (y), sediment of Last Glaciation 2–3, (x), interstadial between Last Glaciation 1 and Last Glaciation 2–3, (w), Last Glaciation 1, (v), last interglacial

TABLE 5.—*Continued*

Core	Thickness of Zone (z) (Cm)	Thickness of Zone (y) (Cm)	Rate of Accumulation of Zone (z) (Cm/1000 Years)	Rate of Accumulation of Zone (y) (Cm/1000 Years)	Thickness of Zone (x) (Cm)	Thickness of Zone (w) (Cm)	Thickness of Zone (v) (Cm)
A179–15	110	>450	10.0	>9.0	..	..	..
A179–16	40	>450	3.6	>9.0	..	..	..
A179–17	20	>520	1.8	>10.4	..	..	..
A179–20	30	>335	2.7	>6.7	..	..	..
A180–1	>360	..	>32.7	..	..	..	..
A180–9*	40	150	3.6	3.0	65	70	>165
A180–10	75	>125	6.8	>2.5	..	..	..
A180–14*	50	375	4.5	7.5	..	..	..
A180–15*	30	300	2.7	6.0	130	>30	..
A180–16*	60	165	5.5	3.3	>142	..	..
A180–32*	35	50	3.2	1.0	80	>90	..
A180–39*	15	95	1.4	1.9	40	45	85
A180–47	220	>233	20.0	>4.7	..	..	..
A180–48	460	>70	41.8	>1.4	..	..	..
A180–49	440	>10	40.0	..	..	..	..
A180–50	270	>210	24.5	>4.2	..	..	..
A180–51	40	>370	3.6	>7.4	..	..	..
A180–53*	25	400	2.3	8.0	..	..	..
A180–56	45	>323	4.1	>6.5	..	..	..
A180–58	220	>148	20.0	>3.0	..	..	..
A180–72*	25	215	2.3	4.3	120	85	>25
A180–73*	20	200	1.8	4.0	130	80	>50
A180–74*	20	280	1.8	5.6	170	>10	..
A180–76*	40	220	3.6	4.4	130	>20	..
A180–79*	15	110	1.4	2.2	75	65	>45
A180–93*	25	100	2.3	2.0	100	100	110
A180–100*	30	90	2.7	1.8	45	40	>201
A180–105*	30	50	2.7	1.0	275	80	..
A181–2*	50	240	4.5	4.8	..	..	..
A185–2	120	>327	10.9	>6.5	..	..	..
A185–3	280	>190	25.5	>3.8	..	..	..
A185–4	275	>45	25.0	>1.0	..	..	..
A185–5	330	>95	30.0	>1.9	..	..	..
A185–8	105	>377	9.5	>7.5	..	..	..
A185–10	155	>248	14.1	>5.0	..	..	..
A185–11	135	>65	12.3	>1.3	..	..	..
A185–17*	25	165	2.3	3.3	90	40	>170
A185–20	30	>382	2.7	>7.6	..	..	..
A185–21*	30	585	2.7	11.7	205	140	>240
C10–14	50	>410	4.5	>8.2	..	..	..
R5–36*	35	265	3.2	5.3	125	150	>45
R5–54*	5	60	0.5	1.2	30	45	40
R5–57	40	>475	3.6	>9.5	..	..	..
R7–7*	80	465	7.3	9.3	..	..	..
R10–1*	35	230	3.2	5.6	..	..	..
R10–2	25	>160	2.3	>3.2	..	..	..
R10–10	110	>305	10.0	>6.1	..	..	..
SP3–33	535	>10	48.6	..	..	..	..
SP8–4*	15	100	1.4	2.0	..	..	..
SP8–12	>185	..	>16.8	..	..	..	..
SP9–3	75	>300	6.8	>6.0	..	..	..
SP9–4*	30	345	2.7	6.9	>110	..	..
SP10–1*	20	285	1.8	5.7	50	>20	..
V2–6	75	>270	6.8	>5.4	..	..	..
V4–1*	80	920	7.3	18.4	..	..	..
V7–67*	55	955	5.0	19.0	>195	..	..

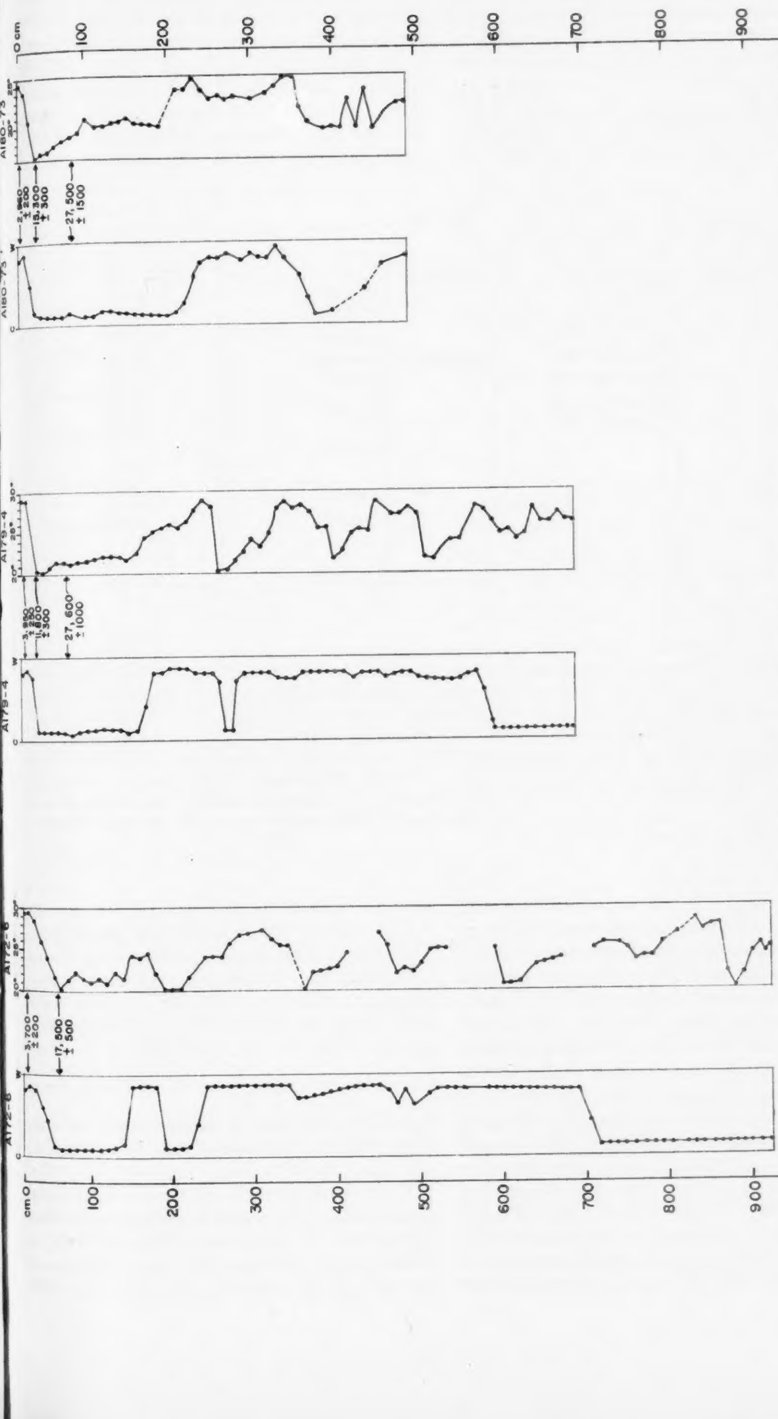

Figure 49. Comparison of Climatic Curves Derived from Variations in Foraminifera with Oxygen-Isotope Paleotemperature Curves. Of each pair of curves the curve to the right shows the isotopic temperatures obtained from *Globigerinoides sacculifera* by Emiliani (1955). The curves to the left are based on the relative numbers of warm- and cold-water planktonic Foraminifera. *C* indicates relatively cold climate and *W* relatively warm climate. Present climate is plotted near *W*, and inferred past climate is plotted with respect to it. Between each pair of curves radiocarbon dates in years B. P. are given with arrows indicating the midpoint of the core sections which were used for dating.

carbon date to another range from 2.2 cm to 274.4 cm per thousand years (Table 6).

Of the 108 cores in Table 5, 46 (marked with asterisks) are considered to contain complete Last Glaciation 2–3 sections (zone (y)). The total thickness of the 46 sections is 11405 cm. The total thickness of the postglacial sections in the same cores is 1740 cm. Thus the years. The average thickness of the Last Glaciation 2–3 section in the 46 cores is 250 cm. From the rates of accumulation calculated from radiocarbon dates in cores A179–4, A180–73, and A180–74, and from comparison of the thicknesses of the postglacial sections with the Last Glaciation 2–3 sections, we conclude that the rate of accumulation during

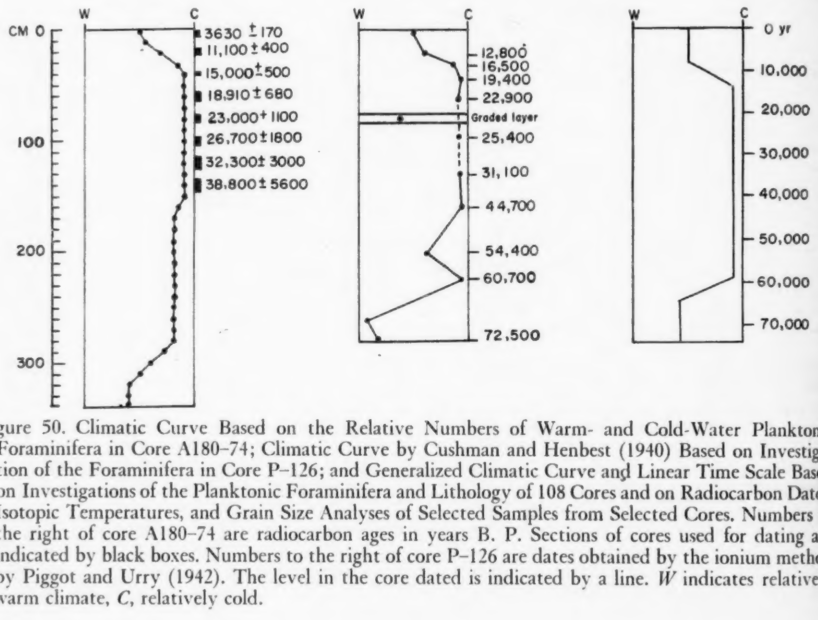

Figure 50. Climatic Curve Based on the Relative Numbers of Warm- and Cold-Water Planktonic Foraminifera in Core A180–74; Climatic Curve by Cushman and Henbest (1940) Based on Investigation of the Foraminifera in Core P–126; and Generalized Climatic Curve and Linear Time Scale Based on Investigations of the Planktonic Foraminifera and Lithology of 108 Cores and on Radiocarbon Dates, Isotopic Temperatures, and Grain Size Analyses of Selected Samples from Selected Cores. Numbers to the right of core A180–74 are radiocarbon ages in years B. P. Sections of cores used for dating are indicated by black boxes. Numbers to the right of core P–126 are dates obtained by the ionium method by Piggot and Urry (1942). The level in the core dated is indicated by a line. *W* indicates relatively warm climate, *C*, relatively cold.

ratio of the length of the postglacial sections to the Last Glaciation 2–3 sections is 1:6.6.

From the extrapolation of radiocarbon dates, the Last Glaciation 2–3 appears to have lasted about 48,000 years in core A179–4, about 50,000 years in core A180–73, and about 55,000 years in core A180–74, the differences presumably being due to local variations in rate of sediment accumulation.

The duration of the Last Glaciation 2–3 can also be extrapolated as follows. The average length of the postglacial section in the 46 cores which have complete Last Glaciation 2–3 sections is 38 cm. Since the duration of postglacial time is believed to be about 11,000 years, the average rate of accumulation in postglacial time in these 46 cores is 3.5 cm in 1000 the Last Glaciation 2–3 was on the average 1 1/2 times as fast as during postglacial time. Thus the average rate of accumulation during Last Glaciation 2–3 in these 46 cores is considered to have been 5.1 cm in 1000 years. Since Last Glaciation 2–3 sections in the cores average 250 cm, the duration of the Last Glaciation 2–3 was $\frac{250}{5.1}$ or 49,000 years. From these two methods of extrapolation we conclude that the duration of Last Glaciation 2–3 was about 50,000 years.

Thicknesses of zone (x) or the interstadial between Last Glaciation 1 and Last Glaciation 2–3 in 30 cores are given in Table 5. These 30 sections total 3010 cm. The total thickness of the postglacial section in the 30 cores is 950

TABLE 5—RADIOCARBON DATES AND RATES OF ACCUMULATION OF SEDIMENT

In calculation of the rate of accumulation, the midpoint of one sample to the next is considered to represent the thickness of sediment deposited between two dates. All dates are based on the carbonate from the total sample except the samples from cores A172–6 and A180–73 and two samples from the lower part of A179–4, which are based on the carbonate from the Foraminifera only. These three cores were dated by Hans E. Suess and the rest of the cores by Wallace S. Broecker and J. Laurence Kulp.

Core	Sample in cm from top	Radiocarbon date in years B. P.	Rate of accumulation cm /1000 years
A164–62	468–488	6990±140	
A172–6	0–10	3700±500	3.6
A172–6	51–61	17,500±250	
A179–4	0–10	3950±250	2.7
A179–4	23–30	11,800±300	3.0
A179–4	70–77	27,600±1000	
A179–8	218–228	10,860±180	
A179–15*	0–3	1000±200	
A179–15	0–1	700±200	14.0
A179–15	49–50.5	4200±200	14.0
A179–15	94–99	7600±130	4.8
A179–15	110–113	10,700±480	4.8
A179–15	129–132	14,700±500	
A180–1	140–170	5130±130	
A180–48	0–12	7000±300	55.7
A180–48	190–210	10,480±380	274.4
A180–48	440–455	11,380±390	
A180–48	490–510	15,300±550	13.6
A180–73	0–8	2960±200	2.4
A180–73	30–38	15,300±300	4.3
A180–73	80–88	27,500±1500	
A180–74	0–5	3630±170	2.2
A180–74	18–21	11,260±460	5.2
A180–74	38–40	15,000±500	
A180–74	57–64	18,910±680	5.5
A180–74	77–83	23,000±1100	4.7
A180–74	97–103	26,700±1800	5.4
A180–74	114–125	32,300±3000	3.5
A180–74	135–146	38,800±5600	3.2
R10–10	0–7	4160±190	170.0
R10–10	35–39	4360±200	
R10–10	60–70	8100±120	7.0
R10–10	90–100	10,680±180	12.0
R10–10	112–120	10,550±420	5.2
R10–10	120–125	11,800±480	12.0
R10–10	165–175	15,820±600	
R10–10	255–275	20,300±900	21.0

*Trigger-weight core

cm. Since the average postglacial section is 31.7 cm thick and the Last Glaciation 1/2 interstadial section is 100.3 cm thick, the ratio of the length of the postglacial section to the interstadial section is 1 to 3.2. If the average rate of accumulation in postglacial time in these 30 cores was 2.9 cm in 1000 years, and assuming that the rate of accumulation during the interstadial was the same as during postglacial time, the duration of the interstadial was $\frac{100.3}{2.9} = 34{,}586$ years or about 35,000 years.

Among the cores listed in Table 5, 18 contain complete Last Glaciation 1 sections. The total thickness of these sections is 1385 cm, and that of the postglacial sections in the same cores is 460 cm. Since the postglacial section is 25.6 cm thick and the Last Glaciation 1 section 71.4 cm, the ratio of the sections is approximately 1 to 3. The average postglacial rate of accumulation in these 18 cores is 2.3 cm in 1000 years. If the rate of accumulation during Last Glaciation 1 was the same as during Last Glaciation 2–3, the duration of Last Glaciation 1 was $\frac{71.4}{2.3 \times 1.5} = 20{,}696$, or about 20,000 years.

Table 5 contains six cores with complete Last Interglacial sections having a total thickness of 1365 cm. In these cores the total thickness of the postglacial sections is 135 cm. Since the average thickness of the postglacial sections is 135 cm and that of the Last Interglacial sections is 227.5 cm, the ratio of the two sections is 1 to 10.1. The average postglacial rate of accumulation in the six cores is 2 cm in 1000 years. Assuming that the rate of accumulation during the Last Interglacial age was the same as that during postglacial time, we estimate that Last Interglacial lasted 113,750 years, or, in round numbers, 110,000 years.

The maximum rate of sediment accumulation as determined by the thickness of the postglacial faunal zone is 63.6 cm in 1000 years. This was found in core A156–4 from the continental rise southeast of Cape Hatteras (Table 5). The maximum rate of accumulation as determined by two radiocarbon dates is 274.4 cm in 1000 years in core A180–48 raised from the bottom of a canyon northwest of Cape Verde, French West Africa (Table 6). These rates of accumulation are considerably greater than any previously reported for deep-sea sediments. For example, the maximum rate Piggot and Urry (1942) found by ionium dating was 24 cm in 1000 years.

Discussion of Late Pleistocene Chronology

Figure 24 gives a chronology of the climatic events recorded in the cores based on radiocarbon dating. This chronology is at variance with radiocarbon dates of wood samples from Pleistocene deposits of the Mississippi Valley region discussed by Horberg (1955). According to these the beginning of the Last Glacial or Wisconsin dates from 22,000 to 25,000 years B.P. Although Horberg cites the internal consistency of the dates, he admits that there are serious geological objections to the chronology based on them. Antevs (1957) has questioned the reliability of radiocarbon dates from samples of wood. He points out that the radiocarbon content of an organic layer such as the spruce-bog peat exposed at Two Creeks, Wisconsin, can be expected to have undergone about equal extra changes, so that several analyses check only one another but not the actual age of the sample.

Flint (1957), however, accepts the greatly shortened chronology to which the dates lead. He states, "All we can say with confidence is that the last major glaciation has occurred within the last 30,000 years."

The chronology presented in Figure 24 is based on radiocarbon dates, and therefore it should be comparable with that discussed by Horberg. We have given our reasons for supposing that zone (x) (Fig. 24) was deposited during an interstadial rather than during the Last Interglacial. Whether this interpretation is correct or not, all evidence indicates that conditions of oceanic climate during accumulation of zone (x) were essentially similar to those of the present.

On the other hand, within the sediment section extending from the top of zone (x) to the base of the uppermost Recent layer there is no evidence that the climate of the Atlantic at any time attained a state similar to that of the present. This conclusion is supported by Emiliani's paleotemperatures from the ratios of oxygen isotopes in the tests of certain species of planktonic Foraminifera. His curves of temperature variations are shown in Figures 41 and 49.

Minor ameliorations of climate must have taken place within the time interval represented by the sediment section between the top of zone (x) and the uppermost faunal zone containing *Globorotalia menardii*. In particular, the interstadial, L.Gl. 2/3, must be included here although it is not represented by any well-defined faunal zone. Since, however, climatic amelioration at the end of the last ice age is obvious in the cores, and since no faunal zone similar to zone (x) or zone (z) is found above the top of zone (x), we conclude that at no other time during the past 50,000 or 60,000 years has the Earth's climate been as warm as it is now.

This serious discrepancy calls for a critical re-examination of the methods and reasoning involved in the derivation of the two chronologies. The possibility that the crystalline crust on the tests of certain species of Foraminifera is acquired at a considerable depth has been discussed. This could lead to incorporation of more or less dead carbon depending upon the rate of deep circulation in the Atlantic. Unfortunately it has not been possible to assay strictly recent tests of Foraminifera from a deep-sea core. Because of the small diameter of the cores, 63 mm, in order to obtain enough material for a radiocarbon determination, one must take a sample which is at least a few centimeters thick and which, therefore, includes some material which may be several thousand years old. On theoretical grounds it is difficult to see how the crystalline crust could introduce an error in excess of 2000 years. Probably the error is much smaller. Such an error would of course reduce the extrapolated dates by about 2000 years, and accordingly the last major age of cool climate in the Atlantic would be included within the last 58,000 years, which leaves the discrepancy between the two chronologies about where it was in the first place.

Important evidence supporting our chronology has been provided by other investigators of deep-sea cores. Arrhenius (1952) in his exhaustive study of a suite of cores from the eastern Pacific has established a sequence of climatic zones based primarily on variation in calcium carbonate content and a chronology which depends upon rate of accumulation of TiO_2 as calibrated by radiocarbon dates. According to his chronology the last major cool period in the eastern Pacific commenced about 70,000 years ago.

Figure 50 shows a curve of climatic change inferred by Cushman and Henbest (1940) from analysis of the planktonic Foraminifera in core P–126 from the North Atlantic. The dates, obtained by Piggot and Urry (1942) by the ionium method, show that a final major period of cool climate began about 60,000 years ago. We have dotted that part of the curve lying between 31,000 and 22,900 years B.P. because of two anomalous layers in this section of the core. A sample from one of these layers was analyzed by Cushman and Henbest. Their assessment of its climatic significance is shown by the isolated point within the graded layer in Figure 50. Bramlette and Bradley (1940) have described this layer in some detail. According to them it has unusually sharp boundaries at both base and top and contains relatively little of the usual fine-grained constituents. Grain size grades from coarse at the base to fine at the top; this gradation applies to the clastic grains as well as to the tests of Foraminifera. Bramlette and Bradley regarded Cushman and Henbest's "temperature" as anomalous and cited it as further evidence that the layer had settled out of suspension following the stirring effect of a submarine slump. We agree.

Fisk and McFarlan (1955) have presented a late Pleistocene chronology based in part on radiocarbon dating of shells and wood samples from deltaic deposits of the Mississippi River. According to them erosion of the Mississippi trench and therefore lowering of sea level because of advancing glaciation commenced about 60,000 years ago, whereas the glacial maximum on the evidence of the lowest point reached by sea level occurred at least 30,000 years ago. The latter date was determined by radiocarbon assay of shells found beneath the weathered surface of the entrenched valley interfluves from a depth of 24 m (80 feet) below sea level in the New Orleans area and a wood sample from the soil zone on the buried valley wall near Donaldsville, Louisiana, at a depth of 83 m (273 feet) below sea level. The latter was found to be more than 28,000 years old, showing that entrenchment of the Mississippi River must have taken place before that date.

In our attempt to correlate evidence of climatic changes in the cores with the sequence of glacial and interglacial deposits on the continents and to derive a tentative chronology of the late Pleistocene, we have not been influenced by any theory of cause of glaciation. We do not find correspondence between our chronology and that derived from the astronomical theory which attributes Pleistocene climatic changes to geometrical variations in the elements of the Earth's orbit. Charlesworth (1957) has reviewed the many objections to this theory raised by geologists and astronomers. It will suffice here to cite the conclusion of van Woerkom (1953) who, with Brouwer, was responsible for a recalculation of the insolation curve, that variations in insolation due to changes in orbital elements of the Earth can cause changes in temperature of no more than 1° or 2° C.; these he regards as insignificant with respect to glaciation.

Gross (1957) called attention to wide differences between the chronology of the Last Glaciation as established by radiocarbon dating and the chronology based on the insolation curve and concluded that the latter must be abandoned.

SUMMARY AND CONCLUSIONS

Investigation of nearly 1000 sediment cores from the Atlantic Ocean and connected seas has led to various conclusions regarding recent processes of sedimentation in deep basins, rates of sediment accumulations, Pleistocene climatic changes, and the nature of sedimentation during the Cenozoic era and Cretaceous period. Data from 221 selected cores, presented in synoptic form, support these conclusions. The cores, ranging in length from 35 to 1275 cm, were taken with a piston corer. There is good evidence that cores taken with this type of corer are truly representative of the sedimentary section *in situ* and that rates of sediment accumulation based on measurements in such cores are not in error because of distortion of the section.

Striking contrasts of lithology in these cores show that two processes of deposition played important roles in the Atlantic during the Pleistocene. These are (1) the slow but continuous settling of fine terrigenous particles and hard parts of pelagic organisms, and (2) catastrophic deposition by turbidity currents in which all particles move together in turbid water. Sediments of catastrophic deposition are as a rule clearly differentiated by color, texture, and chemical, mineral, and organic composition from the slowly and continuously deposited sediment types with which they are usually interbedded. Transportation and deposition by turbidity currents are indicated by the nature of the beds and also by their areal distribution with respect to bottom topography. Evidence from the beds includes the coarse texture of many layers, good particle-size sorting, grading of particle sizes from coarse at the bottom to fine at the top, sharply defined basal contacts of the individual layers, absence of disturbance by burrowing except in the uppermost few centimeters, high calcium-carbonate content at deep stations where the normal sediment is low in carbonate, locally abundant plant detritus, shells of shallow-water mollusks, particles of calcareous algae, and common tests of Foraminifera of shallow-water environment. Distribution of the beds with respect to topography shows clearly that bottom configuration has guided the transportation of the sediment. The sediments occur in depressions or on broad smooth plains, but in no cases on isolated rises. For example, they have been found in submarine canyons, on the smooth floors of the deep basins of the Atlantic and Caribbean, and in the Puerto Rico Trench. They are absent from cores taken on the divides between canyons, on isolated rises in the deep basins, and on the flanks of the Puerto Rico Trench.

Because of the extremely rapid deposition of the individual layers, which may be several meters thick, the net rate of sediment accumulation varies greatly from place to place depending upon the local topography. Various features of bottom topography, otherwise difficult to explain, may be due to the rapid filling of depressions by sediment transported by turbidity currents.

Forty-one cores containing sediments ranging in age from Cenomanian to Pliocene have been described. Evidence is presented that in many cases these older sediments lie within reach of the coring tube in consequence of removal of former cover through submarine slumping. Elsewhere, as in the Hudson Submarine Canyon, exposures of older sediments are probably due to erosion by turbidity currents.

The presence of submarine outcrops of sediments of Neogene and Eocene age along the continental slope opposes the view that the continental slope is analogous to a delta front. We suggest that instability of sediments along the slope as shown by the outcrops is a result of late Cenozoic faulting or steepening of the slope by monoclinal folding parallel to the continental margin. Steepening of slope by concentric faulting is also postulated to explain the zone of exposures of older sediments surrounding the Bermuda Islands.

Absence of submarine outcrops of sediments antedating the Cretaceous period and the restricted thickness of unconsolidated sediment as measured by seismic methods in both the Atlantic and Pacific basins suggest that a drastic reorganization of that part of the Earth's crust now covered by the oceans took place at some time during the latter part of the Mesozoic era.

In consequence of removal of sediment by slumping or because of intercalation of displaced material by turbidity currents, long uninterrupted records of Pleistocene climatic changes are found only where the topographic conditions are exceptional. The nearly level tops of isolated rises afford the most favorable setting for uninterrupted slow sediment accumulation. However, since layers deposited by turbidity currents are usually fairly easily recognized, it is sometimes possible to obtain a complete record by sampling only the interbedded layers due to particle-by-particle accumulation. Removal of a part of the section by slumping or submarine erosion is less easy to detect. Proof of an unbroken climatic record is provided by layer-by-layer correlation between two or more cores from fairly widely separated stations within the same oceanographic province.

The study of many cores tested by correlation has established the reality of several Pleistocene faunal zones in the sediments of the North Atlantic and connected seas. These are distinguished by assemblages of planktonic Foraminifera which are either essentially similar to the assemblage now living in the particular region or by dominance of species now abundant only in higher latitudes.

Emiliani (1955) has measured paleotemperatures as registered by oxygen-isotope ratios in the calcium carbonate of the tests of certain species of planktonic Foraminifera in three cores in the Lamont collection. For the upper two-thirds of the cores there is general agreement between Ericson's climatic sequence based on species frequencies and the isotopic temperatures. Lower in the sections there is a marked divergence.

According to radiocarbon dates in a series of selected cores, the last important faunal change in the North Atlantic took place 11,000 years ago. We suppose that this corresponds to the close of the last glacial age. Extrapolation of rates of sediment accumulation based on 40 radiocarbon dates shows that the last glacial age began about 60,000 years ago. Any variation of water temperature which may have occurred between 60,000 and 11,000 years B. P. must have been of insufficient intensity or of insufficient duration to have left a discernible mark on the faunal record. According to our interpretation of the climatic record no core in the Lamont collection includes all Pleistocene time. The longest record reaches the top of a zone of mild climate which we believe to be equivalent to either the penultimate interglacial or a mild interstadial in the penultimate glacial age.

Our correlation between faunal zones in the cores and the generally accepted sequence of Pleistocene climatic events will remain tentative until the entire Pleistocene section has been obtained in longer cores. Development of a coring tube to take cores more than 20 m long is in progress at Lamont. We are confident that by means of suites of long cores tested for continuity by cross-correlation, it will be possible to establish a standard Pleistocene stratigraphic section.

REFERENCES CITED

Andersen, S. T., 1957, New investigations of interglacial fresh-water deposits in Jutland: Eiszeitalter und Gegenwart, v. 8, p. 181–186

Andrée, K., 1920, Geologie des Meeresbodens, *in* Bodenbeschaffenheit, nutzbare Materialien am Meeresboden, Bd. 2: Leipzig, Gebrüder Borntraeger, 689 p.

Antevs, E., 1957, Geological tests of the varve and radiocarbon chronologies: Jour. Geology, v. 65, p. 129–148

Arrhenius, G., 1952, Sediment cores from the East Pacific: Swedish Deep-Sea Exped. (1947–1948) Repts., v. 5, fasc. 1, 227 p.

Arrhenius, G., Kjellberg, G., and Libby, W. F., 1951, Age determination of Pacific chalk ooze by radiocarbon and titanium content: Tellus, v. 3, p. 222–223

Bé, A. W. H., 1959, Ecology of Recent planktonic Foraminifera, Part I, Areal distribution in the western North Atlantic: Micropaleontology, v. 5, p. 77–100

Beerstecher, E., Jr., 1954, Petroleum microbiology: New York, Elsevier Press, Inc., 375 p.

Bolli, H., 1950, The direction of coiling in the evolution of some Globorotaliidae: Contrib. Cushman Found. Foram. Res., v. 1, p. 82–89

— 1951, Notes on the direction of coiling of Rotalid Foraminifera: Contrib. Cushman Found. Foram. Res., v. 2, p. 139–143

Bramlette, M. N., and Bradley, W. H., 1940, Geology and biology of North Atlantic deep-sea cores, Part I, Lithology and geologic interpretations: U. S. Geol. Survey Prof. Paper 196-A, p. 1–34

Bramlette, M. N., and Riedel, W. R., 1954, Stratigraphic value of discoasters and some other microfossils related to Recent Coccolithophores: Jour. Paleontology, v. 28, p. 385–403

Brandtner, F., 1954, Jungpleistozäner Löss und fossile Böden in Niederösterreich: Eiszeitalter und Gegenwart, v. 4/5, p. 49-82

Charlesworth, J. K., 1957, The Quaternary era, v. 2: London, Edward Arnold Ltd., p. 595–1700

Cushman, J. A., 1936, Geology and paleontology of the Georges Banks Canyons, Part IV, Cretaceous and late Tertiary Foraminifera: Geol. Soc. America Bull., v. 47, p. 413–440

— 1939, Eocene Foraminifera from submarine cores off the eastern coast of North America: Contrib. Cushman Found. Foram. Res., v. 15, p. 49–76

Cushman, J. A., and Henbest, L. G., 1940, Geology and biology of North Atlantic deep-sea cores, Part II, Foraminifera: U. S. Geol. Survey Prof. Paper 196-A, p. 35–50

Daly, R. A., 1936, Origin of submarine canyons: Am. Jour. Sci., v. 27, p. 401–420

Deshayes, G. P., 1832, Encyclopédie méthodique; Histoire naturelle des vers: Paris, tome 2, pt. 1, 256 p.

D'Orbigny, A., 1826, Tableau méthodique de la classe des Céphalopodes: Ann. Sci. Nat., Paris, ser. 1, tome 7, p. 96–314

Edwards, A. M., 1883, L'expédition du Talisman faite dans l'Océan Atlantique: Bull. Ass. Sci. Fr., v. 2, p. 138–139

Emiliani, C., 1954, Depth habitats of some species of pelagic Foraminifera as indicated by oxygen isotope ratios: Am. Jour. Sci., v. 252, p. 149–158

— 1955, Pleistocene temperatures: Jour. Geology, v. 63, p. 538–578

Ericson, D. B., and Wollin, G., 1956a, Correlation of six cores from the equatorial Atlantic and the Caribbean: Deep-Sea Research, v. 3, p. 104–125

— 1956b, Micropaleontological and isotopic determinations of Pleistocene climates: Micropaleontology, v. 2, p. 257–270

Ericson, D. B., Ewing, M., and Heezen, B. C., 1952, Turbidity currents and sediments in the North Atlantic: Am. Assoc. Petroleum Geologists Bull., v. 36, p. 489–511

Ericson, D. B., Wollin, G., and Wollin, J., 1954, Coiling direction of *Globorotalia truncatulinoides* in deep-sea cores: Deep-Sea Research, v. 2, p. 152–158

Ewing, M., Ericson, D. B., and Heezen, B. C., 1958, Sediments and topography of the Gulf of Mexico, p. 995–1053 *in* Weeks, L., *Editor*, Habitat of oil: Am. Assoc. Petroleum Geologists, 1384 p.

Ewing, M., Heezen, B. C., Ericson, D. B., Northrop, J., and Dorman, J., 1953, Exploration of the northwest Atlantic Mid-Ocean Canyon: Geol. Soc. America Bull., v. 64, p. 865–868

Ewing, M., Sutton, G. H., and Officer, C. B., Jr., 1954, Seismic refraction measurements in the Atlantic Ocean, Part VI: Seismol. Soc. America Bull., v. 44, p. 21–38

Fisk, H. N., and McFarlan, E., Jr., 1955, Late Quaternary deltaic deposits of the Mississippi River, p. 279–302 *in* Poldervaart, Arie, *Editor*, Crust of the Earth: Geol. Soc. America Special Paper 62, 762 p.

Flint, R. F., 1957, Glacial and Pleistocene geology: New York, John Wiley & Sons, Inc., 553 p.

Foreman, F., 1951, Study of some Bermuda rocks: Geol. Soc. America Bull., v. 62, p. 1297–1330

Fornasini, C., 1899, Le Globigerine fossili d'Italia: Palaeontogr. Italica, v. 4, p. 203–216

Furon, R., 1949, Sur les trilobites dragués à 4255 m de profondeur par le Talisman (1883): Acad. Sci. Paris, tome 228, p. 1509–1510

Gross, Hugo, 1957, Die Fortschritte der Radiokarbon-Methode 1952–1956: Eiszeitalter und Gegenwart, v. 8, p. 141–180

Hamilton, E. L., 1956, Sunken islands of the Mid-Pacific mountains: Geol. Soc. America Mem. 64, 97 p.

Heezen, B. C., Tharp, M., and Ewing, M., 1959, The floors of the oceans, Part I, The North Atlantic: Geol. Soc. America Special Paper 65, 122 p.

Horberg, L., 1955, Radiocarbon dates and Pleistocene chronological problems in the Mississippi Valley region: Jour. Geology, v. 63, p. 278–286

Hvorslev, H. J., and Stetson, H. C., 1946, Free-fall coring tube; a new type gravity bottom sampler: Geol. Soc. America Bull., v. 57, p. 935–950

Kane, J., 1953, Temperature correlations of planktonic Foraminifera from the North Atlantic Ocean: Micropaleontologist, v. 7, p. 25–50

Koch, R., 1923, Die jungtertiare Foraminiferenfauna von Kabu (Res. Surabaja Java): Eclogae Geol. Helv., v. 18 (1923–1924), p. 342–361

Krumbein, W. C., and Pettijohn, F. J., 1938, Manual of sedimentary petrography: New York, D. Appleton-Century Co., 549 p.

Krumbein, W. C., and Sloss, L. L., 1951, Stratigraphy and sedimentation: San Francisco, W. H. Freeman and Co., 497 p.

Kuenen, Ph. H., 1950, Marine geology: New York, John Wiley & Sons, Inc., 551 p.

—— 1953, Significant features of graded bedding: Am. Assoc. Petroleum Geologists Bull., v. 37, p. 1044–1066

Kuenen, Ph. H., and Menard, H. W., 1952, Turbidity currents, graded and nongraded deposits: Jour. Sed. Petrology, v. 22, p. 83–96

Kuenen, Ph. H., and Migliorini, C. I., 1950, Turbidity currents as a cause of graded bedding: Jour. Geology, v. 58, p. 91–127

Kullenberg, B., 1947, The piston core sampler: Svenska Hydrog.-Biol. Komm. Skr., s. 3, bd. 1, h. 2, 46 p.

—— 1955, Deep-sea coring: Swedish Deep-Sea Exped. Repts., v. 4, fasc. 2, p. 37–95

Loeblich, A. R., Jr., and collaborators, 1957, Studies in Foraminifera: U. S. Nat. Museum Bull. 215, Smithsonian Inst., Washington, D. C., 323 p.

Maerz, A., and Paul, M. R., 1930, A dictionary of color: New York, McGraw-Hill Book Co., 207 p.

Murray, F., and Philippi, E., 1908, Die Grundproben der Deutschen Tiefsee Expedition: Wiss. Ergebn. Deut. Tiefsee-Exped. Valdivia, v. 10, p. 7–206

Murray, F., and Renard, A. F., 1891, Report on deep-sea deposits based on specimens collected during the voyage of H.M.S. Challenger in the years 1872 to 1876: Challenger Repts., London, Govt. Printer, 525 p.

Natland, M. L., 1938, New species of Foraminifera from off the west coast of North America and from the later Tertiary of the Los Angeles Basin: Scripps Inst. Oceanography Bull., Tech. Ser., v. 4, 149 p.

Northrop, J., and Heezen, B. C., 1951, An outcrop of Eocene sediment on the continental slope: Jour. Geology, v. 59, p. 396–399

Passega, R., 1954, Turbidity currents and petroleum exploration: Am. Assoc. Petroleum Geologists Bull., v. 38, p. 1871–1887

Pettersson, H., 1953, The Swedish Deep-Sea Expedition, 1947–48: Deep-Sea Research, v. 1, p. 17–24

Philippi, E., 1910, Die Grundproben der Deutschen Sudpolar-Expedition, 1901–1903: Berlin, G. Reimer, bd. II, h. 6, Geog. Geol., p. 411–616

Phleger, Fred B, Parker, F. L., and Peirson, J. F., 1953, North Atlantic Foraminifera: Swedish Deep-Sea Exped. (1947–1948) Repts., v. 7, fasc. 1, 122 p.

Piggot, C. S., and Urry, W. D., 1942, Time relations in ocean sediments: Geol. Soc. America Bull., v. 53, p. 1187–1210

Raitt, R. W., 1956, Seismic refraction studies of the Pacific Ocean Basin, Part I, Crustal thickness of the Central Equatorial Pacific: Geol. Soc. America Bull., v. 67, p. 1623–1640

Revelle, R. R., 1944, Scientific results of Cruise VII of the CARNEGIE during 1928–1929, Marine bottom samples collected in the Pacific Ocean: Carnegie Inst. Washington Pub. 556, Oceanography—II, Pt. 1, 193 p.

Revelle, R. R., Bramlette, M., Arrhenius, G., and Goldberg, E. D., 1955, Pelagic sediments of the Pacific, p. 221–236 *in* Poldervaart, Arie, *Editor*, Crust of the Earth: Geol. Soc. America Special Paper 62, 762 p.

Rhumbler, L., 1909, Die Foraminiferen (Thalamophoren) der Plankton-Expedition: Ergebnisse der Plankton-Expedition der Humbolt-Stiftung, v. 3, 337 p.

Richards, H. G., and Ruhle, J. L., 1955, Mollusks from a sediment core from the Hudson Submarine Canyon: Penna. Acad. Sci. Proc., v. XXIX, p. 186–190

Ross, C. S., Miser, H. D., and Stephenson, L. W., 1929, Water-laid volcanic rocks of early Upper Cretaceous age in southwestern Arkansas, southeastern Oklahoma, and northeastern Texas: U. S. Geol. Survey Prof. Paper 154, p. 175–202

Schott, W., 1935, Die Foraminiferen in dem aequatorialen Teil des Atlantischen Ozeans: Meteor, Bd. III, T. 3, Lf. 1, B, p. 43–134

Shepard, F. P., 1948, Submarine geology: New York, Harper & Bros., 338 p

— 1952, Composite origin of submarine canyons: Jour. Geology, v. 60, p. 84–96

Shepard, F. P., and Emery, K. O., 1941, Submarine topography off the California coast: canyons and tectonic interpretation: Geol. Soc. America Special Paper 31, 171 p.

Stetson, H. C., 1936, Geology and paleontology of the Georges Bank Canyons. Part I, Geology: Geol. Soc. America Bull., v. 47, p. 339–366

Tauber, H., and de Vries, H., 1958, Radiocarbon measurements of Würm-Interstadial samples from Jutland: Eiszeitalter und Gegenwart, v. 9, p. 69–71

Twenhofel, W. H., 1950, Principles of sedimentation: 2d ed., New York, McGraw-Hill Book Co., Inc. 673 p.

Van Woerkom, A. J. J., 1953, The astronomical theory of climatic changes, p. 147–157 *in* Shapley, Harlow, *Editor*, Climatic change (symposium): Cambridge, Harvard Univ. Press, 318 p.

Vašíček, M., 1953a, Changes in the ratio of sinistral and dextral individuals of the Foraminifer *Globorotalia scitula* (Brady) and their use in stratigraphy: Sborník Ústředního Ústavu Geologického, Svazek XX, 76 p.

— 1953b, Graded bedding and some sedimentary mineral deposits: Sborník Ústředního Ustavu Geologického, Svazek XX, Nakladatelstvi Ceskoslovenske Akademie, Praha, 52 p.

Veatch, A. C., and Smith, P. A., 1939, Atlantic submarine valleys of the United States and the Congo submarine valley: Geol. Soc. America Special Paper 7, 101 p.

Wentworth, C. K., 1922, A scale of grade and class terms for clastic sediments: Jour. Geology, v. 30, p. 377–392

Wiseman, J. D. and Todd, I., 1959, Signification des variations du taux d'accumulation de *Globorotalia menardii menardii* d'Orbigny dans une carotte de l'Atlantique Équatorial: Colloques Internat. du Centre National de la Recherche Scientifique, LXXXIII, Topographie et Géologie des profondeurs océaniques, p. 193–206

Young, J. A., Jr., 1939, Minerals from deep-sea cores and surface deposits of Bermudean calcareous sediments: Am. Jour. Sci., v. 237, p. 798–810

Zeuner, F. E., 1954, Riss or Würm?: Eiszeitalter und Gegenwart, v. 4/5, p. 98–103

MANUSCRIPT RECEIVED BY THE SECRETARY OF THE SOCIETY, JULY 7, 1958
LAMONT GEOLOGICAL OBSERVATORY CONTRIBUTION NO. 467

DON

Sta

in

Abstr
mecha
phase
posses
maint

Sev
1959)
exten
veloci
crust
miner
a che
rock.
pothe
eclogi
identi
of the
erals j
bearin
veloci
km/se
result
denser
basalt.
The
and ex
(1957)
albite
sents a
eclogit
takes
temper
at M in
(1959)
conditi
mantle
Alth
at M i
tractive
sider it
The
point c

Geologi

DONALD C. NOBLE *Dept. Geology, Stanford University, Stanford, Calif.*

Stabilization of Crustal Subsidence in Geosynclinal Terranes by Phase Transition at M

Abstract: Isostatic calculations indicate that a mechanism of geosynclinal subsidence based on a phase transformation at the M discontinuity possesses an inherent stability that will tend to maintain the upper surface of sediments near sea level regardless of fluctuations in the rate of geoisotherm depression or in the rate of sedimentation.

This effect may help in the understanding of sedimentation in geosynclinal and stable-shelf terrane.

Several papers (Lovering, 1958; Kennedy, 1959) have appeared recently supporting and extending Fermor's (1914) concept that the M velocity discontinuity separating the earth's crust and mantle results from a high-pressure mineralogic phase transition rather than from a chemical change from mafic to ultramafic rock. According to the phase-transition hypothesis, the earth's upper mantle consists of eclogitic material with a chemical composition identical to that of the "basaltic" lower portion of the crust but consisting of the denser minerals jadeitic pyroxene (omphacite) and lime-bearing almandine-pyrope. The increase in velocity of compressional waves from 6.8–7.2 km/sec to 8.0–8.3 km/sec at M is then a direct result of the larger elastic constants of the denser eclogite phase as compared to those of basalt.

Theoretical calculation (Kelley *et al.*, 1953) and experimental work by Robertson *et al.* (1957) and Kennedy (1956) on the transition albite + nepheline $\rightleftarrows$ jadeite, which represents a crude approximation of the basalt $\rightleftarrows$ eclogite transition, show that this transition takes place under conditions of pressure and temperature which can be reasonably assumed at M in continental regions. Boyd and England (1959) have shown that pyrope is stable at *P-T* conditions thought to occur in the upper mantle.

Although the concept of a phase transition at M is at present an unproven, although attractive, hypothesis, it is interesting to consider its effects on vertical crustal movements.

The position of M will be determined by the point of intersection of the *P-T* curve for the earth's crust and the *P-T* curve for the basalt-eclogite phase transition (Fig. 1). A low-temperature gradient under the ocean basins will place M near the earth's surface, while a steeper gradient under continental regions (Birch, 1955) will cause M to occur at greater depths. Even steeper temperature gradients under mountain ranges will cause the crust to extend as deep as 40–50 km, forming the "roots" of mountain ranges.

Warming or cooling of the crust at any point —*i.e.*, vertical geoisotherm movements—will cause conversion of eclogite to basalt or basalt to eclogite. This conversion, by decreasing or increasing the average density of the column of material in the crust and upper mantle, will bring about isostatic rise or fall of the earth's surface.

Kennedy (1959) has suggested that geosynclinal sinking is a result of a general geoisotherm depression beneath the geosynclinal tract. The lowering of the geothermal gradient will cause the feldspar-pyroxene assemblage at the base of the crust to become unstable and convert to the denser eclogitic phase. This "contraction" of part of the original crustal material will increase the average density of the rock column above the original position of M. It is evident that the upper surface of the column must subside if the column is to remain in isostatic equilibrium.

If the crust is loaded by sediments and/or water, the rate of crustal sinking relative to sea level will depend both on the rate of geoisotherm depression and on the nature of the materials deposited at the surface. A low rate of sedimentation, permitting the accumulation of

---

Geological Society of America Bulletin, v. 72, p. 287–291, 3 figs., February 1961

low-density water in the sinking trough, will allow less crustal subsidence than would occur if sedimentation were sufficient to fill the trough completely. Conversely, increased pressure at M caused by excess sediments deposited subaerially during periods of rapid sedimentation will bring about additional crustal subsidence by forcing the conversion of basalt to eclogite.

depth are ignored. The model is assumed to remain in isostatic balance at all times. The long time available for isostatic adjustments during the slow process of geosynclinal accumulations justifies this assumption.

The loading of the model by sediments or water will require removal of material below M if isostatic balance is to be maintained. Measurements of isostatic rebound in glaciated

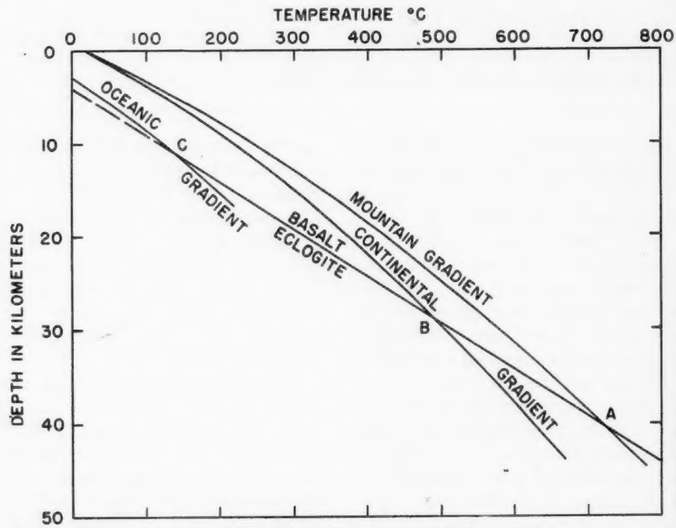

Figure 1. Variation in Position of *M* as Determined by Variations in Temperature Gradients under Mountain Ranges (A), Continental Areas (B), and Oceanic Regions (C). After Kennedy (1959)

The quantitative effects of variation of the rates of isotherm depression and sedimentation may be computed using a simplified model of a geosynclinal section at a time of sedimentary accumulation. Eclogite, with a density $\rho_3 = 3.35$ gm/cm^3, is separated by M from overlying "basaltic" material with a density $\rho_2 = 2.95$ gm/cm^3. Uncompacted sediments with a density $\rho_1 = 2.25$ gm/cm^3 are being deposited at sea level. The density of sea water, ρ_4, is taken as 1.02 gm/cm^3. Specific values for the thickness and density of the material below the unconsolidated sediments and above the basalt are not necessary for the calculations. Reasonable variations in the values ρ_1, ρ_2, and ρ_3 will not basically alter the results.

Calculations are made with an Airy model in which the small gravity variations with

regions, which show that subcrustal material lacks long-term strength, indicate that plastic flowage at depth can be expected to effect this removal quickly.

Constant values for dT/dP near M are used. This simplification is not strictly correct in view of the differences in the thermal conductivity of basalt and eclogite, but it should not affect the validity of the results since thermal equilibrium must be approached for geoisotherm depression to continue. The presence of a zone of transition rather than a sharp boundary at M caused by a lag in the reactions will not affect the calculations if the zone retains the same thickness and phase proportions as it moves vertically.

Referring to the model, the relative amounts of geoisotherm depression with respect to sea level necessary to cause a unit distance of crustal subsidence (Fig. 2) for two cases, *a* and *b*, can be computed. In Case *a*, one unit thickness of sediments of density ρ_1 is deposited below sea level; in Case *b*, one unit thickness of sea water accumulates instead.

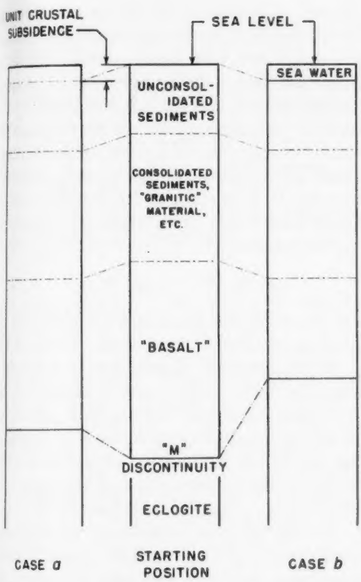

Figure 2. Diagram Illustrating Original Position and new Positions of *M* Relative to Sea Level after unit Crustal Subsidence. Scale greatly exaggerated.

Since in effect basaltic material at depth is being replaced by lower-density sediments at the surface, M must shift to a new position above its original location relative to sea level to maintain the column in isostatic equlibrium. The amount of shift is determined by the density contrast of the sediments and the basaltic material they in effect replace in the column as compared to the density contrast between basalt and eclogite.

For Case *a*, this relation may be represented by

$$(\rho_2 - \rho_1) \times (\textit{amount of surface subsidence}) =$$
$$(\rho_3 - \rho_2) \times (\textit{amount of upward movement of M})$$

Thus, for Case *a*, M must rise

$$\frac{(\rho_2 - \rho_1)}{(\rho_3 - \rho_2)} \times 1$$

unit distance surface subsidence, or

$$\frac{2.95 - 2.25}{3.35 - 2.95} = 1.75$$

units of distance relative to sea level for the model to remain in isostatic equlibrium (Fig. 2).

Likewise for Case *b*, where one unit thickness of water accumulates instead of one unit thickness of sediments, M must be raised

$$\frac{(\rho_2 - \rho_4)}{(\rho_3 - \rho_2)} = \frac{1.93}{0.40} = 4.82$$

units of distance relative to sea level if isostatic balance is to be maintained.

At the original position of M with regard to sea level, the decrease in pressure caused by the "replacement" of basalt by sediments (or water) in the column above M is exactly balanced by the increased pressure caused by the conversion of basalt to eclogite below the new position of M.

Since pressure is proportional to density times thickness, the relative differences in pressure between the original and final positions of M are:

Case *a*

$$\begin{aligned}\triangle P = P_{(M\ original)} - P_{(M\ final)} &\sim \\ [-1.00 \times (\rho_2 - \rho_1)] &= -0.70 \\ +[-1.75 \times \quad \rho_2 \quad] &= \underline{-5.16} \\ &\quad -5.86\end{aligned}$$

Case *b*

$$\begin{aligned}\triangle P = P_{(M\ original)} - P_{(M\ final)} &\sim \\ [-1.00 \times (\rho_2 - \rho_4)] &= -1.93 \\ +[-4.82 \times \quad \rho_2 \quad] &= \underline{-14.23} \\ &\quad -16.16\end{aligned}$$

The quantity $\triangle T$, the change in temperature at points near M necessary to raise the basalt-eclogite phase boundary to the position necessary for isostatic balance, is expressed in terms of $\triangle P$ by the equation (Fig. 3):

$$\triangle T = \left[\left(\frac{dT}{dP}\right)_{phase\ transition} - \left(\frac{dT}{dP}\right)_{earth}\right]\triangle P$$

Substituting the relative pressure drops for Case *a* and Case *b* in the above relation and solving the two resulting equations:

$$\triangle T_{water} = \frac{16.16}{5.86}\triangle T_{sediments} = 2.76\triangle T_{sediments}$$

The geoisotherms may be depressed just enough to keep the surface at sea level as sediments are deposited. But if the isotherms are depressed at a greater rate the accumulation of water instead of sediments will reduce the rate of subsidence because of the lower density of the water.

For example, consider the situation where the rate of sedimentation equals the rate of crustal subsidence. If the rate of geoisotherm depression is then doubled, the sea will not deepen one unit for every unit thickness of sediments deposited.

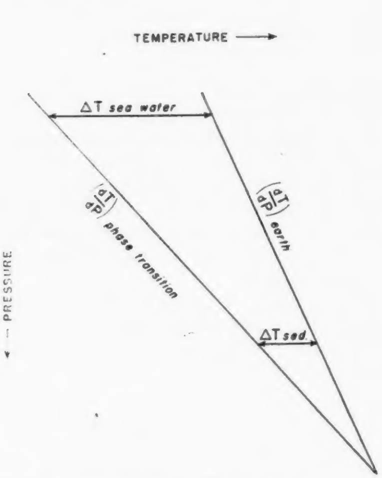

Figure 3. Diagrammatic Representation of the Difference Between $\triangle T$ *water* and $\triangle T$ *sediment* Necessary for Unit Crustal Depression.

This can be shown as follows: The amount of phase conversion at depth allowed by half of the new rate of geoisotherm depression will allow crustal subsidence sufficient to accommodate the newly deposited sediments. It has been shown above that, for equal thicknesses of sediments and water,

$$\triangle T_{water} = 2.76 \triangle T_{sediments}.$$

Therefore, since water is now accumulating in lieu of sediments, the additional geoisotherm depression will allow $1/2.76 = 0.36$ additional units of crustal subsidence.

Thus, even though the rate of geoisotherm depression has been doubled, the sea will deepen only 0.36 unit for every unit of sediments deposited. The rate of geoisotherm depression would have to increase approximately 3.8 times to allow equal thicknesses of water and sediments to accumulate.

The effect of a decrease in the rate of geoisotherm depression can also be calculated. Consider again the situation where the rate of sedimentation equals the rate of crustal subsidence. The rate of geoisotherm depression is now halved. At first sight it might appear that this would permit sediments to accumulate for a considerable thickness above sea level. But this will not occur. By increasing the pressure at M and thus causing basalt to transform to eclogite, the extra sediments initially deposited above sea level will bring about additional crustal subsidence. Subsidence will continue until the pressure increase on M caused by the sediments remaining above sea level equals the pressure decrease caused by the "replacement" of basalt by sediments in the column above M.

The fraction, x, of the total sediments remaining above sea level may be computed using the relation

$$x\rho_1 = (R - x)(\rho_2 - \rho_1)$$

where R equals the fractional reduction in the rate of geoisotherm depression. Thus, if the rate of geoisotherm depression is halved, R equals 0.5, and x will equal 0.119; 11.9 per cent of the sediments will remain above sea level, or, for every foot of sediments deposited below sea level, 0.135 foot of sediments will accumulate above the surface of the water.

From these calculations, it can be seen that the rate of surface subsidence in a system governed by a phase transition is not directly proportional to either the rate of sedimentation or to the rate of geoisotherm depression. The effect on subsidence of large fluctuations in either rate is considerably damped by phase conversion controlled by the P-T conditions at M.

This damping, which would tend to keep the surface of sedimentation near sea level, may help in explaining the irregular, but generally sympathetic, variations in sedimentation and subsidence that appear to have occurred in geosynclinal and stable-shelf areas. In particular, the prolonged accumulation of shallow-water sediments may be somewhat easier to understand.

ACKNOWLEDGMENTS

The writer wishes to thank Professor George A. Thompson of Stanford University for critically reading several drafts of the manuscript and for many instructive and stimulating discussions of the problem. Appreciation is also due Professor Konrad B. Krauskopf and Mr. Robert L. Christiansen for critical reading of the manuscript.

REFERENCES CITED

Birch, Francis, 1955, Physics of the crust, p. 101–117 *in* Poldervaart, A., *Editor*, Crust of the earth—a symposium: Geol. Soc. America Special Paper 62, 762 p.

Boyd, F. R., and England, J. L., 1959, Experimentation at high pressures and temperatures—Pyrope: Annual Report of the Director of the Geophysical Laboratory for 1958–1959, p. 83–87

Fermor, L. L., 1914, The relationship of isostasy, earthquakes, and volcanicity to the earth's infra-plutonic shell: Geol. Mag., v. 51, p. 65–67

Kelley, K. K., Todd, S. S., Orr, R. L., King, E. G., and Bonnickson, K. R., 1953, Thermodynamic properties of sodium-aluminum and potassium-aluminum silicates: U. S. Bur. Mines Rept Invest. 4955, 21 p.

Kennedy, G. C., 1956, Polymorphism in the feldspars at high temperatures and pressures (Abstract): Geol. Soc. America Bull., v. 67, p. 1711–1712

— 1959, The origin of continents, mountain ranges, and ocean basins: Am. Scientist, v. 47, p. 491–504

Lovering, J. F., 1958, The nature of the Mohorovičić discontinuity: Am. Geophys. Union Trans., v. 39, p. 947–955

Robertson, E. C., Birch, F., and MacDonald, G. J. F., 1957, Experimental determination of jadeite stability relations to 25,000 bars: Am. Jour. Sci., v. 255, p. 115–137

Manuscript Received by the Secretary of the Society, June 20, 1960

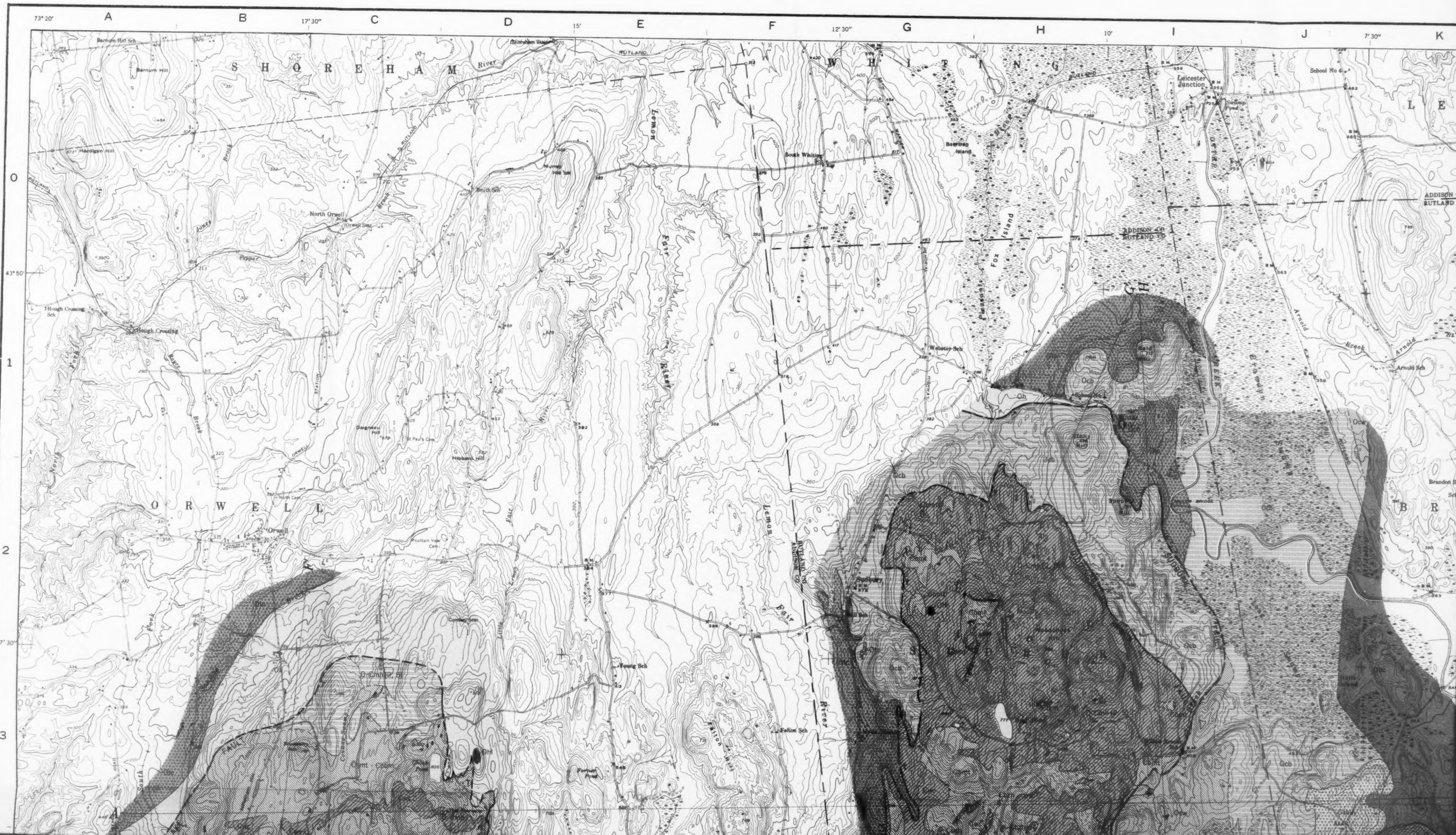

73° 20'
A
B
17' 30"
C
D
15'
E
F
12' 30"
G
H
10'
I
J
7' 30"
K
S H O R E H A M
W H I T I N G
L E
O R W E L L
B R
Barnum Hill
Lemon Fair River
North Orwell
Hough Crossing
Orwell
Leicester Junction
South Whiting
Webster Sch
Fox Island
ADDISON CO
RUTLAND CO
Sudbury
Hibbard Hill
Young Sch
Fallon Sch
Arnold Brook
Brandon Sta
School No 6

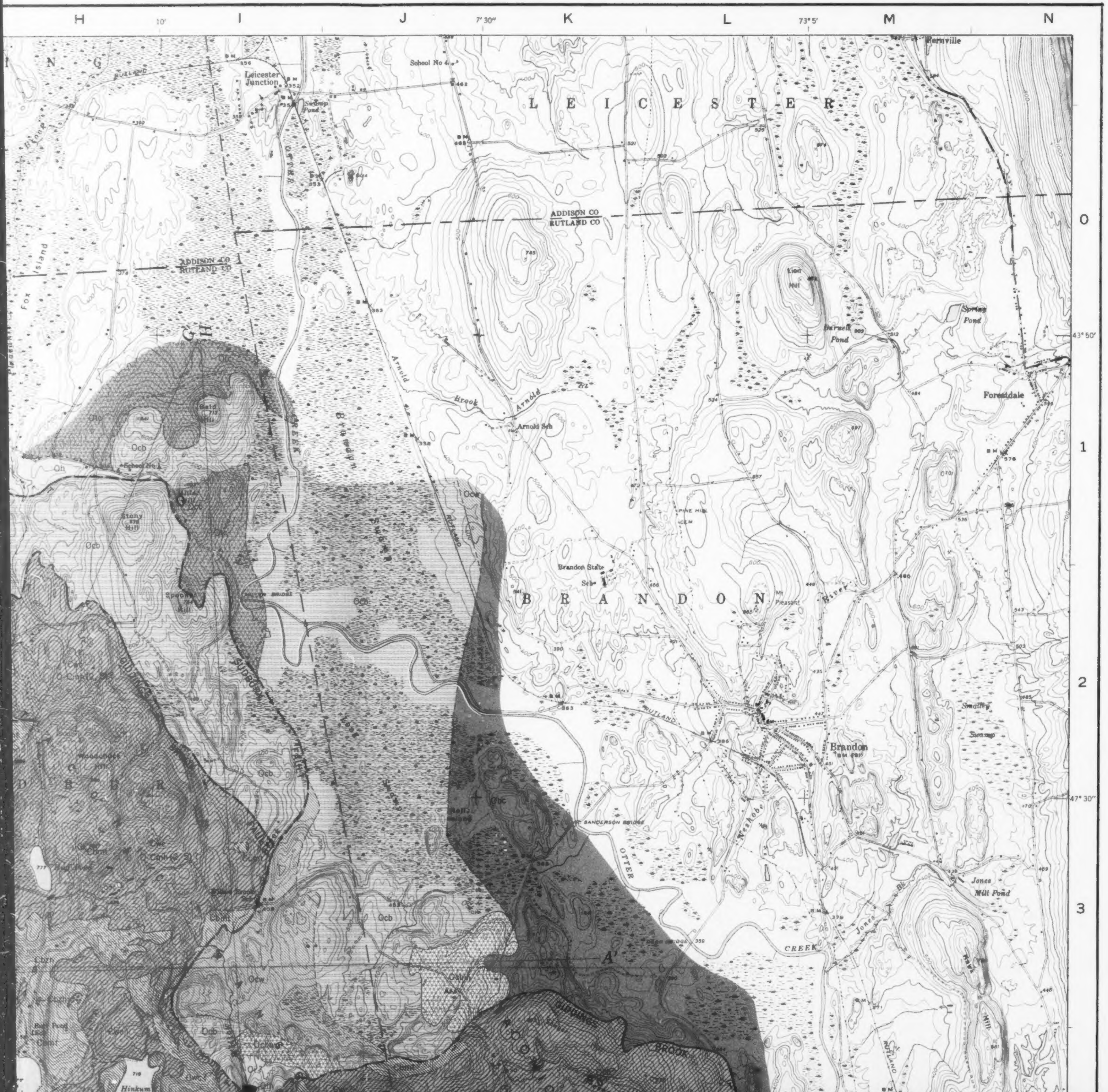

EXPLANATION

SYNCLINORIUM SEQUENCE

MIDDLE ORDOVICIAN

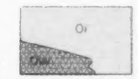

Ira formation
(East side of Taconic Sequence)

Oi; *black, siliceous to graphitic phyllite, locally limy or with beds rich in albite porphyroblasts and dark to greenish grey in color.*

Oiw; *Whipple marble member: dark bluish grey-weathering dark grey marble, generally finer-grained than the Lower Ordovician carbonates. Basal to the Ira formation, but locally interbedded with the lower strata of the slates and phyllites.*

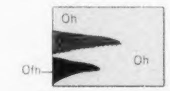

Hortonville formation
(West side of Taconic Sequence)

Oh; *black, siliceous to graphitic slate, locally limy or silty and weathering reddish.*

Ofh; *Forbes Hill conglomerate: angular and poorly sorted quartzite-and-slate pebbles in black slate matrix.*

Ohl; *coarse limestone-pebble, limy-matrix conglomerate in black slate.*

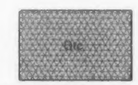

Undifferentiated Mid-Ordovician limestones
(Middlebury, Orwell, and Glens Falls)

Otc; *Undifferentiated dark grey, thin-to-medium bedded limestone and marble, with local interbedding of thin brown-weathering dolomitic layers. Local siliceous and black phyllitic partings in the limestone.*

LOWER ORDOVICIAN

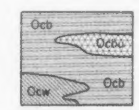

Chipman formation

Ocb; *Beldens member: grey, massive marble with interbedded massive creamy dolostone; white massive marble with red hematite streaks.*

Ocbu; *Burchards member: similar to Beldens member but characterized by buff-weathering dolomitic mottles in limestone and marble beds.*

Ocw; *Weybridge member: grey fine marble interbedded with brown-weathering, slightly dolomitic layers at equal intervals of about 3 inches. Locally these contrasting strata show cross-bedding.*

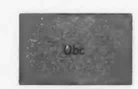

Bascom formation

Obc; *grey, streaky marble; grey marble with dolomitic mottles; massive white marble; interbedded massive grey dolostone and grey marble; interbedded thin grey-white marble and brown-weathering siliceous dolostone and limestone; massive spongy-weathering dark grey dolomitic quartzite; grey sugary marble with pale siliceous or micaceous partings.*

TACONIC SEQUENCE

MIDDLE ORDOVICIAN

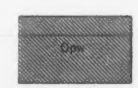

Pawlet formation

Opw; *silver grey to jet black, locally graphitic and pyritiferous, micaceous silty slate interbedded with grey, locally calcareous greywacke. The greywacke weathers dull brown and commonly shows graded bedding. Grains of subangular quartz, feldspar, and rock fragments up to ⅛ inch in a calcareous and argillaceous matrix. Beds up to 4 feet thick. Basal part of the formation carries graptolites.*

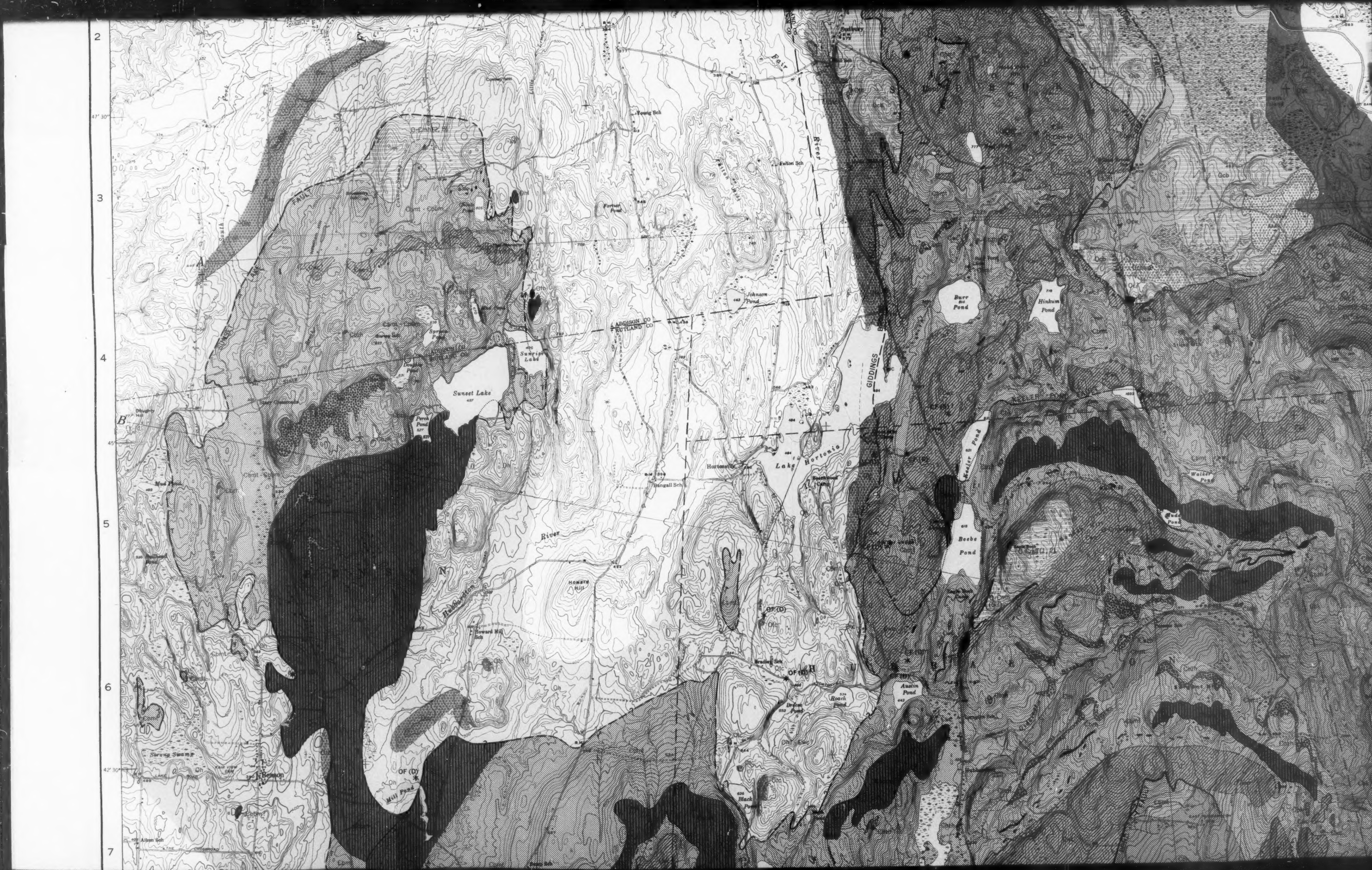

Bascom formation

Bascom formation

Obc; *grey, streaky marble; grey marble with dolomitic mottles; massive white marble; interbedded massive grey dolostone and grey marble; interbedded thin grey-white marble and brown-weathering siliceous dolostone and limestone; massive spongy-weathering dark grey dolomitic quartzite; grey sugary marble with pale siliceous or micaceous partings.*

TACONIC SEQUENCE

MIDDLE ORDOVICIAN

Pawlet formation

Opw; *silver grey to jet black, locally graphitic and pyritiferous, micaceous silty slate interbedded with grey, locally calcareous greywacke. The greywacke weathers dull brown and commonly shows graded bedding. Grains of subangular quartz, feldspar, and rock fragments up to ⅛ inch in a calcareous and argillaceous matrix. Beds up to 4 feet thick. Basal part of the formation carries graptolites.*

UPPER CAMBRIAN TO MIDDLE ORDOVICIAN

Mount Hamilton Group

O-Cmh; *black, grey, green, purple, to red hard slates, weathering white (units 1, 2, and 3 of the text); with beds of ankeritic quartzite from a few inches to several feet thick (unit 5,* bright red*); latter may contain layers of an edgewise conglomerate. Some of the slates are interbedded with thin cherty quartzites or ribbon limestones a few inches apart. A red, smooth, soft slate is included (unit 4), as well as a lime-matrix polymict limestone conglomerate (unit 6), including black chert pebbles. Lithology of the group varies rapidly along strike and separation from* Cwc *is not always easy. Abundant cross-bedding, channel-filling, etc.*

LOWER CAMBRIAN

West Castleton formation

Cwc; *grey siliceous to black, graphitic, pyritiferous slate and phyllite, locally with interbedded thin dark grey dolostone and grey quartzite and arkosic layers. Thin, white sandy laminae common in the graphitic variety.*

Cwcb; *Beebe limestone member: massive, lenticular black limestone weathering blue-grey. Fossiliferous.*

Bull formation

Cbmt; *Mettawee slate facies: bulk of the formation. Purple, green-grey, and variegated slate and phyllite, non-chloritoid bearing; minor beds of white to green quartzite and creamy limestone near the top of the formation.*

Bright blue; *North Brittain conglomerate member: limestone-pebble conglomerate in a non-calcareous green to purple slate matrix. Thickness extremely variable. The conglomerate is intraformational and may pass visibly into boudinaged limestone beds. Fossiliferous. Near West Castleton village, the unit is a grey ribbon-limestone in a dark grey slate matrix.*

Bright green; *Mudd Pond quartzite: white to grey, vitreous, medium-grained orthoquartzite with local dolomitic pods (concretions?). Locally dark grey quartz-grit in a slaty matrix (Eddy Hill lithology). Rock generally weathers white and smooth, with a waxy luster.*

Cbzh; *Zion Hill member: green, vitreous, chloritic quartzite or greywacke with common limonite spots. Base of the unit is commonly a pebble conglomerate and top may be a siltstone. Unit as a whole is massive and lenses in and out rapidly. Weathers white and tends to form cliffs. East of Lake Bomoseen, it is stratigraphically below the Bomoseen greywacke, but west of the lake, it is above the Bomoseen.*

Cbbm; *Bomoseen greywacke member: green to olive-colored arkose and greywacke, carrying visible flakes of mica and rock fragments, and microscopic stilpnomelane. Weathers pale red to white. Massive and uniform, locally with white quartzite layers.*

Biddie Knob formation

Cbk; *purple and green chloritoid-bearing slate and phyllite. Minor beds of white to green quartzite and rarely limestone seams. Especially south of Castleton River but also locally north thereof, the Zion Hill quartzite is actually within, though near the top of, this formation.*

CONTACTS

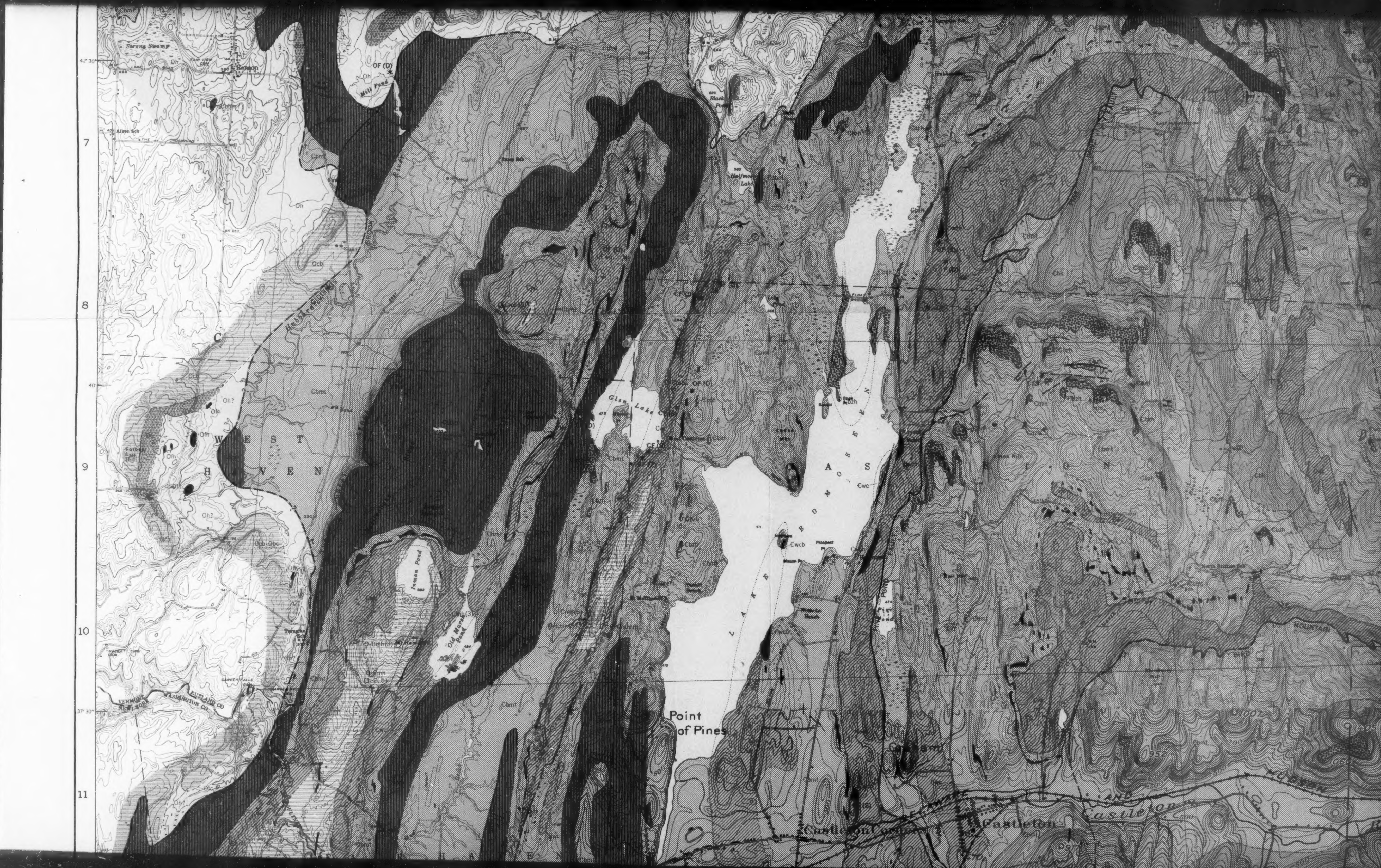

grained orthoquartzite with local dolomitic pods (concretions?). Locally dark grey quartz-grit in a slaty matrix (Eddy Hill lithology). Rock

grained orthoquartzite with local dolomitic pods (concretions?). Locally dark grey quartz-grit in a slaty matrix (Eddy Hill lithology). Rock generally weathers white and smooth, with a waxy luster.

Cbzh; *Zion Hill member: green, vitreous, chloritic quartzite or greywacke with common limonite spots. Base of the unit is commonly a pebble conglomerate and top may be a siltstone. Unit as a whole is massive and lenses in and out rapidly. Weathers white and tends to form cliffs. East of Lake Bomoseen, it is stratigraphically below the Bomoseen greywacke, but west of the lake, it is above the Bomoseen.*

Cbbm; *Bomoseen greywacke member: green to olive-colored arkose and greywacke, carrying visible flakes of mica and rock fragments, and microscopic stilpnomelane. Weathers pale red to white. Massive and uniform, locally with white quartzite layers.*

Biddie Knob formation

Cbk; *purple and green chloritoid-bearing slate and phyllite. Minor beds of white to green quartzite and rarely limestone seams. Especially south of Castleton River but also locally north thereof, the Zion Hill quartzite is actually within, though near the top of, this formation.*

CONTACTS

Sedimentary contact

Dashed where inferred or interpolated, dotted where concealed. Queried where interpreted.

Fault contact

Generally low-angle reverse (thrust) faults. T *on upper plate. Dashed where inferred or interpolated, dotted where concealed. Queried where interpreted.*

*

Fossil locality

CF (Z): *Cambrian locality; this report.*

CF (S): *Cambrian locality; reported by Swinnerton and Schuchert.*

CF (F): *Cambrian locality; reported by Fowler*

CF (D): *Cambrian locality; reported by Dale and assistants (notebooks)*

OF (D): *Ordovician locality; reported by Dale and assistants (notebooks)*

Point of Pines
Castleton Corners
Castleton
Hydeville
Low Hampton
H A M P T O N
W H I T E H A L L
Pond Hill
Parker Hill
Old Knob
Spruce Knob
Hampshire Hollow
East Whitehall
East Poultney
Hampton
11
12
13
14
15

Castleton
Hudson River
Pond Hill
Bird Mountain
Clark Hill
Herrick Mountain
Old Knob
Spruce Knob
Ira
Ira Brook
Bird Mountain
E'
11
12
13
14
15

Williams & Heintz Map

Base from U. S. Geological Survey 7½-minute topographic sheets: Benson (1946), Bomoseen (1944), Brandon (1946), Orwell (1949), Proctor (1944), Sudbury (1946), and Thorn Hill (1946), U.S.G.S. 15-minute topographic sheet: Castleton (1895). U. S. Soil Conservation Service aerial photographs, DCC series, 1941-42.

Scale of Castleton sheet 1:62,500; Scale of other sheets 1:24,000

BEDROCK GEOLOGY OF THE CASTLETON AREA, VERMONT

Scale 1:48 000

1 0 1 2 Miles

ZEN, PLATE 1

Geological Society of America Bulletin, volume 72

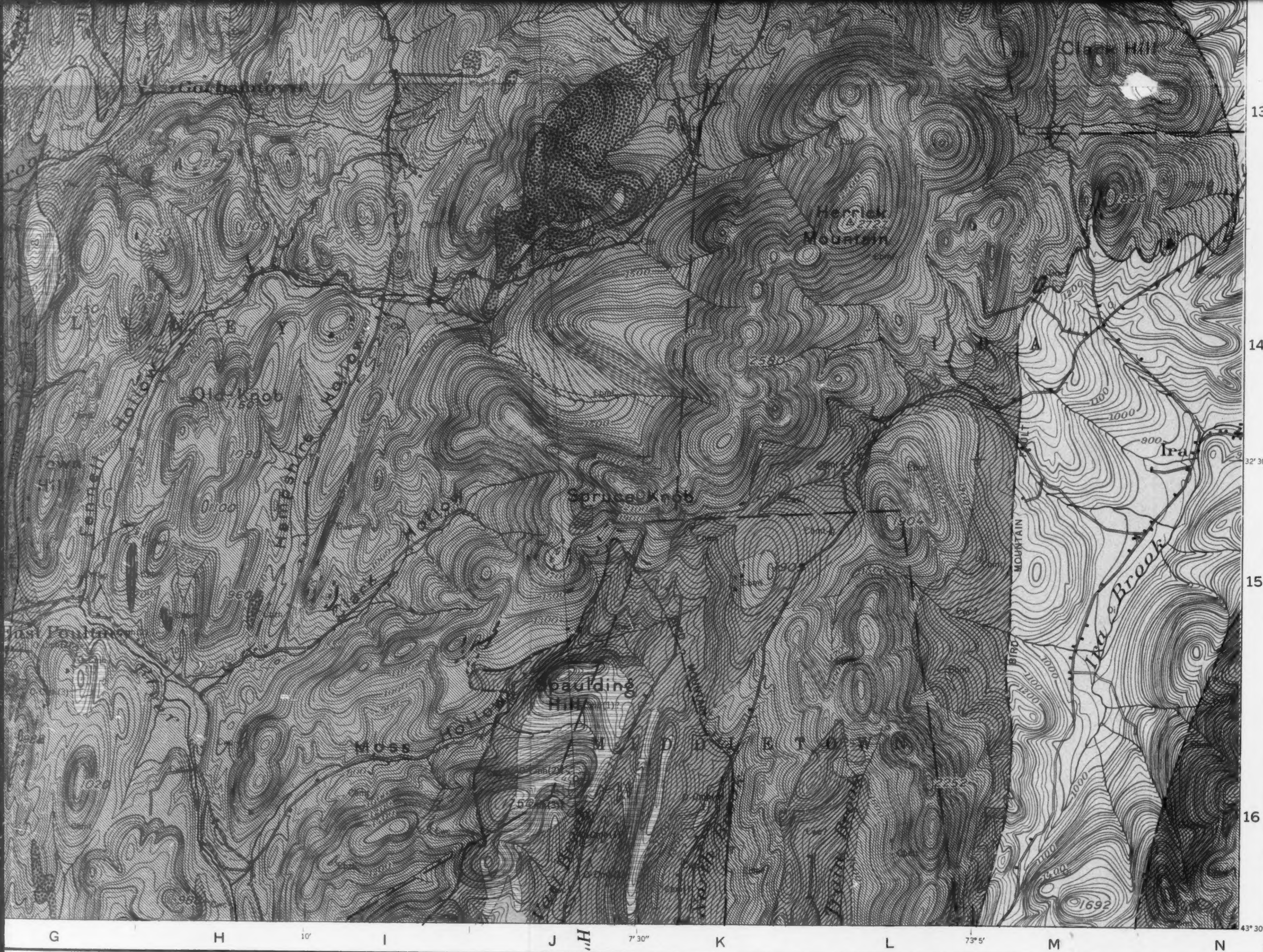

Williams & Heintz Map Corporation Washington 27, D. C.

Geology by E-an Zen, assisted by W. D. Means, A. J. Murray, and D. Harwood, 1953-58.

T THE CASTLETON AREA, VERMONT

Scale 1:48 000

0 1 2 Miles

E-AN

Stra

of

Abstra
at the
centra
Pau
greyw
Mo
green
stone
Camb
We
with
brian
Bu
(
muds
bulk
(
intra
glome
(
ortho
(
wack
cong

medi
Bi
purp
of lin
Th
give
Zion
Bom
Ham
bedd
St
nest
Alth
stra
dow
cult
Bro
twe
fold
was
zon
the
hav

Ge

E-AN ZEN *U. S. Geological Survey, Geophysics Branch, Acorn Building, Silver Spring, Md.*

Stratigraphy and Structure at the North End of the Taconic Range in West-Central Vermont

Abstract: The stratigraphy of the Taconic sequence at the north end of the Taconic Range in west-central Vermont has been revised as follows:

Pawlet formation: interbedded black slate and greywacke; Middle Ordovician

Mount Hamilton group: undivided black, gray, green, and red argillite, with minor limestone, limestone conglomerate, and ankeritic quartzite; Upper Cambrian to Middle Ordovician

West Castleton formation: black slate and phyllite, with a limestone unit near the base; Lower Cambrian

Bull formation: Lower Cambrian

(1) *Mettawee facies.* Purple and green slate, mudstone, and phyllite; this facies constitutes the bulk of the formation.

(2) *North Brittain conglomerate member.* An intraformational limestone-pebble, slate-matrix conglomerate

(3) *Mudd Pond member.* A thin but persistent orthoquartzite

(4) *Zion Hill member.* A discontinuous graywacke or sub-graywacke unit ranging from a pebble conglomerate to a mudstone

(5) *Bomoseen member.* A massive, olive-drab, medium-grained graywacke

Biddie Knob formation: a chloritoid-bearing purple and green slate and phyllite with minor beds of limestone and quartzite. Lower Cambrian (?)

The sense of the Lower Cambrian succession is given by load casting and graded bedding in the Zion Hill, and in rare arkoses mapped with the Bomoseen. The sense of succession in the Mount Hamilton group is given by cross-bedding, graded bedding, and by channel filling.

Structurally, the Taconic sequence consists of nested thrust slices subsequently folded together. Although each slice has its own characteristic stratigraphy and structure, correlation of the units, down to the formational level, presents little difficulty. The structure is typified by the Giddings Brook recumbent bottoming fold in the area between the Taconic Range and Lake Bomoseen. The fold is at least 5 miles in amplitude, the movement was east to west, and the axial plane is nearly horizontal. Digitations on this major structure explain the map pattern. Key units of the Taconic sequence have been recognized east of the Taconic Range; the east flank of the Range is now underlain by an inverted sequence of Lower Cambrian rocks.

The Sudbury nappe at the north end of the map area is composed of the Lower Ordovician Chipman formation. The structure does not root in the east limb of the Middlebury synclinorium as reported by Cady, but is a thrust slice, whose southeast edge tucks under the Taconic sequence. Structurally, this unit is part of the latter.

The Whipple marble at the north end of Whipple Hollow is part of the Lower Ordovician Bascom formation, which in this area has been moved westward over the younger black phyllite through a recumbent fold involuted into the Taconic sequence. This structure indicates the persistence of intense deformation after the development of the Taconic structure.

Topologically, the Taconic sequence is in the southward continuation of the Middlebury synclinorium. Coupled with the discovery of the inverted Lower Cambrian rocks east of the Taconic skyline, the evidence supports an allochthonous origin of the Taconic sequence. The gradational contact between the green and black phyllites east of the Taconic Range, and the presence in the black phyllite of beds characteristic of the Taconic sequence show that part of the black phyllite here is allochthonous.

The thrusting is dated as Late Trenton on the basis of exotic blocks of Taconic rocks in an autochthonous black slate at Forbes Hill. Similar rocks have also been found elsewhere at the periphery of the Taconic sequence. The thrusting may have occurred as submarine gravity slides of soft rocks; slump structure is indeed abundant in the Taconic sequence. The intimate mixing of the black slates of the Taconic sequence and of the Trenton mud may make the mapping of the Taconic fault unfeasible even in principle. Continued deposition of black mud after the emplacement of the Taconic nappes could account for the reported Trenton unconformity at the margin of the Taconic sequence south of the Castleton area.

The Taconic sequence probably was deposited in the area of the present Green Mountains. The upper part of the Mount Hamilton group correlates by fossils with the Moretown-Cram Hill formations of eastern Vermont. The Mount Hamilton group

Geological Society of America Bulletin, v. 72, p. 293–338, 7 figs., 5 pls., February 1961

is free of volcanic rocks and is thin, in contrast with the Moretown-Cram Hill formations; this change is consistent with paleogeographical requirements, as the Cambro-Ordovician, typically eugeosynclinal deposits of eastern Vermont, must somehow change into the synchronous, but typically miogeosynclinal deposits of western Vermont and eastern New York.

CONTENTS

INTRODUCTION

The Taconic Range and Berkshire Hills of Vermont and Massachusetts, and the foothills region extending westward to the Hudson River in New York, have been famous in the geological literature because of their great complexities. Since the days of Emmons, Hall, and Dana, geological work here has been marked by a series of controversies. The latest of these debates has been whether the so-called Taconic sequence is autochthonous or allochthonous. The nature and magnitude of the problem were underscored by Keith's hypothesis of a Taconic klippe (1912); he held that the Taconic sequence was brought from the east to its present location by a major thrust—an idea apparently first suggested by Ruedemann in 1909. For nearly four decades this view was accepted by most other workers in this region—

Swinnerton (1922, Thesis, Harvard Univ.), Prindle and Knopf (1932), Rodgers (1937), Larrabee (1939), Kay (1941; 1942), Goldring (1943), Cady (1945), Kaiser (1945), Fowler (1950), and Rodgers, Thompson, and Billings (1952). Within the last decade, however, an increasing number of geologists have opposed this view and hold that the rocks are in fact autochthonous, the supposed fault being reinterpreted by them as a Trenton unconformity (Lochman, 1956; MacFadyen, 1956; Bucher, 1957; Weaver, 1957; Craddock, 1957).

Despite the extensive interest in the origin of the Taconic rocks, much of the region is still

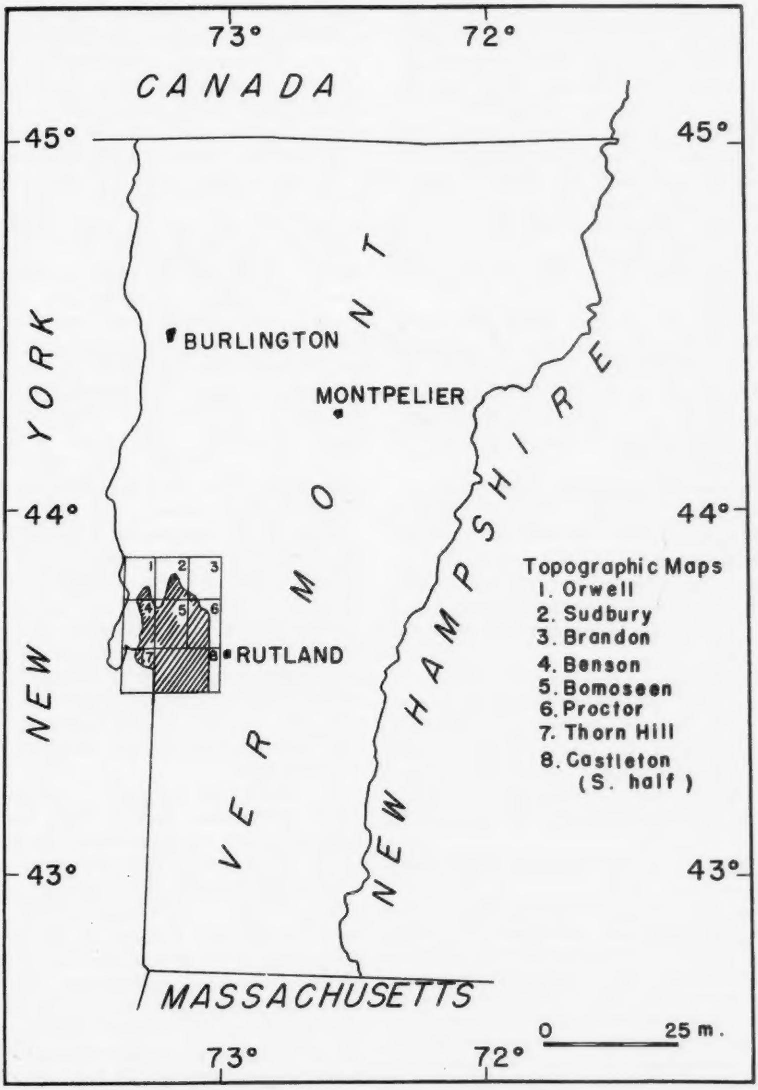

Figure 1. Index Map of the Castleton Area, Vermont

not mapped in detail. The writer, therefore, spent the summers of 1953 through 1957 remapping, in detail, the stratigraphy and structure of the north end of the Taconic region, in the hope of contributing toward a solution of the problem. This particular region was chosen for study because good topographic maps are available; outcrops are generally numerous; and the geology of the immediately adjacent areas is generally understood (Cady, 1945; Osberg, 1952; Rodgers *et al.*, 1952; Brace, 1953). In addition, the area is critically important, in that to the west, north, and east the Taconic rocks, largely argillites, are in contact with a sequence, largely carbonate and orthoquartzite, that is unquestionably autochthonous. Relation with this latter sequence,[1] therefore, affords a two-dimensional control on the geometry of the structure; it was hoped that this might yield clues not available in regions where the formations run in straight, parallel belts.

The map area occupies about 200 square miles in western Vermont and the adjoining parts of New York (Fig. 1). Much of the area is now covered by recent 7½-minute topographic sheets, as well as by U. S. Soil Conservation Service aerial photographs at a scale of approximately 1:20,000.

The area is easily accessible. The major highways include U. S. Routes 4 and 7, Vermont Routes 3, 30, 73, 22A, and 140, and there are numerous local roads. A large part of the area consists of open pastureland; the only sizable forested areas are in the main Taconic Range and in the area between Lake Bomoseen and Route 22A.

The area was covered by traversing, both transverse and parallel to the strike of the units, with Brunton compass and a 50-foot-interval altimeter. The course of a traverse was dictated by local geology. Where the geology is complex, the writer has covered most if not all of the outcrops and traced the key beds in detail.

To aid in the location of topographic features mentioned in the text, a grid system is added to the geologic map. Each rectangle of the grid is a quarter of a ninth of a 7½-minute quadrangle, and after each locality name a number, A-1, etc., is given.

ACKNOWLEDGMENTS

I wish particularly to thank Marland P. Billings and James B. Thompson, of Harvard University, John Rodgers of Yale University, and Wallace M. Cady of the U. S. Geological Survey. These people visited me in the field, discussed numerous problems, and freely contributed ideas. I also thank Tom N. Clifford, of the University of Leeds, for a germane discussion on the structural geology of the area.

The manuscript was read by Billings, Cady, Thompson, Walter H. Wheeler of the University of North Carolina, and Alfred H. Chidester and Walter S. White of the U. S. Geological Survey. Their criticism and comments have resulted in a greatly improved text.

For exchanges of ideas with workers in adjacent areas, I am indebted to Rodgers, Thompson, Marshall Kay, Donald W. Fisher, Donald B. Potter, George Theokritoff, and Robert Shumaker. I also thank F. Fitz Osborne, of Laval University, under whose guidance I visited the problematic rock units of the Quebec City area which have shed much light on the Taconic problem.

Harry B. Whittington of Harvard University, William B. N. Berry of the University of California, and Allison R. Palmer of the U. S. National Museum helped to collect or to identify fossils from the area. G. Arthur Cooper of the U. S. National Museum has spent many hours trying to locate, albeit unsuccessfully, the fossil collection of T. Nelson Dale. The Vermont Marble Company courteously permitted me to study their unpublished drill-hole data.

My special gratitude goes to the Geological Survey of Vermont and the State Geologist, Charles G. Doll, for permission to incorporate, on the geologic map, data from areas which I mapped for the State in the summer of 1958. This is the area south of Castleton River and approximately east of Route 30. Discussion of the geology of this area, as well as presentation of the structural data, however, will be reserved for publication by the State of Vermont. For this reason, the various considerations in the following pages may not specifically apply to this region, although all available data are consistent with the conclusions here arrived at.

[1] Because this autochthonous sequence constitutes the south-plunging Middlebury synclinorium (Cady, 1945, p. 562), it will hereafter be referred to as the "Synclinorium sequence." The term is interchangeable with "valley sequence" as used in the literature (Kaiser, 1945, p. 1096; Fowler, 1950, p. 13; Rodgers *et al.*, 1952, p. 15), but the proposed term emphasizes the fact that the same sequence is found west as well as east of the Taconic sequence, a point of paramount importance in the interpretation of the regional structure.

Parts of three field seasons were made particularly enjoyable through the pleasant and able assistance of Winthrop D. Means, Anthony J. Murray, and David Harwood.

The expenses for the field work were paid for in part by a generous grant from the Penrose Bequest of The Geological Society of America; for this I am grateful. Field work and map preparation were also paid for in part by numerous grants from the Division of Geological Sciences, Harvard University; for these I express my sincere appreciation. An award

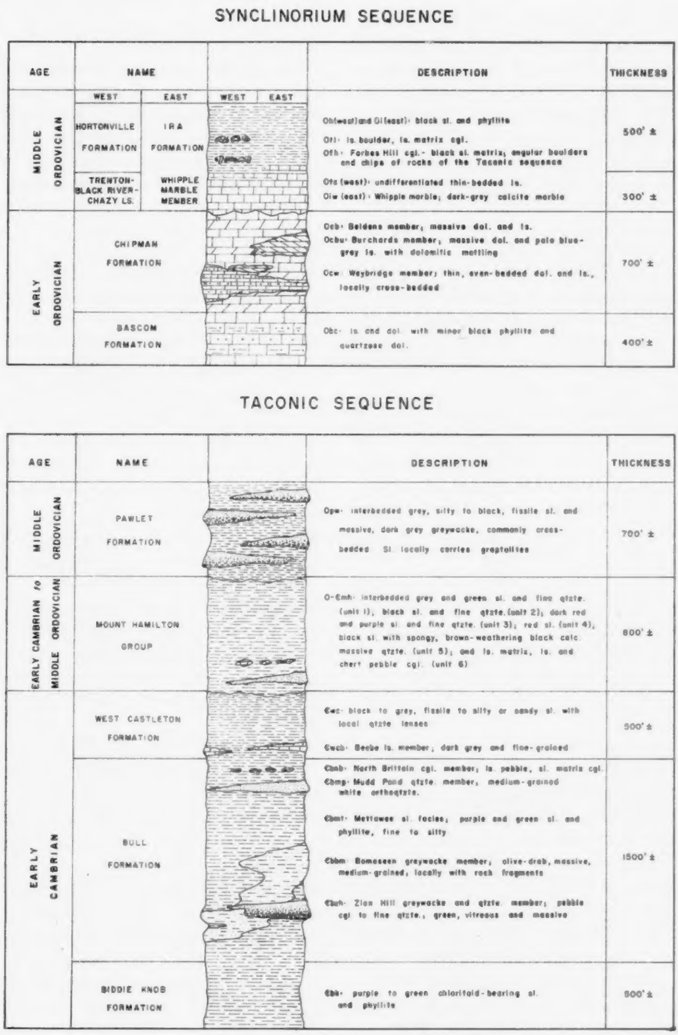

Figure 2. Columnar Sections of the Taconic Sequence and of the Synclinorium Sequence. The Mount Hamilton group of the Taconic sequence is probably the age equivalent of most of the Synclinorium sequence except the Hortonville formation above the Forbes Hill conglomerate.

from the University Research Council of the University of North Carolina has partially paid for the cost of typing.

Finally, I thank the local people of the Castleton area for their warm hospitality.

STRATIGRAPHY

General Remarks

Except for a few post-metamorphic diabasic dikes, all the rocks in the Castleton area are of sedimentary origin. Most of the map area is underlain by clastic rocks, chiefly pelites with subsidiary, but mappable, beds of carbonate rocks and psammites. These units are Early Cambrian through Middle Ordovician. Peripheral to these, to the north, east, and west, is a thick sequence of calcitic and dolomitic carbonate rocks with only minor argillaceous beds. These are Early to Middle Ordovician.

The rocks have undergone low-grade metamorphism so that the argillaceous rocks are now slates or phyllites, and the carbonates are marbles in the eastern part of the area. The original characteristics of the strata are generally preserved, however, so that most of the lithologic features can be referred to original sedimentary features.

During the mapping, a number of key beds have been recognized. These are principally thin but persistent strata with distinctive individual lithologic characteristics and unique composite sequence so that they are of great help not only in correlation and structural

TABLE 1.—CHART OF STRATIGRAPHIC SYNONYMIES IN THE MAP AREA

The units are placed in approximately their age order. Horizontal line indicates the Cambro-Ordovician boundary according to the various authors. Letter symbols in parentheses under column 7 (Dale) are his division designations. Letters not in parentheses indicate equivalent stratigraphic units: (a) capital letters indicate complete synonymies, (b) lower-case letters indicate partial equivalences.

Zen (this report) Cady and Zen (1960)	Swinnerton (1922)	Keith (1932)	Fowler (1950)	Kaiser (1945)	Larrabee (1939)	Dale (1898)
Pawlet formation P		"Black slate" P?				Hudson grit (Ig) P
MT. Hamilton group: Unit 4 N Unit 2 M Units 1 and 3 L Unit 5 G Unit 6		Indian River slate n Poultney River slate L,M,g	Normanskill g,L,M,N,P	Normanskill g,L,M,N,P	Normanskill N,L,M,P	Hudson red and green slate (Irs) N Hudson white beds (Hw) ℓ, m Hudson thin quartzite (Hg) ℓ Hudson shale (G) ℓ m Calciferous (F) ℓ, m Berkshire schist (Sb) A, D
Ordovician						Ordovician
Cambrian						Cambrian
			Zion Hill quartzite C	Zion Hill quartzite C Bird Mtn. grit C	Zion Hill quartzite G	Ferruginous quartzite (E) C, g
				Wallace Ledge formation K, d, a		
W. Castleton formation H and Hortonville formation (in part) h	Hooker slate H	Hooker slate H	Schodack formation H	Schodack formation H	Schodack H	Black slate (D) H
Beebe limestone member F		Beebe limestone F				
Bull formation D: North Brittain conglomerate memb j Mudd Pond quartzite member E, j	Stiles phyllite a, d		Eddy Hill grit J	Eddy Hill grit J Berkshire schist A, D	Eddy Hill grit J	Black patch grit (C) J, c
Mettawee slate facies d	Bull slate d	Bull slate d	Mettawee slate d, a	Mettawee fm. D, a	Mettawee a, d Rowe a, d	Roofing slate (B) D, a
Zion Hill quartzite member C	Barker quartzite C, e	Barker quartzite C, e Hubbardton a, d				
Bomoseen graywacke member B, j		Stiles a, d, f	Bomoseen grit B	Bomoseen grit B	Bomoseen grit B	Olive grit (A) B
	Wallace slate d, K, a	Brezee h	Nassau formation a, b (Including Bird Mountain grit C)			
Biddie Knob formation A						

definition but also in the disentanglement of stratigraphic details—in showing, for instance, whether a given lithologic change is due to lateral facies change or vertical succession. The procedure assumes, of course, that the chosen beds are indeed time-lithologic units. The stratigraphic column and the synonymy of names used in the literature are given in Figure 2 and in Table 1.

Taconic Sequence: Lower Cambrian Units

Biddie Knob formation. The Biddie Knob formation is predominantly a purple or green slate which, by definition, carries chloritoid porphyroblasts. The formation is so named because of the excellent outcrops west and south of Biddie Knob (K-6) in the Taconic Range; according to the present interpretation it is the lowest unit in the geologic column in the map area. The contact between the Biddie Knob formation and the overlying Bull formation is drawn above the highest bed containing chloritoid.

LITHOLOGY: The Biddie Knob formation is predominantly green, gray, or purple, ranging from a soft slate in the western part of the area to a smooth, lustrous phyllite in the Taconic Mountains (H-2 to L-10). The color variations have no time-stratigraphic significance: purple and green varieties pass into each other both along strike and across and seem to reflect original compositional differences that are now reflected in the mineral assemblages:[2] chloritoid-chlorite-muscovite-quartz-rutile; chloritoid-chlorite-muscovite-paragonite-quartz-rutile; chloritoid-chlorite-muscovite-hematite-quartz-rutile; chloritoid-chlorite-muscovite-hematite-magnetite-epidote-rutile. There are also minor beds within this formation devoid of chloritoid.

In a hand specimen, chloritoid is recognized as tiny, dark-green randomly oriented flakes. The proportion and grain size of chloritoid in the rock increases eastward; in some of the relatively high-grade rocks to the east it makes up half the rock by volume. Where abundant, the chloritoid imparts a sandy texture to the rock, which becomes friable. Weathered outcrops are typically rounded and low, and either dull white or rusty gray.

The Biddie Knob formation may in places include other rock types:

(1) Fine-grained, white to green, dull to locally glassy quartzite. The beds are rarely more than a couple of feet, and commonly only a few inches, thick. The beds generally carry chlorite, feldspar, and pyrite, as well as quartz, but no chloritoid. The beds are apparently lenticular and cannot be traced; commonly they are sheared to a confused mass of slivers.

(2) Rare beds of rusty-weathering, white limestone a few inches thick.

AGE: No fossils are found in the Biddie Knob formation in the Castleton area. However, it apparently underlies Lower Cambrian rocks conformably; it is thus probably of Early Cambrian age.

CORRELATION: As defined, the Biddie Knob formation is probably equivalent, at least in part, to the Wallace slate of Swinnerton (1922, Thesis, Harvard Univ., p. 63, 65), which underlies the Barker quartzite, another name for the Zion Hill quartzite. It also can be correlated in part with the Mettawee-Wallace Ledge sequence of Kaiser (1945, p. 1085, 1089), the Mettawee and Nassau formations of Fowler (1950, p. 38, 47), and the Stiles-Hubbardton sequence of Keith (1932, p. 400, 401), but the basis of definition is different, and the correlations are not exact.

The Greylock formation of Dale (1891, p. 5), the Mount Anthony formation of MacFadyen (1956, p. 28), and the chloritoid-bearing beds reported by Balk (1953, p. 841) are lithologically similar to the Biddie Knob formation. Similar rocks have been observed in the intervening area. MacFadyen considers the Mount Anthony formation to be Middle Ordovician, however; until more detailed stratigraphic work is done it is hazardous to attempt a correlation.

ADDITIONAL COMMENTS: Because of the manner in which the formation is defined, the question remains whether it is a time-rock unit or merely a transgressive sedimentary facies. There is also the problem of whether the defining feature—*i.e.*, the presence of chloritoid—is not simply the result of metamorphism, and whether this formation occupies areas of higher metamorphic grade than does the possibly equivalent Bull formation.

The writer considers the Biddie Knob formation stratigraphically significant because (1) its upper contact follows the pattern outlined by other distinct units, such as the Mudd Pond quartzite and the Zion Hill quartzite; (2) with a few exceptions, the over-all stratigraphic se-

[2] The mineralogy and petrology of the rocks in the Castleton area are studied in a separate report (Zen, 1960).

quence is consistent, and in the field it has been possible to predict areas of the Biddie Knob formation by the map pattern; and (3) the nonchloritoid-bearing Bull formation is also present east of the Biddie Knob formation, east of the Taconic Range, even though the metamorphic grade increases eastward. Although the detailed position of the upper contact of the formation may be affected by the varying metamorphic grade, the effect is probably minor.

Bull formation. Swinnerton (1922, Thesis, Harvard Univ., p. 69) proposed the name Bull formation to include all purple and green slates overlying the Barker quartzite; the name is from Bull Hill (H-10) north of Castleton (H-11). Thus defined, the Bull formation is the correlative of the Mettawee of Kaiser and Fowler and is part of the "Cambrian roofing slate" of Dale (1898, p. 178).

The name Bull formation here includes the heterogeneous units between the Biddie Knob formation and the overlying black West Castleton formation. The dominant rock type is the purple and green slate, here for convenience and clarity referred to as the Mettawee slate facies of the Bull formation. It is the "matrix" in which the other members of the formation are set. These members are: the North Brittain conglomerate, the Mudd Pond quartzite, the Zion Hill quartzite and graywacke, the the Bomoseen graywacke (Fig. 2; Pl. 1).

THICKNESS: Because of deformation the true thickness of the Bull formation cannot be determined. The outcrop width of this formation, directly south of Mudd Pond (G-5), is about 0.5 mile; with a representative dip of 30°, this gives a thickness of about 800 feet. This is comparable to the outcrop width just south of Biddie Knob, where the average dip is considerably steeper. A thickness of between 1000 and 2000 feet, however, may be more representative of the area as a whole.

METTAWEE SLATE FACIES: The name Mettawee slate was applied by Ruedemann (*in* Cushing and Ruedemann, 1914, p. 69) to the "Cambrian roofing slate" of Dale (1898, p. 180). As used here, it is dominantly a soft purple and green slate, much like the Biddie Knob formation except for the lack of chloritoid. Consequently, the rock tends to be less friable. In the Taconic Range, this unit is largely a phyllite.

The Mettawee slate also includes several minor rock types:

(1) A medium-grained, hard phyllite, with albite porphyroblasts up to 1 mm and constituting as much as two-thirds of the bulk. It is chiefly green but may be dark gray. On a slightly weathered surface this unit is characterized by minute "pimples" of albite. The unit is discontinuous and is found only along the eastern flank of the Taconic Range near the contact with the adjacent black phyllite into which it grades.

(2) A hard, siliceous, poorly cleavable, green to purple mudstone occurs irregularly in the unit but seems to be best developed low in the Bull formation. Excellent exposures are found near West Castleton (E-9) and in the large tract of the Bull formation east of Castleton.

(3) Rusty-weathering, cream-white limestone beds up to 1 foot thick, commonly confined to the uppermost part of the Bull formation and best developed in the vicinity of Glen Lake (E-9).

The Mettawee slate may also carry numerous

PLATE 2.—SEDIMENTARY FEATURES

Figure 1. Bottom contact of Zion Hill quartzite (graywacke phase) with green slate. "Boulders" are actually load-casting features. West side of peninsula southeast of Float Bridge, east shore of Lake Bomoseen. Looking east

Figure 2. North Brittain conglomerate, showing gradation of "pebbles" into beds of limestone. Road cut on Route 22A, 1.6 miles north of Fair Haven town green. Top of outcrop to right of photograph

Figure 3. Cross-bedding in the West Castleton formation (?). Lamination shown by sandy layers in limestone seam. Top of picture is to the west. East limb of Mount Hamilton syncline in Poultney River, north of Harlow School Road

Figure 4. Mount Hamilton group. Interbedded buff-weathering quartzite and green argillite (unit 1). West bank of Poultney River, north of Harlow School Road

Figure 5. Unit 2 of Mount Hamilton group, showing alternating layers of slate and calcareous quartzite. Cut on Route 22A, 2.0 miles north of Fair Haven town green

Figure 6. Forbes Hill conglomerate. East of Benson Road and northeast of Forbes Hill

FIGURE 1

FIGURE 2

FIGURE 3

FIGURE 4

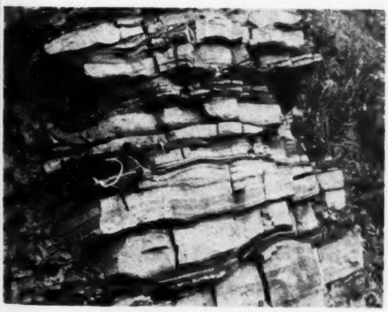

FIGURE 5

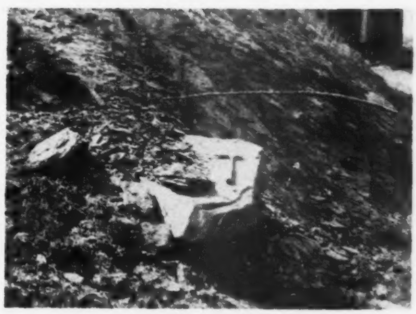

FIGURE 6

SEDIMENTARY FEATURES

Figure 1

Figure 2

Figure 3

Figure 4

Figure 5

Figure 6

STRUCTURAL FEATURES

discontinuous quartzite layers much as does the Biddie Knob formation.

Typical mineral assemblages of the Mettawee slate are as follows (those in parentheses are not everywhere present): muscovite-chlorite-quartz (rutile, calcite, dolomite); muscovite-chlorite-albite-quartz (rutile, carbonate); muscovite-chlorite-hematite-quartz (albite, rutile); muscovite-chlorite-magnetite-quartz (albite, rutile).

BOMOSEEN GRAYWACKE MEMBER: Dale (1898, p. 179) describes an "olive grit" from the Castleton area, which Ruedemann (*in* Cushing and Ruedemann, 1914, p. 69) named the Bomoseen grit for its typical outcrop near Hydeville (E-12), southwest of Lake Bomoseen. Subsequent maps of the area (Larrabee, 1939; Kaiser, 1945; Fowler, 1950) indicate some confusion as to the nature of the unit.

The Bomoseen graywacke is typically hard and poorly cleaved. It is olive gray and weathers white or pale brick red. On a fresh surface flakes of white mica can be seen, aligned parallel to the cleavage. Grains of quartz and feldspar as much as 1 mm across are common, and dark fragments of rocks are found, although rarely. The typical mineral assemblages are: muscovite-chlorite-albite-stilpnomelane-quartz (carbonate, rutile, hematite); muscovite-chlorite-albite-microcline-stilpnomelane-quartz (carbonate, rutile, hematite); muscovite chlorite-albite-microcline-quartz (carbonate, rutile, hematite, biotite?).

At many places, such as east of Route 22A south of Sunset Lake Road (B-6), the Bomoseen graywacke is a well-cleaved slate, grading into the Mettawee slate. Locally, as at Brandon Mountain Road (J-5), it is interbedded with many white quartzite beds, each a few feet thick and lithologically like the Mudd Pond quartzite member. Since this is one place where the two units are close together, the quartzite beds in the Bomoseen graywacke confused the problem of tracing the Mudd Pond member. These quartzite beds are not found interbedded with the Bomoseen graywacke elsewhere.

South of Sargent Hill (I-6 to J-6), the base of the Bomoseen graywacke is a black pebble conglomerate. The pebbles are as much as 5 mm across and show excellent graded bedding; they are chiefly quartz but include feldspar and rare slate fragments, all in an argillaceous matrix. This may be part of the Eddy Hill grit of previous workers.

The Bomoseen graywacke underlies large areas west of Glen Lake. A narrow neck of this rock west of Mill Pond (C-7), previously not recognized, links the main body of the Taconic sequence with that of the Sunset Lake area (C-4). In the latter area, however, the Bomoseen graywacke has not been identified as a traceable unit. The bulk of the slate in the Sunset Lake area is coarse and greenish gray, intermediate lithologically between the Mettawee slate and the Bomoseen graywacke, and grading locally into rocks more typical of either type. This relation is interpreted as a lateral facies

PLATE 3.—STRUCTURAL FEATURES

Figure 1. Recumbent syncline near top of Bull formation. Lighter-colored bands visible along nose of fold are thin limestone seams. Fold is overturned to west and plunges south. Slaty cleavage parallels axial plane of fold. Cedar Mountain quarry, west shore of Lake Bomoseen

Figure 2. Overturned fold of West Castleton formation. Interbedded sandy dolostones show up as dark beds. East shore of Glen Lake near West Castleton, along Scotch Hill Road. Looking north. Immediately to the east and west of the fold are purple and green slates, substantiating stratigraphic succession and sense as given in text

Figure 3. Sudbury thrust fault. Massive Beldens dolostone resting on and truncating thin-bedded Middlebury limestone. South of Route 73, due north of Spooner Hill. Looking northwest

Figure 4. Taconic thrust fault. Bomoseen graywacke resting on Beldens dolostone. Window at William Miller Chapel. Looking east

Figure 5. Cleavage banding, mimicking bedding, in West Castleton formation. True bedding, indicated by color banding, shown by wavy line slanting down from left to right (west-east). Southeast of Hooker Hill, between Hooker and East Hubbardton Roads. Looking north

Figure 6. Disharmonious folds, presumably caused by differences in rock competence. Unit 1 of Mount Hamilton group folded against unit 5. Notice limestone conglomerate in the latter. West bank of Poultney River, north of Harlow School Road. Outcrop is horizontal, and unit 1 is east of unit 5 here

variation in the original sedimentary basin, although the Sunset Lake area is probably a separate thrust slice.

Facies variation may also explain the relations just north of Hampton Hill (A-12) west of Fair Haven, where locally the Mettawee slate is missing between the Bomoseen and the West Castleton formation. Lithological changes here are also gradual. As it lacks marker beds, however, it is difficult to demonstrate extensive facies changes of this sort everywhere.

West of Glen Lake the Bomoseen is stratigraphically below the Zion Hill member. East of this meridian, however, it is above the Zion Hill member. Although the outcrops are not continuous, there is no doubt as to the lithological identity of the Bomoseen graywacke on either side of Glen Lake. Assuming the Zion Hill to be a time-stratigraphic unit, the Bomoseen must be a lithofacies that becomes progressively older, and probably thicker, to the west. West of Lake Bomoseen, the Bomoseen may be in part a facies of the Biddie Knob formation, but even here the Biddie Knob may persist, unexposed, below the Bomoseen graywacke. Such a lowering of stratigraphic position for the Biddie Knob formation, relative to the Zion Hill, is indeed suggested by the increase in distance between these two units from the Taconic Range westward to Lake Bomoseen.

West of Glen Lake the Bomoseen graywacke is the lowest unit exposed, and its thickness cannot be determined. South of Ganson Hill, the Bomoseen is probably no more than 400 feet thick. North of Mudd Pond, on the normal limb of the Ganson Hill syncline, the graywacke appears to be thicker but even here is probably no more than 1000 feet.

ZION HILL QUARTZITE AND GRAYWACKE MEMBER: The Zion Hill member of the Bull formation corresponds to the "ferruginous quartzite" of Dale (1898, p. 183) and was named by Ruedemann (Cushing and Ruedemann, 1914, p. 70) after Zion Hill (I-8). It is the Barker quartzite of Swinnerton (1922, Thesis, Harvard Univ.) and Keith (1932). Both type localities are in the Castleton area, but Zion Hill has priority, is better known, and is therefore retained.

The Zion Hill quartzite is considered a member in the Bull formation for several reasons. It occurs within (generally near the base of) the Mettawee slate. It is not a continuous unit, and so it is not feasible to map identical rocks on either side of it separately. Whether all Zion Hill quartzites and graywackes are contemporaneous or whether they are merely lenses (channel fillings?) staggered in a general zone of the Bull formation cannot be resolved at this time.

About $1\frac{1}{2}$ miles north-northwest of Biddie Knob, two large lenses of the Zion Hill member, here a graywacke, occur near the top of the Biddie Knob formation. The Biddie Knob-Bull contact may transgress, slightly, the surface defined by the Zion Hill member. Such a relationship, however, is exceptional in this area.

The Zion Hill member is predominantly a massive, green to grayish-green, vitreous, chloritic quartzite but ranges to graywacke. Besides chlorite and quartz, the rock contains much muscovite, alkali feldspars, pyrite now altered to limonite, and rare graphite flakes. The rock weathers to a rough surface but is glistening white at a distance. Grain size varies considerably. The base of the rock is commonly a conglomerate, at places a few feet thick and interbedded with the Mettawee slate. The conglomerate contains pebbles of slate, limestone, and fresh, angular crystals of feldspar, quartz, and muscovite. The pebbles may be up to 3 inches across but more commonly are less than a quarter of an inch. Most of the rock is massive and contains well-sorted quartz grains, and minor feldspar. Graded bedding is not uncommon. The highest beds are locally fine-grained and grade into a mudstone, as is well displayed at Wallace Ledge (H-8) and Page Point (G-9).

The bottoms of the conglomerate beds are hummocky, so that the rock might be mistaken for a coarse boulder conglomerate. These hummocky surfaces, however, are actually due to load casting and scour-and-fill and as such are useful in determining tops of beds (Pl. 2, fig. 1).

ZION HILL MEMBER

Locality	Thickness (Feet)
Zion Hill	20–200 (p. 82)
Wallace Ledge	*ca.* 50 (p. 85)
Front Ridge (I-8) (eastern continuation of Wallace Ledge)	70 (p. 90)
Barker Hill (I-9)	60 (p. 92)
Crystal Ledge (780-foot hill; H-9)	*ca.* 40 (p. 99)
1234-foot hill, near E. Hubbardton (J-6)	40 (p. 104)
S. end of peninsula, southeast of "Float Bridge" (G-8)	*ca.* 80 (p. 105)
Flint Hill (690-foot knob, E-9)	60 (p. 115)

The Zion Hill member ranges widely in thickness within a few hundred feet. Taped sections of this competent, and therefore presumably little thickened or thinned, unit have been given by Swinnerton (1922, Thesis, Harvard Univ.) as shown in the tabulation.

Larrabee (1939, p. 51) correlates the Zion Hill member with a quartzite at Hampton, New York (D-15) and suggests that it be assigned to the Ordovician. There is no valid lithologic basis for the correlation inasmuch as the quartzite at Hampton is a dark-gray, calcareous, clean quartzite, weathering brown and punky, totally unlike the typical Zion Hill quartzite and graywacke.[3] Its stratigraphic position, above a black slate which in turn rests on a green slate, also belies the correlation.

The writer confirms the correlation of the Bird Mountain (K-12) grit with the Zion Hill member, suggested by Swinnerton (1922, Thesis, Harvard Univ., p. 196), Keith (1932, p. 401), and Kaiser (1945, p. 1090) on the basis of lithologic resemblances and stratigraphic succession. Details of this area, however, will be presented in a separate report.

Lochman (1956, p. 1336) points out that the Eagle Bridge quartzite, correlated by Prindle and Knopf (1932, p. 277) with the Zion Hill, may be Ordovician. The Eagle Bridge is also lithologically quite different from the Zion Hill. On the other hand, the writer suggests correlating the Zion Hill and the grits within the "Nassau" formation near Ashley Hill, Kinderhook quadrangle, New York (Dale, 1904b, p. 23; Balk, 1953, p. 831; Craddock, 1957, p. 694). These two units are lithologically similar, and at Ashley Hill also the grit or graywacke occurs within the purple and green slates which are capped by a slate-matrix limestone conglomerate, bearing an Early Cambrian *Elliptocephala* fauna (Dale, 1904b, p. 22; Balk, 1953, p. 831; Lochman, 1956, p. 1340; Craddock, 1957, p. 694); this conglomerate, in turn, is succeeded by a black slate unit. The sequence is much the same as in the Castleton area.

MUDD POND QUARTZITE MEMBER: The name Mudd Pond is proposed for a quartzite found within about 100 feet of the top of the Bull formation; excellent outcrops of this unit may be seen at the type locality, Mudd Pond (I-5).

The Mudd Pond quartzite is hard, vitreous, buff to gray, uniform and medium-grained; quartz is its predominant constituent. Locally the rock has a slightly dolomitic cement and may carry brown, punky-weathering dolostone lenses (concretions?) up to 1 foot across. The quartzite weathers white to buff and smooth, with a waxy luster. Locally the quartzite grades into a gray arkosic grit, with black argillaceous cement. Thus the Mudd Pond quartzite may be in part equivalent to the "Eddy Hill grit" (Larrabee, 1939, p. 51; Kaiser, 1945, p. 1086). The type Eddy Hill[4] grit, indeed, occupies the stratigraphic position of the Mudd Pond member.

The Mudd Pond quartzite is well exposed near Ganson Hill (I-5) where it outlines the structure. West of Glen Lake it occurs around belts of slates of the West Castleton formation, and fresh surfaces are typically dark gray. Within the Pine Pond (G-10) thrust slice, it is found only along Eaton Hill Road (H-9 to I-10) and south of Bull and Hooker hills. East of the crest of the Taconic Range typical Mudd Pond quartzite occurs south of Biddie Knob and on the 2034-foot knob (K-6) to the north, not far from the black-phyllite contact.

The Mudd Pond quartzite is 6 to 20 feet thick but commonly about 10 feet thick. Near the southeast end of Ganson Hill Road (I-5), this quartzite occurs as two beds, each about 6 feet thick, separated by about 20 feet of green slate. These beds are not mapped separately.

NORTH BRITTAIN MEMBER: This name is proposed for a slate-matrix, limestone-pebble conglomerate, which forms an excellent marker bed, principally near or at the top of the Bull formation, although locally at the extreme west side of the map area it is just above the bottom of the West Castleton formation. Wherever the two are found together, it lies immediately above the Mudd Pond quartzite. The name refers to its excellent outcrops along North Brittain brook (I-10 to J-9) in the town of Castleton.

The North Brittain conglomerate commonly contains poorly sorted pebbles of limestone in a green to gray slaty, noncalcareous matrix; the ratio of matrix to pebbles varies. The pebbles in a given outcrop range from a quarter of an inch to 3 feet across and are dominantly either dark-gray limestone weathering dove gray, or white to creamy limestone weathering buff. South of Graham Hill (G-11), salmon-colored, hematitic limestone pebbles are abundant in a purple slate matrix, and south of Hooker Hill

[3] Dale (1904a, p. 187) made a similar error in correlating some quartzites at the north end of the map area.

[4] Eddy Hill is not shown on the topographic maps nor is the name now known to local inhabitants. Its location is obtained through a label on one of Dale's fossil collections (USNM 193z), which gives also a station no. 371; this was found on Dale's field map, now in the U. S. Archives. Eddy Hill, thus located, is the 650-foot knob (D-12) just outside the southeast corner of the village (not town) of Fair Haven, shown on the geologic map as underlain by the West Castleton formation.

pebbles of buff-gray lithographic limestone are found.

Rarely, for example in the outcrop 0.5 mile southeast of Beebe Pond (H-5), the matrix is a dark-gray arkose like the Eddy Hill grit.

In the quarries in West Castleton, at Cedar Mountain (F-9), and along Scotch Hill Road (E-9 to E-10), near the top of the Bull formation a unit of gray limestone seams, each a few inches thick, is embedded in black slate. The limestone seams are commonly brecciated and simulate a conglomerate. It raises the possibility that many of the pebbles in the North Brittain conglomerate, throughout the area, represent locally fragmented and rounded limestone seams, formed penecontemporaneously with the matrix. This hypothesis is strengthened by these facts: (1) many of the pebbles are lithologically like the buff-weathering limestone beds occurring near the top of the Bull formation, for instance near Glen Lake; (2) locally, for example northeast of Hooker Hill and on East Hubbardton Road (I-10 to J-9) southeast of Hooker Hill, beds of limestone are found in the conglomerate; and (3) in the Poultney River bed (B-11 to H-16) west of Fair Haven (D-12), and again in cuts along Route 22A 1.6 miles north of Fair Haven (Pl. 2, fig. 2), the North Brittain member shows all gradations between good limestone beds and limestone pebbles.

The North Brittain conglomerate ranges from only 1–2 feet thick, as in the Poultney River bed west of Fair Haven, to more than 20 feet as on the cliff at Hooker Hill. Because bedding is poorly developed, the thickness is difficult to determine; there is also doubtless considerable tectonic thinning and thickening in addition to primary sedimentary lensing.

Schuchert (1937, p. 1039) reports Early Cambrian fossils from this unit at West Castleton: *Obolella crassa*, *Hyolithellus micans*, and *Eodiscus speciosus*. *E. speciosus* is also found in the slate quarry at Cedar Mountain, where the limestone pebbles are definitely brecciated beds, so the Early Cambrian age must also apply to the enclosing matrix. Since the North Brittain conglomerate is the highest member of the Bull formation, this age must apply, as an upper limit, to the formation as a whole. The dating agrees with the Early Cambrian age assigned to the fossils in the overlying West Castleton formation, as well as with the Early Cambrian age of the fossils from the green slates farther south in the slate belt, recently restudied by Lochman (1956).

West Castleton formation. The West Castleton formation is predominantly a black slate or phyllite. The name refers to its characteristic outcrops just south of the village of West Castleton, along Scotch Hill Road, where fossils of Early Cambrian age are found. It is the Hooker formation of Swinnerton (1922, Thesis, Harvard Univ., p. 74) and Keith (1932, p. 402). The type locality of the Hooker, however, is unfossiliferous, and therefore its stratigraphic position cannot be established. It is also Dale's Cambrian black slate (1898, p. 182), to which the name Schodack was later assigned (Ruedemann, *in* Cushing and Ruedemann, 1914, p. 70; Fowler, 1950, p. 50), probably incorrectly (Theokritoff, 1957).

LITHOLOGY: The West Castleton formation ranges from a dark-gray, hard, poorly cleaved, sandy or cherty slate that weathers white or pale red to a jet-black, fissile, graphitic and pyritic slate that contains many paper-thin white sandy laminae and commonly also black cherty nodules, and when weathered displays much alum bloom. Locally interbedded in the fine black slate are beds of buff- to yellow-weathering black dolostone or dolomitic quartzite, a few inches thick, some of which, however, become massive, siliceous, and heavily bedded in the harder black slate. The varieties of black slate do not form mappable units but grade into each other along strike. In open pastures the soft, fissile type is commonly concealed, whereas the siliceous type may stand out as low, rounded bumps. In the eastern part of the map area, and especially east of the Taconic Range, the rock is a phyllite. Typical mineral assemblages are muscovite-chlorite-quartz-graphite (rutile, biotite); muscovite-chlorite-albite-quartz-graphite.

Other rock types included in the West Castleton formation are as follows:

(1) A black, fine-grained, massive limestone, weathering dark gray and abundantly crisscrossed with calcite veins, Keith's Beebe limestone (1932, p. 402), occurs near the base of the formation. It may be as much as 20 feet thick, but it is commonly absent. This unit is here designated the Beebe limestone member of the West Castleton formation.

(2) A black, pebbly conglomerate, with scanty, slate matrix. The pebbles, less than a quarter of an inch across, are largely quartz and feldspar. The unit is discontinuous and occurs in the lower part of the formation. Typical examples may be seen in the pasture at 580-foot elevation northeast of Hooker Hill and east-

southeast of the 922-foot knob (H-10); just west of Murphy Road (H-8), south of the sharp 670-foot knob; and at 840 feet elevation in a small gully about a quarter of a mile due northwest of the East Hubbardton cemetery (K-7). This rock is similar to Fowler's Eddy Hill grit (1950, p. 49) east of the main road (Route 30) between Poultney (E-16) and Castleton Corners (F-11).

AGE: The following Early Cambrian fossils have been reported by Swinnerton (p. 77–79) from the Beebe limestone within the map area:

Olenoides fordi Walcott (free cheek) from Brown farm 1 mile northeast of Castleton Corners ;(the locality is referred to as "Sunset Hill," which is the 650-foot hill on the Castleton topographic sheet. G-11)
Atops trilineatus Emmons (glabella) and
Elliptocephalus (thoracic segment) from Davis farm 1¼ miles northwest of Wallace Ledge
Lingulella or *Obolella*, ½ mile east of Fair Haven
Protospongia spicules and fragments of *Olenellus* (?), on top of hill by Twin Lakes (Keeler Pond, H-5, and Beebe Pond).

Swinnerton also reports that he saw one glabella of *Olenellus* by the roadside cliff south of Glen Lake. These last two localities have also been reported by Schuchert (1937, p. 1039).

Fowler (1950, p. 52–53) lists two more Early Cambrian localities, 1¼ miles southeast of Blissville (E-12) and in Poultney River half a mile northeast of Hampton, New York. The writer found fossils in the Beebe limestone at a low road cut on Scotch Hill Road, at the junction with the dirt road leading to O'Brien Point (E-9) on Glen Lake. The road cut is now obliterated by road widening. A. R. Palmer (letter, April 9, 1958) identified these as probably *Acrotreta saggitalis taconica* or a closely related form (1 pedicle valve, 1 brachial valve) and *Kutorgina* (?). An Early Cambrian age is thus confirmed.

Relation between the Bull and the West Castleton formations. The separation of the West Castleton formation from the Bull formation is based on a color change in the slates. Using the Beebe limestone and the North Brittain conglomerate as reference planes (assuming these to be parallel), the West Castleton–Bull contact undulates in the western part of the map area. In the abandoned quarry on Scotch Hill Road, on the Benson sheet, the lowest bed of Beebe limestone is actually within the green slate, although only a few feet below the contact with the black slate. On the cliffs southeast of Cobble Knoll (D-8) and north of the gully, the Mudd Pond quartzite is within the black slate a short distance above the black–green contact; the limestone conglomerate is entirely in the black slate. Thus, relative to the quartzite and the conglomerate, the base of the West Castleton formation is lower here than in the area east of Lake Bomoseen, comparable with the relation between the Zion Hill quartzite and the Bomoseen graywacke.

Order of succession of the Cambrian stratigraphic units. As most of the Lower Cambrian formations are unfossiliferous, it is imperative that good sedimentary-tops sense be established. The most compelling arguments for the given sense to the section follow.

(1) The bottom of the Zion Hill quartzite is commonly conglomeratic and shows scour-and-fill features against the underlying slate. Southeast of the "float bridge" (G-8) it gives a tops-east sense (Pl. 2, fig. 1). The top of the quartzite is locally a fine siltstone interbedded with sandy green slate. This is shown at Page Point and gives a tops-west sense; this is supported by graded bedding as well as by drag folds. These two quartzite bands on opposite shores of Lake Bomoseen define an overturned anticline plunging and closing to the south. The east limb dips conformably under the West Castleton formation. The west limb of this anticline is the east limb of a south-plunging recumbent syncline, the axis of which is exposed at Cedar Mountain quarry; this syncline opens southward at Neshobe Island (F-9) to include black slate of the West Castleton formation.

(2) On the south slope of Sargent Hill (J-6), the base of the south-dipping Bomoseen graywacke is a black pebbly grit showing graded bedding. The beds are right side up.

(3) Graded bedding in the Zion Hill quartzite at Crystal Ledge (780-foot hill; H-9), at Wallace Ledge, at Zion Hill, and at the 1234-foot hill east of Sargent Hill indicates that the quartzite is younger than the Biddie Knob formation and older than the West Castleton formation. At Flint Hill (690-foot knob, E-9) the quartzite is above the Bomoseen graywacke but below the West Castleton formation.

(4) In Poultney River north of the road from Fair Haven to Harlow School, the east limb of a syncline is exposed. Near the contact with the Bull formation, the black slate of the West Castleton formation (?) shows delicate cross-bedding at several places (Pl. 2, fig. 3); abundant graded bedding and channel filling

are found in the overlying quartzites of the Mount Hamilton group. All these primary structures give a consistent tops-west sense to indicate that the syncline is normal and that the West Castleton (?) formation and the Mount Hamilton group are indeed stratigraphically above the Bull formation.

Other occurrences of cross-bedding, all supporting the present tops sense, are in the thin dolomitic quartzites interbedded with black slate of the Mount Hamilton group. Two localities are:

(1) At 450-foot level on the west side of the 530-foot knob just south of Sheldon Road (C-10), in the woods immediately east of open pastures.

(2) At 940 feet, in an open valley northeast of the 990-foot knob, 1500 feet west of the Pinnacle (D-3) near Choate Pond (D-3).

Structural arguments for the same tops sense will be presented in a later section.

Taconic Sequence: Post-Lower Cambrian Units

Mount Hamilton group. The Mount Hamilton group is a lithologically heterogeneous unit yet of such close stratigraphic association that the various types can be mapped together. The name group is preferred, because additional work in adjacent areas shows that the unit is separable into formations. The group is named after the excellent section on Mount Hamilton (C-10) north of Fair Haven.

LITHOLOGY: Six rock types are included in the Mount Hamilton group:

(1) The most common is a green or grayish-green, very fine-grained argillite, commonly interbedded with a slightly calcareous, fine-grained quartzite at intervals of about 1 foot. The quartzite weathers buff to brown and stands out in relief (Pl. 2, fig. 4). It is commonly cross-bedded or shows channel filling and/or graded bedding against the underlying strata. The argillite weathers to an opaque white coating which is probably responsible for Dale's term "Hudson White Beds" (1898, p. 185). Thin layers of differing composition, indistinct on a fresh surface, tend to weather into bands of sharp color contrast. Although the rock looks cherty, the typical mineral association is quartz-alkali feldspar (microcline; less commonly albite)-chlorite-muscovite (plus carbonate locally), not very different from a typical shale.

Rock unit 1 is well developed in the Mount Hamilton (C-10)–Poultney River section and also occurs in the Ganson Hill area, south of Glen Lake, and southwest of Gorhamtown (H-13). It is largely Keith's Poultney slate (1932, p. 403).

(2) A dark-gray to sooty-black, "cherty" looking, siliceous argillite, commonly with a glazed appearance. It is also interbedded with thin, brown-weathering quartzite (Pl. 2, fig. 5) and itself weathers white. Except for the color it is much like unit (1). It is well developed in the Mount Hamilton syncline and is exposed in the Poultney River section, northwest of unit (1).

(3) A deep-red to purple, hard argillite which, in addition to its color, differs from unit (1) in that the quartzites (generally less than 1 inch thick) in it weather white to green, rather than buff (Dale's Hudson thin quartzite, 1898, p. 186). The argillite also weathers into a thick opaque white coating. Although it locally appears cherty, its mineral association is like that of unit (1) with hematite added. It differs from the purple Mettawee slate in its weathering, in being much harder and less well cleaved, and in its stratigraphic succession. This rock occurs on the 830-foot knob (C-10) west of Mount Hamilton and to the west; it forms the core of the syncline. It also occurs at the south end of the synclinal ridge, immediately east of the 424-foot BM (E-10) on Scotch Hill Road, and in the area east of East Poultney (G-15).

(4) A purplish-red to vermillion, soft slate, with interbedded thin green quartzites. On weathered surfaces it is dull red. The rock is weak, and outcrops are poor. Mineralogically it differs little from unit (3) except possibly for its lower quartz content. In the map area, it occurs southwest of Gorhamtown. This rock unit is Keith's (1932, p. 403) Indian River slate.

(5) A massive, dark-gray calcareous quartzite, which on a fresh surface glistens with rounded quartz grains, generally well sorted and less than half a mm across; the quartzite is interbedded with black slate like that of unit (2) and upon weathering becomes red brown, loose and spongy, ribbed with thin white quartz veins. Individual beds range from a few inches to 10 feet thick. Graded bedding is locally found near its base. At places—for instance in the road cut on Route 22A near Hampton, New York, and in the Poultney River bed—the base of this quartzite is an edgewise limestone conglomerate or breccia, with dove-gray-weathering, angular to subrounded pebbles as much as several inches across embedded in the brown-weathering

quartzite matrix (Pl. 3, fig. 6). Other excellent examples of this rock may be seen (1) on the south slope of Signal Hill (H-3) near Sudbury (G-2), and (2) in the woods south of Eagle Rock (H-5) at the west end of Ganson Hill.

This quartzite presents many baffling problems. Although it occurs in black slates mapped as Mount Hamilton group, similar rocks might occur within the West Castleton formation. The problem is augmented by the apparent local transition of the Mudd Pond quartzite, northeast of Inman Pond (C-10), into a similar rock through the addition of an iron-rich calcite.

The quartzite does not carry fossils in the map area. The Eagle Bridge quartzite (Prindle and Knopf, 1932, p. 277) may be Ordovician and has the same appearance. On the other hand, the Diamond Rock quartzite of Lansingburgh, New York, also similar, has fossils of Early Cambrian age (Donald W. Fisher, 1956, oral communication)*. It thus appears that there are at least two similar rock units and sequences of different ages.

(6) A limestone conglomerate in a dove-gray, and gray-weathering limestone matrix. The pebbles, which constitute the bulk of the rock, are rounded to subrounded, range from a fraction of an inch to several inches across, and include at least four lithologic types: gray limestone, gray limestone with thin sandy layers, sandstone, black chert. In the map area, the rock occurs in the synclinal ridge extending south-southwest from West Castleton, on either side of unit (3); another locality is an isolated outcrop 0.5 mile north of West Castleton, just east of Moscow Road (E-9 to F-7), in the same syncline. Lithologically, this unit resembles that in the brook north of Bald Mountain near Schuylerville, New York, correlated by Rodgers *et al.* (1952, p. 49) with other similar conglomerates bearing Deepkill fossils. No fossils are found in the present area, however.

RELATIONSHIPS OF THE ROCK TYPES: The relative positions of the six rock types at the areas of outcrop north of Castleton River are tabulated, with the oldest rocks at the bottom, wherever the relative ages are known. The other areas will be described in a later publication.

Although unit (5) may occur at several levels, it is generally the lowest unit. Units (1) and (3) seem to be lateral equivalents. Unit (6) is definitely below (1) and (3), but its relation to (5) is not established. The relation of (4) to the others will be considered in another report.

DISTRIBUTION: The black argillite (2) greatly resembles some of the Lower Cambrian West

Ganson Hill	*Scotch Hill*	*Mt. Hamilton*	*Poultney River west of Fair Haven*	*Sunset Lake area*
			Unit 2	
		Unit 2	Unit 5	
Units 1 and 2	Units 1 and 3	Units 1 and 3	Unit 1	
Unit 5	Unit 6	Unit 5	Unit 2	Unit 5
	(intermittent)			

Castleton formation, and the boundary is at many places arbitrary. Thus the distribution of the Mount Hamilton group may be more extensive than is mapped, but without fossils this point cannot be settled.

AGE: Paleontological and stratigraphic evidence from adjacent areas establishes the Mount Hamilton group as of Late Cambrian to Middle Ordovician age (Berry, *in* Zen, 1959). In the areas to the south, subdivision of the group into distinct formations has also proved feasible. This problem will be considered in another paper.

Pawlet formation. The name Pawlet formation (Shumaker, 1960, Thesis, Cornell Univ., p. 38) is here published for the first time and refers to a thick sequence of interbedded silty to fissile slate and graywacke beds, of Middle Ordovician age and overlying all other units of the Taconic sequence. These beds are Dale's Hudson grits (1898, p. 187) and have been mapped as Normanskill by Fowler (1950).

LITHOLOGY: The Pawlet formation consists, in the present area, of roughly equal amounts of slate and graywacke; the base of the formation is everywhere a slate. The slate ranges from silky gray and silty to jet black, graphitic and pyritiferous; these types do not seem to have stratigraphic significance. In places the jet-black and fine-grained slate is graptoliferous. At intervals of a few inches to tens of feet are beds of massive graywacke which is dark gray on a fresh surface but weathers rusty gray

* *Note added in proof:* For published reference to the age of the Diamond Rock quartzite, *see* D. W. Fisher, 1956, The Cambrian system of New York State: XX Internat. Geol. Cong., The Cambrian system, v. 2, pt. 2, p. 321–351 (especially p. 331).

brown. The graywacke ranges from a few inches to 6 feet thick. It contains subangular grains of quartz, with subsidiary feldspar and slate fragments, in a gray argillaceous matrix which is locally slightly calcareous. The graywacke commonly shows graded bedding and in the present area gives a right-side up sense to the Pawlet formation.

Because of an important regional unconformity within the present area the Pawlet formation unconformably rests on the Bull formation, the West Castleton formation, and the Mount Hamilton group. No direct contact between the Pawlet formation and the Biddie Knob formation has been found.

AGE: Within the map area, the only locality that yields fossils from the Pawlet formation is about 500 feet south of the bridge at East Poultney, on the east side of the paved road. This locality, first found by W. B. N. Berry, carries *Nemagraptus gracilis* and other forms characteristic of the *Climacograptus bicornis* zone (Berry, *in* Zen, 1959, p. 62, and Table G-1; also oral communication). Similar forms are abundant in this unit in the Pawlet quadrangle (Shumaker, *in* Zen, 1959, p. 59). The Pawlet formation is thus of Normanskill age and may be equivalent to the Black River beds of the carbonate sequence (Twenhofel *et al.*, 1954).

Problems relating to the Pawlet formation will be discussed in detail in a later publication.

Synclinorium Sequence: Beekmantown Group

Bascom formation (Cady, 1945, p. 542). The Bascom formation is a heterogeneous group, consisting principally of thin beds of white to gray marble with thin white siliceous or black phyllitic partings. Also abundant are brown-weathering, dark, calcareous sandstones, a few inches to several feet thick, which stand out on a weathered surface, as well as massive, dove- to dark-gray, dense dolostone beds as much as several feet thick. These dolostone beds weather creamy white to reddish and present a craggy surface; they may contain abundant calcite or quartz veins. Locally snow-white and massive marble beds exist, as well as gray marble with abundant clots of dolomite that appear mottled on weathered surfaces (Cady, 1945, p. 544). The Bascom grades upward into the Chipman formation.

A particularly significant rock type is a massive, homogeneous, coarse gray marble, with darker gray streaks, and rarely siliceous or phyllitic partings, that occurs on the main east limb of the Middlebury synclinorium, about 1.5 miles south of the Brandon–Proctor quadrangle boundary, as well as farther south along the strike. It is identical with the marble mapped by Fowler (1950) as Whipple marble at the north end of Whipple Hollow (L-7 to N-10). Fowler (1950, p. 33–34) supposes the Whipple marble to be Glens Falls equivalent and to be interbedded with the Hortonville black slate of Trenton age. However, these particular marbles contain the thin and massive dolostone beds and siliceous partings, characteristic of the Bascom formation; the writer therefore suggests that they are actually part of the Bascom. Structural evidence also indicates that these marble patches are parts of the Bascom formation.

Within the Bascom marble and in direct contact with the black slate is locally a thin-bedded, fine-grained black limestone. Whether this is a limestone of Chazy–Trenton age ("Whipple") or a lithologic variant in the Bascom formation cannot be determined.

The age and faunal relationships of the Bascom formation have been discussed by Cady (1945). The patch of "Whipple" marble, now reinterpreted as Bascom, east of Biddie Knob, contains abundant fragments of crinoid or cystoid stems. Identical fossils are also abundant in similar rocks at the following localities, all in the east limb of the Middlebury synclinorium:

(1) At 600 feet elevation, north slope of 690-foot knob (M-6), 1 mile northwest of Smith Pond (M-6), Florence (N-6) (first noticed by W. M. Cady in the company of the writer).

(2) At 420 feet elevation, in the ledge west of dirt road three-quarters of a mile south of Arnold School (K-1), Brandon (M-2). Here fossils occur abundantly in thin layers.

(3) On the 440-foot knob (K-2) immediately west of the same dirt road, just north of Route 73 (road between Brandon and Webster School, G-1). The fossils are found in a unit immediately above, and west of, the fossiliferous Bascom zone 1; it is therefore presumed to be zone 2.

(4) At 490 feet elevation on the middle knob of Halls Island (K-2), at the junction of the 7½-minute Brandon and Sudbury topographic sheets.

Chipman formation (Cady and Zen, 1960). The name Chipman formation is proposed by Cady and Zen to include the Beldens (Cady, 1945, p. 550), the Weybridge (Cady, 1945, p.

550), the Bridport (Cady, 1945, p. 545), and the Burchards (Kay and Cady, 1947, p. 601) as members. Details of lithologic characteristics and stratigraphic relationships, as well as paleogeographic implications, are discussed by Cady and Zen.

Within the map area, the Synclinorium sequence contains all except the Bridport member of the Chipman formation. The Weybridge member at many places shows channel filling and cross-bedding. Near Willow Brook School (I-3), these features consistently yield a tops-south sense and indicate a normal sequence. The Chipman formation overlies the Bascom conformably and in turn underlies Middle Ordovician limestones. In the Sudbury thrust slice (fig. 3), however, only the Beldens member occurs. A band of the Beldens also occurs south of the Weybridge member near Willow Brook (I-3 to I-4), dipping south under the black slate of the Taconic sequence. This belt may be in the autochthone, but might also be part of the Sudbury slice re-emerging from under the slate and lying pseudoconformably on the Weybridge member. In the field, no structural discordance has been found along this line.

Patches of Beldens member occur near the Turnpike School (B-10) in West Haven town; Beldens and fossiliferous Weybridge limestones also occur southwest of Johnson Pond (F-4; Cady, 1945, Pl. 10; 1959, letter).

In the map area, cystoid or crinoid stems have been found in the Weybridge member of the Chipman formation on the west side of the 430-foot knoll (J-1) three-quarters of a mile south-southwest of Arnold School, immediately east of the railroad tracks; and on the most northeasterly of four 620-foot prominences just southeast of Willow Brook School (I-3).

Synclinorium Sequence: Carbonate Rocks of Chazyan, Black River, and Trentonian Age

To this group of carbonate rocks belong the Middlebury, the Orwell, and the Glens Falls formations (Cady, 1945; Cady and Zen, 1960), as well as portions of the Whipple marble (Fowler, 1950). The rocks contrast strongly with the Bascom–Chipman sequence in that they are dark gray, fine-grained, and commonly thin-bedded; locally they have black phyllitic partings or brown-weathering thin dolomitic layers. They are all post-Canadian in age. East of the Taconic sequence, in Whipple Hollow, these rocks occur either at the base of, or interbedded with, the basal strata of the black phyllite of the Ira formation; they are accordingly designated on the map as the Whipple marble member (Oiw) of the Ira formation. West of the Taconic sequence, the beds are mapped as undifferentiated Chazy-Black River-Trenton limestone (Otc).

The stratigraphic relations and age problem of the Whipple marble are complex; they will be discussed in detail in a later publication.

In the east limb of the Middlebury synclinorium, the Chipman formation locally appears to grade upward into the younger limestones. The relations are best seen on the slopes of Bald Hill (I-1) and the 641-foot hill west of it (H-1). However, the contact can be easily drawn, just above the highest of the massive dolostone beds that characterize the Chipman. In this area, both the Chipman and younger carbonates are discordantly overlain to the south by black slate assigned to the Hortonville formation; whether the relation represents an unconformity or a thrust fault is not clear. The entire sequence is in turn truncated by the Sudbury thrust, whose trace is mapped just south of School No. 1 (H-1).

Limestones of the Chazy-Black River-Trenton sequence occur near Hyde Manor (G-3), where they dip under the Chipman beds of the Sudbury thrust slice. The beds are at least in part Glens Falls in age, for in a road cut on Route 30 near the north end of Lake Hortonia (F-5) the guide fossil *Cryptolithus tesselatus* is abundant.

Extensive areas of similar limestones occur west of the slate belt, between Route 22A south of Sunset Lake Road and West Haven. Between Mill Pond and Howard Hill School (C-6), Cady (1945) mapped these limestones as Glens Falls.

Surrounded by black Hortonville slate in the area between Lake Hortonia and Black Pond (F-7) are a number of isolated patches of a dark-gray limestone that weathers light blue gray. The limestone is rather massive and is nowhere interbedded with the black slate. These patches appear to be anticlinal crests. Fragments of brachiopods, Bryozoa, and crinoids are generally abundant. In the largest patch east of Black Pond, the writer found *Cryptolithus tesselatus*. Probably all these limestone patches are of the same age.

Prompted by the supposed discovery by Wing of *Cryptolithus* in one of two patches of limestone at the two ends of the Ganson Hill syncline Cady (1945) mapped them as fensters of Glens Falls and

Orwell limestone. Through the kindness of W. M. Cady, the writer has studied Wing's original notes, which are quoted below.

"It is equally true that beds of limestone found in different localities in the slate are all inverted anticlinals of the Trenton limestone dipping east. A good example of this is the limestone found in Hubbardton on the road from Hortonville to the slate Quarries in West Castleton, about one mile south of Hortonville, a little south of a large red farmhouse on the east side of the road. Here in a small elevation of Trenton limestone holding *Trinucleus concentricus* [synonym for *Cryptolithus tesselatus*] etc., sixty yards wide between slate all dipping E. Not 100 rods further on, after turning the corner east by the School House and passing a *white* farmhouse another small bed some 10 feet wide occurs, also holding Trenton fossils and further on by Mr. Hunt's about two miles north of a slate quarry in the northwest corner of Castleton, another, or may be, the same belt of limestone occurs. This too is Trenton by fossils." (Book II, letter to Dana, May 13, 1869).

Kaiser (1945, p. 1087) surmises that "the limestone bed referred to must be that northeast of Hubbardton village." However, from Wing's descriptions it seems clearly to be the patch at Black Pond. There is no reason to suppose that the limestone at Ganson Hill is not Beebe limestone, Early Cambrian in age.

Rocks of Uncertain Age and Relation: The Hortonville and Ira Formations

Name and lithology. Keith (1932, p. 369) suggests that the black slate typically occurring in the village of Hortonville (F-5) be named after this place and correlated with the Snake Hill formation of New York, which in turn is correlated by Kay (1937, p. 272) with the Canajoharie formation. Keith's correlation is based on lithologic similarity and the occurrence of Trenton (Glens Falls) fossils in one limestone patch enclosed in the Hortonville. Cady (1945) extended this unit, with reservations, around the northern periphery of the slate belt, and other workers since (Fowler, 1950; Rodgers *et al.*, 1952; MacFadyen, 1956) have correlated the black phyllite along the eastern base of the Taconic Range (Keith's Ira slate, 1932, p. 398) with the Hortonville formation as well.

In this report, the black slate and phyllite of the Middlebury synclinorium, east of the Taconic Range and south of Brandon, will be included in the Ira formation, which is an extension of Keith's name Ira slate (1932, p. 398). The formation includes the black phyllite and also the Whipple marble members. The separation of black phyllite and slate on the two sides of the Taconic sequence is desirable because these belts cannot be traced into each other, and their stratigraphic equivalence cannot be demonstrated pending better age determination of the fossils they carry. For convenience, however, these two formations will be discussed here together.

In the field, the Hortonville and Ira formations are indistinguishable from the Lower Cambrian West Castleton formation. In the western part of the area, the Hortonville ranges from a black, fissile, graphitic and pyritic slate to a dark-gray, sandy, poorly cleaving argillite. East of the Taconic Range, the Ira formation is a black pyritic phyllite which may, in places, be rather massive because of its sandiness. Thin, white sandy laminae and brown limy beds occur abundantly, as well as black, thick-bedded pebbly grit.

Other rock types found in the Hortonville and Ira formations include:

(1) A dark-gray dolostone, either thin-bedded or massive, commonly with black slate partings and weathering reddish brown. This unit is rarely more than a few feet thick and does not form traceable units. It occurs, for instance, on the top of Biddie Knob, on the sharp knob west of High Pond (F-7) near Black Pond[6], and sporadically along the east flank of the Taconic Range. Lithologically it is identical with a dolostone in the West Castleton formation, found on the 1360-foot knob (I-5) southwest of Mudd Pond.

(2) A black dolomitic quartzite, identical in lithologic characteristics and thickness with the quartzite in unit (5) of the Mount Hamilton group, for instance on Signal Hill. Like its counterpart in the Taconic sequence, it occurs a short distance from the Bull formation. It is best seen north of Castle Hill (L-4) and east of Brandon Mountain Road near Seager Hill (K-4 to L-4).

(3) A coarse, massive, albitic phyllite, with porphyroblasts of albite making up to 50 per cent of the bulk. On a fresh surface the albite cleavage faces are easily recognizable; on a weathered surface these commonly show up as minute pimples. The rock may be dark gray or green. It is discontinuous and occurs exclusively in the Ira formation on the east side of the Taconic Range, apparently because of the higher grade of metamorphism there. It

[6] Not to be confused with High Pond (I-4) near Walker Pond (J-5).

occurs near the contact with the Bull formation.

Forbes Hill conglomerate (breccia?) in the Hortonville slate. At several places in the black slate mapped as Hortonville a breccia (conglomerate?) has been found. The first is near the north end of the slate belt. The best outcrop is in Willow Brook at 750 feet elevation. In a black-slate matrix are embedded numerous subrounded pebbles of green slate, buff-weathering limestone, dolomitic sandstone, and brown-weathering dark dolostone. The pebbles range from half an inch to 1 foot across and are unsorted; the cleavage in the slate pebbles is parallel to the main cleavage. All the rock types in the pebbles may be reproduced from rocks within the Lower Cambrian sequence which overlies the black slate at 820-foot level in the brook. The conglomerate (?) can be found also immediately east and west of the ravine, but it does not form a continuous unit.

On a small ledge at 800-foot level (G-2), 2300 feet N.70°W. of Signal Hill, a similar conglomerate or breccia is found in close association with a patch of green slate. The enclosed rocks are green slate and quartzite, with rock cleavage oriented with the matrix. It has been impossible to ascertain whether this isolated outcrop represents a breccia or conglomerate.

A third area is west of Route 22A, 2000 feet N.17°W. of the junction with West Haven Road (B-10). Here, on a west-facing slope at 320 feet elevation and 100 feet horizontally from the underlying Ordovician limestone, the black slate encloses angular quartzite several inches across, as well as numerous small, angular chips of green slate and a calcareous sandstone. Again, the pebbles are reminiscent of the Taconic sequence. The angularity of the pebbles suggests that the rock may be a breccia.

A large tract of a similar rock occurs just east of the gravel road, due east of Forbes Hill (A-9). The black slate encloses boulders of black quartzite, similar to the Mudd Pond, up to 4 feet across (Pl. 1, fig. 6); other pebbles are of the Bomoseen graywacke type, a dolomitic quartzite, up to 6 inches across, and innumerable angular green slate chips and sandstone chips less than 1 inch across. The degree of comminution seems to be related to rock resistance. Poor outcrops prevent tracing out of this rock.

A fifth area is at an elevation of 600 feet, at the base of the steep slope due west of the 830-foot knob (D-3) north of Sunrise Lake (D-4). The pebbles include gray slate and massive to thin-bedded buff-weathering sandstone. The sandstone tends to form slabs whose parallel orientation gives the bedding attitude and indicates that there the black slate structurally overlies the green slate immediately to the west.

Distribution. Rocks tentatively mapped as the Hortonville and Ira formations include most of the black slates marginal to the slate belt on the west side; the black slates around the type localities; and the large belt of black slate extending from Seager Hill southward through Whipple Hollow toward West Rutland (N-12).

The writer has been unable to differentiate the black slates at the north end of the slate belt into an allochthonous and an autochthonous unit. On the basis of existing fossil evidence, most of these have been mapped as allochthonous; on Plate 1 these areas were labeled Ꞓwe?, O-Ꞓmh?, and/or Oh?.

Age of the Hortonville and Ira formations. The Taconic sequence is separated from the Synclinorium sequence by an almost continuous belt of black slate and phyllite, a large part of which has been called the "Hortonville formation," of mid-Trenton age (Cady, 1945; Fowler, 1950; Rodgers *et al.*, 1952). Since the unravelling of the Taconic problem depends on an understanding of the relations between the Taconic and the Synclinorium sequences, it is important to review carefully the evidence for the age of the "Hortonville" formation in the immediate environs of the Taconic sequence.

EVIDENCE FOR A TRENTONIAN AGE: The original assignment of the Hortonville formation to the Trentonian is based on the fossils found in the Glens Falls limestone patches that it encloses, on the assumption of a normal stratigraphic superposition. Additional arguments were based on the lithic similarity with the Snake Hill formation with which, however, the Hortonville has no direct contact. The Glens Falls limestone and the black slate are not interbedded within the map area, although they are near Johnson Pond (F-4). Near Hortonville village, the contact is everywhere sharp, and the limestones appear to be anticlines. In a complex area such as the present one, the possibility that the limestone areas may be windows cannot be ignored.

Just east of Hyde Manor, the black slate rests in the center of a syncline outlined by the Glens Falls (?) limestone. Kay (1956, oral communication; also *in* Zen, 1959, Pl. B-1) tentatively considers this evidence for the conformable relation between these units, and therefore the black slate is taken to be Trentonian. This area of black slate, however, is continuous, on the south, with the main body of black slate that lies to the east, and this main body is generally accepted as part of the Taconic sequence. Two explanations are possible: the western black slate might be Ordovician, brought into contact with the eastern belt by a fault; alternatively, both belts of black slate may be Lower Cambrian, thrust over the limestone and lying, pseudoconformably in part, above the Ordovician limestone units. Since the two belts of black slate are identical and no evidence exists for a fault here within the black slate, the latter alternative is adopted in this report, and the thrust separating slate and limestone is shown as folded in the syncline.

Cady (1945) shows the type Hortonville as directly traceable into the black slate in the core of the Middlebury synclinorium north of the Sudbury thrust. Furthermore, the black slate on the east side of the Taconic Range is traceable into the belt of black phyllite within the marble belt, north of West Rutland; this latter belt apparently rests unconformably on Ordovician limestones, ranging, according to Fowler (1950), from the Bascom to the Glens Falls-equivalent Whipple marble and therefore must be no older than Trentonian. The writer, in the summer of 1958 discovered black limestone, carrying Trenton fossils, interbedded with black phyllite, in a ravine at 1100-foot level, west of the road three-quarters of a mile southeast of the 1850 foot Knob (M-13) north of Ira (N-15). Finally, in the Pawlet quadrangle, black phyllite apparently continuous with this Ira band contains lenses of limestone carrying Ordovician fossils (Rodgers *et al.*, 1952, p. 17; *see also* Foerste, 1893, p 441).[6]

Dale (1898, Pl. XIII) reports numerous graptolite localities in the Hortonville formation (mapped by Dale as "Ordovician slate") contiguous with the type locality, as well as in the central portion of the synclinal belt that extends from Fair Haven through West Castleton. No authentic identifications of these graptolites were made, and the specimens cannot be located. The writer visited all these localities but found no fossils. If, however, the fossil evidence is accepted, then the type Hortonville must be Ordovician.

EVIDENCE FOR AN EARLY CAMBRIAN AGE: Swinnerton (1922, Thesis, Harvard Univ., p. 79) reports Early Cambrian fossils from the Beebe limestone from a hilltop northwest (?) of Twin Lakes. These fossils were identified by Schuchert (1937, p. 1039). The locality is probably the south slope of the 887-foot knob (H-4) north of Keeler Pond. Since this limestone is in black slate of the West Castleton formation which is traceable into the black slate around Signal Hill and Woodchuck Hill (H-2), this latter tract is regarded as Lower Cambrian. Furthermore, from the Keeler Pond area the black slate can also be traced continuously into the type Hortonville. Thus there is reason to regard the type Hortonville formation as Lower Cambrian as well.

Lithologic and stratigraphic evidence strongly suggests that at least parts of the Hortonville and Ira formations are Lower Cambrian. The presence, in the black slates near Black Pond, near Castle Hill, and east of the Taconic Mountain, of quartzites and dolostones identical in appearance and in position with rocks in the West Castleton formation (?) or Mount Hamilton group (?) has been indicated. Moreover, both north and south of Biddie Knob, typical Mudd Pond quartzite occurs in the green phyllite, a short distance west of the black phyllite (of Whipple Hollow); the relation is exactly like that between known West Castleton and Bull formations. West of the Mudd Pond quartzite typical Zion Hill quartzite occurs also, strengthening the view that the Biddie Knob formation forms an anticline with matching limbs; on the west limb, however, the black slate carries Early Cambrian fossils.

A similar situation exists at Barber Ledge, where the Mudd Pond quartzite and the North Brittain conglomerate occur in the Bull formation near the black slate contact, in a way typical of the Bull–West Castleton relationship.

The contact relation between the Bull formation and the Hortonville and Ira formations can be studied in detail at many places. Many, although not all, of these contacts are gradational; a few of the localities are:

[6] The patches of Orwell limestone reported by Fowler (1950, p. 31) cannot be used as evidence for the age of the black phyllite, as the limestone is in every case under the black phyllite rather than interbedded with it.

(1) On the south shore of a small reservoir (N-13), at 850 feet elevation, 7/8 mile east-southeast of Clark Hill (M-13),

(2) Near West Rutland, by the connecting road across the Whipple Hollow swamp, due west of the mills of Vermont Marble Company (M-11),

(3) On the 940-foot knob (M-10), 1 mile northwest of Whipple Hollow School *site* (M-10),

(4) On the slopes (L-7) west of the 629-foot road junction, northwest of Butler Pond (M-7), in Whipple Hollow.

West of the slate belt, the gradational contact may be seen at

(5) The north slope of Barber Ledge (G-5), and

(6) On the northeast and south shores of Mill Pond.

East of the Taconic Range, no evidence has been found for a dislocation between the green and the black phyllites. Even where the color contrast is sharp, the contact appears to be conformable.

SUMMARY OF THE EVIDENCE: One could either (1) accept the unconfirmed fossil reports of Dale and Schuchert and assume a major break in the black slate terrane, or (2) ignore the fossil reports as specious and accept the black slate as a single unit, of Early Cambrian age, on the basis of the stratigraphic parallelism, down to minute lithic details, between the Biddie Knob-Bull-West Castleton (and Mount Hamilton) and the Biddie Knob-Bull-Hortonville (and Ira) sequences. Whichever alternative is accepted, however, a major discordance, presumably a fault, must exist within the black phyllite east of the Taconic Range even as on the west side of the Taconic sequence, separating the Trenton black phyllite, Ira, and Hortonville from the sequence of Lower Cambrian through Normanskill. The location of this fault remains conjectural.

Another possibility, independently conceived also by Rodgers (1957, oral communication), is that the major tectonic movement involving the Lower Cambrian rocks took place during Trenton time; in this movement the rocks, including the black slates, were shoved into the sea in which black mud was accumulating. Thus the two black pelites may have become too intimately commingled for field separation. This scheme would account for the continuity of the outcrops, the lithic similarities, and the finding of both Early Cambrian and Ordovician fossils. It also accounts for the breccia or conglomerate at Forbes Hill and other places, as blocks of Lower Cambrian rocks shed into the Ordovician sea in front of an advancing thrust sheet.[7] Finally, it allows for the existence of Trenton black slates resting unconformably on the Taconic sequence, reported by Bucher (1957) from the south end of the slate belt.

The problem of the Hortonville slate has been gone into in considerable detail, as upon it hinges the interpretation of the regional structure. This interpretation—that part of the Hortonville is Lower Cambrian—will be used later in one version of the regional synthesis; however, it must be remembered that ultimately it hinges on an unproven hypothesis.

STRUCTURAL GEOLOGY

General Statement

For the purpose of discussion of the geologic structure, the area may be divided into the eight tectonic units shown in Figure 3. Five of these tectonic units are in the Taconic sequence; the other three involve the surrounding Synclinorium sequence. Because the structural style and indeed detailed stratigraphy differ from one unit to another, they are conveniently discussed separately. Nonetheless, these differences are not very profound. The discussion of the area as a whole will be taken up under the heading of Regional Synthesis.

Because of the complexity of the structures, two new terms are introduced. By ***topping fold*** is meant a fold whose core contains the relatively youngest beds. By ***bottoming fold*** is meant one whose core contains the relatively oldest beds. For rocks that have been only simply folded, these terms are equivalent to synclines and anticlines, respectively; however, for rocks which have been complexly deformed, these terms are not necessarily synonyms. Anticline and syncline, as used in this report, are strictly geometric terms; however, topping- and bottoming folds are terms with stratigraphic connotations. Thus an anticline whose axial plane has been overturned beyond the horizontal becomes a syncline, but it re-

[7] Another outcrop of the Forbes Hill conglomerate has been traced to a black slate with interbedded black limestone. The limestone carries Middle(?) Ordovician fossils. The relations will be reported in detail in a later communication.

mains a bottoming fold regardless of the degree of rotation. The *sense* of a topping fold or a bottoming fold is given by its *direction of facing*,[8] which is shown on Plate 4.

Structural Details

Pine Pond thrust slice. Although a number of outcrops locally indicate the presence of the fault, the strongest argument for mapping the Pine Pond thrust is the areal pattern. The black West Castleton formation everywhere forms the footwall of the fault. As one follows the fault from northeast to the southwest, however, successively younger formations are encountered in the upper plate, ranging from the Biddie Knob formation to the highest unit of the Bull formation. In both plates, the section is right-side up; a major dislocation is the only explanation for the geometric relationships. The fault is named after Pine Pond (G-10) because the fault surface is exposed there.

A thrust fault, locally striking N.45°E. and dipping 25° SE., is exposed on Route 30 at the north end of Bomoseen village (G-10). Here Mettawee slate rests discordantly on the West Castleton with much drag folding, shearing, and fracturing in both formations. The disturbed zone is about 10 feet thick. This fault appears to be a subsidiary fault in front of the main thrust.

The attitude of the Pine Pond thrust is suggested by the above fault, by the measured attitude near Pine Pond (30°E.) and in Sucker Brook (H-8), and by the effect of topography on the trace of the fault in Sucker Brook. All evidence indicates an east-dipping low-angle thrust.

This fault cannot be traced farther than shown on the map. Possibly at both ends the thrust dies out into flexures. Failure to recognize the fault caused Dale (1898) to suggest that the Zion Hill quartzite and associated purple and green slates rest stratigraphically above the black slate. This succession is clearly untenable. Swinnerton seems to be the first to have detected the fault and established a more nearly correct stratigraphic succession.

STRUCTURE IN THE PINE POND THRUST SLICE: In general, the structure in the Pine Pond slice is simple. The beds tend to be nearly flat lying in normal sequence; this may be seen at Zion Hill. South and southeast of Wallace Ledge, however, the Zion Hill quartzite is repeated at least four times. Each band of this unit dips south, and graded bedding indicates that the beds are right side up. Thus, if the quartzite bands are one and the same, there must be a series of imbricate faults here.[9] These faults are complicated by later folding, which has folded the fault surface, and possibly by transverse faulting.

Southeast of Hooker Hill, the structure is locally complex, as may be seen between Hooker Road (I-10) and East Hubbardton Road. The upper part of the Bull formation and the lower part of the West Castleton formation are involved here; the beds strike easterly and dip vertically. The beds young to the north. The anomalous structure here is interpreted as a local drag fold formed when the tectonically higher Bird Mountain slice rode over the Pine Pond slice (Pl. 1, H-11 and I-11; Pl. 5, section D-D′).

Giddings Brook fold complex. North and west of the Pine Pond thrust, the West Castleton formation forms a tenuous but persistent belt with north-south strike on the west side, swinging gradually into east-west strike north of the fault. The dips are everywhere gently toward the fault. This flat-lying belt passes southwestward under the alluvium of the Castleton River (G-11) but re-emerges to form the hills northwest of Gorhamtown.

The eastern continuation of the West Castleton is found in a series of isolated synclines on the west flank of the Taconic Range, commonly forming tops of knobs. Where exposures are favorable, for example in many mountain ravines, the reverse (east) limbs of these folds are commonly broken by thrust faults dipping very gently east. Some of these faults are drag-folded, others have quartz veins, but many are clean cut, and only truncation of bedding shows their presence.

The West Castleton formation is underlain by the Bull formation, which in turn is underlain by the Biddie Knob formation except on the west side of the Pine Pond thrust where,

[8] The term facing is used in the sense defined by Cummins and Shackleton: "A bed or succession is said to *face* towards the side which was originally the top. Extending the term to structures, we say that a fold faces in the direction, normal to its axis and in its axial plane, in which younger beds are met. Beds intersected by a cleavage or schistosity are said to *face* along such a structure, normal to the intersection, towards the younger beds." (1955, p. 353).

[9] One excellent exposure of such a fault may be seen on the cliffs of Wallace Ledge, where an upper band of Zion Hill quartzite dips at right angles into a lower, nearly flat-lying band.

because of the southerly plunge, this formation does not extend far enough west to crop out.

The concentric belt of Biddie Knob formation is overturned radially outward to the west and north, on the west and north sides, respectively (Sections C-C′ and H-H′). The apparent direction of overturn along the eastern branch of the structure cannot be determined with certainty because of lack of key beds in

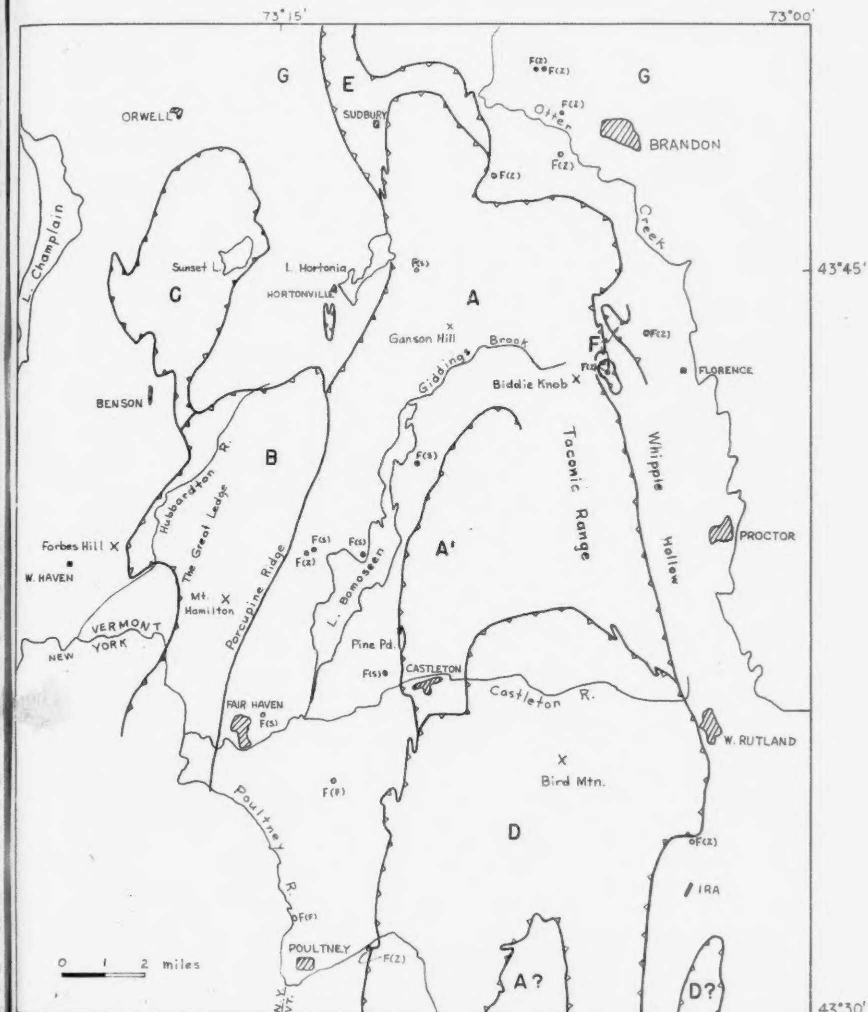

Figure 3. Sketch Map of the Major Tectonic Units in the Map Area. A, the Giddings Brook bottoming fold; A′, the Pine Pond thrust slice; B, the Porcupine Ridge–Great Ledge bottoming fold; C, the Sunset Lake slice; D, the Bird Mountain slice; E, the Sudbury slice; F, the Florence nappe; G, the Middlebury synclinorium. F(F), fossil locality of Fowler (1950); F(S), fossil locality of Swinnerton (1922) and/or Schuchert (1937); F(Z), fossil locality described in this report. Hachures are on the upper plate.

the Taconic Range. However, the gentle westerly dips of the Zion Hill quartzite near East Hubbardton (see J-6) and the steep bedding in the Mudd Pond and Zion Hill quartzites near Biddie Knob (see K-6) suggest an upward closure and thus a slight apparent overturn to the east, now in part obscured by later folding with a westerly overturn.

The Biddie Knob formation appears to form the core of a bottoming fold along the Giddings Brook valley (H-6 to I-6), which is indeed the topographic expression for this weak formation. On or near the apparent crest is a small recumbent syncline containing Mettawee slate and Zion Hill quartzite; the attitude of this structure, as well as those of several minor folds exposed on Monument Hill Road (H-6) west of Parsons School site (I-6), yields a northeasterly trend for the hinge of the bottoming fold and a northwesterly sense of movement.

West of the meridian of Brandon Mountain Road, the north, or lower, limb of the Giddings Brook bottoming fold becomes the south limb of a recumbent syncline, the Ganson Hill syncline (also a topping fold), again with an apparent east-west axis. The closure of the syncline is shown by the band of dolomitic quartzite near Eagle Rock, although through a series of axial undulations the black slate can be traced west of Lake Bomoseen and passes into the folds farther southwest. At the east end of the syncline, the closure is demonstrated by the convergence of two bands of Mudd Pond quartzite from the two limbs of the syncline. The two bands have been traced to within 200 feet of each other, the normal separation of the individual quartzite outcrops. The tracing is complicated by intricate folding within the quartzite and by similar quartzites in the top of the Bomoseen graywacke; however, the location of the closure is not likely to be greatly in error.

Bedding on both limbs of Ganson Hill syncline dips gently south, demonstrating the recumbent isoclinal nature of the fold. The minimum amplitude of the fold may be estimated by the depth of the re-entrant in the West Castleton-Bull contact between the 1330-foot knob (I-5) and the 1351-foot knob (I-6) to the southwest. The amplitude is about 1500 feet. The actual amplitude must be considerably greater.

A later, relatively minor set of folds with north-south axis is superimposed on the major structure. The folds are open, with poorly developed axial-plane cleavages dipping moderately east. This set of folds invariably plunges south, probably reflecting the pre-existing southerly dips of the beds.

At places the extreme deformation on the reverse limb of the Giddings Brook bottoming fold can be seen, as in the Giddings Brook ravine, west of the 730-foot knob (H-6), 1 mile northeast of Hubbardton village. The Zion Hill quartzite is represented by a number of blocks, 10 feet or more across, enclosed in the intricately folded Mettawee slate. The normal

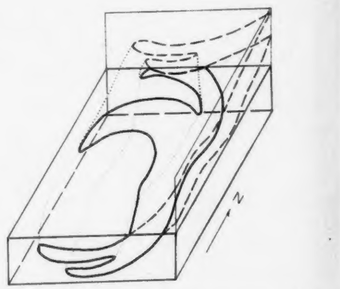

Figure 4. Schematic Diagram Showing the Geometry of the Giddings Brook Bottoming Fold. Surface shown is the top of the Biddie Knob formation; topographic effect is ignored. Heavy lines: intersection of the stratigraphic surface with the faces of the block diagram. Light dashed lines: trace of the surface of the Biddie Knob formation *not* on the faces of the block diagram. Dotted lines: hinge lines of the recumbent fold and its digitations.

limb of the quartzite is also fractured, however. On Route 30, a quarter of a mile south of the Murphy Road junction (H-7), gently dipping Zion Hill quartzite rides over a block of itself embedded in the Mettawee slate.[10]

The Giddings Brook-Ganson Hill fold system appears to be part of a series of such folds extending farther north (Fig. 4). The bulge in the map pattern of the Biddie Knob formation northeast of Sargent Hill is the elbow of a second, although discontinuous, belt of this formation that extends as far as Keeler Pond. Part of its north limb appears to be faulted out; the fault is suggested by the discordant relation between the Bull and West Castleton formations on the east shore of High Pond

[10] Detailed field relationships in this, as well as several other important areas, are described in a separate paper (Zen, *in* Zen, 1959, p. 10).

plunges
existing

on the
ttoming
Brook
, 1 mile
ne Zion
mber of
d in the
normal

the Ge-
ng Fold.
e Knob
. Heavy
surface
t dashed
e Knob
diagram.
ent fold

d, how-
e south
gently
a block
te.[10]
old sys-
ch folds
bulge in
rmation
w of a
of this
r Pond.
faulted
cordant
astleton
n Pond

as several
ate paper

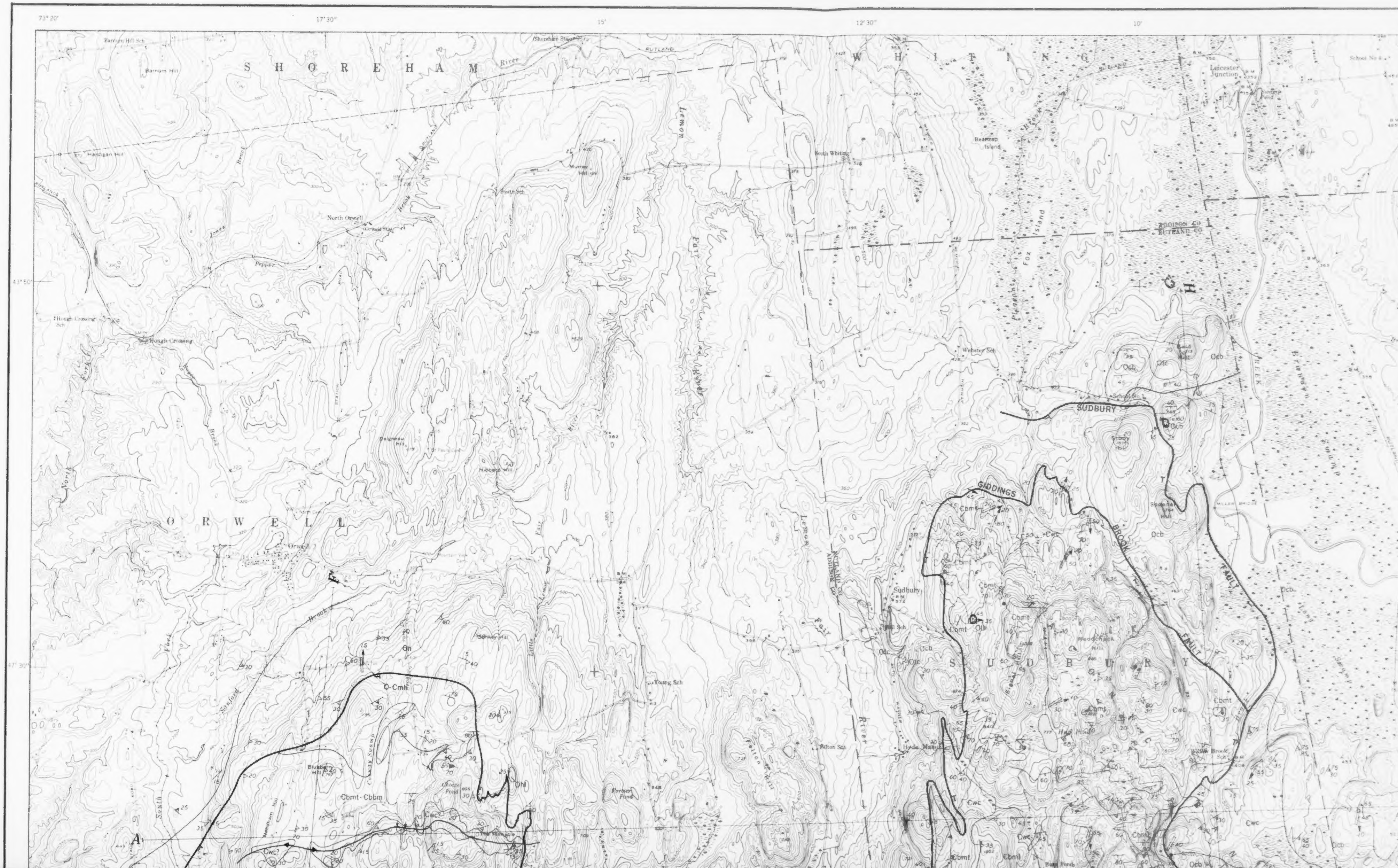

73° 20'
17' 30"
15'
12' 30"
10'
43° 50'
47' 30"
SHOREHAM
WHITING
ORWELL
SUDBURY
SUDBURY
GIDDINGS
BROOK
FAULT
FAULT
ADDISON CO
RUTLAND CO
Barnum Hill
Hardigan Hill
North Orwell
Hough Crossing
Orwell
Beantrap Island
Fox Island
Leicester Junction
South Whiting
Webster Sch
Sudbury
Woodchuck Hill
Hyde Manor
Young Sch
Fair Haven
Lemon Fair
Lemon Fair River
O-Cmh
Cbmt-Cbbm
Ocb
Otc
Cbmt
Cwc
Oh
A

EXPLANATION

CONTACTS

Normal sedimentary contact
Degree of control not specified

Fault contact; commonly low-angle reverse fault
T *on the side of the upper plate. Degree of control not specified*

STRUCTURE SYMBOLS

Note: All data recorded and plotted to the nearest five degrees

50
Strike and dip of bedding
Including inverted beds

Strike of vertical bedding

Horizontal bedding

70
Strike and dip of cleavage

Strike of vertical cleavage

30
Strike and dip of bedding with parallel cleavage

Strike of vertical bedding and parallel cleavage

15 20
Bedding and cleavage with parallel strike
First figure gives the dip of the bedding; second figure gives the dip of the cleavage

30 55
Bedding and cleavage with parallel strike, but dip in opposite directions

40 25
Bedding and cleavage not parallel
Point of junction of the truncated symbols represents the location of the outcrop

60 30
Two cleavages with parallel strikes, but different dips
First figure refers to (a) the earlier cleavage, if the sequence is determinable; (b) the better formed of the two cleavages, including foliation in the phyllites; or (c) the more closely-spaced of the two cleavages.

25 70
Two non-parallel cleavages from the same outcrop

45 10

SUNSET LAKE FAULT
GIDDINGS BROOK FAULT
B E N S O N
H U B B A R D
KEELER POND
GANSON HILL
FOLD
ADDISON CO
RUTLAND CO
Sunset Lake
Lake Hortonia
Hortonville
Burr Pond
Hinkum Pond
Johnson Pond
Howard Hill
Benson
Mill Pond
Strong Swamp
Bump Sch
Black Pond
Beebe Pond
Stacy Crossroads
Bishop Hill
Bullhead Pond
Hubbardton River
Sargent Hill
Cbmt
Cbbm
Cwc
Cbk
Otc
Oh
Ocb
Cbmt-Cbbm
A
B
C

60 30

Two cleavages with parallel strikes, but different dips
First figure refers to (a) the earlier cleavage, if the sequence is determinable; (b) the better formed of the two cleavages, including foliation in the phyllites; or (c) the more closely-spaced of the two cleavages.

25 70

Two non-parallel cleavages from the same outcrop

45 10

Axial plane of fold
Arrow gives the direction and amount of the true plunge as measured in a vertical plane

65

Axial plane of fold with no plunge

35

Vertical axial plane
Arrow gives sense and amount of the plunge

10

Lineation, with sense and amount of the true plunge as measured in a vertical plane
Butt-end of arrow indicates location of outcrop

45 35

Bedding with lineation
Arrow gives direction and amount of the plunge

80 65

Cleavage with lineation
Arrow gives direction and amount of the plunge

30

Strike and dip of exposed fault surface

SYMBOLS PERTAINING TO AXIAL SURFACES

Trace of axial surface on the topography
Arrow indicates the projected sense of the axial plunge

Axial trends of simple anticlines

Axial trends of simple synclines

Axial trends of simply overturned anticlines

Axial trends of simply overturned synclines

Trace of axial surface of bottoming fold on the topography
Arrow gives approximate direction and sense of plunge of the axis of the fold at the particular locality, and barb is on that side of the arrow in the direction of facing

Trace of axial surface of topping fold on the topography
Arrow gives approximate direction and sense of plunge of the axis of the fold at the particular locality, and barb is on that side of the arrow in the direction of facing

SYMBOLS FOR THE FORMATIONS

WEST HAVEN
FAIR HAVEN
CASTLETON
LAKE BOMOSEEN
GREAT LEDGE
BOTTOMING FOLD
PORCUPINE RIDGE SYNCLINE
SCOTCH HILL SYNCLINE
ANTICLINE
CEDAR MTN SYNCLINE
GRAHAM HILL SYNCLINE
HOOKER HILL SYNCLINE
PINE POND FAULT
MOUNTAIN FAULT
GIDDINGS BROOK FAULT
Point of Pines
Graham Hill
Castleton Corners
Castleton
Castleton River
HUDSON
West Castleton
Avalon Beach
Neshobe Beach
Crystal Beach
Barker Hill
Hooker Hill
Blueberry Hill
Zion Hill
Half Moon Lake
Black Pond
Glen Lake
Cedar Mtn
Coons Den
Beaver Meadow
Carver Falls
VERMONT
NEW YORK
WASHINGTON CO
RUTLAND CO
Cbmt
Cbbm
Cwc
Cbk
Otc
Oth
O-Cmh

Axial trends of simple anticlines

Axial trends of simple synclines

Axial trends of simply overturned anticlines

Axial trends of simply overturned synclines

Trace of axial surface of bottoming fold on the topography
Arrow gives approximate direction and sense of plunge of the axis of the fold at the particular locality, and barb is on that side of the arrow in the direction of facing

Trace of axial surface of topping fold on the topography
Arrow gives approximate direction and sense of plunge of the axis of the fold at the particular locality, and barb is on that side of the arrow in the direction of facing

SYMBOLS FOR THE FORMATIONS

Oi:	Black slate and phyllite of the Ira formation.
Oiw:	Whipple marble member of the Ira formation.
Oh:	Black slate of the Hortonville formation, including the Forbes Hill conglomerate.
Otc:	Undifferentiated Chazy, Black River, and Trenton limestone.
Ocb:	Beldens member of the Chipman formation.
Ocbu:	Burchards member of the Chipman formation.
Ocw:	Weybridge member of the Chipman formation.
Opw:	Pawlet formation.
O-Ꞓmh:	Mount Hamilton group; figures following the symbol indicates lithologic units.
Ꞓwc:	West Castleton formation.
Ꞓbmt:	Mettawee facies of the Bull formation, but including the North Brittain conglomerate member, the Mudd Pond quartzite member, and the Zion Hill member.
Ꞓbbm:	Bomoseen member of the Bull formation.
Ꞓbk:	Biddie Knob formation.

Point of Pines
Graham Hill
Castleton Corners
Castleton
Hydeville
Parker Hill
Bissville
Fair Haven
FAIR HAVEN
Pond Hill
Bird Mountain
Gorhamtown
Herrick Mountain
HAMPTON
POULTNEY
Old Knob
Town Hill
Fennell Hollow
Hampshire Hollow
Clark Hollow
Spruce Knob
Spaulding Hill
East Poultney
WHITEHALL
Low Hampton
Hampton Flats
East Whitehall
Bartholomew Hill
Morris Hill
Thorn Hill
Hampton
Cedar Swamp
Castleton River
Poultney River
GIDDINGS BROOK
HAMILTON
MOUNT
CEDAR MTN
DELAWARE AND HUDSON R.R.
RUTLAND AND WASHINGTON R.R.
DELAWARE AND HUDSON R.R.
FAULT
MOUNTAIN
Cbmt
Cwc
Cbbm
O-Cmh
Cbk
Opw
VERMONT
NEW YORK


Point of Pines
Graham Hill
Castleton Corners
Castleton
Castleton River
Hydeville
Parker Hill
Fair Haven
Blissville
Pond Hill
Bird Mountain
Clark Hill
Gorhamtown
Herrick Mountain
Old Knob
Town Hill
Fennell Hollow
Hampshire Hollow
Clark Hollow
Spruce Knob
Ira
DELAWARE AND HUDSON R.R.
RUTLAND AND WASHINGTON R.R.
AND HUDSON
HAVEN
POULTNEY
IRA
FAULT
D′
E′

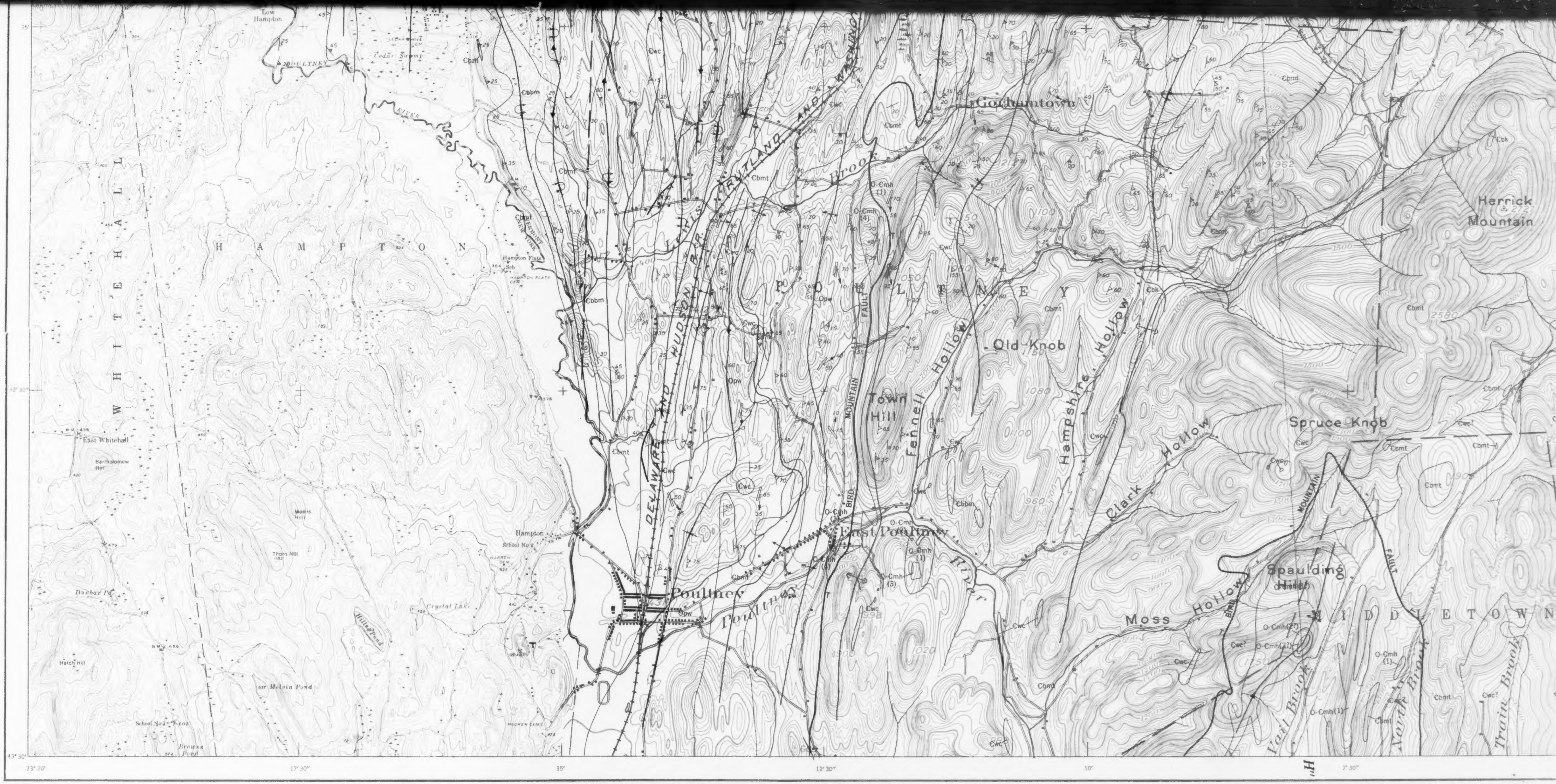

SELECTED STRUCTURAL DATA OF THE BEDROCK GEOLOGY, CASTLETON AREA, VERMONT

Scale 1:48 000

1 0 1 2 3 4 5 Miles

ZEN, PLATE 4

Geological Society of America Bulletin, volume 72

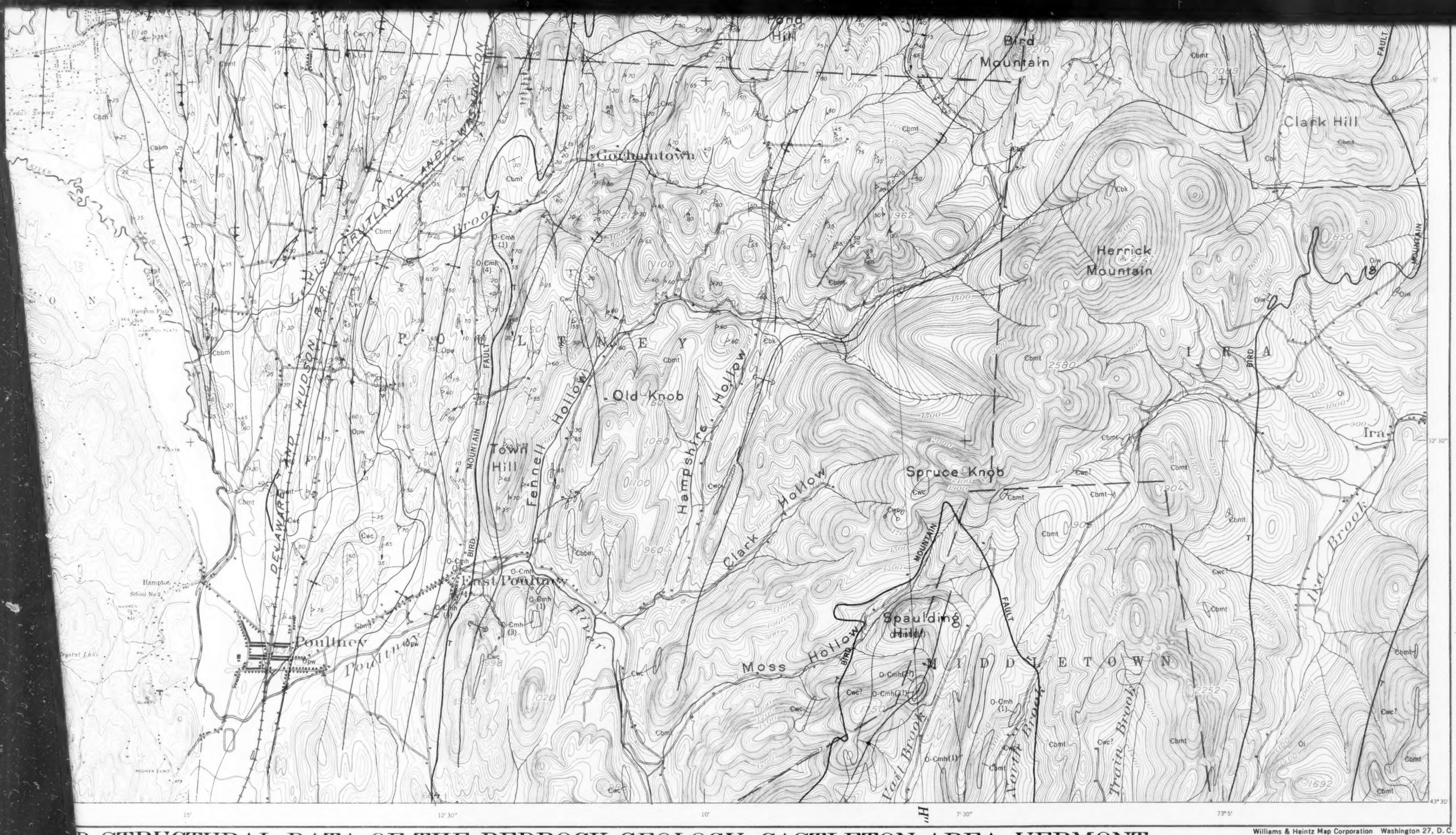

Williams & Heintz Map Corporation Washington 27, D. C.

D STRUCTURAL DATA OF THE BEDROCK GEOLOGY, CASTLETON AREA, VERMONT

Scale 1:48 000

1 0 1 2 3 4 5 Miles

(I-4) nea
of Biddi
one, app
fold, alt
understo
eastern
formatio

The s
the slate
beds. Th
patches;
Mudd
glomera
pected s
relation
Mettaw

Deter
between
by the
places.
largest
bury vi
south 1
Signal
north s
black s
dips st
compre
quartzi
green
gently
sistent
posed

Mos
demon
to the
traced
crop c
the W
the re
this a
repres
botto
"float
but t
dence
beds.

In
fault,
mapp
form
Here
soft,
area,
comm

Th

(I-4) near Walker Pond. A third, and last, belt of Biddie Knob formation, northeast of this one, appears to form yet another bottoming fold, although the details are very poorly understood owing to the lack of key beds. The eastern terminus of this belt of Biddie Knob formation rests directly against black slate.

The structure at the extreme north end of the slate belt is obscure because of lack of key beds. The green slate occurs largely in isolated patches; nonetheless, occasional outcrops of Mudd Pond quartzite, North Brittain conglomerate, and Zion Hill quartzite, at their expected stratigraphic positions, justify the correlation of the green slate patches with the Mettawee.

Determination of the geometric relations between the green and black slates is hampered by the lack of bedding in these units in most places. This much, however, seems certain: The largest patch of green slate northeast of Sudbury village dips north on both the north and south limbs; the large area of green slate near Signal Hill dips south, nearly vertically on the north side and moderately on the south; the black slate on the south slope of Signal Hill dips steeply and includes a series of tightly compressed folds defined by the dolomitic quartzite. Finally, the northern contact of the green slate south of Huff Pond (H-3) dips gently south. Clearly these data are not consistent with any simple structural scheme composed of simple anticlines of the green slate.

Most of the black slate in this area can be demonstrated to overlie Ordovician limestones to the north, west, and east, and also can be traced into a fossiliferous Lower Cambrian outcrop of black slate. It is therefore mapped as the West Castleton formation (?). In view of the recumbent structure immediately south of this area, the green slate at the north end may represent remnants of the core of a large bottoming fold, the remnants now actually "floating" within the stratigraphically higher but tectonically lower West Castleton. Evidence is needed to confirm the tops sense of beds.

In addition to the Keeler Pond-High Pond fault, a fault is suggested (although not so mapped) around the elongate area of Bull formation (G-3) just south of Hyde Manor. Here the slate is purple and green, and very soft, unlike the common Mettawee slate in this area, which is preponderantly green and hard, commonly quartzitic.

The area east of Hinkum Pond (H-4), between Stiles Mountain (J-4) and Castle Hill, is notable in that green Mettawee slate here overlies the black slate. Dips range from steeply to moderately south, and, where determined, bedding in both formations parallels the contact, yielding an apparently normal sequence. The stratigraphy, however, indicates a fault or an overturned section, depending on whether the black slate is autochthonous or allochthonous. Several outcrops of green slate in the ravine of Willow Brook just south of the limestone–slate contact might indicate at least local faults.

To the east, in Whipple Hollow, the black phyllite dips westward under the green Mettawee slate. The Mettawee slate is present everywhere except for about a mile northeast of the 2034-foot knob; in fact, south of Biddie Knob it includes the Mudd Pond and Zion Hill quartzites and shows a tops-east stratigraphic sense by the order of succession. The extremely complex interfolding of the slate and limestone units all along the east flank of the Taconic Range also proves that the Taconic and the Synclinorium sequences have been deformed as a unit.

Structural elements west of Lake Bomoseen. The first major structural feature west of Lake Bomoseen is the Cedar Mountain syncline, beautifully exposed in the large abandoned quarry on the south slope of the mountain (Pl. 3, fig. 1). A recumbent syncline in the upper beds of the Bull formation, overturned westward, plunges south. This syncline is found again on Neshobe Island (F-9), which is underlain largely by the West Castleton formation, with only a narrow stretch of nearly vertical Mettawee slate at the island's eastern extremity. On the west side of the island the slate is nearly horizontal. On the east shore of the south end of Lake Bomoseen, the same belt of West Castleton slate dips isoclinally and gently east on both limbs of the fold.

The next syncline to the west, the Scotch Hill syncline, is simple. The east limb is nearly vertical, and the west limb dips gently east. This open fold is exposed on a low cliff on the road southeast of Glen Lake (Pl. 3, fig. 2). The simplicity of the structure and the relation of the West Castleton slate to the underlying Bull formation at this locality support the proposed relative ages of the two units.

The anticline separating the two synclines is shown by the north-plunging Bomoseen graywacke southwest of Avalon Beach (F-10). Through an east-west axial culmination, this area of graywacke joins, between Hydeville and Fair Haven, another band that extends north and south through the village of Fair Haven. This culmination is suggested by the north-plunging syncline of North Brittain conglomerate northeast of Fair Haven—the southern termination of the Scotch Hill syncline—and its south-plunging counterpart as well as the isolated area of West Castleton formation, near Eddy Hill southeast of Fair Haven.

West of the Scotch Hill syncline, the most important structure is the complex fold defined by the Bomoseen graywacke. The east branch of this structure is a simple anticline that runs from Porcupine Ridge (D-10), by Glen Lake, toward Black Pond; the west branch runs from the Great Ledge (B-9 to C-9) through Cobble Knoll and north. The two branches join west of Black Pond and yield a hairpin pattern. On both limbs of each branch the dip is east; however, at the arch bend of the hairpin the dip is gently south on both limbs.

Within this Great Ledge-Porcupine Ridge fold is nested a simple syncline, the Mount Hamilton syncline. The West Castleton formation in the syncline differs in detail from the same formation in the Scotch Hill syncline, in the much greater development of the Mudd Pond quartzite in the former structure, and in the occurrence here of a limestone conglomerate, correlated with the North Brittain conglomerate, within the black slate. The black slates in both synclines apparently face up throughout and pass into the Mount Hamilton group.

Three geometric reconstructions of the compound structure may be considered: (1) two separate and initially distinct anticlines may have been joined by an east-west cross-fold, which locally overturns to the north to give the observed attitude at the north end. Such a cross-fold, however, is not reflected in the units beyond the Bomoseen graywacke.

(2) The compound fold and associated structures may represent a distinct thrust slice tectonically above the rocks now exposed to its east. The east-dipping section between O'Brien Point and Coon's Den (D-9), with tops-east sense given by the basal conglomerate of the Zion Hill quartzite at Flint Hill (690-foot knob, E-9), however, argues strongly against this.

(3) The hairpin structure may be a compound bottoming fold, with the west belt of the Bomoseen graywacke representing the core of the fold but the east branch merely a later anticline on the normal limb. The two branches have coalesced through a south plunge of the flat-lying axial plane (Pl. 5, Sections C-C′ through G-G′; Fig. 5). The Mount Hamilton syncline then becomes an incidental flexure on the back of the major structure, and the black slate northeast of Black Pond would be interpreted as part of the Taconic sequence in the inverted limb.

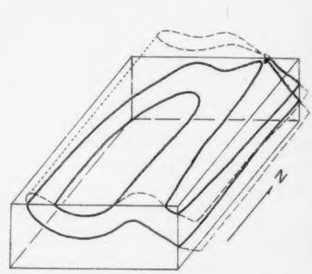

Figure 5. Schematic Diagram Showing the Geometry of the Great Ledge–Porcupine Ridge Bottoming Fold. Surface shown is the top of the Bomoseen graywacke; topographic effect is ignored. Heavy lines: intersection of the stratigraphic surface with the faces of the block diagram. Light dashed lines: continuation of the heavy lines beyond the confines of the block diagram. Dotted line: hinge line of the recumbent fold. The effect of a boudinage is shown at the north end of the diagram.

The structural relationship of the black slates of Ganson Hill, Barber Ledge, and Black Pond to the structure in the Mount Hamilton syncline must be explained. Two alternatives will be considered.

If the black slate north of Black Pond were autochthonous, then a concealed discordance must exist between it and the Lower Cambrian black slate at Barber Ledge. The discordance must be a thrust fault of the Cambrian rocks over the Hortonville slate since at the south end of Black Pond the Hortonville slate plunges under the Bull formation. The black slates at Ganson Hill, Barber Ledge, and west of Moscow Pond (E-8) would bear no direct structural relation to one another. The belt of Mettawee slate on top and north of Barber Ledge could thus be either a simple isoclinal recumbent anticline or a structural syncline with an upside-down sequence (latter explanation shown in Section B-B′ of Plate 5.).

One very disturbing feature is that nearly everywhere the green Bull formation, which is the middle unit of the Lower Cambrian section, comes in contact with the Hortonville slate. The entire contact must of course be a fault, but what could bring about the anomalous relationship? To add to the difficulty, locally the Bull–Hortonville slate contact is in fact gradational: for instance on the ridge just southwest of High Pond (F-7) near Moscow Pond.

These anomalous relations become comprehensible if part of the black slate at Black Pond is considered West Castleton. The consistent juxtaposition of the Bull formation and black slate then becomes a simple inverted section, and the patches of Glens Falls limestone become windows. The black slate at Barber Ledge becomes part of the lower limb of the recumbent structure, and the green slate within it part of an inverted sequence in a later syncline. The belt of Bull formation between Ganson Hill and Barber Ledge thus represents the entire core of the bottoming fold at this locality (Pl. 5, Section B-B′). Finally, the hairpin anticline of Bomoseen graywacke, as well as the West Castleton slate within it, fits naturally into the scheme.

Since green slate appears to be missing between the Bomoseen graywacke and the black slate north of Mill Pond, and possibly also east of Forbes Hill, the above scheme cannot be directly applied to these areas. The explanation may be lateral pinching out of the green slate, faulting, or incorrect age assignment of the black slate here.

Finally, the structure around William Miller Chapel (A-12) west of Fair Haven remains to be described. Here is an area of Beldens limestone and dolostone, nearly flat lying but in detail intensely folded, surrounded pseudoconformably to the west, north, and east by the Bomoseen graywacke. On the south there is no outcrop. The Bomoseen graywacke is overlain by green Mettawee slate followed by West Castleton slate. The Beldens limestone is thus a window, exposed through a local anticline, and the allochthonous units over it are in their normal sequence. Locally, then, no recumbent fold exists in the Taconic sequence (Pl. 3, fig. 4).

Structure of the Sunset Lake area (C-4). In the vicinity of Oak Hill (C-4) the Zion Hill quartzite is flat lying and caps the hills; an isolated outcrop of it is found on the hilltop just east of Old Stage Road (A-3 to A-6), south-southwest of Stacy Crossroads (B-4). Graded bedding in the quartzite and graded bedding and channel filling in thin quartzites within the underlying slate indicate that the section here is right side up.

Three more bands of Zion Hill quartzite appear south of here. The northernmost band is the same as above; here it dips south under more green-gray slate. The section is repeated a short distance to the south, where clear-cut thrust faults seen on the cliff face just east of Route 22A indicate that the repetition is probably due to faulting. The third band resembles the Mudd Pond quartzite and may represent a higher unit than the bulk of the cliff-forming Zion Hill quartzite.

Two isolated outcrops of Zion Hill quartzite are found north of the Oak Hill belt, northwest of Bishop Hill (C-4) and northeast of Spruce Pond (C-4); these beds dip steeply south and are not traceable, although they trend parallel to the strike of the Oak Hill belt. They are interpreted as sheared remnants of the Zion Hill quartzite in the reverse limb of a major anticline overturned to the north.

The next structural unit to the north consists of areas of black slate, elongate parallel to the areal trend. These are synclinal, overturned steeply northward so that both limbs dip gently south. The structures were refolded along north-south axes much as the structure in the Ganson Hill area were. The synclinal nature of the black slate belt is shown by the presence of the North Brittain conglomerate on both limbs and by cross-bedding in the black slate. The age of the black slate within the Taconic sequence, however, is uncertain; in appearance it resembles part of the Mount Hamilton group.

The contact between the Taconic sequence and the surrounding autochthonous units is drawn on both structural and lithological grounds. At the north end, the Taconic black slate is in contact with the black Hortonville slate; however, the two units are quite distinct, and generally there is little confusion: the Taconic slate is jet black, splintery to fissile, with interbedded brown-weathering dolomitic quartzite, whereas the Hortonville slate is dark gray, hard, siliceous to soft and limy, but homogeneous and uniform. Along Pond Woods Road (D-3 to D-4), moreover, the Taconic structures trend east-west by actual tracing of the units; but all the trends in the autochthonous units are north-south. The regional picture leaves little doubt that a major discordance exists.

North of Sunrise Lake, the "Forbes Hill" type of breccia is exposed at the base of a low cliff, east of and overlying Taconic rocks. This black slate, on the 790-foot knob to the east (D-4), includes a large lens of limestone breccia containing Ordovician fossils.[11] If the slate is correctly dated as Trentonian (Cady, 1945, Pl. 10), the breccia might indicate a local overturn of the discordant contact. The same black slate is traced along the eastern and northern margins of the Sunset Lake area of Taconic rocks.

RELATION WITH THE MAIN TACONIC REGION: The Sunset Lake area is shown on all published maps (Cady, 1945; Keith, 1933; Rodgers, 1937; Rodgers, *et al.*, 1952) as a separate unit, not connected with the main Taconic belt. Although forming a distinct tectonic unit, rocks of the Sunset Lake area are, nevertheless, contiguous with the main Taconic sequence through a narrow but persistent neck of sheared Bomoseen graywacke. Although outcrops are poor south-southwest of Mill Pond, they show that this "neck" connects with the main area to the south. East of the junction of Route 22A and Sunset Lake Road, outcrops are again scanty, but enough occur west of the road to establish the southward connection.

Structure south of the Castleton River. In the area west of the Castleton-East Poultney line, the stratigraphy is the normal Bomoseen–Bull–West Castleton–Mount Hamilton sequence. The West Castleton formation includes the fossiliferous Beebe limestone (Fowler, 1950, p. 52). The structures consist of narrow, north-south trending folds that, except near Fair Haven, plunge southward. An example of this attitude is the syncline south of Hydeville, outlined on the map by the double-pronged pattern of Bomoseen graywacke and the canoe-shaped termination of West Castleton formation and in the field by the alignment of quarries in the upper Mettawee slate. The folds are at places recumbent, for instance in the big quarry operated by the Vermont Structural Slate Company, just south of the road leading west from Route 30 at its crossing with the Delaware and Hudson Railroad tracks, south of Blissville (E-12).

South of Fair Haven, extensive areas of Bomoseen graywacke occur with variable fold plunges. The map pattern suggests two anticlines, en echelon to the anticlines north of Castleton River. Although the extensive alluvial deposits in the Castleton River valley make structural correlation across the river difficult, there is little doubt that the anticline of Bomoseen graywacke strikes into the north-plunging anticline of the same unit west of the Scotch Hill road.

South of Glen Road, Castleton, in a small ravine called the "Glen" excellent outcrops show the North Brittain conglomerate dipping east under the black slate. Bedding in the conglomerate is well exposed and shows no repetition or folding. West of the ravine more black slate occurs without repetition of the conglomerate. The black slate is intensely disturbed near the contact but less so farther west. The contact is taken, then, to be the southern extension of the Pine Pond thrust.

In the vicinity of Poultney village, the Lower Cambrian sequence terminates against slates of the Mount Hamilton group. The nature of the junction is unknown because of poor outcrop; possibly an unconformity separates these rocks. Similarly, on the east side of this area, north-south belts of the Middle Ordovician Pawlet formation rest directly on the Bull formation and the West Castleton formation and, near the Castleton–East Poultney line, probably also on the Mount Hamilton group. The base of the Pawlet formation marks an important unconformity in the Taconic sequence; all the existing data fit this interpretation. Detailed discussion however must await a later report.

AREA EAST OF THE CASTLETON–EAST POULTNEY LINE: The details of this area, likewise, will be presented in a later report, and only the tectonic relation of this area to the areas north will be considered here.

South of Belgo Road (J-10), the black slate of the West Castleton formation, in the Hooker Hill syncline, is underlain to the north by a conformable and normal sequence of the Bull formation. To the south, the black slate is in turn overlain, with sharp contact, by purple and green silty slates devoid of key beds. The sharp break and lithologic contrast of the Mettawee slate on the two sides of the black slate are persistent.

In the ravine southeast of the east end of Belgo Road, black slate is continuously exposed up to the 1960-foot level. It is confined to the ravine, however; on the banks green slate crops out. The relationship indicates either a thrust fault or a recumbent syncline; the lithologic contrast favors the former hypothesis.

[11] John Rodgers showed the writer this outcrop.

Between Hooker and East Hubbardton roads 1 mile east-northeast of Castleton, the structure trends east-west, and the beds are nearly vertical. The outcrops disappear in the North Brittain Brook valley. Across the valley, 1000 feet east, these structural and rock units are absent and are replaced by the purple, green, and gray silty slates of the Bull formation.

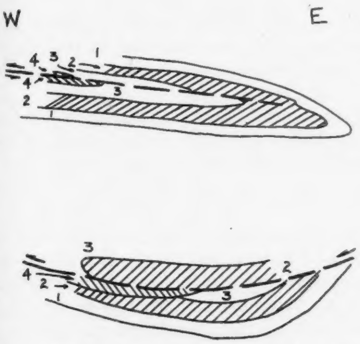

Figure 6. Schematic Representation of the Alternative Interpretations of the Sudbury Thrust Slice. A, according to Cady (1945); B, present interpretation. The units marked 1, 2, 3, and 4 may be identified with the Bascom formation, the Chipman formation, the Middlebury–Orwell–Glens Falls sequence, and the Hortonville formation, respectively. In 6B, the Hortonville formation is shown to overlie the older units unconformably; the contact, however, may be a thrust fault.

These indications of structural and stratigraphic discordance suggest a fault contact; the intersection of the contact with topography indicates a low dip. The area south of the Pine Pond slice and east of the Castleton–East Poultney line is therefore referred to as a fault slice, here named the Bird Mountain slice. The hypothesis of a thrust fault naturally explains the southern termination of the belt of Biddie Knob formation in the core of the Giddings Brook fold, along the Taconic Range northwest of West Rutland.

Structure in the limestone terrane north of the slate belt. The geology of part of the Ordovician limestone terrane north of the slate belt has been remapped in an effort to understand better the relationships between the two sequences. Considerable reinterpretation resulted. The Sudbury thrust slice, instead of being rooted in the east limb of the Middlebury synclinorium (Cady, 1945), is now regarded as a separate unit rooted farther east and closely related structurally to the Taconic sequence (Fig. 6).

In the vicinity of Bald Hill (I-1) and Miller Hill (I-1), at the northeast corner of the town of Sudbury, the Chipman formation (Beldens facies) and Middlebury limestone are involved in a tight, recumbent anticline with a south-dipping axial plane. A key outcrop of Middlebury limestone, next to Brandon swamp (J-1 to J-2) northeast of Bald Hill, shows that the under limb of the fold dips south persistently at a gentle angle, instead of swinging north to join the east limb of the Middlebury synclinorium (Cady, 1945, p. 570). The contact between the two formations is marked by a zone of red, hematitic limestone; on the map, the top of the Beldens is drawn where the massive dolostone disappears. As the Middlebury formation is part of the autochthonous synclinorium sequence, the gradational contact, probably marking an unconformity rather than a fault, indicates that the Beldens belongs to the same tectonic unit. The attitude of minor folds in the two formations indicates that the Bald Hill anticline closes westward and plunges south.

South of Route 73, between Stony Hill (H-1) and Webster School, is a line of scarps of Beldens dolostone and limestone which can be traced to the vicinity of Lemon Fair River (F-2), where these units overlie Middlebury limestone in an overturned section. This inversion, however, may be a local phenomenon, and contrary to Cady's interpretation (1945, Pl. 10, section C-C′) there is no evidence within the bulk of the Sudbury slice that the section is not normal.

The scarp-forming Beldens south of Route 73 overlies, southeast of Webster School, a black slate which can be traced northwestward into the core of the Middlebury synclinorium and which is thus Trenton or younger. Northeast of Stony Hill and just south of Route 73, an isolated patch of black slate displays the same relation to the Beldens and itself overlies the Beldens limestone of the Bald Hill anticline (H-1; section G-G′). Although there is a gap in outcrops between this area of black slate and that southeast of Webster School, there is little doubt that the slates belong to the same unit. These slates lie discordantly upon the autochthonous Beldens either through thrusting or through a Trenton unconformity.

The contact between the Middlebury limestone of the upper, normal limb of the Bald Hill anticline and the Beldens limestone of the Sudbury thrust slice can be traced southeastward; it disappears finally in Long Swamp (J-2 to J-3). The map shows clearly that the contact is an irregular surface; on the other hand the lithologic break is clear and unequivocal. The massive dolostone and pale limestone of the Beldens everywhere rest upon the younger, thin-bedded, dark-gray Middlebury. Near Willow Brook School, the Taconic sequence is in contact with units of the synclinorium sequence, here the Weybridge member of the Chipman formation.

Discordance at the base of the thrust slice has been found at two places: (1) At a bluff just off Route 73 southwest of Miller Hill, isolated Beldens dolostone dips steeply southeast and is much contorted; it rests upon, and is surrounded by, Middlebury limestone gently dipping west. (2) Due north of Spooner Hill (I-2) (Pl. 2, fig 3) and 500 feet south of Route 73, massive Beldens dolostone rests upon and truncates the Middlebury.

A number of isolated outcrops of Beldens limestone and dolostone occurs south of Seager Hill. These are on strike with the main belt of Beldens northwest of Seager Hill and have been interpreted as minor anticlines (Cady, 1945, Pl. 10). If the black slate surrounding these patches is part of the Taconic sequence, the limestone may then be windows or possibly even small klippen.

Northeast of Castle Hill, a small area of limestone, lithologically identical with the upper Bascom formation, is infolded or interbedded in the black slate. The outcrop is on strike with the Bascom formation to the north and may hold the same relation as the patches of Beldens limestone to the west.

Structures at the north end of Whipple Hollow. Large tracts of fossiliferous Ordovician marble within areas of black slate, at the north end of Whipple Hollow and east of Biddie Knob, have been mapped by Fowler (1950) as Whipple marble, roughly Glens Falls equivalent, and basal to or interbedded with the black slate which he calls Hortonville and considers Trentonian. The Whipple marble at this locality, however, is here correlated with, or is directly traceable into, the Bascom formation on the east limb of the Middlebury synclinorium.

At 820 feet elevation east of the 2034-foot peak and just south of a mountain brook in Whipple Hollow, a simple, open syncline plunges gently south; it contains massive, brown-weathering dolostone underlain by black phyllite. The dolostone is overlain to the south by massive, sugary, dove-gray, streaky marble. The dolostone is much shattered, but the fractures are healed by calcite veins. This syncline is the north end of the roughly dumb-bell-shaped marble patch (L-6) on the map. The marble–phyllite contact can be traced around the patch on all sides, and the marble definitely rests upon the phyllite.[12] The marble patch, in fact, defines a doubly plunging syncline; it is not anticlinal and in contact with Taconic green slate, as Fowler suggests (1950, p. 33, Pl. 2).

Lithologically identical marble is also found about half a mile east, across a belt of black phyllite in an elongate tract interpreted by Fowler as intertongued Whipple. The western contact of the marble against phyllite is exposed, for instance three-quarters of a mile west of Florence, just south of a gravel road; the marble dips east moderately, overlying the phyllite. A similar attitude can be seen on the west wall of the abandoned quarries to the north and in the outcrops between these quarries and the black phyllite to the west. The main part of the quarries and the knobs to the north, however, show a flattening of the dip so that the beds are nearly horizontal. Continuing eastward, a broad anticline brings the black phyllite to the surface. Outcrops are sufficiently good to show that everywhere the black phyllite underlies the marble rather than being interbedded with it.

Farther east, the dip of the marble steepens, and the structure becomes part of the overturned homoclinal sequence on the east limb of the Middlebury synclinorium.

The structural interpretation of the area is as follows: The marble belongs to the inverted limb of a recumbent anticline (the Florence nappe) which has traveled westward. The forward part of the nappe has become isolated, by erosion, to form the patch east of Biddie Knob. The extension of the marble westward and upward, just east of the 2034-foot peak, may then be the remnant of the hinge.

A single outcrop of coarse gray marble, at 730 feet elevation on the south slope of the

[12] On a shoulder of the 2034-foot peak, the marble extends westward and upward to the 1250-foot level, is underlain by black phyllite, and exhibits extreme shearing and strong lineation caused by the smearing of the color bands. The lineation strikes southeast and is down dip.

810-foot hill (M-6) west of Florence, is interpreted as a remnant of the marble that once connected the area east of Biddie Knob with the main belt of marble. A second outcrop, in the mountain ravine east of the 2034-foot peak, however, is clearly within the black phyllite and is interpreted as due to subsidiary thrusting in the inverted limb of the nappe.

It has been impossible to determine how much of the black phyllite surrounding the Bascom marble of the Florence nappe is Ordovician and how much is Cambrian.

Status of isolated "klippen" in Whipple Hollow. Fowler (1950) maps two patches of "Mettawee" slate in Whipple Hollow, one near Butler Pond (M-7) and the other 1¼ miles farther south. The patch at Butler Pond is really a belt of gray to greenish-gray phyllite, commonly albitic and quartzitic, that trends north-northwest and dips steeply east. This unit crops out for about 2 miles, is intercalated with the typical black phyllite, and appears to grade into it. The writer interprets this unit as a stratum of the Ordovician black phyllite rather than part of the Taconic sequence.

The "klippe" 1¼ miles south of Butler Pond is areally more restricted than Fowler shows and occurs in two separate patches. These patches consist of green slates typical of the hard Mettawee slate of the nearby Taconic Range. Structural evidence of its relations to the surrounding jet-black phyllite, however, is lacking, as well as evidence for the age of the black phyllite itself.

Minor Structures

Introduction. Before proceeding to a structural synthesis for the area, a few remarks will be made on the minor structures. As no detailed study of minor structures as such has been made, only features relevant to the regional study will be considered. Dale (1895) has described some of the features in detail.

Planar features. The planar features here considered include bedding and several types of cleavage.

BEDDING: The bedding as mapped includes not only such typical features as limestone or quartzite beds, but also fine compositional banding such as that shown by thin limy or sandy laminae in slates. While there is some risk in using these features in intensely metamorphosed rocks because of the possibility of metamorphic differentiation, in the slate belt this danger is slight. Color contrasts within the slate have been used only sparingly, for these may merely reflect local irregularities in the rock and do not represent bedding.

For contorted beds, the trend and average dip of the beds are recorded as more meaningful.

CLEAVAGE: Two or more sets of cleavage are common in a typical slate outcrop. Of these, the best developed is the "slaty" cleavage, which generally parallels the bedding; where noses of folds are exposed, however, the cleavage may turn out to be the axial-plane cleavage and therefore cut the bedding. Thus the common parallelism of the bedding and slaty cleavage may be due merely to isoclinal folding. This relationship is excellently illustrated at, for example, the Cedar Mountain quarry.

Slaty cleavage has customarily been attributed to flowage (Leith, 1905, p. 23, 99). There is, true enough, strong orientation of mica flakes within the cleavage plane, as can be easily verified by X-ray study of oriented specimens; however, flowage is only one of many ways to achieve this. Dale (1895, p. 563) suggests that slaty cleavage is simply well-developed slip cleavage due to minor shearing; in the field the writer finds all gradations between these two megascopic features. The problem of the origin of slip cleavage has been reviewed by White (1949) and Brace (1953).

Whatever their origin, distinct sets of cleavage can be mapped in the field. In general the later set of "slip cleavage" is more coarsely spaced than the typical "slaty" cleavage, displaces the latter, and commonly indicates a secondary axial plane along which the slaty cleavage itself is folded. The slip cleavage seems also to be genetically related to fractures in the more competent layers, such as quartzite and limestone; these fractures in turn are invariably healed by quartz or calcite veins and suggest that the formation of the late slip cleavage is penecontemporaneous with metamorphism.

Another feature, called "cleavage banding" by Dale (1895, p. 561), is common in the more sandy variety of the argillites. This consists of subparallel layers of hard, dense argillite, locally quartzitelike in appearance, about 1 inch thick, interspersed with fine slates with parallel orientation of the cleavage. The quartzitelike layers may persist for a few feet or more before pinching out. The entire structure looks very much like bedding. However, where exposures are good, these features cut unquestioned bedding, including dolomitic beds in slate. They are thus the result of intense shearing, and the slatelike and quartzitelike layers differ only in texture (Pl. 3, fig. 5).

As an aid in differentiating cleavage banding from true bedding, many of the planar surfaces of the former show, upon close examination, faint lineation caused by color streaks. This is, in fact, the trace of faint color or compositional banding in the rock and reflects the true bedding orientation.

RELATION OF BEDDING TO CLEAVAGE: As mentioned, slaty cleavage does not necessarily parallel bedding. It is, however, risky to use the bedding–cleavage relationship to decipher the major structure, for, in an area of intense large-scale isoclinal folding, the first cleavage may be parallel to the bedding over long distances, and a second cleavage may develop so well that it in turn may be styled a slaty cleavage. Obviously relations between this second cleavage and bedding cannot be indiscriminately used in mapping the regional structure. As an example, the bedding–cleavage relationships just south of Mudd Pond and also northwest of Parsons School both indicate a right-side up sense. However, stratigraphy indicates that at Parsons School the section faces down, and at Mudd Pond it faces up.

Thus the cleavage–bedding relation is useful only when one is certain that the cleavage in question is of the first generation: a difficult decision at best. It is most useful in the Taconic Range where the first cleavage has developed into a crude schistosity, whereas the later slip cleavages remain widely spaced.

Linear features. Linear features here considered include rodding, boudins, and fractures, and elongation of pebbles in conglomerate beds.

RODDING: Rodding is due to the intersection of two sets of cleavage at nearly right angles; the slate breaks up into pencils or rods. It occurs thus on the noses of folds in cleavage and furnishes valuable clues to the attitude of these folds.

BOUDINS AND FRACTURES: Boudins and fractures occur in the relatively competent beds. In the Castleton area, boudins involving rock flowage are found only in dolostone layers embedded in limestones; the quartzite beds embedded in slate break largely along simple fractures. The boudinage or fracture cavities are commonly filled with secondary minerals. Those in the quartzites are most commonly milky quartz but also include chlorite, albite, ankerite, and pyrite, in order of decreasing frequency.

The orientation of the boudins is one of the most constant attitudes in the area. The boudins invariably lie in the northwest-southeast quadrants, generally west-northwest to east-southeast. They form approximately *a* lineations.

ELONGATIONS: Elongated pebbles are common, especially in the North Brittain conglomerate. The pebbles are generally elongated in a west-northwest direction and, like the boudins, give one of the most constant directions in the area. This direction is obliquely down the limbs of visible folds. However, along the axes of folds the pebbles commonly change abruptly into parallel orientation with the axes and become, thus, *b* lineated.

Rotational features. Minor structures indicating rotational movements include minor folds and rotated porphyroblasts.

MINOR FOLDS: Minor folds range from a few inches to tens of feet in wave length and amplitude. Their orientation and directions of closure yield useful clues to the larger structures to which they are directly related. However, the preceding discussions make clear that they may not be used blindly. If the minor folds involve folding of the slaty cleavage, they are secondary. Minor folds undoubtedly primary in origin—*i.e.*, related to the first folding—have not been found. The minor folds, with few exceptions, plunge south. This may simply reflect the fact that the regional dip of the beds before the second deformation had a southerly component.

ROTATED CRYSTALS: A few rotated pyrite crystals are found. The "tails" of quartz in the lee of these pyrite crystals give the sense of rotation of the rock. At Cedar Mountain quarry, for instance, such an occurrence corroborates the larger structures nicely. Unfortunately, such rotational features are far too rare to be of much assistance over the area as a whole.

REGIONAL SYNTHESIS

Introduction

Before proceeding to synthesize the stratigraphic and structural data into coherent regional pictures, it is desirable to set forth the basic information that may be regarded as objective and reliable and that is the foundation of the syntheses.

(1) The order of stratigraphic section is as indicated.

(2) Most of the rocks of the Taconic sequence are, by consensus of paleontologists,

Lower Cambrian. However, rocks as young as Upper Normanskill (Berry, *in* Zen, 1959, Table G-1) also exist.

(3) Rocks within the slate belt maintain an essential lithologic unity at least as far as the southern margin of the Pawlet quadrangle (Shumaker, 1960, Thesis, Cornell Univ.) and probably even farther south.

(4) On the eastern slope of the Taconic Range, green slate and black slate grade into each other. In the green slate, also, key beds exist which resemble units in the Lower Cambrian formations of the slate belt.

(5) Thrust faults and recumbent and isoclinal folds exist in the slate belt.

(6) The map pattern, particularly peripheral to the Pine Pond thrust slice, is as shown, with apparent sense of overturn to the west, west of Lake Bomoseen; to the north, around Giddings Brook; and with suggestions of overturn to the east in the Taconic Range, based primarily on the bedding attitude of a few key units.

(7) In the central portion of the map area, bedding strikes east-west and dips gently south.

(8) The structure of the slate belt is synclinal as a whole, with southerly plunge, in apparent continuity with the Middlebury synclinorium.

(9) Inverted stratigraphic relation exists between the Taconic sequence and the Lower to Middle Ordovician rocks along the margin of the slate belt.

Autochthonous Hypothesis (Figure 7B)

Because no Taconic fault has been located on the east side of the slate belt, and because no other similar compelling evidence exists, the regional structure may be interpreted, with internal consistency, by assuming that the Taconic sequence is autochthonous. A geometric reconstruction on this basis would require a series of concentric mushroom folds, each of which may be isoclinal and recumbent and which may be combined with local thrust faults where these are indicated. The geometric relationships demanded by the autochthonous hypothesis are so improbable, however, that they raise more serious problems than they solve. For this reason such a synthesis will not be pursued in detail. Enough information has been given so that the reader could make his own reconstruction.

A few of the objections to this hypothesis will be discussed. Perhaps the most celebrated is the necessary assumption of a rapid facies change, for the largely argillaceous Taconic sequence is supposed to be contemporaneous with the orthoquartzite and carbonate sequence of the Middlebury synclinorium immediately around it. Although one might perhaps avoid this problem by correlating the Lower Cambrian Taconic rocks with the Mendon series (Craddock, 1957, p. 717), this still leaves the lithological contrasts of the Upper Cambrian, Lower Ordovician, and Middle Ordovician rocks unexplained.

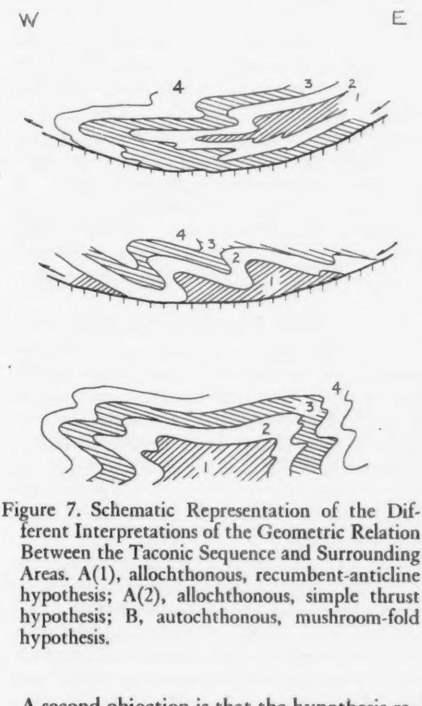

Figure 7. Schematic Representation of the Different Interpretations of the Geometric Relation Between the Taconic Sequence and Surrounding Areas. A(1), allochthonous, recumbent-anticline hypothesis; A(2), allochthonous, simple thrust hypothesis; B, autochthonous, mushroom-fold hypothesis.

A second objection is that the hypothesis requires an easterly sense of overturn in the Taconic Range, whereas the regional-movement sense, in particular that of the Florence nappe in Whipple Hollow, which involves the Bascom formation, clearly is westerly.

A third objection is that the autochthonous hypothesis cannot explain the geometry of relations in the Sunset Lake area. The size of the area is limited, and the structure in it is fairly well understood, so that no possibility of a hidden anticlinal core exists here, such as is required by the hypothesis. For the Sunset Lake area at least, a fault slice seems to be certainly indicated.

The autochthonous hypothesis demands that somewhere in Whipple Hollow, as well as northwest of Lake Hortonia, the black West Castleton slate must pass into a black identical-looking Ira slate, presumably across a thrust fault. No such thrust has been found, and location of it on the map would be purely arbitrary. The contact cannot be a simple unconformity because the Cambrian rocks rest *above* the Ordovician rocks. It should be remarked, however, that this defect is common to all the hypotheses, and is the most baffling aspect of the Taconic problem itself.

The autochthonous hypothesis pictures the north end of the slate belt as involved in mushroom folds, overlapping into the adjacent tectonic units on at least three sides. It thus implies considerable, although perhaps superficial, horizontal telescoping of the rocks, both in the north-south and in the east-west directions. The geometric problem posed by this requirement is enormous and, combined with the other arguments, constitutes formidable argument against the autochthonous hypothesis.

In favor of this hypothesis, one might mention the finding of Trenton rocks unconformably on the Taconic rocks, as reported by Bucher (1957) from the southern part of the slate belt. However, the idea that the Taconic sequence may have been emplaced into a Trenton sea in which black mud was depositing makes it possible to incorporate Trenton unconformities into an allochthonous scheme, and so this evidence is not compelling.

The autochthonous hypothesis avoids the embarrassing problem of large-scale transport of rock units over long distances, as well as the problem of locating a root zone for such transported masses. This problem is indeed immense when account is taken of the entire slate belt. Arguments against the autochthonous hypothesis are so strong, nevertheless, that other ideas should be seriously considered.

Allochthonous Hypothesis (Figure 7A)

The hypothesis that the Taconic rocks represent a mass thrust into their present position is of long standing. It was first proposed by Ruedemann (1909, p. 189) and later defined by Keith (1912; 1913). Keith (1913) places the thrust plane at the contact of the black phyllite and the Ordovician carbonate sequence; however, Fowler (1950, p. 36) considers this contact to represent a mid-Trenton unconformity and proposes to locate the thrust at the contact of black and green phyllites (1950, p. 65), which he calls Hortonville and Mettawee, respectively.

The present writer pictures a series of nested thrust slices of the Taconic rocks. Each slice is internally folded and faulted; the folds may be recumbent and isoclinal. Because of the many similarities between this picture and the simple thrust idea of Keith, the two concepts will not be separately discussed. The writer's interpretation can be simply adapted to Keith's hypothesis merely by relaxing certain geometric requirements to allow the presence of truncated structures.

The favored hypothesis assumes the existence of a major recumbent and isoclinal bottoming fold in the Giddings Brook area. The fold is not rooted in place; instead the core projects into the air east of the Taconic Range (Fig. 4; Pl. 5, Section C-C′). During the formation of the Middlebury synclinorium, both limbs of the fold have been folded as a unit to yield a broad, south-plunging synclinal form.

The axial plane of this recumbent bottoming fold is taken to be nearly horizontal, with a gentle south dip. The fold must close westward along a north-south line, with the possible exception of the extreme north end where the closure may swing north-northeast. The above conclusions are based largely on the regional tectonic trend. The Green Mountain anticlinorium, the Vermont valley carbonate belt, and the Taconic slate belt all have north-south trends and are relatively narrow in the east-west direction. Therefore, if rocks of the slate belt are allochthonous, they presumably conform to the general regional trend. This notion is supported by the north-south trend of the structural elements within the major portion of the slate belt. The westward closure of the Giddings Brook bottoming fold conforms to the general westward tectonic transport observed in central and western Vermont. The stratigraphic displacement across the Pine Pond thrust, with older strata resting upon younger units to the west, is also compatible with a westward direction of movement.

Under this hypothesis, the east-west bedding strike with gentle southward dip, across the central part of the area, has no fundamental significance. This feature is interpreted as the superimposition of a locally accentuated southerly axial-plane dip upon both limbs of a nearly flat-lying fold.

The amplitude of the topping fold at Ganson Hill must be considerably less than the east-west extent of the Ganson Hill syncline, for two reasons. The Scotch Hill syncline, which corresponds to the same tectonic position, is a simple overturned fold with the West Castleton formation closing locally, as can be seen on a cliff on Scotch Hill Road (Pl. 3, fig. 2): This would not be so if the structure has great depth to it. Furthermore, if this topping fold has great depth, one might expect this to be reflected in the trace of the base of the West Castleton slate on the west side of the Ganson Hill patch, which should then continue much farther south on the map than it does. One must therefore conclude that the trend of closure swings northeast near the north end of Lake Bomoseen.

The bulge in the map pattern of the Biddie Knob formation northeast of Sargent Hill leads, under this hypothesis, into the fragmentary anticline of Biddie Knob formation near Keeler Pond. This, as well as the area of Biddie Knob formation south of Castle Hill, represents relatively minor folds or digitations on the main structure.

According to the interpretation presented in these paragraphs, the girdle of black slate at the extreme north end of the slate belt is the lower limb of the bottoming fold, facing down. Similarly, the belt of Bull formation from Barber Ledge to Huff Pond is the core of a syncline with upside-down sequence; this fits well with the structural data. It dips south, in turn, under the West Castleton formation. The first face-up section of the West Castleton formation is encountered in the belt running east-west near High Pond (near Walker Pond), and the close approach of these two sections of West Castleton formation is taken to be the result of extreme attenuation of the section here.

The Pine Pond thrust slice is taken to be another digitation on the upper limb of the bottoming fold that has broken through to form a thrust. There is thus naturally no thrust fault on its east side.

The structural units from Pine Pond thrust westward as far as the Great Ledge all belong to the upper limb of the postulated bottoming fold. The Cedar Mountain and Scotch Hill synclines are parts of minor digitations on this limb; they may be formed in part by the later deformation which has refolded all the structural elements along north-south axes with westerly overturn, and which also created the folds in the earlier cleavage.

The compound hairpin structure of Porcupine Ridge and Great Ledge, however, cannot, because of its northward coalescence on the map, be explained so simply. It is interpreted as the frontal portion of the Giddings Brook bottoming fold, at a higher stratigraphic level, with a dominant westerly movement sense but with sufficient south plunge to give it its northerly closure (Fig. 5). The Mount Hamilton syncline is therefore nested within this structure. The Mettawee slate west of Great Ledge is taken to belong to the inverted limb of the anticline. Unfortunately, outcrops in this area are so poor that the true structure may never be known. The structural position of the Bomoseen graywacke east of Forbes Hill, for instance, is not clear.

Since the Scotch Hill syncline is the geometric continuation of the Ganson Hill syncline, one expects the Porcupine Ridge digitation to be the continuation of the fragmentary Keeler Pond digitation. Thus the Bomoseen graywacke in the core of the former should be connected with the belt of Bomoseen graywacke north of Ganson Hill. A large patch of Bomoseen graywacke does exist south of Austin Pond (G-6). The presence of the small area of West Castleton formation southeast of Austin Pond, however, shows that the Bomoseen graywacke must be located on the culmination of a synclinal axis and thus represents a continuation of the inverted belt of Bomoseen graywacke south of Ganson Hill.

The discontinuous nature of the Bomoseen graywacke between Halfmoon Lake (F-7) and Beebe Pond is best explained by excessive local attenuation of the section, or large-scale boudinaging (Fig. 5). Thus, at many places, only a narrow belt of Bull formation separates the normal and inverted beds of the West Castleton. One such constriction is southwest of Hinkum Pond, another is south of Beebe Pond, and a third is at Halfmoon Lake. These narrows line up along the strike. They are interpreted as the loci of boudinaging. The isolated patch of Bomoseen graywacke just east of Halfmoon Lake may be a remnant of this process as it lies on the northwest side of the Scotch Hill syncline; this patch, however, cannot be traced, nor can its structural role be established. No mappable unit of Bomoseen graywacke exists just south of Beebe Pond, although isolated outcrops are locally lithologically similar to it.

Under this interpretation, the black slate at Black Pond, and possibly even as far as Hortonville, is the inverted West Castleton formation. The local stratigraphic, lithologic, and structural arguments in favor of this idea have been discussed.

The concept of large-scale boudinaging is not new. For example, it has been used in the interpretation of the Beinn Dronaig area (McIntyre, 1952), where the Lewisian gneiss is supposed to be the severed core of a nappe. Similar features are shown by Thompson (*in* Rodgers *et al.*, 1952, map) for some structures on the Chester dome.

The Sunset Lake area poses a problem. If the Great Ledge–Porcupine Ridge structure is a recumbent bottoming fold, the Sunset Lake area cannot be directly connected with it. This is a matter of solid geometry, but agrees with the divergent stratigraphy and structure of the two areas. The Sunset Lake area must then be regarded as a separate unit, a distinct thrust slice.

At the southeast part of the map area, the Bird Mountain slice must also be a distinct unit.

The belt of Biddie Knob formation along the east flank of the Taconic Range is supposed to connect with the root zone from above. The Bull formation and at least part of the black phyllite, to the east, therefore, belong to the inverted limb and should dip west. That this appears to be the case is shown by the reentrant outcrop pattern in a number of mountain ravines; elsewhere the paucity of reliable bedding dips makes determination of structure difficult.

Finally, the Sudbury thrust slice is taken to be a sliver of Ordovician bedrock dragged along the sole of the recumbent bottoming fold. The Bald Hill anticline is interpreted as a drag fold formed by the motion of the major structure.

One feature that cannot be conveniently explained by the recumbent bottoming-fold hypothesis is related to the Great Ledge-Porcupine Ridge structure. If, consistent with previous discussions, this structure is the severed frontal part of the Keeler Pond digitation, and if the Bomoseen graywacke transgresses down into the lower Mettawee slate and possibly supplants part of the Biddie Knob formation, then the Bomoseen graywacke might be expected to reappear in the inverted limb of the bottoming fold east of the Taconic Range. Such is not the case. One must therefore assume that in the sedimentary basin the Bomoseen graywacke was confined to a narrow median belt which has now by coincidence become the frontal part of the structure. Such an assumption is admittedly artificial and unconfirmable. On the other hand, this problem is neatly disposed of by the hypothesis of a simple thrust sheet as envisioned by Keith and later workers. Whereas in any hypothesis predicated on a geometrically integral unit one must explain this problem by rapid and perhaps improbable facies change, the simple thrust hypothesis explains the observed relations by invoking different depositional environments whose initial relative dispositions are to be worked out according to particular ideas of sedimentary pattern.

The recumbent-fold hypothesis is inconsistent with the local evidence at William Miller Chapel, which supports the idea of the simple thrust hypothesis. However, the observed structural relations may be explicable in terms of local thrust faults. The bulk of evidence definitely supports the recumbent-fold idea.

The recumbent-fold hypothesis demands the existence, in the black-phyllite and slate terrane peripheral to the Taconic sequence, of a major thrust fault. This fault can be located with reasonable certainty on the west side of the Taconic sequence and locally is even demonstrable; however, on the north and east sides the location of a fault is conjectural. This problem of a hypothetical fault exists also, however, for the autochthonous hypothesis and seems to be intrinsic to the Taconic problem itself.

The allochthonous hypotheses demand a root zone for the Taconic sequence and suppose that colossal masses of rocks have been transported as coherent units over long distance. The root zone is probably to be sought to the east. The nearest region where the root zone could conceivably be located is the Green Mountains, which thus gives a minimum distance of transport of 20 miles. This figure is undoubtedly low since erosion must have reduced the westward extension of the Taconic sequence. Erosion, moreover, presumably has also denuded higher levels of the Taconic sequence so that a developed, or palinspastic, map of the slate belt would yield only the minimum original east-west extension of the sedimentary basin.

Keith (1932, p. 404) suggests that the root zone lies near the base of the Paleozoic sequence of eastern Vermont. His line corresponds to the base of the Pinney Hollow formation (Thompson, *in* Rodgers *et al.*, 1952, p. 20). Field work in that area by Hawkes (1941, p. 660–664), Thompson (1950, Thesis, Mass. Inst. Technology), and Chang (1950, Thesis, Harvard Univ.), however, seems to have conclusively ruled out this possibility. Hawkes' suggestion (1941, p. 655) that the root zone may be located along the western front of the Green Mountains does not seem to be borne out by later, more detailed mapping in that area (Brace, 1953).

The answer may lie in gravity sliding, perhaps in part submarine (indeed, much of the complex structure within the Taconic sequence may have resulted from earlier soft-rock deformation); this accords with the explanation of the Forbes Hill conglomerate. A tectonic root zone then becomes unnecessary. Similar features of comparable magnitude have been attributed to gravity sliding in the Alps (DeSitter, 1956, p. 277; 279 ff.), in the Apennines (Migliorini, 1948; DeSitter, 1956, p. 286), in the Scottish Highlands (Cummins and Shackleton, 1955), to mention but a few examples; indeed it has been suggested by various workers for the Taconic sequence itself. (See, for instance, Fowler, 1950, p. 68; Rodgers, *et al.*, 1952, p. 12.) However, structures in the best-studied area, the Alps, have been interpreted to mean that sliding is a secondary phenomenon in orogenic movements superimposed upon causative recumbent folding (DeSitter, 1956, p. 290). In addition, Hubbert and Rubey (1959, p. 153) have shown that, if anomalous water pressure in the sediments has aided in the occurrence of thrusting, the situation could be brought about most effectively by the application of tectonic stresses in the horizontal direction. The tectonic as well as geographic problem of a root zone, therefore, remains.

Summary

Hypothesis: AUTOCHTHONOUS

Structural Motif: Concentric mushroom folds locally passing into recumbency; break thrusts in the southeastern portion of the map area; normal fault or thrust in the northwestern portion

Merits:

(1) Avoids the need for large-scale transport of rock units from distant sources
(2) Avoids the need for a root zone, as yet unlocated
(3) Faunal evidence suggests an intermediate position between the Atlantic and the Pacific provinces (Lochman, 1956, p. 1353)

Defects:

(1) Unconventional sense of movement (particularly in the Taconic Range), in conflict with observable structures
(2) Geometric difficulties associated with concentric, recumbent folds
(3) Need for arbitrary fault contacts within the black slate on all sides
(4) Need for rapid facies change in Early Cambrian through Middle Ordovician times

Sequence of Events:

(1) Deposition
(2) Mushroom folding with thrusting, at least in part during or after Trenton time
(3) Emplacement of the Florence nappe
(4) Shallow folding with westerly movement sense, producing most of the readily observable structures and folding of the earlier cleavages.

Hypothesis: ALLOCHTHONOUS, SIMPLE THRUST SLICES

Structural Motif: Shallow thrust sheets; anticlines may be without roots and not directly connected with one another

Merits:

(1) Avoids reinterpretation of the Hortonville formation
(2) Avoids need for intricate geometric relationships
(3) Thick section of Bomoseen graywacke west of Lake Bomoseen readily explained
(4) Divergent structures at Sunset Lake and at Bird Mountain readily explained
(5) Uniquely explains the relations at William Miller Chapel

Defects:

(1) The youngest, rather than the oldest, units of the section come most commonly in contact with the autochthone
(2) Need for arbitrary faults within the black-slate terrane
(3) Need for a root zone (unlocated) and a site of deposition for the rocks that continue as far south as the Catskill quadrangle, New York
(4) Mechanical problem of the movement of large masses of incompetent rocks over large distances

Sequence of Events:

(1) Deposition
(2) Possible folding
(3) Break thrusting or sliding, resulting in the emplacement of the rock units at the present site during or later than mid-Ordovician time, with concurrent folding, thrusting, and local development of recumbent folds
(4) Emplacement of the Florence nappe
(5) Shallow folding with westerly movement and development of late structures, including cleavage folds

Hypothesis: ALLOCHTHONOUS, RECUMBENT FOLD COMPLEX

Structural Motif: Large recumbent folds in the central part of the area, with both limbs preserved; hinge lines of the folds are north-south; complex digitations on the folds locally passing into thrust faults

Merits:

(1) Explains readily the east-west trending beds in the central part of the area

(2) Readily explains the fact that the youngest beds most commonly come in contact with the autochthone

(3) Explains the lithologic and stratigraphic correspondences between slate of the West Castleton formation and the black slate underlying the Taconic sequence

(4) Explains the apparent westerly dip on the east flank of the Taconic Range

Defects:

(1) Difficulty in explaining the absence of Bomoseen graywacke in the eastern portion of the map area

(2) Demand for large-scale boudinaging

(3) Need for arbitrary faults within the black-slate terrane

(4) Need for an unlocated root zone and a wide original sedimentary basin

(5) Incapability of explaining the Sunset Lake and Bird Mountain areas as integral units

(6) Inconsistent with structures around William Miller Chapel

(7) Mechanical difficulties in transporting large masses of incoherent material

Sequence of Events:

(1) Deposition

(2) Formation and emplacement of the recumbently-folded units

(3) Cross-folding of the axial plane on an east-west axis, at places recumbent

(4) Late shallow folding producing the visible structures, with westward sense of movement

SOURCE OF SEDIMENTS AND LOCATION OF SEDIMENTARY BASIN

A structural synthesis of the area leads to the question of the paleogeography of early Paleozoic time in New England. This problem has recently been dealt with by Lochman (1956) on the basis of lithologic and faunal evidence, and on the assumption that the Taconic rocks are autochthonous. It is therefore pertinent to restate this problem in the light of the present findings.

Before delving into the details, it will be useful to set down the following relevant features of the sediments as found in the Castleton area:

(1) The rocks are predominantly clastic, with very little carbonate and no volcanic rocks. Among the clastic rocks, argillites predominate, and graywackes and arkoses are also important. Orthoquartzites are rare.

(2) The rocks are Early Cambrian to Middle Ordovician in age although the Cambrian fossils are not identical with those found in northwestern Vermont or immediately west of the Green Mountain front. Lochman, after an analysis of the faunas, suggests (1956, p. 1360) that the distinction is due to ecological rather than geographical barriers.

(3) The rock units are thin. Dale (1898, p. 178) gives an estimated maximum thickness of 830 feet for the Cambrian, while Swinnerton measures several incomplete sections and gives thicknesses between 2000 and 3000 feet (1922, Thesis, Harvard Univ., p. 145, 148, 151, 153). Swinnerton's figures may be too high owing to his failure to consider repetition of beds, whereas Dale's is likely low since he excludes the "Berkshire schist" to which belong most of the Biddie Knob formation and the lower part of the Bull formation. A figure of 2000 feet for the exposed Taconic sequence seems to be a fair estimate.

(4) The arkoses and graywackes in the Taconic sequence commonly contain coarse grains of quartz and feldspar. At the base of the Zion Hill quartzite, especially, pebbles have been found consisting of muscovite books and quartz grains still retaining their crystal outlines. Thus the source must have been coarsely crystalline and probably nearby.

(5) Rocks of the Taconic sequence continue south from the map area at least as far as the Catskill quadrangle, in Dutchess County, New York (Ruedemann, 1942; Goldring, 1943).

If the autochthonous hypothesis is correct, the sediments may be derived from outside, or from islands within the basin of deposition. The second alternative is attractive because it furnishes a nearby source. However, not the slightest indication for these islands exists. If the sediments were derived from outside, two alternatives exist: an easterly or a westerly source.

The sediments may be derived from the Green Mountains or even from sites farther east, depending in part on the age assignment of the Paleozoic section east of the Green Mountains. One might object to this source, as between the Green Mountains and the Taconic Range the country is underlain by a thick section of Lower Cambrian through Middle Ordovician orthoquartzites and carbonates (Thompson, *in* Rodgers *et al.*, 1952; Brace, 1953).

A possible westerly source remains to be considered. Between the areas of the Taconic sequence and the Precambrian rocks of the

Adirondack region, the oldest Paleozoic rocks are Upper Cambrian, followed by carbonates ranging into the Middle Ordovician (Rodgers, *in* Rodgers *et al.*, 1952, p. 34–36). Thus, although the contrasts in rock types cannot be invoked against a western source for the Lower Cambrian sequence, they remain for the Upper Cambrian to Middle Ordovician Mount Hamilton group. For an autochthonous hypothesis, source areas inside the basin of deposition seem necessary. Such interior sources are unlocated, and available data are against their existence.

If the Taconic rocks were allochthonous, then the two alternatives, east and west, still remain, both as possible sources of sediments and as possible sites of sedimentation.

If the site of deposition were the present Green Mountain core, a source area to the west is ruled out because of the intervening belt of contemporaneous carbonate deposits. A source area to the east is left open.

One possible objection is that the sedimentary basin required by the Taconic rocks may be too wide for the known Green Mountain area. However, what is exposed of the latter today may be only the root zone of the original structure which may have been much more extensive.

Another objection is that, since the Taconic rocks, if allochthonous, must have been emplaced no earlier than Late Normanskill or Trenton time, and since these rocks continue southward uninterrupted at least to Dutchess County, New York, the fact that the Lower Cambrian Cheshire quartzite wraps around the south-plunging Green Mountain anticlinorium near Williamstown, Massachusetts (Prindle and Knopf, 1932), is against the hypothesis. However, Prindle and Knopf show a thrust fault just east of Clarksburg Mountain (1932, p. 269, also sections B, C), bridging the Precambrian rocks of the Green Mountains with those south of Adams. Thompson (*in* Rodgers *et al.*, 1952, p. 18) suggests that this fault may in fact be a mid-Ordovician unconformity; this is also so shown on Herz's map of the Cheshire quadrangle (1958). Exact dating of this break, whatever its nature, is necessary in order to determine whether it could resolve the dilemma.

An alternative possibility is that the Taconic rocks were deposited over portions of the Adirondack basement and later transported eastward. Strong arguments against this idea may be given. Such a sense of movement contradicts all known structural data and regional trend west of the Green Mountains. Furthermore, the Precambrian core of the Adirondacks terminates southward north of the Mohawk valley and is overlain by Upper Cambrian and Lower Ordovician units. These facts are incompatible with the requirement that the Taconic allochthone be emplaced no earlier than Trenton time.

REGIONAL CORRELATION

Introduction

The results of the present study lead to possible correlations with rock units elsewhere in New England, in eastern New York, and in southern Quebec. Correlation with the eastern New York section has been indicated throughout the discussion and is summarized in Table 2; the other correlations will be briefly discussed.

Correlation with the Eastern Vermont Section

In eastern Vermont a thick section of dominantly clastic rocks of Early Paleozoic age rests unconformably on the Precambrian of the Green Mountains (Thompson, *in* Rodgers *et al.*, 1952; Brace, 1953). The best-dated of these units is the Cram Hill formation, which grades into the Moretown formation below (Thompson, *in* Rodgers *et al.*, 1952, p. 18) but is separated from the Shaw Mountain formation above by an unconformity (Currier and Jahns, 1941, p. 1501). Currier and Jahns (1941, p. 1496) correlate the Cram Hill formation with the fossiliferous Magog slate at Castle Brook, Magog, Quebec (Ells, 1886, p. 16). According to Ruedemann (1947, p. 69, 70), the Magog slate is Late Normanskill and perhaps slightly younger; by and large it is correlative with the upper beds of the Mount Hamilton group and/or the Pawlet formation —certainly a correlation between the Upper Mount Hamilton and parts of the Moretown formation (or Beauceville in Quebec; Osberg, 1956) is indicated.

Apart from effects of metamorphism, the Moretown and Cram Hill formations have many features reminiscent of much of the Mount Hamilton group. The Moretown is dominantly gray or green, finely interbedded quartzites and pelites, including the "pin-stripe" type, but in places contains magnetite which, in lower grades of metamorphism, may be hematite which would color the rock red or purple. (For description of the Moretown and Beauceville, see Clark, *in* Cooke, 1937; Thompson, 1950; *in* Rodgers *et al.*, 1952;

Rosenfeld, 1954, Thesis, Harvard Univ.; Cady, 1956a; Albee, 1957.) The pin-stripe lithology is regarded by Thompson (1950, Thesis, Mass. Inst. Tech., p. 42) and Rosenfeld (1954, Thesis, Harvard Univ. p. 43) as due to primary sedimentary banding and may be compared with the fine interbedding of quartzite and slate in the Mount Hamilton group. (*See* also Dale, 1898, p. 190.)

The Whetstone Hill member of the Moretown formation (Thompson, 1950, Thesis, Mass. Inst. Tech., p. 42) contains numerous manganiferous bodies, comparable to the manganiferous lenses in the "Hudson red and green slates," now mapped as part of the Mount Hamilton group, described by Dale (1898, p. 190, 260).

This correlation, however, is not without its difficulties. Thus, the Cram Hill and less so the Moretown (Thompson, *in* Rodgers *et al.*, 1952; Cady, 1956a), as well as the Beauceville (Gorman, 1954) carry assorted volcanic rocks which are absent from the Mount Hamilton group. Lateral pinchout of the volcanic rocks is one explanation; indeed such pinchouts are known within the area of the eastern Vermont sequence (Thompson, *in* Rodgers *et al.*, 1952, p. 40; 1959, oral communication). However, it is an additional assumption that has not been verified.

The Mount Hamilton group lacks good pin-stripe structure. Such a structure, however, is probably an accentuation of original compositional banding, and the quartzose-slaty interlayers of the banded Mount Hamilton group may well be the protolith.

The contrasting thicknesses of the Moretown–Cram Hill and the Mount Hamilton

TABLE 2.—CORRELATION OF FORMATIONS IN ADJACENT AREAS

	N.W. Taconics Zen (this report) Cady (1945)	E. Taconics and Vt. Valley Thompson (1952) Brace (1953) MacFadyen (1956)	S.W. Quebec Cady (1956b) Cooke (1937; 1950) Dresser and Denis (1944) Osberg (1956)	N. Central Vermont Albee (1957) Cady (1956a)	S.E. Vermont Thompson (1950; 1952) Rosenfeld (1954)	Quebec City Area Rasetti (1946) Osborne (1956)	E. New York Dale (1904b) Ruedemann (1914)	
Middle Ordovician	Hortonville and Ira (including Forbes Hill) Pawlet	Mt. Anthony Walloomsac	Stanbridge Magog Beauceville	Moretown	Cram Hill	Quebec City (including Citadel)	Snake Hill (including Rysedorph) Normanskill	Middle Ordovician
Lower Ordovician	Mount Hamilton Autochthonous carbonate sequence of the synclinorium	Canadian limestone	Beauceville ?		Moretown Whetstone Hill	Levis (Ville Quay)	Deepkill Schaghticoke	Lower Ordovician
Upper Cambrian		Clarendon Springs Danby	Monsonville	? Stowe Ottauquechee	? Stowe Ottauquechee ?	Lauzon		Upper Cambrian
Middle Cambrian					?	? ?		Middle Cambrian
Lower Cambrian	West Castleton Bull Biddie Knob	Winooski Monkton Dunham Cheshire Mendon	? Sutton Schist ?	Camels Hump	Pinney Hollow Grahamville Tyson	Charny ?	Diamond Rock Schodack Nassau	Lower Cambrian

sequences pose another problem. The Moretown–Cram Hill sequence is thick: Thompson (*in* Rodgers *et al.*, 1952, p. 40) gives 3700 feet for the Moretown alone, and Cooke (1950, p. 45) gives 10,000 feet for the Beauceville which includes the Magog slate, correlative of the Cram Hill. The Mount Hamilton group on the other hand is relatively thin. Dale (1898, table facing p. 178) gives a cumulative maximum thickness of about 1000 feet, which is undoubtedly high. Whether such rapid thinning is plausible is a question.

The Beauceville is correlated with the Stanbridge slate of the Granby area (Osberg, 1956; Dresser and Denis, 1944, p. 396), which is said to overlie unconformably, at least in part, the Sillery (Ells, 1896, p. 53; W. M. Cady, letter, November 27, 1958). This might appear inconsistent with a correlation of the Beauceville with the allochthonous Mount Hamilton group. In an earlier section it was, however, proposed that the emplacement of the Taconic sequence may be a Trenton event, and therefore some Normanskill slate may unconformably overlie the Taconic sequence.

The correlation of the units below the Moretown and the upper Mount Hamilton group is more problematical, partly because of the uncertain age of the pre-Moretown formations. In southern Quebec, Osberg (1956) correlates the Mansonville, which includes the Ottauquechee formation (Cady, 1956b), across the Sutton Mountain axis, with the Sweetsburg slate, which in turn is correlated by Booth (1950, p. 1138, 1153) with the Middle Cambrian Skeels Corners formation in northwestern Vermont (Shaw, 1958, p. 532). Thus the Hoosac–Pinney Hollow formations in eastern Vermont, underlying the Ottauquechee (*in* Rodgers *et al.*, 1952, p. 40), could be correlative of the Lower Cambrian Taconic rocks. These rocks are indeed lithologically similar, but detailed correlation is still risky.

Correlation with the Quebec City Area

The geology of Quebec City and vicinity has been restudied and summarized by Osborne (1956), who gives detailed lithologic data. The fossil records have received modern study by Rasetti (1945). The Lower Cambrian Charny formation (Rasetti, 1946, p. 698; Osborne, 1956, p. 175) contains the *Austinvillia* fauna (Rasetti, 1945) which according to Lochman (1956, p. 1350) is slightly younger than the *Elliptocephala* fauna of the Taconic region. Nevertheless, the Lower Cambrian rocks of the Quebec City area and the Taconic sequence of the Castleton area are similar, and a broad correlation is indicated (Rasetti, 1946; Osborne, 1956, p. 177–178). The Charny formation is succeeded by the Middle and Upper Cambrian Lauzon formation (Osborne, 1956, map; Upper Cambrian to Canadian according to Rasetti, 1946, p. 701), lithologically similar but containing numerous limestone conglomerate beds resembling those in the overlying Beekmantown Levis formation, into which it grades (Rasetti, 1946, p. 701). The Lauzon formation apparently is not everywhere present, for Rasetti describes a pseudoconformable contact between the Lower Cambrian and Canadian units at Ville Guay (1946, p. 695) with few intervening strata.

The limestone conglomerate, common in the Lauzon and Levis formations (Osborne, 1956, p. 181, 183, 185), has gray limestone blocks in a quartz-carbonate matrix. The writer examined this unit at Fort Lauzon under the guidance of Professor Osborne in 1957 and found the unit strikingly similar to the "edgewise conglomerate" in unit (5) of the Mount Hamilton group, although parts of it also resemble unit (6). The Levis formation is classical for its Deepkill graptolite fauna (Ruedemann, 1947, p. 56–57), whose age supports the suspected age of the middle portion of the Mount Hamilton group.

MAJOR UNSOLVED PROBLEMS

Relation Among Different Tectonic Units

Four distinct tectonic units within the Taconic sequence have been discussed: the Giddings Brook bottoming fold and its related units; the Great Ledge–Porcupine Ridge area; the Sunset Lake area; and the Bird Mountain slice. Although the map patterns have been traced out in some detail, their proper relations cannot always be uniquely determined.

The stratigraphic contrast between the Pine Pond slice area and the Bird Mountain slice has been mentioned. It was concluded that a dislocation probably exists between these units. Such an idea fits with the termination of the Biddie Knob formation in the Taconic Range; however, it brings a host of its own problems: What is the nature of the fault? Before the movement how closely related were the rocks from the two sides of the fault?

The structural relation between the Porcupine Ridge–Great Ledge fold and the surrounding units remains obscure. Evidence suggests that a recumbent bottoming fold combined with a rapid facies change in the Mettawee slate-Bomoseen graywacke sequence best suits the data; however, this decidedly is not a unique solution. A proper understanding of this tectonic unit will go far toward unraveling the regional structure as well as toward reconstruction of the paleogeography of the sedimentational basin.

The Sunset Lake area is so distinct from the adjacent region to the southeast in its detailed lithology, stratigraphy, and structural trend that there is little question that a separate slice in involved. In support of this, the geometric pattern at the north end of the Great Ledge fold makes it virtually impossible to construct a cross section for the Sunset Lake area, incorporating the latter in a single tectonic unit. Just where the dislocation occurs, however, is largely speculative; the natural place to put it seems to be along Hubbardton River (C-7) which separates the Great Ledge structure from the rocks of the Sunset Lake area.

Differentiation of Black Slates

Perhaps the biggest unsolved problem in the area, both in scope and regional significance, is the differentiation of the several black slates and phyllites. At least four black slates are known in the area: the Lower Cambrian West Castleton formation, the Lower (?) Ordovician black slate (units 2 and 5) of the Mount Hamilton group, the Middle Ordovician Pawlet formation, and the Trenton black slate of the Synclinorium sequence. In the field, these black slates cannot always be distinguished, and their stratigraphic relations with units of the Bull formation are also commonly curiously alike. Possibly at places the various autochthonous and allochthonous black slates are so commingled that they cannot even in principle be mapped separately. Since, however, much of the structural interpretation—or even definition—of the Taconic problem depends on the proper recognition of the different black slates, this remains the most urgent point to be settled. The local details have been considered; only a few salient points need to be mentioned as summary:

(1) What is the age of the black phyllite on the east slope of the Taconic Range? If part of it is Early Cambrian, where is the contact? Decision on this point will affect not only the interpretation of the geometry of the Giddings Brook bottoming fold, but through its control limit the geometry, and therefore the possible origin, of the Taconic sequence as a whole.

(2) What is the black slate north of Huff Pond as far as the Ordovician marbles to the north, and what is its relation to the type Hortonville? What, in fact, is the age of the Hortonville slate itself?

(3) What is the age of the black slate matrix of the Forbes Hill conglomerate? Decision on this point is vital because if it is Trenton it will figure prominently in the chronologic and tectonic reconstruction of the emplacement of the Taconic sequence.

(4) A proper delineation of the contact between the West Castleton formation and the Mount Hamilton group is vital to an understanding of the Cambro-Ordovician boundary. For instance, does the contact mark a low-angle unconformity, simple nondeposition, or a continuous record with a vastly attenuated and unfossiliferous intervening section? Much of this question can be intelligently discussed only when the age of the black slate found between the fossiliferous Lower Cambrian and the unquestioned Upper Cambrian can be determined.

(5) Because of their lithologic similarity, the proper age assignment of most of the black slates in the map area is suspect wherever no fossil evidence exists. Among such areas may be mentioned the bulk of the Ganson Hill syncline, the Hooker Hill syncline, the Graham Hill syncline, the numerous patches of black slate west of the crest of the Taconic Range, the black slate patches in the Sunset Lake area, and the extensive areas of black slate within and around the Bird Mountain slice. Although the regional structure would not be changed much by an age shift from the Early Cambrian, say, to the Early Ordovician, detailed reconstruction of the geologic history would be affected.

Age of the Biddie Knob Formation

In this report, the purple and green, chloritoid-bearing phyllite has been called the Biddie Knob formation and assigned to an Early Cambrian age because of its apparently conformable relation with the overlying fossiliferous Early Cambrian units. This unit lithologically resembles the Greylock or Mount Anthony formation which MacFadyen gives a Middle Ordovician age (1956, p. 29). J. B. Thompson, Jr., has pointed out that, once a fault contact is admitted between the Lower

Cambrian units and the synclinorium sequence, then it is an open question where it lies; in particular, there is no *a priori* reason why the Biddie Knob formation cannot be autochthonous. At least part of the Biddie Knob formation—that in the Giddings Brook bottoming fold—is almost certainly Lower Cambrian because northwest of Biddie Knob this unit contains, near its top, the Zion Hill quartzite which may be directly correlated with the Zion Hill quartzite to the west along the same structure, where (*e.g.*, 1234-foot knob east of Sargent Hill; on Lake Bomoseen by the "float bridge") primary tops sense, if extrapolated eastward, indicates an inverted section on the east slope of the Taconic Range. Even such tenuous control as this, however, is lacking south of Castleton River, and one cannot exclude the possibility of autochthonous rocks in the Bird Mountain slice, although the writer judges this unlikely. Finally, it is yet conceivable that the age assignment of the Mount Anthony formation may be altered again, thus affecting the problem of correlation.

Geometry of the Sudbury Thrust Slice

Interpretation of the geometric possibilities at the north end of the map area, where the crucial junction with the Ordovician Synclinorium sequence occurs, depends upon a proper understanding of the geometry of the Sudbury thrust slice. Because of the present reinterpretation of this slice as a detached unit rather than part of the Middlebury synclinorium, the stratigraphic tops within this unit, which Cady (1945) assumed to be upside down, ought to be critically re-examined. The writer has found no evidence that the section is not right side up; it is hoped that current detailed work by Marshall Kay and his students in this area will shed light on this problem.

Mechanical Problem of Thrusting Large Masses of Weak Material

If the Taconic sequence is allochthonous, then the classical problem of the mechanism by which such a large, and presumably relatively thin, mass of incoherent material could be transported as a unit over large distances becomes pressing. The dynamic difficulties are reviewed by Hubbert and Rubey (1959). However, Hubbert and Rubey show that many modern deep drill-hole records indicate that at depth the fluid pressure in the rocks may approach the rock pressure; under such circumstances the effective load of the rock approaches zero (1959, p. 135). These authors use this idea to explain some large thrust faults in western Wyoming (Rubey and Hubbert, 1959). The concept may be applied directly to the Taconic problem; the idea that the thrusting occurred before the rocks were completely consolidated makes the fluid-pressure mechanism attractive. The mechanism is particularly applicable to argillaceous rocks for which the porosity is high but permeability is low; the Taconic rocks fit the requirement. The mechanism, however, requires rapid sedimentation or rapid increase in tectonic stresses, and thus rapid increase in fluid pressure; hence the events of thrusting and folding must have taken place in short time periods, before the excess pressure could have been appreciably dissipated by leakage of the fluid. Thus quantitative testing of the fluid-pressure hypothesis requires data on the mechanical properties of unconsolidated argillaceous rocks under pressure, as well as on the relative rates of sedimentation and escape of interstitial water. These data are not as yet available.

REFERENCES CITED

Albee, A. L., 1957, Bedrock geology of the Hyde Park quadrangle, Vermont: U. S. Geol. Survey Geol. Quadrangle Map 102

Balk, R., 1953, Structure of graywacke areas and Taconic Range, east of Troy, New York: Geol. Soc. America Bull., v. 64, p. 811–864

Booth, V. H., 1950, Stratigraphy and structure of the Oak Hill succession in Vermont: Geol. Soc. America Bull., v. 61, p. 1131–1168

Brace, W. F., 1953, The geology of the Rutland area, Vermont: Vt. Geol. Survey Bull. 6, 124 p.

Bucher, W. H., 1957, Taconic klippe—a stratigraphic-structural problem: Geol. Soc. America Bull., v. 68, p. 657–674

Cady, W. M., 1945, Stratigraphy and structure of west-central Vermont: Geol. Soc. America Bull., v. 56, p. 515–558

Cady, W. M., 1956a, Bedrock geology of the Montpelier quadrangle, Vermont. U. S. Geol. Survey Geol. Quadrangle Map 79

—— 1956b, Stratigraphic relationships in northern Vermont and southern Quebec (Abstract): Geol. Soc. America Bull., v. 67, p. 1811–1812

Cady, W. M., and Zen, E., 1960, Stratigraphic relationships of the Lower Ordovician Chipman formation in west-central Vermont: Am. Jour. Sci., v. 258, p. 728–739.

Cooke, H. C., 1937, Thetford, Disraeli, and eastern half of Warwick map areas, Quebec: Geol. Survey Canada Mem. 211, 160 p.

—— 1950, Geology of a southwestern part of the eastern townships of Quebec: Geol. Survey Canada Mem. 257, 142 p.

Craddock, J. C., 1957, Stratigraphy and structure of the Kinderhook quadrangle, New York, and the "Taconic klippe:" Geol. Soc. America Bull., v. 68, p. 675–724

Cummins, W. A., and Shackleton, R. M., 1955, The Ben Lui recumbent syncline (S. W. Highlands): Geol. Mag., v. 92, p. 353–363

Currier, L. W., and Jahns, R. H., 1941, Ordovician stratigraphy of central Vermont: Geol. Soc. America Bull., v. 52, p. 1487–1512

Cushing, H. P., and Ruedemann, R., 1914, Geology of Saratoga Springs and vicinity, N. Y. State Mus. Bull. 169, 177 p.

Dale, T. N., 1891, The Greylock synclinorium: Amer. Geologist v. 8, p. 1–7

—— 1895, Structural details in the Green Mountain region and in eastern New York: U. S. Geol. Survey Ann. Rept. 16, pt. 1, p. 543–570

—— 1898, The slate belt of eastern New York and western Vermont: U. S. Geol. Survey Ann. Rept. 19, pt. 3, p. 163–307

—— 1904a, The geology of the north end of the Taconic Range: Am. Jour. Sci., 4th ser. v. 17, p. 185–190

—— 1904b, Geology of the Hudson valley between the Hoosic and the Kinderhook: U. S. Geol. Survey Bull. 242, 63 p.

DeSitter, L. U., 1956, Structural geology: New York, McGraw-Hill Book Company, 552 p.

Dresser, J. A., and Denis, T. C., 1944, Geology of Quebec II. Descriptive geology: Quebec Dept. Mines Geol. Rept. 20, 544 p.

Ells, R. W., 1886, Report on the geology of a portion of the eastern townships of Quebec: Geol. Survey Canada Ann. Rept., new ser., v. 2, pt. J, 70 p.

—— 1896, Report on a portion of the Province of Quebec: Geol. Survey Canada Ann. Rept., new ser., v. 7, 157 p.

Foerste, A. F., 1893, New fossil localities in the early Paleozoics of Pennsylvania, New Jersey, and Vermont, with remarks on the close similarity of the lithologic features of these Paleozoics: Am. Jour. Sci., v. 146, p. 435–444

Fowler, P., 1950, Stratigraphy and structure of the Castleton area, Vermont: Vt. Geol. Survey Bull. 2, 83 p.

Goldring, W., 1943, Geology of the Coxsackie quadrangle, New York: N. Y. State Mus. Bull. 332, 374 p.

Gorman, W. A., 1954, Ste. Justine area: Quebec Dept. Mines, Geol. Surveys Br., Prelim. Rept. no. 297, 5 p.

Hawkes, H. E., Jr., 1941, Roots of the Taconic fault in west-central Vermont: Geol. Soc. America Bull., v. 52, p. 649–666

Herz, N., 1958, Bedrock geology of the Cheshire quadrangle, Massachusetts: U. S. Geol. Survey Geol. Quadrangle Map 108

Hubbert, M. K., and Rubey, W. W., 1959, Role of fluid pressure in mechanics of overthrust faulting, I. Mechanics of fluid-filled porous solids and its application to overthrust faulting. Geol. Soc. America Bull., v. 70, p. 115–166

Kaiser, E. P., 1945, Northern end of the Taconic thrust sheet in western Vermont: Geol. Soc. America Bull., v. 56, p. 1079–1098

Kay, G. M., 1937, Stratigraphy of the Trenton group: Geol. Soc. America Bull., v. 48, p. 233–302

—— 1941, Taconic allochthone and the Martic thrust: Science, v. 94, p. 73

—— 1942, Development of the northern end of the Taconic thrust sheet in western Vermont: Geol. Soc. America Bull., v. 53, p. 1601–1657

Kay, G. M., and Cady, W. M., 1947, Ordovician Chazyan classification in Vermont: Science, v. 105, p. 601

Keith, A., 1912, New evidence on the Taconic question (Abstract): Geol. Soc. America Bull., v. 23, p. 720–721

— 1913, Further discoveries in the Taconic Mountains (Abstract): Geol. Soc. America Bull., v. 24, p. 680

— 1932, Stratigraphy and structure of northwestern Vermont: Washington Acad. Sci. Jour., v. 22, p. 357–379, 393–406

— 1933, Outline of the structure and stratigraphy of northwestern Vermont: 16th Internat. Geol. Cong. Guidebook I, p. 48–61

Larrabee, D. M., 1939, The colored slates of Vermont and New York: Eng. Mining Jour., v. 140, no. 12, p. 47–53

— 1940, The colored slates of Vermont and New York: Eng. Mining Jour., v. 141, no. 1, p. 48–52

Leith, C. K., 1905, Rock cleavage: U. S. Geol. Survey Bull. 239, 216 p.

Lochman, C., 1956, Stratigraphy, paleontology, and paleogeography of the *Elliptocephala asaphoides* strata in Cambridge and Hoosick quadrangles, New York: Geol. Soc. America Bull., v. 67, p. 1331–1396

MacFadyen, J. A., Jr., 1956, The geology of the Bennington area, Vermont: Vt. Geol. Survey Bull. 7, 72 p.

McIntyre, D. B., 1952, The tectonics of the Beinn Dronaig area, Attadale: Edinburgh Geol. Soc. Trans., v. 40, p. 258–264

Migliorini, C. I., 1948, Composite wedges and orogenic landslips in the Apennines: 18th Internat. Geol. Cong. Rept. of the Sessions, pt. 13, p. 186–198

Osberg, P. H., 1952, The Green Mountain anticlinorium in the vicinity of Rochester and East Middlebury, Vermont: Vt. Geol. Survey Bull. 5, 127 p.

— 1956, Stratigraphy of the Sutton Mountains, Quebec; key to stratigraphic correlation in Vermont (Abstract): Geol. Soc. America Bull., v. 67, p. 1820

Osborne, F. F., 1956, Geology near Quebec City: Le Naturaliste Canadien, v. 83, p. 157–223

Prindle, L. M., and Knopf, E. B., 1932, Geology of the Taconic quadrangle: Am. Jour. Sci., 5th ser., v. 24, p. 257–302

Rasetti, F., 1945, Fossiliferous horizons in the "Sillery formation" near Lévis, Quebec: Am. Jour. Sci., v. 243, p. 305–319

— 1946, Cambrian and Early Ordovician stratigraphy of the lower St. Lawrence valley: Geol. Soc. America Bull., v. 57, p. 687–706

Rodgers, John, 1937, Stratigraphy and structure in the upper Champlain valley: Geol. Soc. America Bull., v. 48, p. 1573–1588

Rodgers, John, Thompson, J. B., Jr., and Billings, M. P., 1952, Geology of the Appalachian highlands of east-central New York, southern Vermont, and southern New Hampshire: Geol. Soc. America Guidebook for field trips in New England. p. 1–71

Rubey, W. W., and Hubbert, M. K., 1959, Role of fluid pressure in mechanics of overthrust faulting, II. Overthrust belt in geosynclinal area of western Wyoming in light of fluid-pressure hypothesis. Geol. Soc. America Bull., v. 70, p. 167–206

Ruedemann, R., 1909, Types of inliers observed in New York: N. Y. State Mus. Bull. 133, p. 164–193

— 1942, Geology of the Catskill and Kaaterskill quadrangles. Pt. I, Cambrian and Ordovician geology of the Catskill quadrangle: N. Y. State Mus. Bull. 331, 188 p.

— 1947, Graptolites of North America: Geol. Soc. America Mem. 19, 652 p.

Schuchert, C., 1937, Cambrian and Ordovician of northwestern Vermont: Geol. Soc. America Bull., v. 48, p. 1001–1078

Shaw, A. B., 1958, Stratigraphy and structure of the St. Albans area, northwestern Vermont: Geol. Soc. America Bull., v. 69, p. 519–568

Theokritoff, G., 1957, Use of the term "Schodack formation" in Washington County, New York (Abstract): Geol. Soc. America Bull., v. 68, p. 1804–1805

Twenhofel, W. H., *et al.*, 1954, Correlation of the Ordovician formations of North America: Geol. Soc. America Bull., v. 65, p. 247–298

Weaver, J. D., 1957, Stratigraphy and structure of the Copake quadrangle, New York: Geol. Soc. America Bull., v. 68, p. 725–762

White, W. S., 1949, Cleavage in east-central Vermont: Am. Geophys. Union Trans., v. 30, p. 287–294

Zen, E., *Editor*, 1959, Stratigraphy and structure of west-central Vermont and adjacent New York; Guidebook for the 51st Annual Meeting of the New England Intercollegiate Geological Conference, Rutland, Vermont, 85 p.

——, 1960, Metamorphism of Lower Paleozoic rocks in the vicinity of the Taconic Range in west-central Vermont: Am. Mineralogist, v. 45, p. 129–175

Manuscript Received by the Secretary of the Society, June 1, 1959

37–294
w York;
nference,

t-central

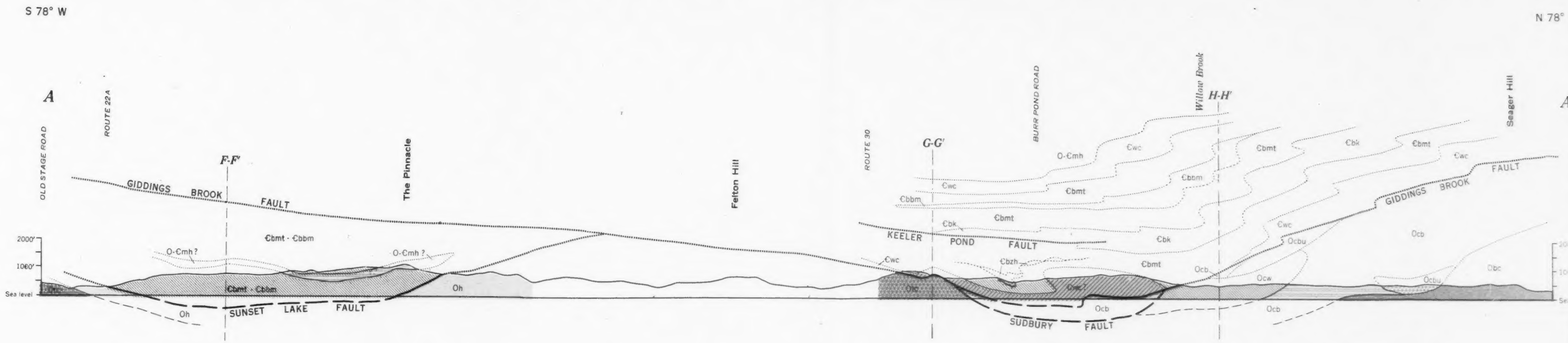
S 78° W
N 78° E
A
A'
OLD STAGE ROAD
ROUTE 22A
F-F'
The Pinnacle
Felton Hill
ROUTE 30
G-G'
BURR POND ROAD
Willow Brook
H-H'
Seager Hill
GIDDINGS BROOK FAULT
KEELER POND FAULT
SUNSET LAKE FAULT
SUDBURY FAULT
2000'
1000'
Sea level
Ɛbmt - Ɛbbm
O-Ɛmh ?
Oh
Ocb
Ocbu
Ocw
Obc
Ɛwc
Ɛbbm
Ɛbk
Ɛbmt
Ɛbzh
O-Ɛmh

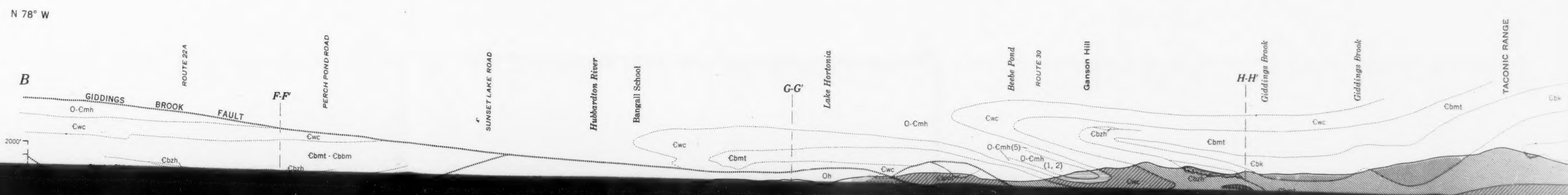
N 78° W
B
ROUTE 22A
F-F'
PERCH POND ROAD
SUNSET LAKE ROAD
Hubbardton River
Bangall School
G-G'
Lake Hortonia
Beebe Pond
ROUTE 30
Ganson Hill
H-H'
Giddings Brook
Giddings Brook
TACONIC RANGE
GIDDINGS BROOK FAULT
2000'
O-Ɛmh
Ɛwc
Ɛbzh
Ɛbmt - Ɛbbm
Ɛbmt
Oh
O-Ɛmh(5)
O-Ɛmh
(1, 2)
Ɛbk

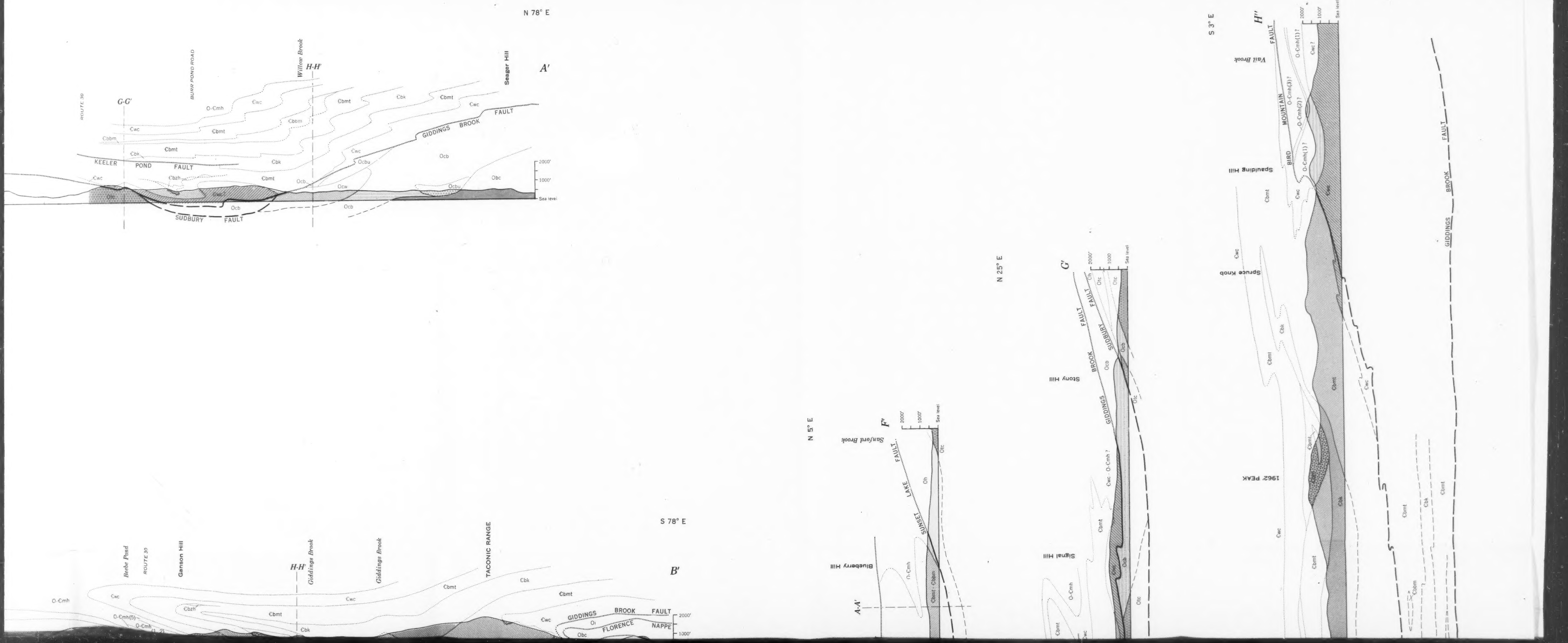

N 78° E
A'
ROUTE 30
G-G'
BURR POND ROAD
Willow Brook
H-H'
Seager Hill
KEELER POND FAULT
GIDDINGS BROOK FAULT
SUDBURY FAULT
2000'
1000'
Sea level
S 78° E
B'
Beebe Pond
ROUTE 30
Ganson Hill
Giddings Brook
TACONIC RANGE
GIDDINGS BROOK FAULT
FLORENCE NAPPE
N 5° E
F'
Sanford Brook
SUNSET LAKE FAULT
Blueberry Hill
A-A'
N 25° E
G'
GIDDINGS BROOK FAULT
SUDBURY
Stony Hill
Signal Hill
S 3° E
H''
Vail Brook
BIRD MOUNTAIN FAULT
Spaulding Hill
Spruce Knob
1962' PEAK
GIDDINGS BROOK FAULT

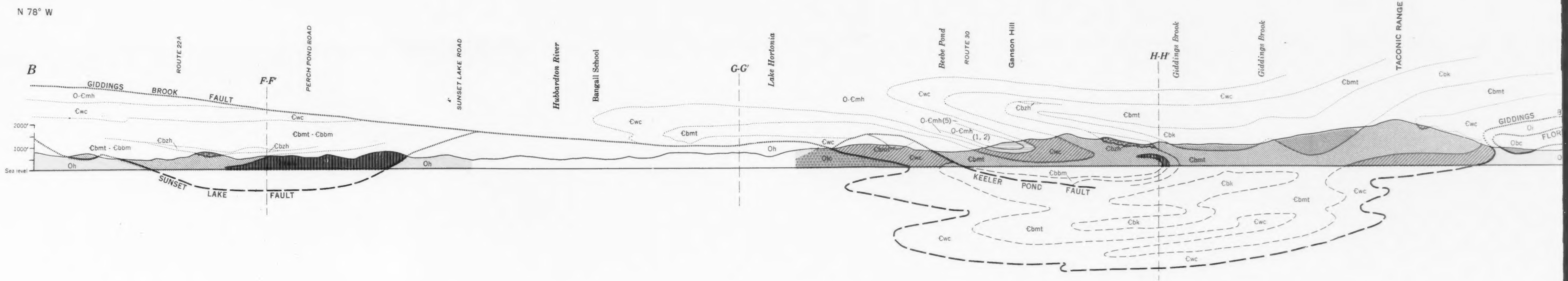
N 78° W
B
ROUTE 22A
PERCH POND ROAD
F-F'
SUNSET LAKE ROAD
Hubbardton River
Bangall School
G-G'
Lake Hortonia
Beebe Pond
ROUTE 30
Ganson Hill
H-H'
Giddings Brook
Giddings Brook
TACONIC RANGE
GIDDINGS BROOK FAULT
SUNSET LAKE FAULT
KEELER POND FAULT
2000'
1000'
Sea level
O-Єmh
Єwc
Єbmt - Єbbm
Єbzh
Єbmt
Єbbm
Єbk
Oh
Obc
Oi
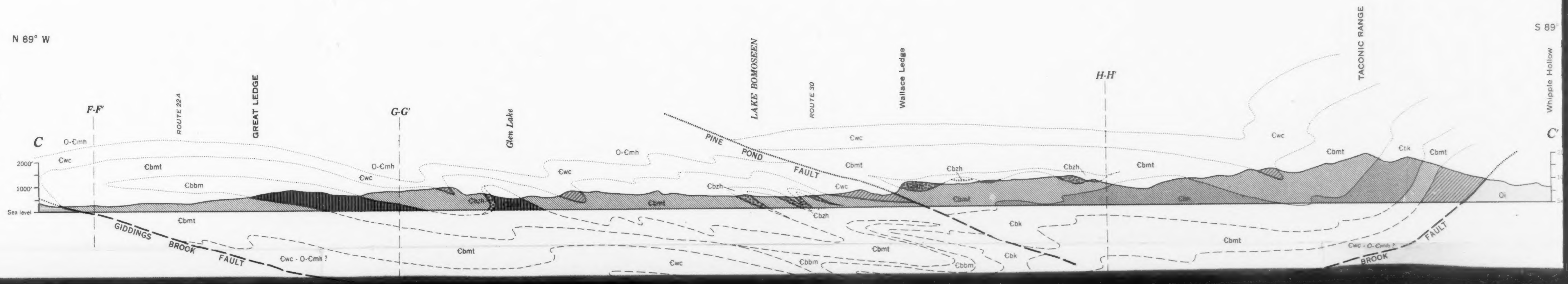
N 89° W
S 89°
C
C'
F-F'
ROUTE 22A
GREAT LEDGE
G-G'
Glen Lake
LAKE BOMOSEEN
ROUTE 30
Wallace Ledge
H-H'
TACONIC RANGE
Whipple Hollow
PINE POND FAULT
GIDDINGS BROOK FAULT
2000'
1000'
Sea level
O-Єmh
Єwc
Єbmt
Єbbm
Єbzh
Єbk
Єwc - O-Єmh ?
Oi

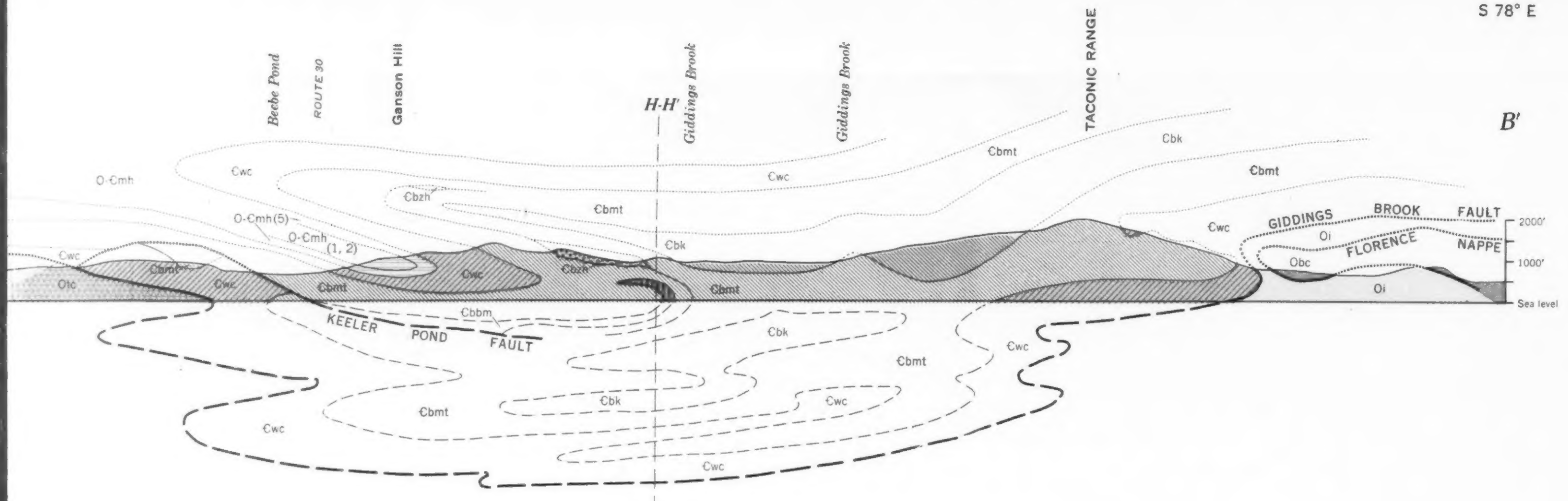
S 78° E
B′
Beebe Pond
ROUTE 30
Ganson Hill
H-H′
Giddings Brook
Giddings Brook
TACONIC RANGE
GIDDINGS BROOK FAULT
FLORENCE NAPPE
KEELER POND FAULT
2000′
1000′
Sea level
O-Cmh
Cwc
Cbmt
Cbk
Cbzh
Cbbm
Otc
Oi
Obc

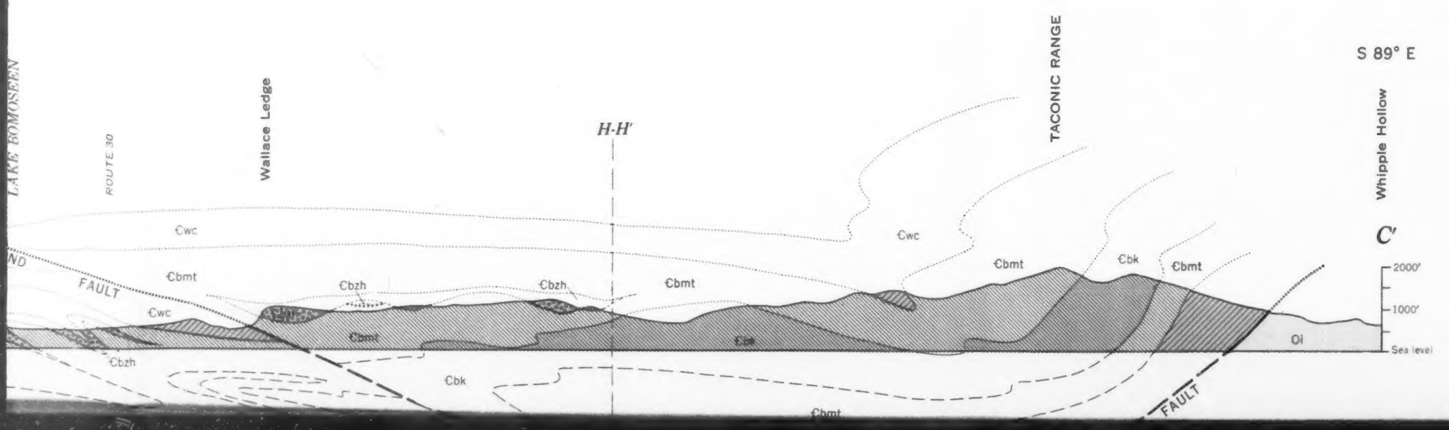
S 89° E
C′
LAKE BOMOSEEN
ROUTE 30
Wallace Ledge
H-H′
TACONIC RANGE
Whipple Hollow
FAULT
2000′
1000′
Sea level
Cwc
Cbmt
Cbzh
Cbk
Oi

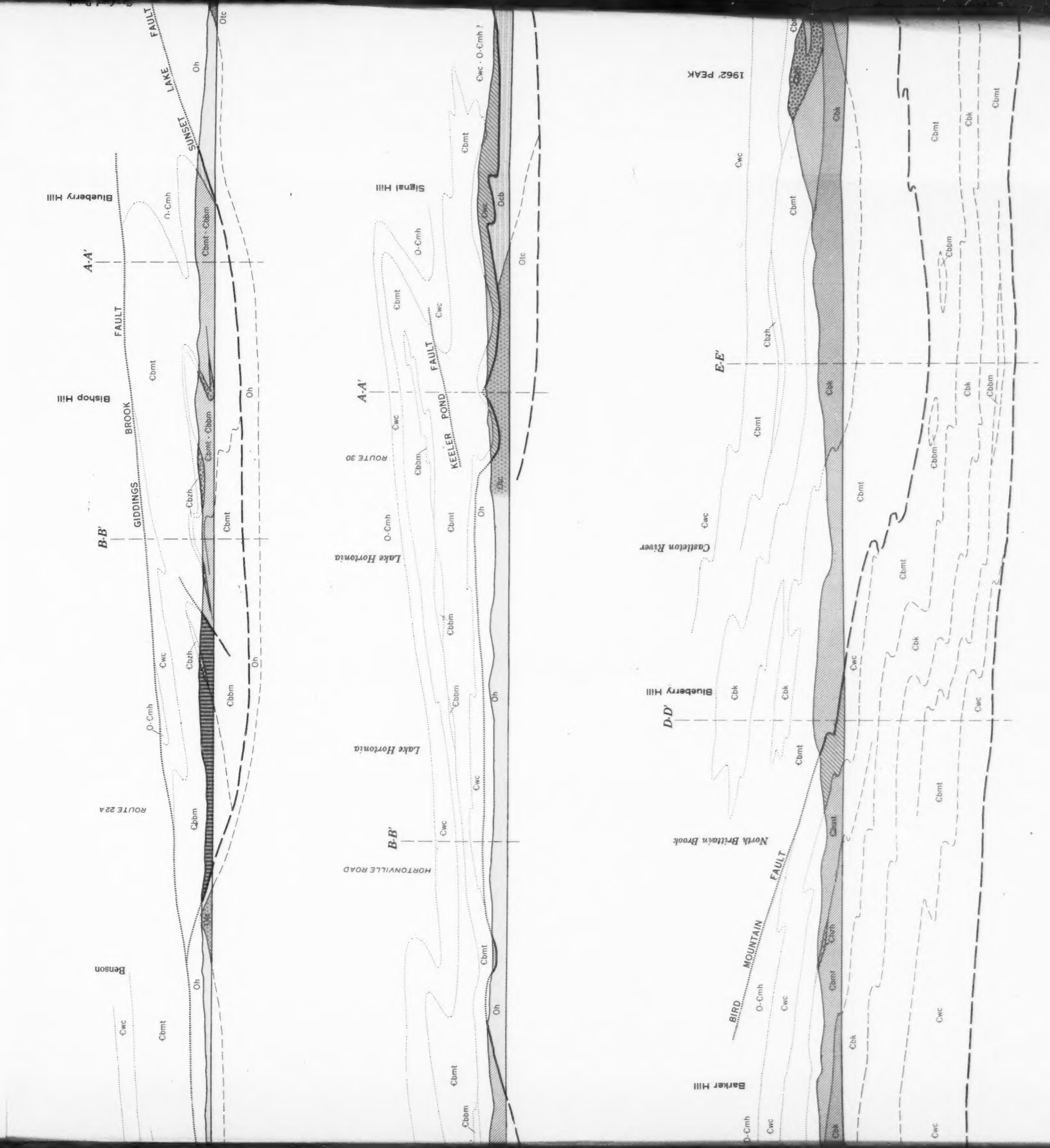
SUNSET LAKE FAULT
GIDDINGS BROOK FAULT
KEELER POND FAULT
BIRD MOUNTAIN FAULT
Blueberry Hill
Bishop Hill
Benson
ROUTE 22A
Signal Hill
Lake Hortonia
ROUTE 30
HORTONVILLE ROAD
1962′ PEAK
Castleton River
North Brittain Brook
Barker Hill
A-A′
B-B′
D-D′
E-E′

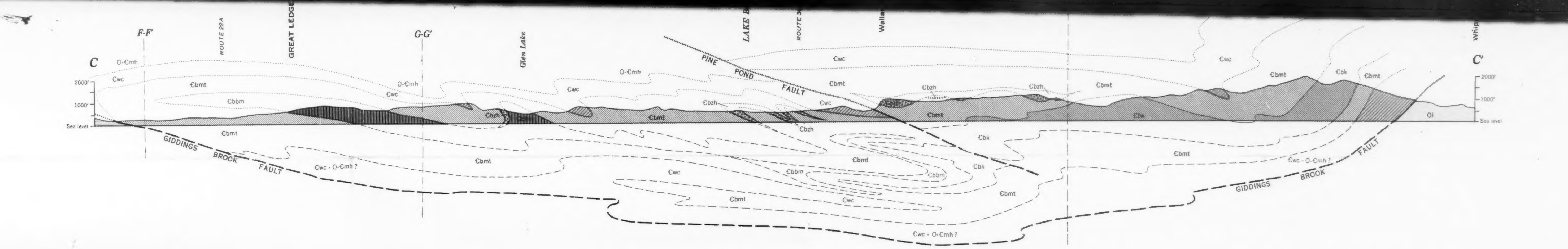
C
C'
F-F'
ROUTE 22A
GREAT LEDGE
G-G'
Glen Lake
ROUTE 30
2000'
1000'
Sea level
O-Ꞓmh
Ꞓwc
Ꞓbmt
Ꞓbbm
Ꞓbzh
Ꞓbk
Oi
PINE POND FAULT
GIDDINGS BROOK FAULT
Ꞓwc - O-Ꞓmh ?

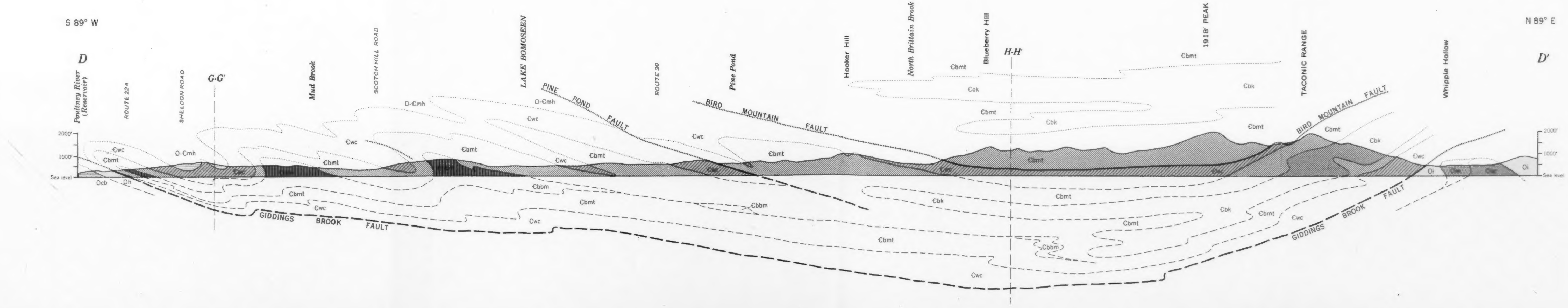
S 89° W
N 89° E
D
D'
Poultney River (Reservoir)
ROUTE 22A
SHELDON ROAD
G-G'
Mud Brook
SCOTCH HILL ROAD
LAKE BOMOSEEN
ROUTE 30
Pine Pond
Hooker Hill
North Brittain Brook
Blueberry Hill
H-H'
1918' PEAK
TACONIC RANGE
Whipple Hollow
2000'
1000'
Sea level
PINE POND FAULT
BIRD MOUNTAIN FAULT
GIDDINGS BROOK FAULT
O-Ꞓmh
Ꞓwc
Ꞓbmt
Ꞓbbm
Ꞓbk
Ocb
Oh
Oi

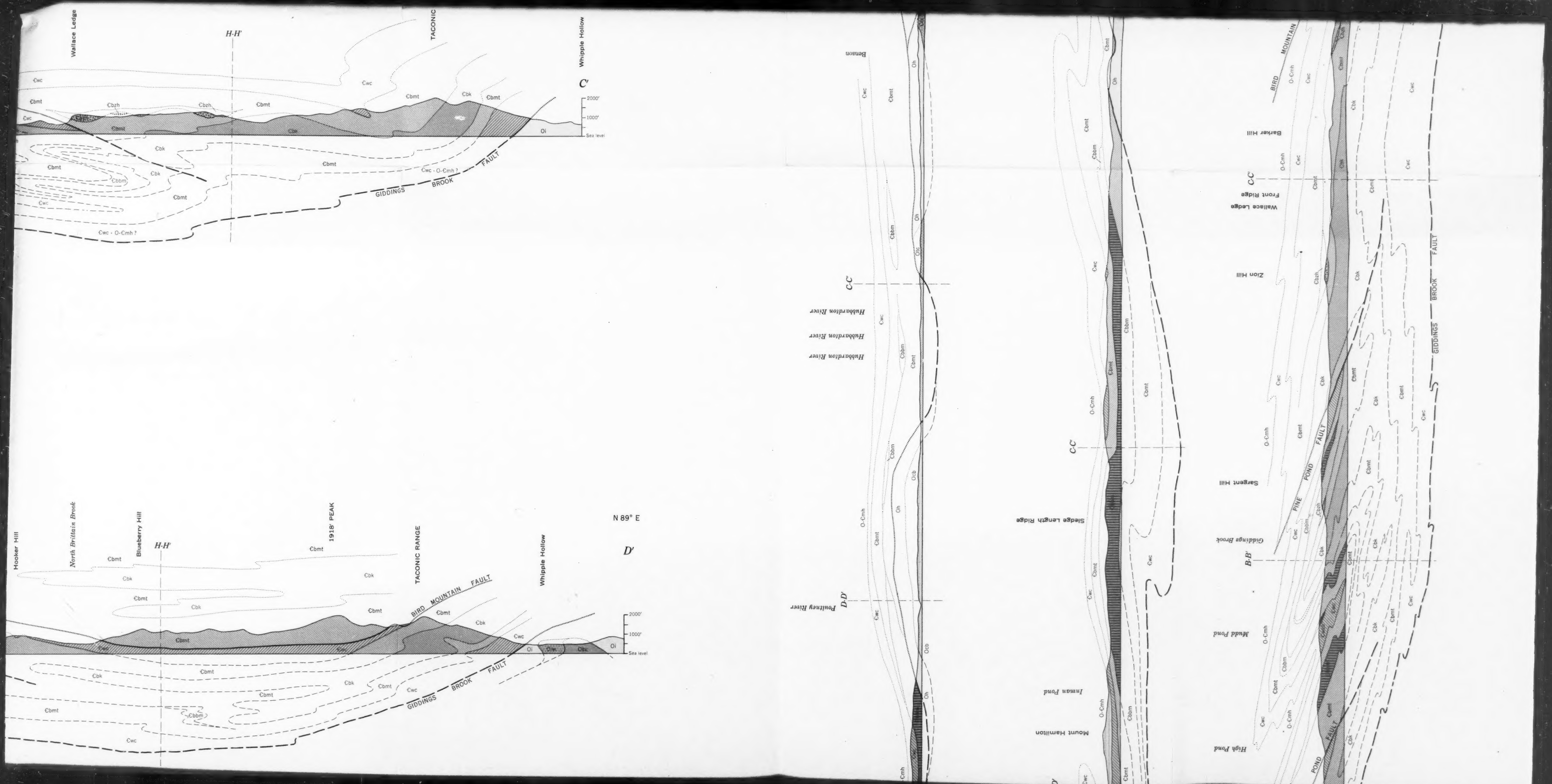

Wallace Ledge
H-H'
TACONIC
Whipple Hollow
C'
2000'
1000'
Sea level
GIDDINGS BROOK FAULT
Hooker Hill
North Brittain Brook
Blueberry Hill
1918' PEAK
TACONIC RANGE
BIRD MOUNTAIN FAULT
N 89° E
D'
Benson
Hubbardton River
Poultney River
Mount Hamilton
Inman Pond
Sledge Length Ridge
Barker Hill
Front Ridge
Zion Hill
Sargent Hill
Giddings Brook
Mudd Pond
High Pond
BIRD MOUNTAIN
PINE POND FAULT
POND FAULT
C-C'
D-D'
B-B'

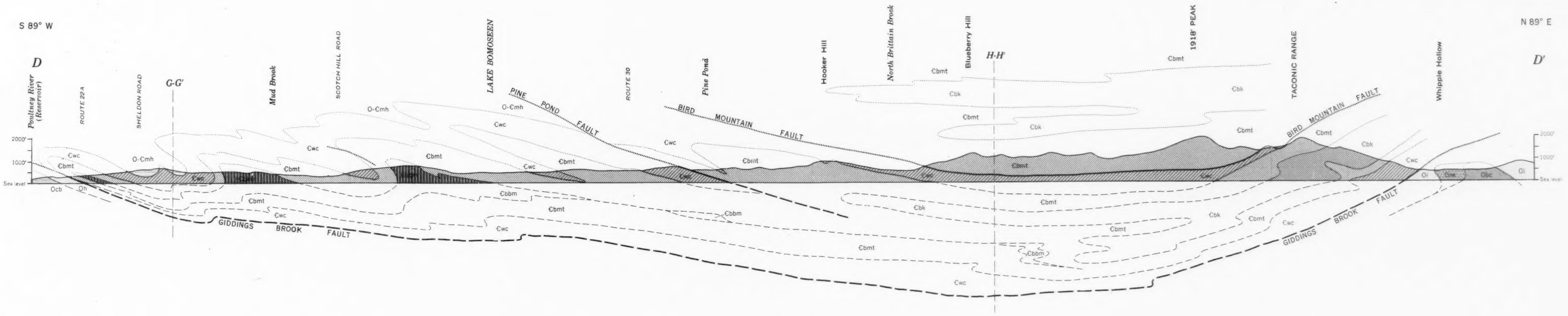
S 89° W
N 89° E
D
D'
Poultney River (Reservoir)
ROUTE 22A
SHELDON ROAD
G-G'
Mud Brook
SCOTCH HILL ROAD
LAKE BOMOSEEN
ROUTE 30
Pine Pond
Hooker Hill
North Brittain Brook
Blueberry Hill
H-H'
1918' PEAK
TACONIC RANGE
Whipple Hollow
PINE POND FAULT
BIRD MOUNTAIN FAULT
GIDDINGS BROOK FAULT
2000'
1000'
Sea level
O-Cmh
Cwc
Cbmt
Cbk
Cbbm
Ocb
Oh
Oi
Obc

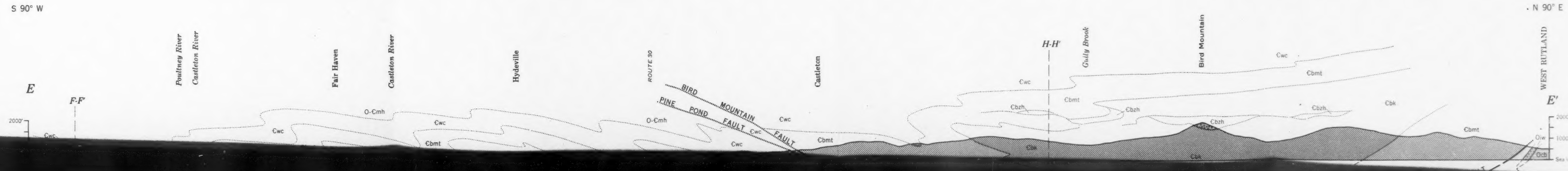
S 90° W
N 90° E
E
E'
F-F'
Poultney River
Castleton River
Fair Haven
Castleton River
Hydeville
ROUTE 30
Castleton
H-H'
Gully Brook
Bird Mountain
WEST RUTLAND
BIRD MOUNTAIN FAULT
PINE POND FAULT
2000'
1000'
Sea level
O-Cmh
Cwc
Cbmt
Cbzh
Cbk
Oiw

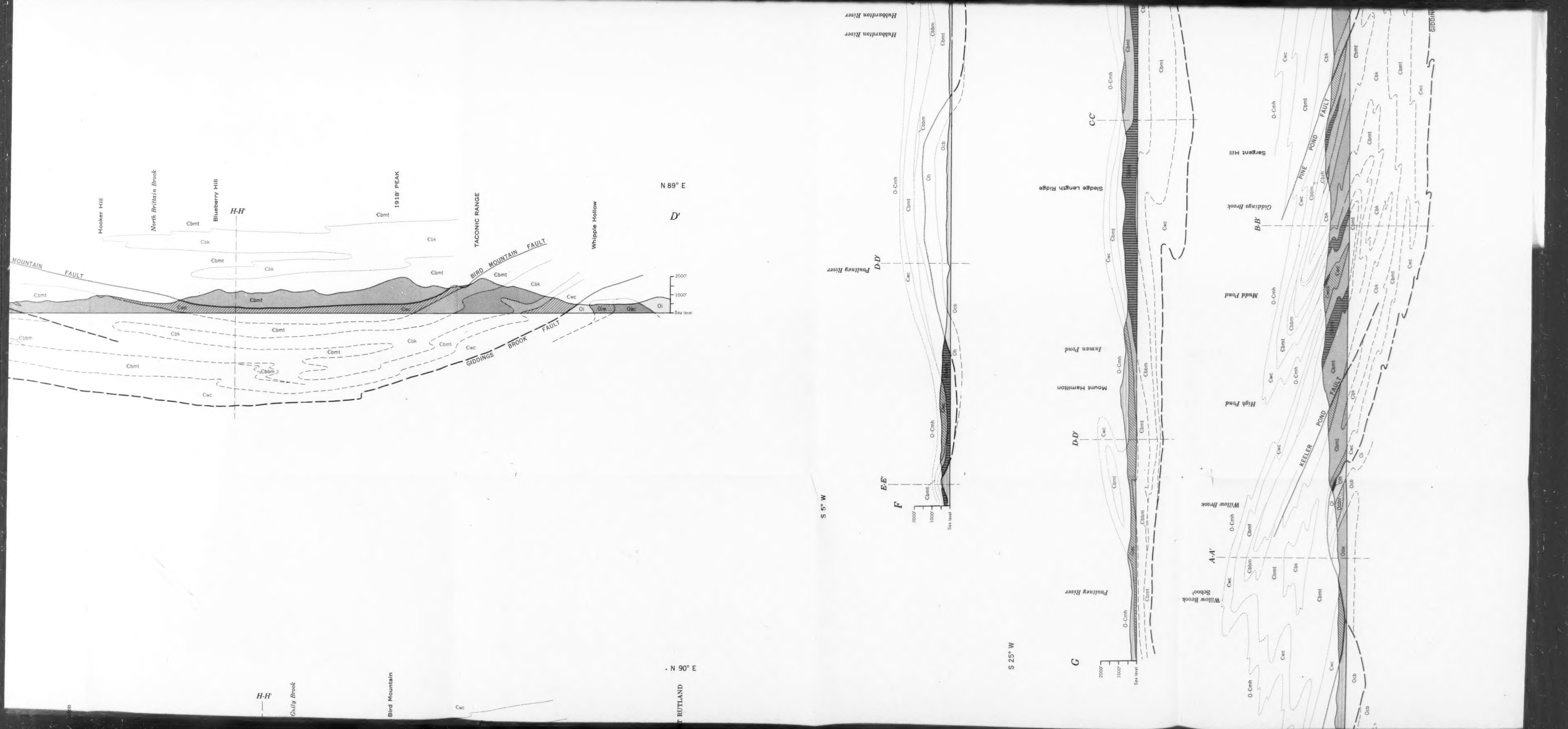
D'
N 89° E
Hooker Hill
North Brittain Brook
Blueberry Hill
H-H'
1918' PEAK
TACONIC RANGE
Whipple Hollow
MOUNTAIN FAULT
BIRD MOUNTAIN FAULT
GIDDINGS BROOK FAULT
2000'
1000'
Sea level
N 90° E
Gully Brook
Bird Mountain
RUTLAND
S 5° W
S 25° W
F
G
E-E'
D-D'
C-C'
B-B'
A-A'
Hubbardton River
Poultney River
Sledge Length Ridge
Inman Pond
Mount Hamilton
Sargent Hill
Giddings Brook
Mudd Pond
High Pond
Willow Brook
Willow Brook School
PINE POND FAULT
KEELER POND FAULT

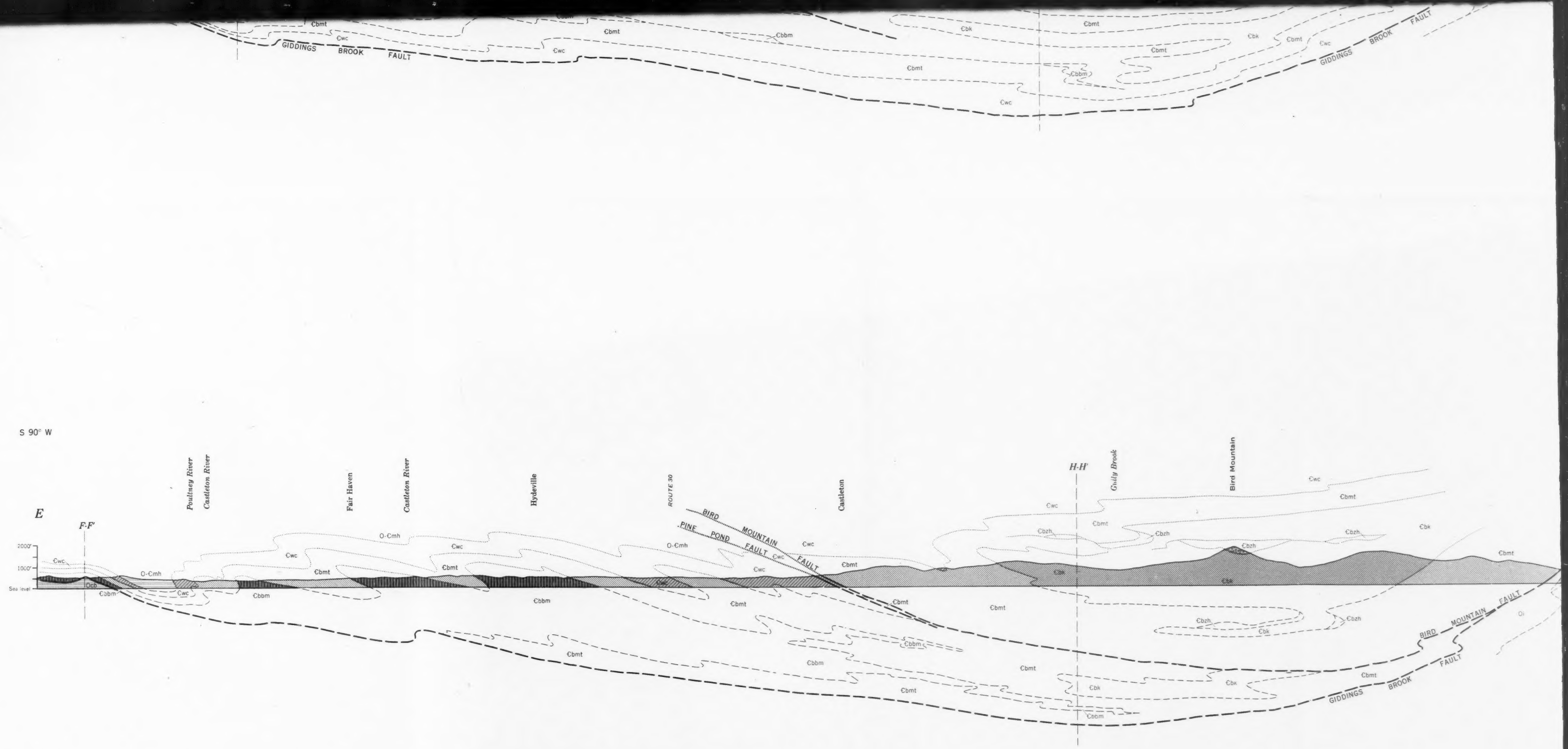

GEOLOGIC SECTIONS ACROSS THE CASTLETON AREA, VERMONT

Scale 1:48 000

1 0 1 2 3 4 5 Miles

ZEN, PLATE 5

Geological Society of America Bulletin, volume 72

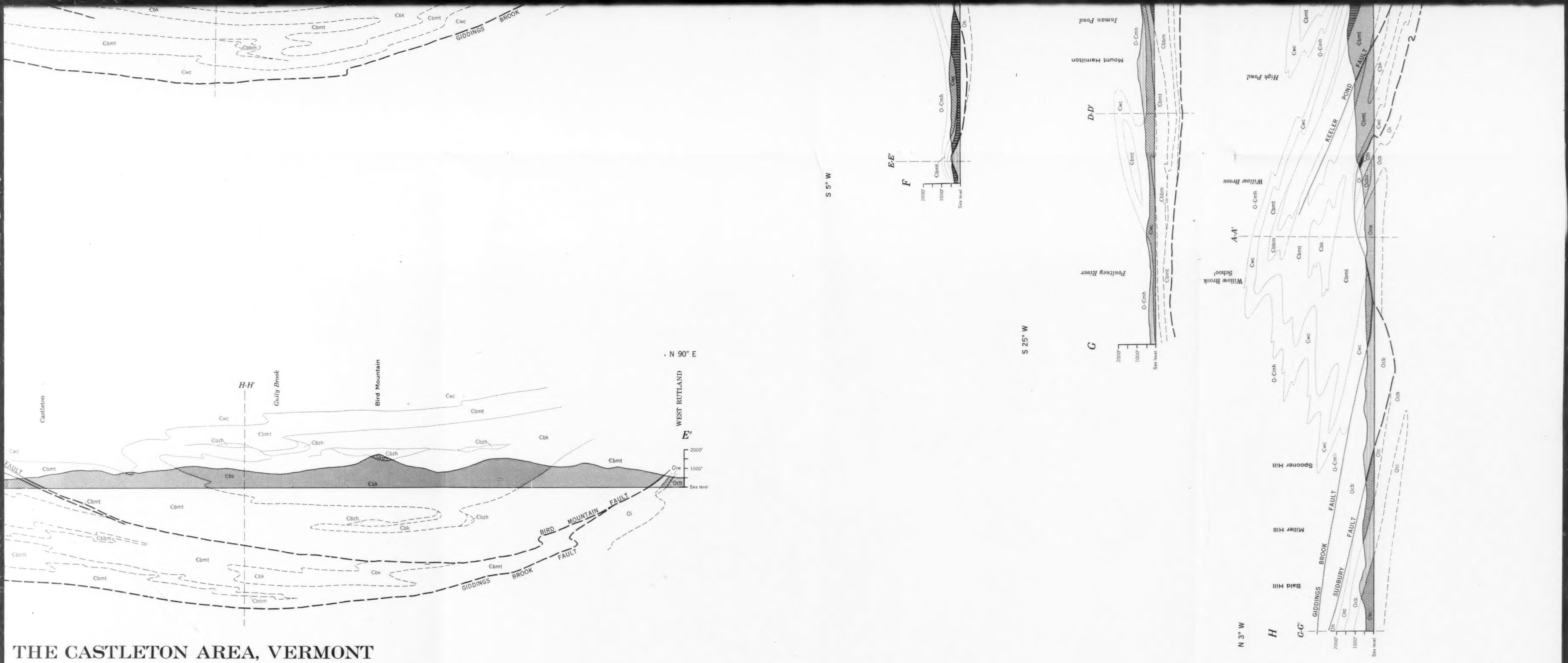

THE CASTLETON AREA, VERMONT

Scale 1:48 000

2 3 4 5 Miles

Williams & Heintz Map Corporation Washington 27, D. C.

Shor

C. A. KA
C. C. SC
J. N. CH

TEKT

Abstra
glass dis
Martha's
be a tek
from on

A fr
disc wa
1959 or
of Mar
Massac
and co
that it
at the
by Sch
Pinson
M. C
Geolog
R. Cl
Washi
the W
rately
The
gms, i
an ap
been
is de
some
conce
disc i
radia
The
surfa
greas
0.00
to b
sculp
alter
and
to s
part
Pl.
T

Ge

Short Note

C. A. KAYE
C. C. SCHNETZLER
J. N. CHASE

TEKTITE FROM MARTHA'S VINEYARD, MASSACHUSETTS

Abstract: A fragment of an oddly sculptured glass disc found on the cliff of Gay Head, on Martha's Vineyard, Massachusetts, is thought to be a tektite. Unless carried to Gay Head by man from one of the known tektite fields, it raises to three the number of tektite localities in the Western Hemisphere. The freshness of surface features and the clarity of glass indicate a recent origin. If, however, it weathered out of the cliff, it may be Late Cretaceous, Miocene, or Pleistocene in age.

A fragment of an oddly sculptured glass disc was found by Chase in the summer of 1959 on the cliff at Gay Head, the western tip of Martha's Vineyard, off the south coast of Massachusetts. The shape, physical properties, and composition of this piece of glass suggest that it is a tektite. Analytical work was done at the Massachusetts Institute of Technology by Schnetzler, under the direction of Wm. Pinson, and by F. Senftle, W. W. Brannock, M. Carron, and I. Friedman of the U. S. Geological Survey, Washington, D. C., and R. Clarke of the U. S. National Museum, Washington, D. C. The results of the work by the Washington group will be reported separately.

The tektite, weighing approximately 17.8 gms, is a 90-degree sector (Pls. 1, 2) broken off an apparently circular disc that must have been about 3 inches in diameter. The surface is deeply sculptured by discontinuous and somewhat ramifying ridges—or grooves—in a concentric arrangement. The edge of the disc is deeply serrated, and in the narrow rim radial grooves replace the concentric grooves. The glass is clear light olive green, but the surface looks opaque black with a slightly greasy luster. The specific gravity is 2.337 ± 0.005. Under magnification the surface is seen to be covered by minute round pits. The sculpturing is sharp, and no wear or secondary alteration of the glass is apparent. The form and sculpturing of this tektite are very similar to several moldavites figured by Suess(1900), particularly a disc from Budweis (Suess, 1900, Pl. XV, fig. 5a, 5b, 5c).

The chemical composition (Table 1) shows several characteristics of tektites: high SiO_2 and high FeO/Fe_2O_3 ratio.

TABLE 1.—CHEMICAL ANALYSIS OF MARTHA'S VINEYARD TEKTITE*

Oxides	Composition in per cent
SiO_2	80.68 ± 1.2†
Al_2O_3	11.43 ± 0.28
FeO	2.22 ± 0.15
Fe_2O_3	0.72 ± 0.10
MgO	0.73 ± 0.02
CaO	0.50 ± 0.05
Na_2O	1.04 ± 0.10
K_2O	2.44 ± 0.12
TiO_2	0.51 ± 0.05
P_2O_5	0.06 ± 0.03
MnO	0.047 ± 0.003
Total	100.38

* Analysis by C. C. Schnetzler, using rapid silicate method

† Errors in accuracy based on monitoring with W-1 and G-1

The fresh appearance of the surface of the tektite and the clarity and seemingly unaltered condition of the glass suggest a recent origin. There is, however, a possibility that it weathered out of the cliff, and therefore the deposits from which it would have been derived are described.

The tektite was found loose in the bottom of a small erosional gully just below the point where most tourists view the cliffs (Pl. 1, fig. 1). It was lying in assorted rock debris that had washed down into the gully from the cliff face

Geological Society of America Bulletin, v. 72, p. 339–340, 2 pls., February 1961

above. For about 25 feet above the point where the tektite was found, the gully is cut into white to nearly white, medium to coarse, clayey quartz sand and fine quartz gravel. The small amount of binder clay in these beds is white kaolinite. The beds are cross-bedded and belong to a sequence of sands, gravels, clays, and lignites that crops out widely in Gay Head and that from plant fossils have been dated by Hollick (1906, p. 27) as of Raritan age (early Late Cretaceous). The entire sequence seems to be continental in origin and most likely was deposited in broad flood plains.

Above the Upper Cretaceous clayey sands and gravels is about 10 feet of very light-greenish-gray clayey quartz sand and gravel. Interbedded in this horizon is a nodular phosphatic bed about 2 feet thick, consisting of quartz gravel, bone, sharks' teeth, phosphate pellets, and miscellaneous organic and inorganic debris variably cemented by dark-gray aphanitic phosphate. This bed, the Aquinnah conglomerate of Woodworth and Wigglesworth (1934, p. 36), weathers out as rounded puddingstone boulders up to 3 feet across. Many of these were lying loose in the gully where the tektite fragment was found. This peculiar zone is mostly a reworking of older deposits that occur in the vicinity—the Cretaceous quartz sand and gravel and the highly fossiliferous bone-bearing greensand of Miocene age which crops out in the cliffs nearby. It seems to be a talus deposit that accumulated in early or middle Pleistocene time at the toe of a cliff cut into Upper Cretaceous, Miocene, and early Pleistocene glacial sediments. Therefore, if the tektite weathered out of this horizon, its age may be Pleistocene, Miocene, or early Late Cretaceous.

Above the fossil talus deposit are sands of middle Pleistocene age and gravels representing two glacial advances and perhaps one interglacial interval. These are capped by about 2 feet of Recent wind-blown sand.

A brief but unsuccessful search was made in the vicinity for other tektites and for the rest of the disc. Until other tektites are found in the vicinity the question will persist whether this tektite marks a new locality or whether it was transported by man. There is little basis for judging the relative probabilities of these two possibilities—both seem equally unlikely, depending on how one looks at the find. If Martha's Vineyard is a true tektite locality, then it is the third, following Texas and Georgia, so far found in the Western Hemisphere.

The writers acknowledge the valuable advice of Professor William Pinson, Massachusetts Institute of Technology. The analytical work was supported by the Geological Research Directorate, Air Force Cambridge Research Center, Bedford, Massachusetts. The manuscript was critically reviewed by J. P. Schafer, P. M. Hanshaw, F. E. Senftle, and I. Friedman of the U. S. Geological Survey and P. D. Lowman and R. S. Clarke of the Smithsonian Institution.

REFERENCES CITED

Hollick, Arthur, 1906, The Cretaceous flora of southern New York and New England: U. S. Geol. Survey Monograph 50, 129 p.

Suess, F. E., 1900, Die Herkunft der Moldavite und verwandter Gläser: Kaiserlich-Königlichen geol. Reichsanstalt Jahrb., Bd. 50, H. 2, p. 193–382

Woodworth, J. B., and Wigglesworth, E., 1934, Geography and geology of the region including Cape Cod, the Elizabeth Islands, Nantucket, Marthas Vineyard, No Mans Land and Block Island: Harvard College Museum Comp. Zoology Mem., v. 52, 322 p.

U. S. Geological Survey, 270 Dartmouth Street, Boston, Mass.; Dept. Geology, Massachusetts Institute of Technology, Cambridge, Mass.; Dept. Zoology, Ohio Wesleyan University, Delaware, Ohio

Manuscript Received by the Secretary of the Society, July 1, 1960

FIGURE 1.—Gay Head. The arrow points to place in gully where tektite was found.

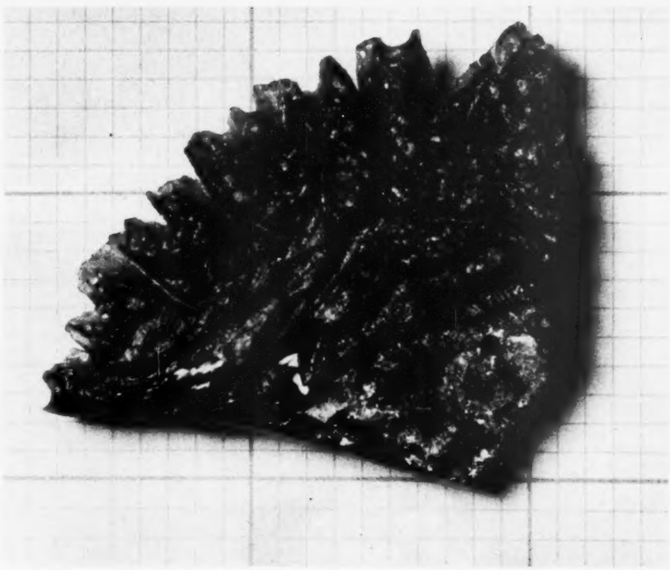

FIGURE 2.—The tektite in reflected light. Co-ordinate paper gives scale: dark lines are 1-inch squares, light lines are 1/10-inch squares.

TEKTITE FROM GAY HEAD, MARTHA'S VINEYARD, MASSACHUSETTS

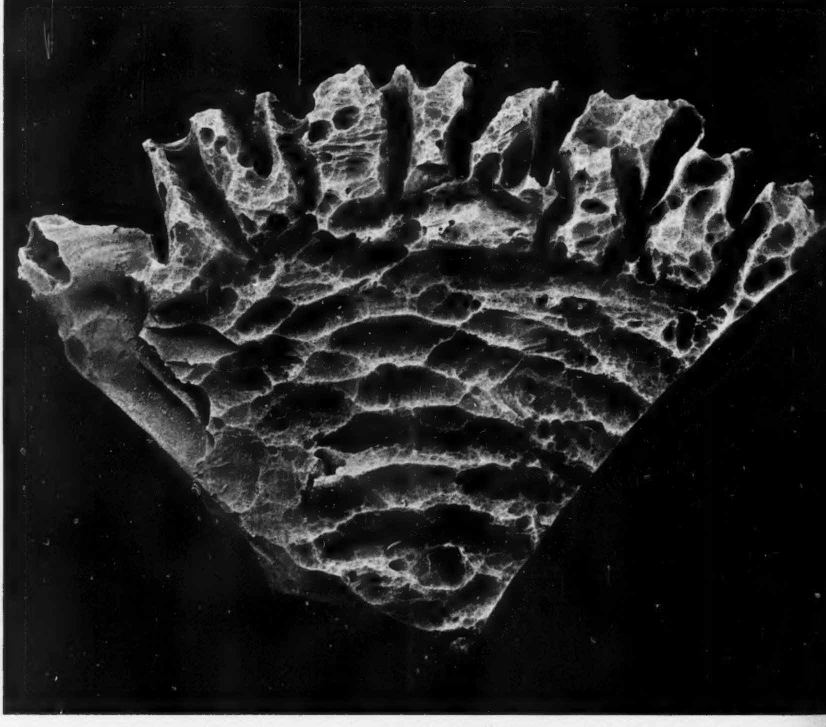

Figure 1.—Tektite smoked with ammonium chloride. Small fragments had been chipped from an edge f analysis.

Figure 2.—Tektite, edge view; smoked with ammonium chloride.

TEKTITE FROM GAY HEAD, MARTHA'S VINEYARD, MASSACHUSETTS